

SYMPOSIUM ON GEOCHEMISTRY AND CHEMISTRY OF OIL SHALE
PRESENTED BEFORE THE DIVISIONS OF FUEL CHEMISTRY, GEOCHEMISTRY
AND PETROLEUM CHEMISTRY, INC.
AMERICAN CHEMICAL SOCIETY
SEATTLE MEETING, MARCH 20-25, 1983

GEOLOGY AND GEOCHEMISTRY OF SOME QUEENSLAND TERTIARY OIL SHALES

By

Arthur W. Lindner

Southern Pacific Petroleum N. L., 143 MacQuarie Street, Sydney, Australia 2000

INTRODUCTION

Oil shale was first recognized almost a century ago in Queensland. The flammable rock aroused some interest for a number of years but the first serious attempt to assess the resource did not take place until World War II. Typically, the Queensland Tertiary oil shales are sparsely exposed and deeply weathered. The distribution and extent of the oil shale has to be determined by drilling.

Southern Pacific Petroleum and Central Pacific Minerals commenced exploration for oil shale in 1974 and defined the Rundle deposit in the Narrows Graben (Figure 1). The search has since been extended to other basins which hold the attraction of proximity to infrastructure facilities and population centers along Queensland's central coast. In five deposits under review, the indicated *in situ* shale oil resource exceeds 17 billion barrels (at a cut off grade of 50 liters/ton).

The drill core is logged for lithology and bulk density, then split and assayed on 2m intervals. From experience with the Queensland shales, an 80 gm charge is used in the Fischer retort. Half drill-core 2 meter intervals provide from 3 to 5 kg. of sample and the assay rejects together with unused core are retained to provide a sample bank for characterization tests carried out on the oil shale seams.

GEOLOGY OF THE DEPOSITS

During the Paleozoic and much of the Mesozoic, the region now represented by eastern coastal Queensland developed by continental accretion to the Australian Shield. The tectonic grain strikes northwest-southeast. Sedimentary basin remnants and uplifts from this earlier period underlie the oil shale deposits.

At the beginning of the Tertiary Period, rifting began to open the Tasman and Coral Seas and relaxation of the former compressive forces resulted in the formation of a number of grabens within the continent, adjacent to the developing ocean to the east. This appears to be the framework in which the thick, essentially lacustrine sequences containing oil shales accumulated in narrow, linear, fault-bounded basins, in some cases with accompanying igneous activity (1).

The Narrows Graben (Figure 2)

The Rundle Formation (580m) contains the oil shale resource in The Narrows Graben preserved in two structurally defined lobes, the Rundle and Stuart deposits (2). The most prospective interval (the upper 320m) comprises 4 seams (Ramsay Crossing, Brick Kiln, Munduran Creek, Kerosene Creek) of predominantly oil shale, one (Humpy Creek) of carbonaceous shale ranging to lignite and one thick unit of barren claystone (Telegraph Creek unit). The average yield is 99 liters per ton at zero moisture (LTOM) for Rundle and 94 LTOM for Stuart. Average moisture is respectively 21 and 19%, and *in situ* bulk density 1.75 g/cc. The calculated *in situ* resource in the graben is 5.16×10^9 barrels oil.

The oil shales, clay and silt in grain size, range from massive to finely laminated, and range in color through combinations of brown, grey and green with the greenish hue more evident in thin barren interbeds within the seams and in the Telegraph Creek unit. There are dark colored carbonaceous horizons in all seams. Ostracods and gastropods are widespread and fragments of reptiles, fish and crustaceans have been found in drill cores. Sedimentary structures (breccias, color grading, slumping) are prevalent and repeated; recent detailed mapping in a cut opened in the Ramsay Crossing seam to provide bulk samples has revealed cyclic sedimentation over a frequency of a few meters (3). Thin, discontinuous, dense limestone beds and lenses are present throughout the sequence.

The sequence dips to the west from 4 to 10 degrees and both flanks of the deposit are in fault-contact with basement. A localized alkaline intrusive has invaded the lower seams of the

Rundle Formation and thermally metamorphosed (pyrolyzed) up to 46m thickness of oil shales. Its minimum age of crystallization has been calculated at 26.8 m. y.

Hillsborough Basin

Prospecting for oil shale has been confined to the west flank of the onshore portion of the Hillsborough Basin where volcanolithic quartz arenites and pelite form economic basement, conformably underlying the Condor deposit. The brown oil shale, the main unit of the Condor deposit is a remarkably monotonous, massive (to slightly laminated) brown, kerogenous mudstone. It ranges from 300-400m in thickness and has been traced for 15 km along strike. About half of the seam has an average yield of 63 LTOM and constitutes the main potential economic zone of the deposit (4). Towards its base, the brown oil shale becomes blackish and at the contact with the basal sandstone, a high yielding (135 LTOM) humic coal and carbonaceous shale occur along much of the strike length of the deposit. The indicated *in situ* resource is 8.45×10^9 barrels of shale oil.

Overlying the brown oil shale are thinly interbedded and laminated oil shales and siltstones, a unit transitional to the youngest horizon (upper unit). A uniform and regular dip to the northeast of 14° takes the top of the brown oil shale to a depth of 500m at the downdip limit of prospecting.

The oil shale at Condor is a tougher, more competent rock than the other Tertiary oil shales and also possesses a lower moisture content (9% by weight). The brown oil shale unit contains scattered collophane nodules and buddingtonite occurs persistently in the unit, comprising almost 10% of the rock (5).

Duaringa Basin

In contrast to other deposits, the Tertiary sequence in the Duaringa Basin has positive relief, standing as steep-sided tablelands up to 100m above surrounding low lying-country and is underlain by Permian rocks of the Bowen Basin.

"Fence line" drill holes across the basin revealed that oil shale occurs at two horizons (Units B and D) above the base of the tablelands and although lying subhorizontally and continuous, is relatively thin. The oil shales are soft, moist, greenish grey mudstones. Traces of oil shale also occur deeper (from 250 to 800 meters below the surface) in the basin. A stratigraphic core hole drilled by the Geological Survey of Queensland (Duaringa 1-2R) proved a depth of 1200 meters of Tertiary sediments, mostly bloturbated silty and sandy, mottled, oxidized claystones, underlain by 180m+ of basalt (Noon, pers. comm.). Basalts also occur interbedded with the shallow oil shale layers in the southern end of the basin. A distinctive and ubiquitous sanidine-rich ash bed of centimeters thickness occurs near the base of Unit B.

The resource is estimated to contain 3.72×10^9 barrels of shale oil.

Byfield

At Byfield, oil shale is contained in a small graben 2 km wide and about 5 km along the western flank of the Water Park Creek Basin. Two oil shale units (TW2, 4) overlie carbonaceous and pale colored claystones and sandstones (TW1) and are separated by about 120m of kerogen-bearing mudstone (TW3). Unit TW2 is 120 m thick of which 50m has an average grade of 58 LTOM with a low (9.5%) moisture and has superficial similarities to the brown oil shale at Condor. At the top of the sequence Unit TW4 (up to 110m) consists of dark brown to black carbonaceous shale-lignitic coal, with interbedded sandstone and siltstone. The shale oil yield is relatively high (up to 100 LTOM) for the appearance of the rock, but averages 77 LTOM for a net 50m. Some of the assay-produced oils contain a tarry fraction, with S.G. >1.0.

COMPOSITION OF THE OIL SHALES

In their study of Queensland Tertiary alginites (exinite material largely of algal origin), Hutton et al. (6) found that they were able to distinguish between accumulations of discrete algal bodies (typical of high grade oil shales, like torbanite and kukersite) and finely banded, lamellar alginite in intimate association with mineral matter (typical Queensland Tertiary alginites). As a result of the study Hutton et al. proposed the terms "Alginite A" and "Alginite B" (or lamosite) as modifications of conventional oil shale maceral terminology. Green algae were shown to be precursors of alginite A, and blue-green algae the precursor of alginite B. Both alginite forms produce Type I kerogen (7).

The Queensland Tertiary lamosites are high moisture, with an organic carbon content rarely exceeding 20% by weight. Pyrite is usually present in trace quantities. An association of silt and clay sized silica and silicate-rich minerals dominates the inorganic constituents. However, generalizations have to be kept in perspective. For example, assaying of the oil has been consistently carried out over two meter intervals and while over this interval, the organic carbon content may rarely exceed 20%, over centimeters within this interval, the range may vary enormously.

Yet, distinctive grade patterns over multiples of the two meter assay interval commonly persist throughout the preserved areal dimension of a deposit, coincident with other lithologic characters of the rock. Thus, the seam classification at Rundle applies also at Stuart, throughout the 28 km length of The Narrows Graben. Likewise, the 10 and 20 m seams (units D and B) at Duaringa persist over a distance of 130 km in the erosional remnants in that basin; and vertical grade changes through the 300 m thick brown oil shale unit at Condor persist for at least 15 km along strike.

MINERALOGY

The distribution of the major elements (expressed as oxides) in the main oil shale seams in three basins, (The Narrows Graben, Duaringa and Hillsborough Basins) are listed in Table I. The most apparent variations are in the inorganic components of the carbonaceous units (Humpy Creek seam in The Narrows Graben; brown-black oil shale and carbonaceous unit at Condor) when compared to the lamossites. At Condor, the increase in Al_2O_3 at the expense of SiO_2 is very pronounced; whereas in the Humpy Creek seam the distribution is reversed. The other aspect to the Humpy Creek is the relatively higher incidence of Na_2O and lower level of CaO and MgO compared to the rest of the seams in The Narrows Graben. In the lamossites, the values of CaO and MgO are lower in the Duaringa and Condor deposits than in Stuart.

Mineral composition, as determined by X-ray diffraction, shows a dominance of clay minerals, although quartz and opaline silica are persistent as sub-dominant or co-dominant (Table II). The clay minerals are commonly interstratified montmorillonite and illite (in all deposits) with kaolinite or illite appearing as accessory or sub-dominant components. A marked contrast in the dominant clay species occurs between the brown oil shale unit and the two units below it at Condor. In these lower units, kaolinite is in greater abundance than other clays as well as quartz, an aspect already indicated in the variations in Table I.

Feldspar occurs as an accessory or trace mineral in all deposits. At Rundle, Stuart and Duaringa it is a K-feldspar and more rarely, plagioclase, while at Condor it is the unusual ammonium feldspar, buddingtonite (5). The presence of buddingtonite in the Condor sequence coincides with the change from kaolinite to montmorillonite dominance. The feldspars in the deposits may be authigenic. At the base of Unit B oil shale at Duaringa, there is a thin (20+ cm), but laterally persistent sandine - rich marker horizon, considered to be of allogenic origin, probably a volcanic ash.

Apart from recurrent thin limestone beds in The Narrows sequence, carbonates are present in all deposits in only trace or accessory amounts. Siderite occurs in all deposits and is persistent through the sequence at Byfield and Condor, except for the carbonaceous units where its incidence is variable. At Condor, a second, possibly calcian siderite, occurs but only with an identical distribution through the sequence to the buddingtonite. Other evaporites, gypsum, halite and jarosite occur only in trace amounts. The sulfates may be a secondary development. Phosphate mineralization occurs in the transitional and brown oil shale units at Condor; a mineral related to jahnsite (5) and ovoidal colophonane nodules up to 5 cm (4). Vivianite is associated with Unit B shale at Duaringa. Barite nodules occur in weathered shale at the surface at Duaringa from about the same horizon in close stratigraphic association with diatomite recorded in that sequence.

Trace element analysis by emission spectroscopy on pyrolyzed shale has not revealed any concentration of metals in anomalous or unusual amounts even though the provenance for the different basins ranges from sedimentary, through igneous and metamorphic sequences.

KEROGENS

In the course of characterization work, a number of kerogen samples have been isolated from different seams in the various deposits. Their elemental composition (on a mineral free basis) has been incorporated into Table III and atomic ratios plotted on the Van Krevelen diagram, Figure 3. The diagram demonstrates the persistence of Type I kerogen in the lamossites from the Queensland Tertiary deposits. Two of the five kerogens from the Condor brown oil shale show unusually high O/C atomic ratios. The other kerogens from this unit appear to be intermediate between Type I and II.

The Carbonaceous units (Condor, Byfield and Humpy Creek seam at Rundle and Stuart) characteristically fall into Type III kerogens implying a lower algal content or the presence of higher plant material. Higher rank for the Condor Type III is apparent. Maturation due to greater burial might also be assumed for the position in the diagram of Type I Condor and for the older kerogens (Ramsay Crossing and Brick Kiln) in The Narrows Graben.

Elemental analyses together with hydrogen/carbon and oxygen/carbon ratios for shale oils have been listed in Table III. The table shows where analyses have been performed on kerogen and derived shale oil, that the hydrocarbon content and the H/C atomic ratio of the oil are higher than for the parent kerogen.

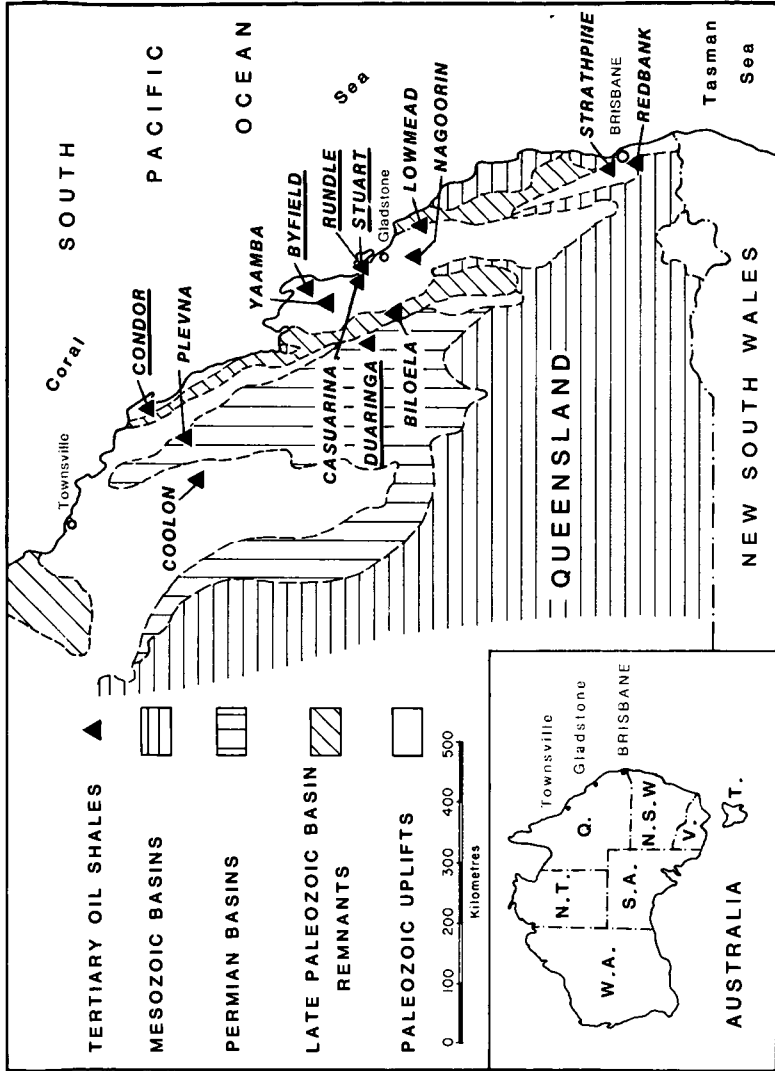


Figure 1. Location of Tertiary oil shale deposits, eastern Queensland.

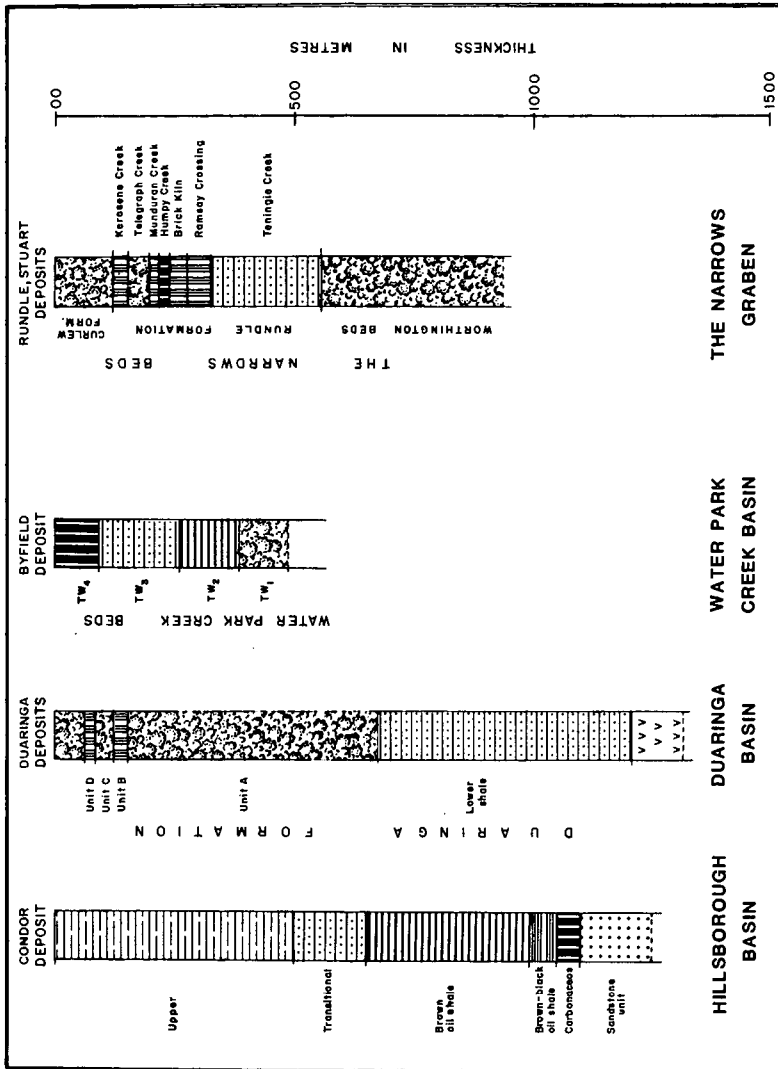


Figure 2. Diagrammatic columnar sections showing oil shales in four basins.

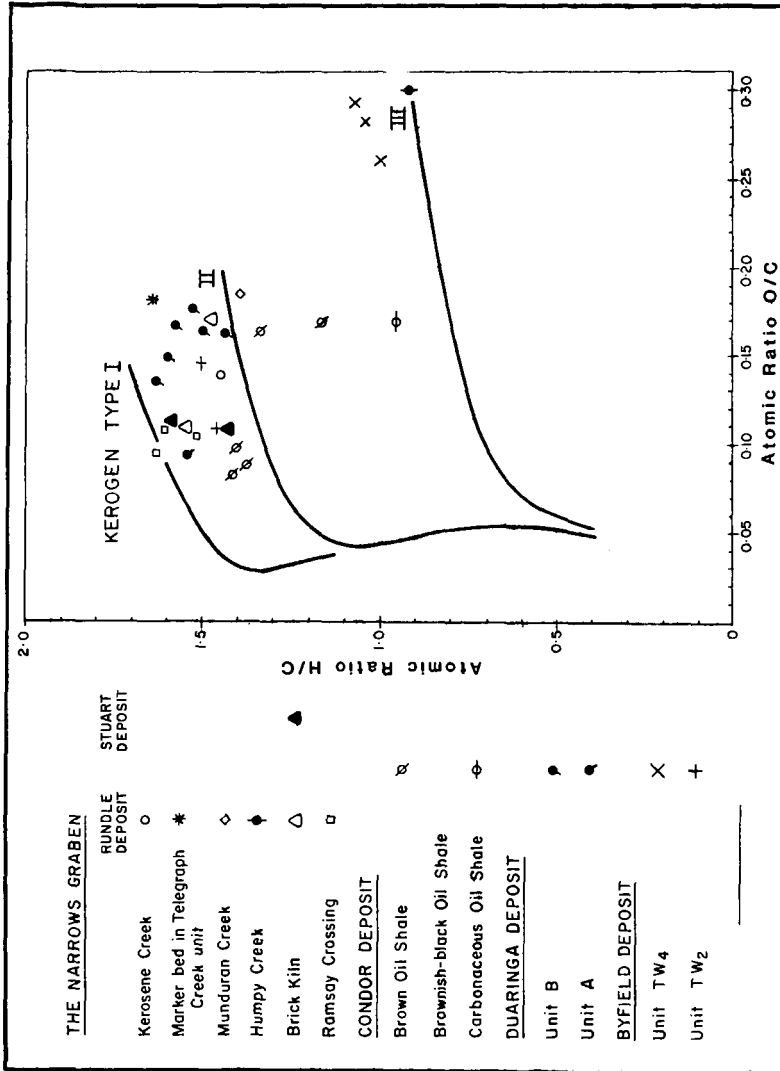


Figure 3. Van Krevelen diagram of some Queensland Tertiary kerogens.

TABLE I
MAJOR ELEMENTS AS OXIDES

Deposit	Seam	Rock Type ^a	No. of Analyses	SiO ₂	TiO ₂	Al ₂ O ₃	Total Fe as FeO ₃	Mno	MgO	CaO	Na ₂ O	K ₂ O	P ₂ O ₅	Range of Yields by mFA ^b (LTOM)	Average Moisture ^c W+%
Stuart	Kerosene Ck.	O.S	4	63.4	0.6	16.3	9.1	0.2	2.4	5.8	0.8	2.2	0.4	45-230	22
	Munduran Ck.	O.S	3	61.8	0.7	16.6	6.7	0.2	2.3	6.3	1.2	2.2	0.3	109-202	18
	Humpy Ck.	C/C.S	3	66.8	0.6	12.1	6.6	0.1	1.5	2.5	2.0	0.9	0.1	81-112	24
	Brick Kiln	O.S	14	61.9	0.8	16.5	9.8	0.2	2.6	6.1	1.2	1.6	0.3	44-193	18
Duaranga	Ramsay														
	Crossing	O.S	9	62.2	0.8	16.0	9.3	0.2	2.9	5.3	1.0	1.9	0.2	25-179	17
	Teningie Ck.	L.O.S	3	66.7	1.0	18.6	7.0	0.1	2.0	3.5	0.9	1.7	0.3	33-43	N.A.
Condor	Unit B	L,M,H,O,S	3	66.2	0.8	19.0	8.6	0.3	1.3	0.6	0.6	2.3	0.3	27, 57, 119	24-33
	Brown oil shale	O.S	18	68.3	0.9	17.1	8.9	0.1	1.4	0.8	0.5	1.0	0.3	25-104	8
Carbonaceous unit	Brown-black oil shale	L.O.S	3	59.1	1.3	25.2	11.7	0.2	1.6	1.1	0.5	1.4	0.3	22-46	9
	Carbonaceous unit	C/C.S	4	58.2	1.4	30.3	5.0	<0.03	1.0	0.7	0.5	1.42	0.2	48-106	155

a. O.S. - Oil shale
C/C.S - Coal, carbonaceous shale
L, M, H, O, S - Low, medium, highgrade oil shale

Analyses are reported on a dry total ash basis. b) Range of oil yields and c) average moisture are included for an appreciation of the organic and volatile components of the various oil shales. Moisture value includes free and combined water. Oil yield is expressed as liters per ton of oil shale on a dry (zero moisture) basis (LTOM).

TABLE II

MINERAL COMPOSITION OF OIL SHALE SEAMS IN THE STUART, DUARINGA, BYFIELD AND CONDOR DEPOSITS

Deposit	Seam	Rock Type	m. PA (TOM)	Amorphous Material	Quartz	Opaline Silica	Montmorillonite	Inter stratified Illite	MICA/Illite	Kaolinite	Feldspar	Buddingtonite	Siderite	Calcan Siderite	Calcite	Calcite (substituted Mg.)	Pyrite	Gypsum	Jarosite	Alunite	Halite	Anatase	
Stuart	Kerosene Ck.	O. S.	45-230	xx/xxxx	xx/xxxx	xxxxx	xxxxx	xxxxx	xx	xx	x/xx	x	x	xx	xx	x/xx	x/xx	x	x/xx	x	x		
	Munduran Ck.	O. S.	109-204	xxx/xxx	xxx/xxx	xxxxx	xxxxx	xxxxx	xx	xx	x/xx	xx	xx	xx	xx	xx	x/xx	x	x/xx	x			
		CL/O. S.	33-47	xx	xx	xxxxx	xxxxx	xxxxx	x/xx	xx	x	xx	xx	xx	xx	xx/xxx	x	x	x/xx	x			
	Humpy Ck.	C. O. S.	81-112	xxx	xx/xxxxx	xxx/xxxxx	xxxxx	xxxxx	x/xx	xx	x	xx	xx	xx	xx/xxx	x	x	x	x/xx	x			
Byfield	Brick Kiln Ramsay	O. S.	50-193	xx	xx	xxxxx	xxxxx	xxxxx	x/xx	xx	x/xx	xx	xx	xx/xxx	x	x	x	x	x/xx	x			
	Crossing	O. S.	25-179	xx/xxx	xx/xxx	xxxxx	xxxxx	xxxxx	x/xx	xx/xxx	x/xx	x/xx	x/xx	xx/xxx	x	x	x	x	x/xx	x			
Duaringa	Unit D	O. S.	29-62	xx/xxx	xx/xxx	xxx	xxx	xxx	xxx	xxx	x	x	x	x	x	x	x	x	x	x			
	Unit B	CL/O. S.	5-20	xxx/xxxxx	xxxx	xxx/xxx	xxx/xxx	xxx/xxx	xx	xxx/xxxx	x	xx	xx	xx	xx	xx	xx	xx	x	x			
	Unit A	O. S.	22-148	xxx	xxx/xxxxx	xxx/xxxxx	xxx/xxxxx	xxx/xxxxx	xx	xx/xxx	x	x/xx	x/xx	x/xx	x	x	x	x	x	x			
Condor	Unit TW4	C. O. S.	~ 80	xxxxx	xxxxx	xxxxx	xxxxx	xxxxx	xxxx	xxxx	xxxx	xxxx	xxxx	xxxx	xxxx	xxxx	xxxx	xxxx	xxxx	xxxx	xxxx	xxxx	xxxx
	Unit TW2	O. S.	~ 80	xxxxx	xxxxx	xxxxx	xxxxx	xxxxx	xx	xx	xx	xx	xx	xx	xx	xx	xx	xx	xx	xx	xx	xx	xx
Byfield	Unit TW4	C. O. S.	~ 80	xxxxx	xxxxx	xxxxx	xxxxx	xxxxx	xxxx	xxxx	xxxx	xxxx	xxxx	xxxx	xxxx	xxxx	xxxx	xxxx	xxxx	xxxx	xxxx	xxxx	xxxx
	Unit TW2	O. S.	~ 80	xxxxx	xxxxx	xxxxx	xxxxx	xxxxx	xx	xx	xx	xx	xx	xx	xx	xx	xx	xx	xx	xx	xx	xx	xx
Condor	B. O. S.	O. S.	25-104	xxxxx	xxxxx	xxx	xxx	xxx	xx	xx	xx	xx	xx	xx	xx	xx	xx	xx	xx	xx	xx	xx	xx
	B/B. O. S.	O. S.	29-46	xx/xxx	xx/xxx	xxx	xxx	xxx	xxxxx	xxxxx	xxxxx	xxxxx	xxxxx	xxxxx	xxxxx	xxxxx	xxxxx	xxxxx	xxxxx	xxxxx	xxxxx	xxxxx	xxxxx
Condor	B. O. S.	C. O. S.	29-46	xx	xx	xx/xxxx	xx/xxxx	xx/xxxx	xxxxx	xxxxx	xxxxx	xxxxx	xxxxx	xxxxx	xxxxx	xxxxx	xxxxx	xxxxx	xxxxx	xxxxx	xxxxx	xxxxx	xxxxx
	B/B. O. S.	C. O. S.	29-46	xx	xx	xx/xxxx	xx/xxxx	xx/xxxx	xxxxx	xxxxx	xxxxx	xxxxx	xxxxx	xxxxx	xxxxx	xxxxx	xxxxx	xxxxx	xxxxx	xxxxx	xxxxx	xxxxx	xxxxx

Reference: - O. S. - Oil Shale C. O. S. - Carbonaceous Oil Shale CL - Claystone
 +++++ Dominant, ++++ Co-dominant, +++ Sub-dominant (>20%), ++ Accessory (5-20%), + Trace (<5%).

TABLE III
ELEMENTAL ANALYSES, KEROGENS AND SHALE OILS; ATOMIC RATIOS H/C, O/C.

Deposit	Unit	Location	Fischer Assay Yield (LTOM)		Elemental Analysis (K=kerosen; O=oil)					Atomic Ratio		
					C	H	N	O	S	H/C	O/C	
Rundle	Kerosene Ck. O.S. Marker in Telegraph Ck.	Auger sample	High grade	K	74.4	9.0	2.0	13.7	0.9	1.45	0.138	
		RDD31 25m	Low grade (<40)	K	71.8	9.9	1.3	14.9	2.1	1.64	0.156	
	Munduran Ck.	RDD31 110.5m	High grade	K	70.9	8.3	1.9	17.4	1.5	1.40	0.184	
	Humpy Ck.	RDD43 80.5m	Medium grade	K	64.9	4.9	3.1	25.9	1.1	0.91	0.300	
	Brick Kiln	RDD31 161.0m	High grade	K	73.4	9.1	1.1	15.1	1.3	1.48	0.154	
	Brick Kiln	RDD25 111.0m	High grade	K	75.5	9.7	2.0	11.0	1.8	1.54	0.109	
	Ramsay Crossing	RDD41 67.5m	High grade	K	76.6	10.3	0.7	10.9	1.5	1.61	0.107	
		RDD41 85.0m	High grade	K	77.6	10.6	1.0	9.6	1.2	1.63	0.093	
		RDD41 99.2m	High grade	K	77.0	9.8	1.5	10.5	1.2	1.52	0.102	
	Stuart	Brick Kiln	SDD51 50- 52m	193	K	74.7	9.9	1.7	11.6	0.2	1.59	0.116
				O	85.4	12.8	0.9	0.7	0.2	1.80	0.006	
SDD51 62- 64m			76	K	72.3	8.6	1.2	17.8	0.3	1.43	0.118	
				O	84.7	13.0	1.0	0.9	0.4	1.84	0.008	
Byfield	TW ₄	BYD1 68- 70m	98	K	66.8	5.8	2.2	25.2	0.5	1.05	0.283	
		BYD1 84- 86m	83	K	67.9	5.7	2.1	23.5	0.8	1.00	0.260	
		BYD1 84- 86m	83	K	65.6	5.8	2.3	25.6	0.5	1.07	0.292	
				O	82.0	10.8	1.0	5.6	0.6	1.58	0.051	
			224-226m	Average grade	K	75.3	9.1	2.2	11.9	1.5	1.44	0.119
		BYD1 290-292m	73	K	72.5	9.2	2.2	14.0	?	1.52	0.144	
			O	84.7	11.8	1.2	1.7	0.6	1.67	0.015		
Duaringa	B	DD10 66- 68m	64	K	71.6	9.5	1.4	14.2	1.4	1.60	0.149	
				K	60.6	7.7	1.0	14.2	4.8	1.53	0.176	
				O	85.9	11.6	1.3	1.4	0.5	1.62	0.012	
		DD10 74- 76m	130	K	71.3	9.4	1.0	15.5	1.4	1.58	0.166	
				K	69.1	9.4	1.2	12.3	3.8	1.63	0.133	
				O	85.1	12.1	1.1	1.3	0.4	1.71	0.011	
		DD52 92- 94m	26	K	68.8	8.6	1.3	14.9	1.2	1.50	0.163	
				K	50.4	6.1	1.3	11.1	5.9	1.44	0.165	
		O	86.1	11.3	0.9	1.5	0.6	1.57	0.013			
	DD6 247.4m	Medium grade	K	78.3	10.0	1.7	9.5	0.5	1.54	0.091		
Condor	Brown Oil Shale	Auger sample	65-77	K	77.5	9.1	2.3	8.3	2.5	1.41	0.081	
		CDD1 380.1m	Average grade	K	72.9	9.0	2.8	9.1	0.4	1.38	0.087	
		CDD6 352-354m	66	K	70.0	8.2	1.9	9.4	4.2	1.41	0.101	
		CDD11 106-108m	82	K	70.2	7.9	1.9	15.1	5.1	1.34	0.161	
		CDD11 68- 70m	62	K	68.9	6.7	2.7	15.4	6.6	1.17	0.168	
		CDD26 308-310m	75	K	72.4	5.7	2.9	16.1	1.4	0.95	0.169	
Stuart	Brick Kiln	SDD51 36- 38m	172	O	85.8	12.3	0.8	0.7	0.4	1.72	0.006	
				O	85.3	12.6	1.1	0.5	0.5	1.77	0.004	
			92- 94m	75	O	85.6	12.3	1.2	0.3	0.5	1.73	0.003
			134-136m	38	O	85.6	12.3	1.2	0.3	0.5	1.73	0.003
Duaringa	B	27 Oils	Range 20-130	O	83.8	11.8	1.1	3.2	0.5	1.69	0.028	
Condor	Brown Oil Shale	18 samples		O	85.3	12.1	1.5	1.0	0.5	1.70	0.009	
				O	83.7	11.2	1.4	2.6	0.6	1.61	0.023	
		Carbonaceous	3	O	84.0	10.5	1.4	5.2	0.6	1.50	0.047	
			3	O	84.0	10.5	1.4	5.2	0.6	1.50	0.047	

This is consistent with the oils being derived primarily from the algal component of the oil shales. The oils derived from the carbonaceous units differ from those derived from lamossites. The carbonaceous units yield oil with a higher heteroatom component, indicating presence of vitrinite or kerogen sourced from higher forms of plant life. The higher aromatic or unsaturates content in oils from carbonaceous units is also supported by a lower oil yield per unit kerogen content as observed by Eckstrom et al. (8).

DEPOSITIONAL ENVIRONMENT

All Tertiary sedimentary basins considered contain a substantial proportion by volume of clastic rocks devoid of organic content. Such units typically contain bioturbated, sandy and silty claystones with reddish and brownish coloring. At Duaringa these units are interbedded with oil shales. In the other deposits, low grade or barren interbeds do not display oxidation colors. It seems that once the conditions supporting growth of plant organisms was established, the regime continued, although variation took place in the amount and type of vegetal matter contributed and preserved in the accumulating deposits. Such variations occur with greater frequency in The Narrows Graben (as shown by numerous carbonaceous horizons interbedded in the lamossite sequence) and cyclicity in this sequence has already been referred to. At Condor, once the lignin-like material was supplemented by the lamellar alginite dominant in the brown oil shale, conditions remained relatively unchanged until several hundred meters of sediment accumulated.

While the evidence (fossils, sediment type, stratification) supports a lacustrine environment for all the deposits, the monotonous sequence at Condor is unique. At Condor, a stratified lake system similar to that proposed by Smith and Lee (9) for density stratification in the Piceance Creek Basin may have developed.

There may be a combination of circumstances in the Queensland Tertiary lakes (sedimentation rate, supply and range of organic matter, water depth, etc.) from which a regional model can be deduced. The relationship of time, climate, provenance and preservation of this energy resource is a topic for much further study and research.

ACKNOWLEDGMENTS

Preparation of a general paper of this nature is only possible from the compilation of effort by many people, from the geologists who have logged core and painstakingly noted unusual features in what commonly appears as a monotonous sequence, to the petrologists and chemists who have dissected and identified the organic and inorganic components usually present in extremely minute particle size. Comments, suggestions and criticisms have particularly been appreciated from John Gannon, John Best and David Henstridge. Permission by the boards and management of Southern Pacific Petroleum and Central Pacific Minerals to produce this paper is gratefully acknowledged.

LITERATURE CITED

- (1) Lindner, A. W. and Dixon, D. A., Australian Petroleum Exploration Assoc., (APEA) Journal, 16, 165 (1976).
- (2) Henstridge, D. A. and Missen, D. D., AAPG Bull, 66, 719 (1982).
- (3) Neale, R. C. and Coshell, L., in "Black Shales and Oil Shales in Australia", Search, 13, 125 (1982).
- (4) Green, P. W. and Bateman, R., APEA Journal, 21, 24 (1981).
- (5) Loughnan, F. C., Roberts, F. E. and Lindner, A. W., "Buddingtonite in the Condor Oilshale Deposit, Queensland, Australia" (in press).
- (6) Hutton, A. C., Kanstler, A. J., Cook, A. C. and McKirdy, D. M., APEA Journal, 20, 44 (1980).
- (7) Tissot, B. P. and Welte, D. H., "Petroleum Formation and Occurrence", Springer-Verlag, Berlin (1978).
- (8) Eckstrom, H., Hurst, H. J. and Randall, C. H., "Aspects of the Chemical and Retorting Properties of Selected Australian Oil Shales", (this symposium).
- (9) Smith, J. W. and Lee, K. K., 15th Oil Shale Symp. Proc., 111 (in press) (1982).

SYMPOSIUM ON GEOCHEMISTRY AND CHEMISTRY OF OIL SHALE
PRESENTED BEFORE THE DIVISIONS OF FUEL CHEMISTRY, GEOCHEMISTRY
AND PETROLEUM CHEMISTRY, INC.
AMERICAN CHEMICAL SOCIETY
SEATTLE MEETING, MARCH 20-25, 1983

GEOCHEMISTRY OF ISRAELI OIL SHALES - A REVIEW

By

M. Shirav (Schwartz) and D. Ginzburg
Geological Survey of Israel, 30 Malkhe Yisrael St., Jerusalem 95501, Israel

INTRODUCTION

The oil shales in Israel are widely distributed throughout the country (Figure 1). Outcrops are rare and the information is based on boreholes data. The oil shale sequence is of Upper-Campanian - Maastrichtian age and belongs to the Chareb Formation (Figure 2). In places, part of the phosphorite layer below the oil shales (Mishash Formation, Figure 2) is also rich in kerogen. The host rocks are biomicritic limestones and marls, in which the organic matter is generally homogeneously and finely dispersed. The occurrence of authigenic feldspar and the preservation of the organic matter (up to 26% of the total rock) indicate euxinic hypersaline conditions which prevailed in the relative closed basins of deposition during the Maastrichtian (1).

Current reserves of oil shales in Israel are about 3,500 million tons (2, 3), located in the following deposits (Figure 1): Zin, Oron, Ef'e, Hartuv and Nabi-Musa. The 'En Bokek deposit, although thoroughly investigated, is of limited reserves and is not considered for future exploitation. Other potential areas, in the Northern Negev and along the Coastal Plain are under investigation.

Future successful utilization of the Israeli oil shales, either by fluidized-bed combustion or by retorting will contribute to the state's energy balance.

CHEMISTRY

Typical analyses of Israeli oil shales are shown in Table I.

TABLE I
CHEMICAL ANALYSES OF OIL SHALE SAMPLES (WT %)

	Ef'e Bor. 1	Ef'e Bor. 1	Hartuv Bor. HRB	Hartuv Bor. HRB
	18-22m	60-70m	62-82m	130-150
SiO ₂	16.9	7.6	7.5	5.0
Al ₂ O ₃	6.8	1.5	1.61	1.32
TiO ₂	0.32	0.16	0.1	0.1
Fe ₂ O ₃	2.8	0.7	1.01	0.57
CaO	34.2	36.1	37.7	38.2
MgO	0.57	0.58	1.67	0.39
Na ₂ O	0.27	0.20	0.14	0.10
K ₂ O	0.42	0.32	0.15	0.14
P ₂ O ₅	1.6	3.5	3.0	2.3
SO ₃	2.3	0.9	0.3	0.26
S (Org)	1.4	2.7	1.7	2.4
Org. Mat.	8.2	24.1	14.8	20.5
L. O. I	33.5	45.7	44.0	49.6

One borehole in the Ef'e deposit, T1, coord. 1167/0544 (Israel Grid) was analyzed meter by meter; the correlation factors between the variables are summed up in Figure 3.

SiO₂ content is 2-14 wt %. The significant correlation with Al₂O₃ and Fe₂O₃ indicate its residence in clay minerals. Free silica, in the form of quartz grains is rare.

CaO (30-40 wt %) constitutes calcite (50-70% of the total rock). Little amounts of CaO are located in apatite and gypsum.

Al₂O₃ is a main component in clay minerals. Al₂O₃ is highly correlative with SiO₂, Fe₂O₃ and TiO₂. The content of Al₂O₃ along the oil shale sequence is 1-7 wt %.

Fe₂O₃ content is 0.5-2 wt % and it is located in clay minerals and pyrite.

Sulfur is shown on Figure 3 as SO₃, which includes organic and inorganic sulfur. Direct observations and isotopic composition of sulfur (4) indicate that kerogen-bound sulfur accounts for 60-80% of the total sulfur in the rock while the remainder is pyritic and gypsum sulfur.

P₂O₅ content within the oil shale is 1-5 wt %, while in the phosphorous Mishash Formation it may exceed 30%.

Organic matter (kerogen) composes 5-26 wt % of the rock. The average content of organic matter in Israeli deposits is 14-16 wt %. Only rocks with more than 10% organic matter, are considered as "economic" oil shales.

Depth shows significant positive correlation with the following variables: organic matter, SO₃, P₂O₅ and negative correlation with Al₂O₃, Fe₂O₃ and SiO₂. As Al, Si and Fe are dependent upon clay content, it is clear that the amount of clay decreases with depth. Organic matter, SO₃ (the part included in organic matter and in gypsum) and P₂O₅ contents increase with depth. Thus, these data represent a mineralogical system of four main variables, changing with geological time (=depth) (Figure 2). The 4 main mineralogical phases are: carbonate, clay minerals (mainly montmorillonite and kaolinite), apatite and organic matter. Other minor constituents are pyrite, gypsum, quartz and feldspar. This system is one clue to the understanding of the paleogeographical set-up during the Maastrichtian in Israel, as well as a main factor for any assessment of oil shale's quality.

Effect of CaCO₃ on Combustion

Fluidized bed technology seems to be preferable for oil shale combustion (5). Series of combustion tests which were run in different temperatures resulted in lower effective calorific value with the increase of operating temperature. Figure 4 shows a DTA curve for a typical Israeli shale. When operating the fluidized bed in the range of 700-800 °C endothermic reactions are only in their beginning, but if the operating temperature exceeds 800-850°C, the endothermic reaction of calcite decomposition has a severe influence on the effective calorific value. Fluidized beds burning coal use a certain amount of carbonate for SO₃ trapping, but in this case more than 60% of the material which is fed to the burner is carbonate. Thus, the necessity of maintaining delicately-controlled conditions during combustion is a direct outcome of the inorganic composition of the oil shale.

CALORIFIC VALUE

The high calorific value of the oil shale was determined by a "bomb" calorimeter on more than 50 composite samples from different deposits and on one-meter samples along borehole sections. The average value is 1000Kcal/Kg and the highest value measured was 1790Kcal/Kg. The correlation between organic matter content to the high calorific value is more than significant (R=0.96). The equation for the Ef'e deposit is:

a) calorific value = 77.8 + 60.2 (org. matter wt %)

and for the Hartuv deposit

b) calorific value = 52.0 + 71.3 (org. matter wt %)

The line for the Hartuv deposit is steeper than that for the Ef'e deposit (Figure 5) i. e.: in the range of 14 wt % organic matter (average for most of the deposits) the difference will be 120Kcal/Kg in favor of the Hartuv deposit. As the overall inorganic composition is similar in the two deposits, we assume that the reason for this difference is due to compositional variations within the organic matter.

FISCHER ASSAY

Fischer assay tests were carried out on several boreholes in the Ef'e deposit (6). The average yield was 15.6 Gal/Ton; sections with high content of organic matter (20-26 wt %) yielded

up to 29 Gal/Ton. Evidently, there is a positive correlation between Fischer assay and the content of organic matter; another interesting relation is illustrated in Figure 6. With the increase of depth, more oil is yielded per wt % of organic matter. The data in Table II suggest that this phenomenon may be related to changes in the elemental composition of the oil shale and/or to the content of bituminous fraction within the organic matter.

TABLE II
ULTIMATE ANALYSES AND OIL YIELD

<u>Sample No.</u>	<u>Org. C %</u>	<u>H %</u>	<u>N %</u>	<u>S %</u>	<u>Oil, Gal/Ton</u>	<u>% Bitumen of TOM</u>
SRV208	7.8	1.28	0.29	2.4	11.9	6.8
SRV215	10.1	1.56	0.35	3.0	16.5	7.1
SRV221	13.6	1.76	0.54	3.1	24.2	7.8

TOM = Total Organic Matter

The average composition of kerogen from the Ef'e deposit is:

C-64.9% H-8.0% N-2.8% S-9.1%

The average composition of retorted oil from the Ef'e deposit is:

C-79.8% H-10.1% N-1.1% S-7.6%

TRACE ELEMENTS

Table III summarizes trace elements concentration data in the oil shale sequence of the Ef'e deposit, the phosphorite layer from the same area (7) and the Green River oil shale (8).

TABLE III
TRACE ELEMENTS DATA (PPM)

	<u>Ef'e 1</u>	<u>Ef'e 2</u>	<u>Phosphate</u>	<u>Green River</u>
Ba	250	200	500	N. D.
Cr	430	450	200	49
Cu	95	100	25	15
Li	17	17	N. D.	850
Mn	30	35	40	34
Ni	125	135	70	11
Rb	10	5	4	29
V	70	75	170	29
Pb	17	35	N. D.	N. D.
Y	34	11	83	1.2
Zn	160	175	430	13
Zr	38	50	N. D.	9.3
U	20	40	150	1

N. D. = not determined

The Ef'e oil shale has higher concentrations of trace elements than the Green River oil shale (except for Li). Concentration of those elements which occur in apatite (7) - V, Zn, Y, U - are much higher in the phosphorite layers. Ni and Cu are correlative with the Fe₂O₃ content (not shown in the Table) suggesting their occurrence in association with pyrite or as an independent phase. Generally, there is not any evidence for an accumulation of trace elements as a result of high concentrations of organic matter.

SUMMARY

The Israeli oil shales may be considered as a multi-variable system, in which the main components influencing their quality are organic matter, carbonate, clay minerals and apatite. As

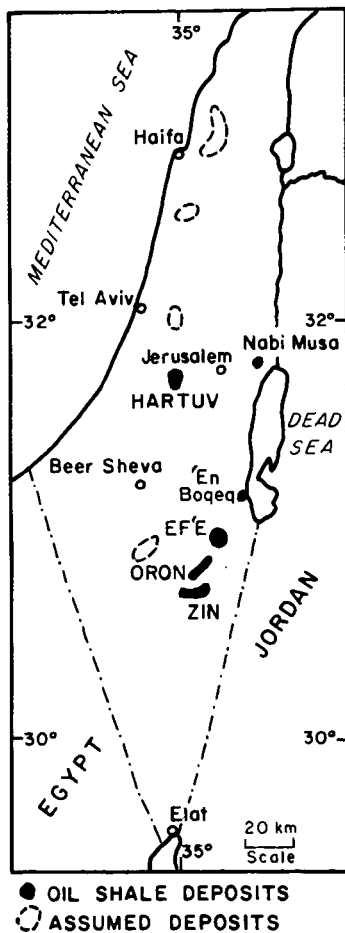
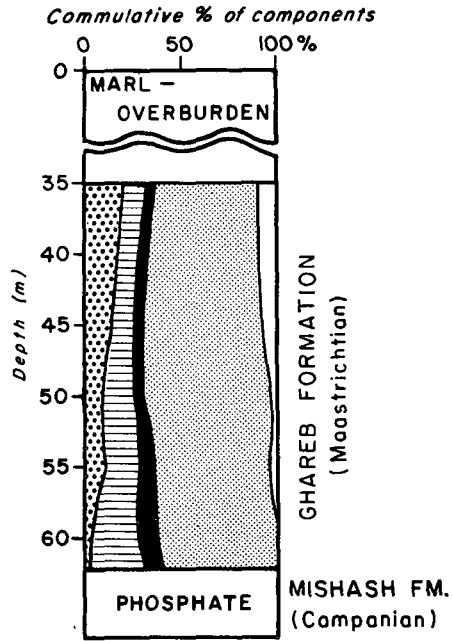


Figure 1. Location Map



LEGEND

-  Clay minerals
-  Organic matter
-  Apatite
-  Calcite
-  Others (Pyrite, gypsum, dolomite)

Figure 2. Mineralogical log (Bor. Ti)

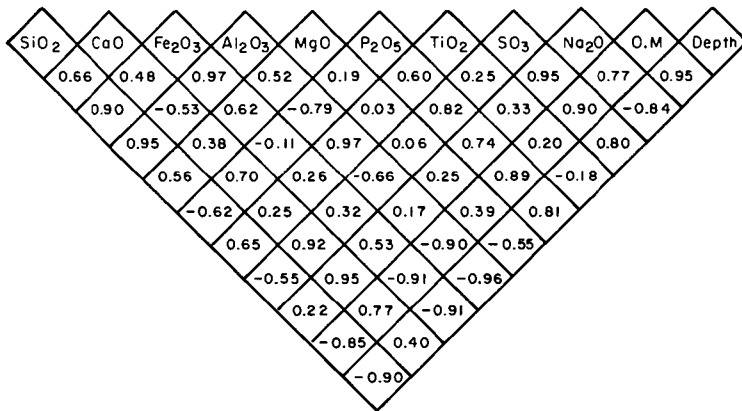


Figure 3. Correlation factors for chemical analyses of samples from Borehole T1, Efe deposit (O.M=Organic Matter)

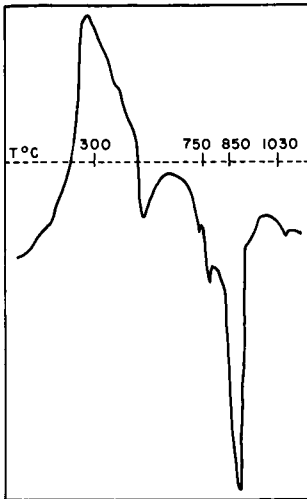


Figure 4. DTA curve for sample HRB-3a

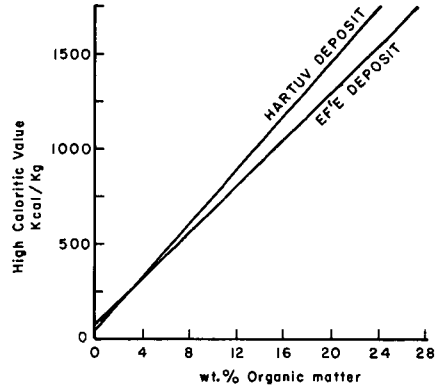


Figure 5. Correlation between organic matter content and high calorific value (Ef'e and Hartub deposits)

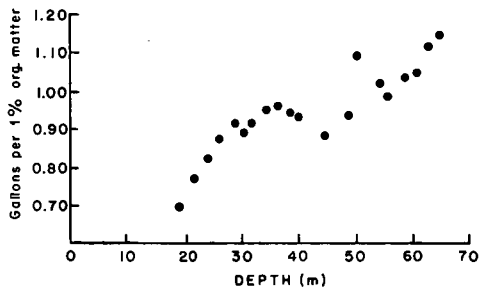


Figure 6. Oil yield per 1 wt % of organic matter as a function of depth (Borehole Bit1, Ef'e)

the percentage of these components varies over the vertical section, depth also plays a significant role whenever a quality assessment of the shale is done. Compositional variations within the organic matter are responsible for changes in the relative calorific value and retorted oil yield while fluidized bed combustion is affected by the inorganic components.

LITERATURE CITED

- (1) Shirav (Schwartz), M. and Ginzburg, D., "Distribution and Depositonal Environment of the Oil Shale Deposits in Israel", 10th Intl. Cong. on Sedimentology, Jerusalem, Israel. Abstracts Vol. II, pp. 601-602 (1978).
- (2) Shirav (Schwartz), M. and Ginzburg, D., "A Guidebook to the Oil Shale Deposits in Israel", Int. Symp. on Oil Shale Chem. and Tech., Jerusalem, Israel, 32 pp. (1978).
- (3) Shirav (Schwartz), M. and Ginzburg, D., "A New Oil Shale Deposit in the Hartuv-Zora' Region, GSI Rep. No. MP 597/80, 15 pp. (1980).
- (4) Dinur, D., Spiro, B. and Aizenshtat, Z., "The Distribution and Isotopic Composition of Sulfur in Organic-Rich Sedimentary Rocks", Chem. Geol. 31, 11. 37-51 (1980).
- (5) Wohlfarth, A., Dibner, I., Keren, Y. and Berkovitz, Y., "Combustion of Oil Shale for Industrial Steam Production", Intl. Symp. on Oil Shale Chem. and Tech., Jerusalem, Israel, Abstract (1978).
- (6) TOSCO Corp., "Efe Oil Shale Deposit", Int. Rep. (1975).
- (7) Nathan, Y., Shiloni, Y., Roded, R., Gal, I. and Deutch, Y., "The Geochemistry of the Northern and Central Negev Phosphorite (Southern Israel)", GSI Bull. No. 73, 41 pp. (1979).
- (8) Cook, E. W., "Elemental Abundances in Green River, Oil Shale Chem. Geol. 11, pp. 321-324 (1973).

SYMPOSIUM ON GEOCHEMISTRY AND CHEMISTRY OF OIL SHALE
PRESENTED BEFORE THE DIVISIONS OF FUEL CHEMISTRY, GEOCHEMISTRY,
AND PETROLEUM CHEMISTRY, INC.
AMERICAN CHEMICAL SOCIETY
SEATTLE MEETING, MARCH 20 - MARCH 25, 1983

GEOCHEMISTRY OF BRAZILIAN OIL SHALES

By

C. Costa Neto
Instituto de Química, Universidade Federal do Rio de Janeiro,
Rio de Janeiro, Brasil

ABSTRACT

A general survey of the main Brazilian oil shale formations presenting their location, oil reserve, age and stratigraphy introduces this paper. It is followed by a comparative survey of the data on chemical composition (elementary, minerals and organic constituents/biological markers) and of thermal alteration indexes in order to define their maturity. The geochemical phenomena involved with a large diabase intrusion in the Irati formation is particularly stressed. The analytical methods of Solid Phase Extraction and Functional Group Marker developed for the analysis of bitumens and kerogens and the results obtained from the application of these methods to Brazilian oil shales are discussed. The paper ends with a brief description of a comprehensive analytical bibliography on Brazilian oil shales prepared to serve as a data base for these organites.

SYMPOSIUM ON GEOCHEMISTRY AND CHEMISTRY OF OIL SHALE
PRESENTED BEFORE THE DIVISIONS OF FUEL CHEMISTRY, GEOCHEMISTRY,
AND PETROLEUM CHEMISTRY, INC.
AMERICAN CHEMICAL SOCIETY
SEATTLE MEETING, MARCH 20 - MARCH 25, 1983

COMPARATIVE ORGANIC GEOCHEMISTRY OF SOME EUROPEAN OIL SHALES

By

A. G. Douglas and P. B. Hall
Organic Geochemistry Unit, Geology Department, The University,
Newcastle upon Tyne, England, NE1 7RU
and
H. Solli
Continental Shelf Institute, Hakon Magnussons Gt.1B, 7001 Trondheim, Norway

The distribution, and geology, of oil shales occurring in Western Europe was described in a substantial paper by Bitterli (1) and briefly in a later paper by Schlatter (2). The interest of the former author was principally the location, depositional environments, mineralogy and organic carbon content of a very large number of bituminous sediments, and he proposed a classification which divided the bituminous rocks into seven categories. Although, in this work, we have followed Bitterli to some extent in the locations from which our samples were collected we have, for convenience, considered Duncan's (3) classification of three main oil shale lithologies. Although there were two major periods of European oil shale formation, namely deposits of Permo-Carboniferous age which are associated, in part, with coal sequences, and Jurassic deposits often of marine origin, the work undertaken in this laboratory has covered eighty samples from twenty deposits ranging in age from Cambrian to Oligocene. These may be divided, using Duncan's classification into a) those believed to have been deposited in shallow marine basins (Cambrian, Sweden; Permian, England; Lower, middle and upper Jurassic, Scotland/England; Oligocene, France), b) those deposited in large Lacustrine basins (Devonian, Scotland; Carboniferous, Scotland; Permian, France), and c) those deposited in small lagoonal basins, often associated with coal swamp environments (Carboniferous, Scotland; middle Jurassic, Scotland; Tertiary, Germany).

The types of analyses of these oil shales, which have been carried out by us include, *inter alia*, microscopical observation and maceral point count, vitrinite reflectance and spore fluorescence, oil assay using a simple mini Fischer-type retort followed by chromatographic analyses of some of the shale-oils, Rock Eval pyrolysis, organic carbon content, extractable bitumens and analyses of the contained hydrocarbons. Elemental analyses, pyrolysis gas chromatography and pyrolysis gas chromatography-mass spectrometry was achieved on some isolated kerogens.

This overview, which will hopefully provide some ground work for further investigations, has given some of the results which follow. Total organic carbon values varied widely: for instance, Devonian shales from N. Scotland had a maximum of 5% whereas in the Carboniferous shales of the Midland valley (Scotland) they ranged to 25% and to very high values in the torbanite-rich shales. The values for organic carbon in the Permian (Autun) samples ranged from 7-18%, lower and middle Jurassic figures ranged from 2% to 15% with the Brora Parrot Shale having the exceptionally high value of 32%. Upper Jurassic (Kimmeridgian) values ranged from 7% to 38%. Soluble bitumens were extracted from the rocks giving values ranging from traces to 3% with aliphatic/aromatic ratios varying from 0.06 to 3.90: in some instances unsaturated hydrocarbons formed the major fraction of the aliphatic fraction. Analysis of the saturated hydrocarbons by molecular sieve separation followed by GC and GC-MS indicate wide variations in distributions, and types, of compounds. Normal alkane distributions vary, as reflected in carbon preference indices, which range from less than 1.0 to 2.5 (exceptionally 6.0) with maxima indicating algal and higher plant contributions to the sediment. Steranes and triterpanes are ubiquitous with the former appearing to be more abundant in marine deposits and the latter in lake basin deposits. In certain of the samples from Autun (France) and Caithness (Scotland), which represent large lacustrine deposits, carotane and C₁₃ to C₂₄ alkyl substituted trimethylcyclohexanes, which are possibly degradation products of carotenoids, were identified by Hall and Douglas (4). Kovats retention indices for almost 70 cyclic compounds including the above, together with hopanes, diasteranes, and regular and nuclear methylated steranes were measured in many of the samples and provide useful data to help in identifications.

Oil assays were obtained using small samples in a simple laboratory-constructed apparatus and indicated that shale oil yields ranging from 2 to 300 liters/tonne could be expected. Twelve of the shale oils were then separated to provide trans- and terminal alkene fractions, together with

saturated hydrocarbons. Yields of saturated hydrocarbons varied from 3% to 23%, of terminal alkenes from 4% to 21% and possibly trans-alkenes from 2% to 16%. In all of the oils there was a large fraction (from 35% to 85%) which was more polar than the terminal alkenes on Ag⁺ thin layer chromatography and presumably represented aromatic, heterocyclic and other polar compounds. Gas chromatographic analyses revealed principally homologies of the aliphatic hydrocarbons noted above: few firm conclusions can be drawn from these analysis although in general it appeared that marine sediments provided mainly normal hydrocarbon homologies superposed on a large unresolved 'hump', whereas non-marine sediments produced extended homologies on a less pronounced 'hump' of unresolved material.

Pyrolysis gas chromatography (and gas chromatography-mass spectrometry) indicates that oil shale kerogens can produce fingerprints that allows some measure of 'typing' the oil shales (5). Algal kerogens, with a substantial contribution from *Botryococcus braunii*, provided easily recognized programs in which the predominant feature is a homology of alkanes, -enes and -dienes: in some marine kerogens the triplet homology is much less predominant than are aromatic molecules. An attempt to use aliphatic/aromatic ratios in typing kerogens has already been made (6).

LITERATURE CITED

- (1) Bitterli, P., *Geol. en Mijnb.*, **42**, 183 (1963).
- (2) Schlatter, L. E., in "The Exploration for Petroleum in Europe and North Africa", Instit. of Petroleum, London, 251 (1969).
- (3) Duncan, D. C., in "Oil Shale", eds. T. F. Yen and G. V. Chilingarian, Elsevier, Amsterdam, 13 (1976).
- (4) Hall, P. B., and Douglas, A. G., in "Advances in Organic Geochemistry", 1981, eds. M. Bjoroy et al., Heyden, London. In press.
- (5) Larter, S. R., and Douglas, A. G., *J. Anal. Appl. Pyrol.*, **4**, 1 (1982).
- (6) Larter, S. R., and Douglas, A. G., in "Advances in Organic Geochemistry", 1979, eds. A. G. Douglas, and J. R. Maxwell, Pergamon, London, 579 (1980).

SYMPOSIUM ON GEOCHEMISTRY AND CHEMISTRY OF OIL SHALE
PRESENTED BEFORE THE DIVISIONS OF FUEL CHEMISTRY, GEOCHEMISTRY
AND PETROLEUM CHEMISTRY, INC.
AMERICAN CHEMICAL SOCIETY

GEO-LIPIDS IN THE OIL SHALE FROM ALEKSINAC (YUGOSLAVIA)

By

D. Vitorović and Mirjana Šaban

Department of Chemistry, University of Belgrade, P. O. Box 550, 11001 Belgrade, Yugoslavia

INTRODUCTION

The oil shale from Aleksinac (Yugoslavia) is a lacustrine sediment of Miocene age. Both the soluble portion of the organic matter (the bitumen) and the insoluble kerogen of this shale were studied extensively. In this paper, isolation and identification of various types of geolipids from the Aleksinac shale, carried out in the last few years, will be reviewed. A thorough examination of the bitumen was expected to give additional data on the origin of the organic matter as well as on the sedimentation conditions and postburial changes.

EXPERIMENTAL PROCEDURES

The shale sample contained 20.4% organic matter (1). It was powdered to -100 mesh (Tyler). In most cases, the bitumen was isolated by 100 h Soxhlet extraction either with benzene or with a mixture of benzene and methanol (1:1).

Various schemes for isolation of different fractions and various separation techniques were used, such as the usual chemical method, chromatographic techniques, molecular sieving and clathration.

Identifications were made by gas chromatography involving coinjection of internal standards, or by a system of gas chromatograph, mass spectrometer and computer.

RESULTS AND DISCUSSION

The yields of the benzene- and benzene-methanol bitumens were 1.25% and 4.27%, respectively. The bitumens consisted mainly of neutral components (Table I).

TABLE I
COMPOSITION OF THE BITUMEN

<u>Constituents</u>	<u>% of the benzene-bitumen</u>	<u>% of the benzene- methanol bitumen</u>
Neutral	81.36	53.48
Acids	6.51	31.46
Phenols	7.28	8.18
Basic	0.21	0.17

n-Alkanes

The n-alkane fraction was found to consist of a C₁₃-C₃₇ homologous series (Figure 1) with a predominance of odd-carbon-numbered members in the C₂₅-C₃₇ range (2). The CPI was 1.46 and 1.75, for the n-alkanes from the benzene- and benzene-methanol bitumen, respectively, indicating that the organic matter of Aleksinac shale was non-mature.

Branched Alkanes

Phytane and pristane, with a dominance of phytane over pristane, were found in considerable amounts. The dominance of phytane over pristane indicated a higher plant's origin of the organic matter of this sediment. Other aliphatic isoprenoid alkanes; C₁₅ (farnesane), C₁₆ and C₁₈ were also identified in the thiourea adduct. In the thiourea adduct of the branched-cyclic fraction, a C₁₈-C₂₈ series of iso- or anteiso-alkanes was suggested by gas chromatography involving coinjection of five standards of iso-alkanes. Two unidentified homologous series containing 7 and 9 members were also found in the thiourea adduct of the branched-cyclic fraction.

Cyclic Alkanes

In the cyclic fraction, the following polycyclic isoprenoid compounds were identified: C₂₇-C₂₉ steranes, methyl-C₂₉ sterane, C₂₇-C₃₂ pentacyclic triterpanes of hopane and lupane type (except C₂₈) and the bicyclic tetraterpane perhydro- β -carotane (Table II).

TABLE II

ISOPRENOID ALKANES IDENTIFIED IN THE ALEKSINAC SHALE BITUMEN

Aliphatic	C ₁₅	C ₁₆	C ₁₈	C ₁₉	C ₂₀		
Steranes	C ₂₇	C ₂₈	C ₂₈	C ₂₉	C ₂₉	C ₂₉	
5 H	α	$\alpha+\beta$?	α	α	α	
14 H	$\alpha+\beta$	β	$\alpha+\beta$	β	$\alpha+\beta$	α	
Triterpanes	C ₂₇	C ₂₇	C ₂₉	C ₂₉	C ₃₀ (4)*	C ₃₁ (3)*	C ₃₂
17 H	α	?	α	?	?	?	α

* Number of isomers

All these compounds have already been known as bitumen constituents of other shales. However, the identified steranes suggest a higher plant's origin of one part of the organic matter of Aleksinac shale. On the other hand, a certain number of identified triterpanes of hopane type may have originated from lower procaryotic organisms in which hopane oxygen compounds were identified lately (3). On the basis of the presence of thermodynamically stable stereoisomers of steranes and triterpanes, nonspecific for biological molecules, such as 14 β H holestane, ergostane and sitostane, 17 α H, 21 β H norhopane and bishomohopane, it is possible to speculate on diagenetic and maturation changes of the organic matter of Aleksinac shale.

Aromatic Hydrocarbons

A few classes of aromatic hydrocarbons were isolated and identified (4): C_nH_{2n-14} (bi-phenyls) and C_nH_{2n-18} (anthracenes and/or phenanthrenes). These aromatic hydrocarbons are presumably products of diagenetic changes characteristic for most ancient sediments.

Aliphatic and Aromatic Acids

A review of various acids identified in the Aleksinac shale is given in Table III. It is obvious that similar types of aliphatic acids were found in benzene- and benzene-methanol bitumen as well as in the extract of demineralized shale and in kerogen hydrolysis product. The only difference was in the range of the members in the homologous series. The list of acids isolated from aqueous extract of the shale is given for comparison (5).

Fatty Acid Methyl Esters

In one of the polar fractions of the benzene-bitumen, methyl esters of fatty acids (C₄-C₂₅) were isolated and identified by high resolution mass spectrometry (4). As far as we know, fatty acid methyl esters had not been found earlier as biolipids or geolipids. If their existence in various shale bitumens should be confirmed, their appearance could be explained either by diagenetic transformation of some precursor biological aliphatic molecules, or they might originate from biolipids so far unknown.

Aliphatic γ - and δ -Lactones

One of the most interesting findings in one of our first investigations of the acidic fraction (6) was the identification of a homologous C₇-C₁₅ series of γ -lactones in this fraction (Figure 2). It was a surprise to find a homologous series of components whose mass spectra had only one significant peak at m/z 85 (Figure 3).

The finding of γ -lactones in the bitumen of Aleksinac shale added a new structural type to the organic compounds found in geological specimens. However, the question was posed whether γ -lactones were indigenous to the organic matter of the shale and appeared in the acidic fraction from the base hydrolysis and subsequent acidification, or perhaps were produced, also during the isolation procedure, from precursors, such as the corresponding 4-hydroxy-acids of Δ -3 or Δ -4 unsaturated carboxylic acids.

Therefore, in another experiment (7), the neutral fraction was isolated by a careful procedure (extraction of bitumen at room temperature and isolation of acids by weak alkali) to avoid the formation of γ -lactones during the Soxhlet extraction of the bitumen and the possible hydrolysis of γ -lactones. Since in this experiment γ -lactones were isolated in relatively high yields, 0.41% and

0.34% relative to the benzene- and benzene-methanol bitumen, respectively, it was proved that they were indigenous to the organic matter of the shale.

Samma-lactones are quite prevalent in biolipids and in microbiological transformation products. Any of these may be the source of γ -lactones. Hydroxy-acids and unsaturated acids may also be the source of γ -lactones in Aleksinac shale. If γ -lactones would be found typical for certain class of sediments, they might shed more light on the source of the organic matter of these sediments.

In addition to γ -lactones, δ -lactones were also added to the organic compounds found in geological samples (8). Mass spectrometric identification of δ -lactones was based on the fragmentation ion m/z 99. However, they were present in very small quantities and their molecular ions in the mass spectra were not particularly pronounced so that it was not possible to establish with certainty which members of the 4-member homologous series were present.

TABLE III

ACIDS IDENTIFIED IN THE ALEKSINAC OIL SHALE

Products identified	Free acids extracted with		Bound acids	
	Water plus acidification (raw shale and bitumen-free shale)	Benzene and benzene-methanol (raw shale)	Kerogen (hydrolysis)	Entrapped (after removal of mineral part)
<u>Aliphatic acids</u>				
<u>Sat. unbranched</u>				
Monocarboxylic	--	C ₆ -C ₁₂	C ₆ -C ₃₃	C ₅ -C ₃₂
Dicarboxylic	C ₆ -C ₁₅	C ₇ -C ₁₈	C ₃ -C ₃₀	C ₃ -C ₂₈
<u>Aromatic acids</u>				
Monocarboxylic	Benzoic Methoxy-benzoic Me-hydroxy-benzoic Hydroxy-benzoic Me-naphthoic	Benzoic Me-benzoic (2)* di-Me-benzoic (4) tri-Me-benzoic Hydroxy-benzoic (2) Methoxy-benzoic Naphthoic (2) Me-naphthoic	Benzoic Me-benzoic	
Dicarboxylic	Benzene (2) Me-benzene Hydroxy-benzene Me-hydroxy-benzene Naphthalene (2)	Benzene Me-benzene (2) Naphthalene		
Tricarboxylic	Benzene (3) Naphthalene (4)	Benzene		

* Numbers in parentheses indicate the number of isomers

Cyclic γ -Lactones

Two cyclic γ -lactones were identified, i. e. γ -lactones of 6-hydroxy-2,2,6-trimethyl-cyclohexylidene acetic acid (dihydroactinidiolide) and 6-hydroxy-2,2,6-trimethyl-cyclohexyl acetic acid (tetrahydro-actinidiolide). Figures 4 and 5 show a comparison of mass spectra obtained with reference spectra of authentic compounds from the literature (8).

It may be supposed that cyclic γ -lactones were formed by lactonization of acids which might represent intermediates in a bacterial or abiogenic oxidation of carotenoids into naphthenic acids. Corresponding acids were isolated from a Californian petroleum and it was assumed that they were formed by oxidation of β -carotene (9).

Other Polar Constituents

Several other compound types were identified in the polar fraction. In addition to isoprenoid ketones 6,10-dimethyl-undecan-2-one (C₁₃) and 6,10,14-trimethyl-pentadecan-2-one (C₁₈), which were not a novelty in the chemistry of geolipids, C₁₃-C₂₄ aliphatic methyl ketones and the triterpenoid ketone adiantone were identified (4).

As far as we know, aliphatic methyl ketones as such were unknown as biolipid constituents. It may, therefore, be assumed that the aliphatic methyl ketones found in the Aleksinac shale bitumen

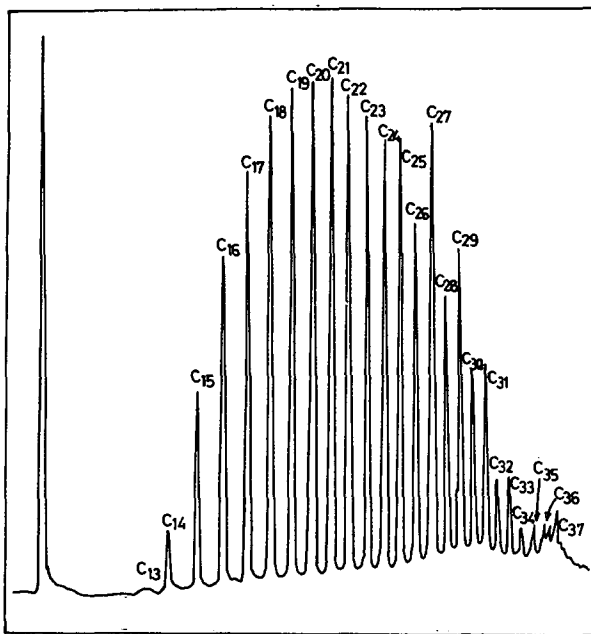


FIGURE 1. - Chromatogram of the n-Alkane Fraction of the Benzene-Bitumen.

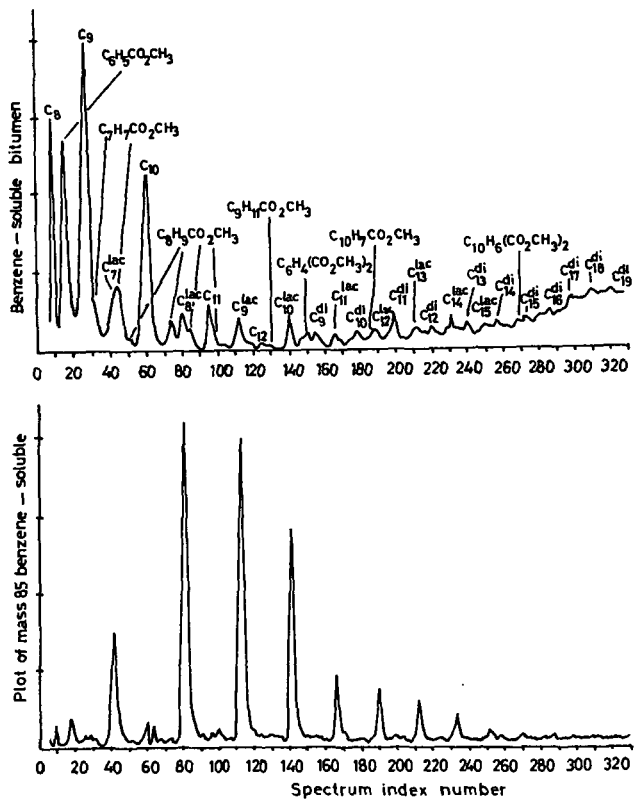


FIGURE 2. - Total Ionization Plot and Plot of Mass 85 for the Benzene Soluble Bitumen.

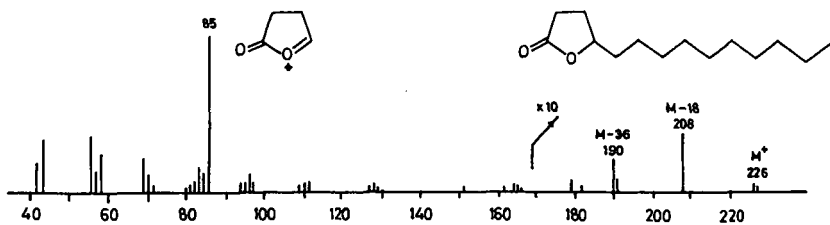


FIGURE 3. - Mass Spectrum Recorded During the GC-MS Analysis of the Lactone Mixture.

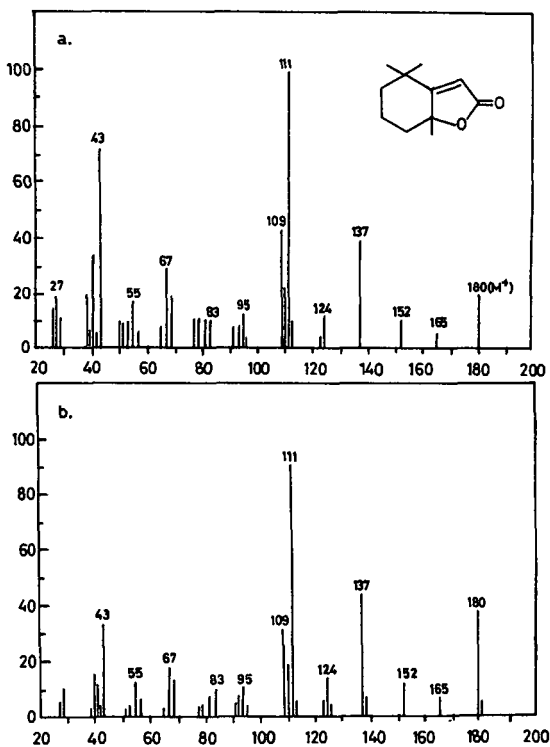


FIGURE 4. - Mass Spectrum of Authentic Dihydroactinidiolide (a) and Mass Spectrum 5 Recorded During the GC-MS Analysis of the Lactone Mixture (b).

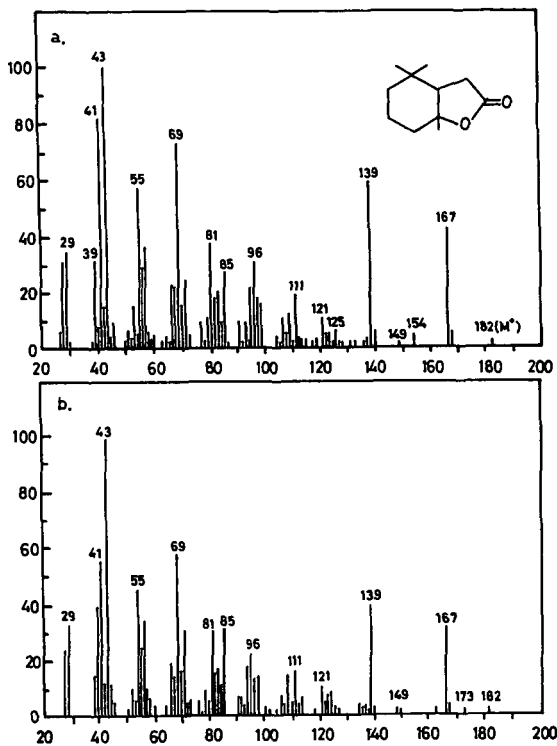


FIGURE 5.—Mass Spectrum of Authentic Tetrahydroactinidiolide (a) and Mass Spectrum ? Recorded During the GC-MS Analysis of the Lactone Mixture (b).

are a product of microbiological oxidation of higher fatty acids or alkanes. This assumption is supported by the fact that methyl ketones have been found in soil and peat as well as in tobacco leaves dried in air and sun for two years. The bitumen of Bouxwiller shale was found to contain higher members (C_{27} - C_{36}) of this homologous series (10).

The triterpenoid ketone adiantone represents an intact biological indicator, which at the same time indicates that one part of the organic matter of Aleksinac shale originates from ferns. Adiantone is also a known constituent of Bouxwiller shale (10).

CONCLUSIONS

Most of the geolipids so far identified in the oil shale from Aleksinac represent well known and ubiquitous constituents of sediments: *n*-alkanes, aliphatic and cyclic isoprenoid alkanes including steranes, triterpanes and tetraterpanes and aliphatic and aromatic mono- and dicarboxylic acids. Moreover, several classes of compounds were identified which were also known as constituents of some ancient sediments but were not found to be ubiquitous, such as aliphatic isoprenoid ketones C_{13} and C_{18} , aliphatic methyl ketones C_{13} - C_{24} and the triterpenoid ketone adiantone.

However, in the Aleksinac shale bitumen geolipid constituents were identified which had not been found earlier in ancient sediments: a homologous C_7 - C_{15} series of aliphatic γ -lactones, a homologous series of 4 members of δ -lactones, two cyclic γ -lactones (dihydro- and tetrahydro-actinidiolide), as well as a homologous series of methyl esters of fatty acids (C_4 - C_{25}).

The composition and distribution of identified geolipids suggest: a) that the Aleksinac oil shale is a non-mature sediment (relatively high content of oxygen compounds with unchanged biolipid molecules, high *n*-alkane CPI values, relatively high amount of unstable stereoisomers in the fraction of steranes and triterpanes) and b) that the organic matter of Aleksinac shale is of mixed origin; the following precursors of the organic substance were incorporated in this lacustrine sediment: residues of continental plants, ferns and algae, as well as residues of micro-organisms, most probably of those which took part in early diagenetic changes of sedimented organic matter.

ACKNOWLEDGMENTS

This work was supported in part by the Research Fund of the S. R. Serbia (Yugoslavia).

LITERATURE CITED

- (1) Jovanovic, S. Lj. and Vitorovic, D., Bull. Soc. chim. Beograd, 17, 347-360 (1952).
- (2) Vitorovic, D. and Saban, M., J. Chromatogr., 65, 147-154 (1972).
- (3) Ensminger, A., Van Dorsselaer, A., Spyckerelle, C., Albrecht, P. and Ourisson, G., Advances in Organic Geochemistry 1973, B. Tissot and F. Bierner, eds., Editions Technip, Paris, pp. 245 (1975).
- (4) Saban, M., Porter, S., Costello, C., Djuricic, M. and Vitorovic, D., Advances in Organic Geochemistry 1979, A. G. Dougals and J. R. Maxwell, Pergamon Press, Oxford, pp. 559 (1980).
- (5) Jovanovic, L. J., Djuricic, M. V., Vitorovic, D. K., Andresen, B. D. and Biemann, K., Bull. Soc. chim. Beograd, 44, 605-613 (1979).
- (6) Hertz, H., Andresen, B. D., Djuricic, M. V., Biemann, K., Saban, M. and Vitorovic, D., Geochim. Cosmochim. Acta, 37, 1687-1695 (1973).
- (7) Saban, M. and Vitorovic, D., Advances in Organic Geochemistry 1975, R. Campos and J. Goni, eds., Enadisma, Madrid, pp. 209 (1977).
- (8) Saban, M., Jeremic, D. and Vitorovic, D., 9th Int. Cong. on Organic Geochemistry, Moscow, Abstracts of Reports, 1, 123.
- (9) Seifert, W. K., Progress in the Chemistry of Organic Natural Products 32, W. Herz, H. Grisebach and G. W. Kirby, eds., Springer Verlag, Vienna, pp. 1 (1975).
- (10) Arpino, P., These soutenue a Strasbourg, Sciences Geologiques, Memoire, 39, 1-107 (1973).

SYMPOSIUM ON GEOCHEMISTRY AND CHEMISTRY OF OIL SHALE
PRESENTED BEFORE THE DIVISIONS OF FUEL CHEMISTRY, GEOCHEMISTRY
AND PETROLEUM CHEMISTRY, INC.
AMERICAN CHEMICAL SOCIETY
SEATTLE MEETING, MARCH 20-25, 1983

THE ORGANIC GEOCHEMISTRY OF THE ORDOVICIAN WHITBY FORMATION -
A POSSIBLE ONTARIO SHALE

By

J. F. Barker and R. D. Dickhout

Department of Earth Sciences, University of Waterloo, Waterloo, Ontario, Canada, N2L 3G1
and

D. J. Russell and M. D. Johnson

Engineering and Terrain Geology Section, Ontario Geological Survey, 77 Grenville Street
Toronto, Ontario, Canada, M5S 1B3
and

P. R. Gunther

Geological Research and Services, Petro Canada, P. O. Box 2844
Calgary, Alberta, Canada, T2P 2M7

INTRODUCTION

Historically, shale oil was produced in Ontario from a plant near Collingwood, on Lake Huron. In 1859, rock of the Ordovician Whitby Formation was retorted to produce fuel and lubricants. In 1863, this operation became uneconomic in the fact of the newly discovered conventional crude oil near Oil Springs, Ontario. Existing data suggested three units were sufficiently organic to warrant an updated assessment -- the Ordovician Whitby and the Devonian Kettle Point and Marcellus Formations. The initial phase of the project involved shallow sampling of the Whitby Formation by diamond drilling at 20 locations stretching from Manitoulin Island to Toronto (see Figure 1) and to Ottawa, where the stratigraphic equivalent Billings Formation is present. Lithological and geophysical logs for these boreholes and preliminary geochemical results are in press (1).

GEOLOGY

The Whitby Formation (Upper Ordovician) overlies the Lindsay Formation - a limestone with interbedded shaley units. The character of the contact with the overlying Whitby Formation is variable and may be an important control over the organic content of the lower part of the Whitby Formation. The Whitby Formation has been subdivided into Upper, Middle and Lower (Collingwood) members. The Upper member is generally a greenish-grey fissile shale between 36 and 52 m thick in the study area. The Middle member is a brownish-grey fissile shale between 5 and 26 m thick. The Lower member or Collingwood is a dark brownish-grey, sometimes highly fossiliferous marl with black shale interbeds and is 1.5 to 7 m thick. The Whitby Formation is overlain by interbedded limestone and shale of the Upper Ordovician Georgian Bay Formation.

The most organic-rich zone of the Whitby is the calcareous Lower (Collingwood) member which occurs in a transition from carbonates of the Lindsay Formation to shales of the Whitby Formation. Hutt, et al (2) suggest the Whitby Formation was deposited under reducing conditions, perhaps in a stagnant, non-aerated basin. Initially, however, restricted circulation with little input of clay and silt produced organic-rich marls (Collingwood member). Increased supply of terrigenous mud diluted the organic matter and produced the less-organic-rich shales of the Middle and Upper members. The Upper and Middle members rarely contain more than 2.5% total organic carbon (TOC) while the Collingwood member often includes intervals of 2 to 5 m with more than 3% TOC. Clearly, the major economic potential lies in the Collingwood member.

OIL YIELDS

The available Fischer Assay (FA) oil yields are less than 40 litres/ton. This oil has a specific gravity in the range 0.895 to 0.942 and the oil yields correlate reasonably well with TOC as shown in Figure 2. For the Whitby samples, the relationship between TOC and Fischer Assay oil yield is:

$$FA(1/t) = 7.7 \text{ TOC } (\%) - 8.8$$

1)

with a correlation coefficient of 0.847. The Whitby Formation samples averaged about 6.8 litres/ton per 1% organic carbon. The non-zero intercept on the TOC axis is consistent with the common observation that the oil yield from oil shales is not limited by organic carbon but rather by hydrogen. Some carbon residual remains after pyrolysis since there is insufficient hydrogen to combine to form hydrocarbons.

GEOCHEMISTRY

Besides evaluating the amount of organic matter present and the yield of hydrocarbons upon pyrolysis, this study examines the nature of the organic matter in the Whitby Formation. Basically, two questions are being addressed. What is the maturation state of the organic matter and what is the chemical nature and origin of the organic matter?

The thermal history of kerogen is usually discussed relative to the optimum time-temperature conditions for hydrocarbon generation. Immature kerogen has not been heated sufficiently to produce oil. At perhaps 40-80°C maximum paleotemperature, the kerogen should have been sufficiently matured to produce oil as well as natural gas. At higher paleotemperatures, 120-160°C, only hydrocarbon gases should be present as liquid hydrocarbons are no longer stable. The associated kerogen is considered overmature. Only kerogen which is immature to perhaps marginally mature can be expected to produce oil upon commercial pyrolysis. In fact, commercial retorting or pyrolysis can be viewed as a much more rapid version of natural oil generation in which the mature and overmature maturation levels are reached in the retort.

Standard petroleum geochemical studies have been undertaken to define the maturation level attained by the Whitby Formation. Preliminary assessment indicates an average vitrinite reflectance in the range 0.44% to 0.57%, corresponding to immature or marginally mature kerogen. Billings Formation shale from the Ottawa area is apparently overmature with reflectance of 1.38%. The thermal alteration index, T. A. I. (3), based on kerogen particle color changes with increased temperature, indicates a mature to overmature level for Ottawa and Manitoulin samples. The conodont alteration index (C. A. I.), values based on microfossil color changes with increased maturation, range from 1.5 to 2.0 at Manitoulin and Collingwood, from 2.0 to 2.5 in the Toronto area and are about 3.0 for the Billings Formation near Ottawa (4). These values correspond to immature or marginally maturation levels except for the overmature level for the Billings shale.

Although maturation studies are continuing, it would appear that the Billings shale in the Ottawa area is not a potential oil shale because of its overmature nature. On the other hand, the immature to marginally mature nature of the Whitby Formation in Ontario is encouraging. In fact, it may be advantageous to explore for less mature areas in order to obtain higher pyrolysis yields per unit of organic matter. Perhaps the high TOC sections in the Manitoulin Island-Collingwood area of the Whitby subcrop should be emphasized in further assessment.

CHEMICAL NATURE OF KEROGEN

Oil generation potential is not only dependent upon the amount and thermal history of organic matter, but also upon its chemical nature. This is controlled by the nature of the source material and by biological and/or chemical transformations upon burial. The classification of kerogen has been made on a number of bases (5). A very useful system for potential oil shales involves the recognition of essentially three "types" of kerogen -- types I, II and III. Type I kerogen is composed of marine or lacustrine organic material. It has the highest H/C of the kerogen types and has a high capacity to generate liquid hydrocarbons. Structurally, kerogen particles are dominantly algal (alginate) or amorphous. Type II kerogen may have a significant component of terrestrial as well as marine material. Its H/C is lower than type I kerogen and its O/C is slightly higher. Exinuous (cutinite, resinite), vitrinous and fusinuous materials are more common relative to amorphous material. Type III kerogen is dominantly terrestrial in origin with higher O/C and lower H/C values than the other types reflecting the increased proportions of polycyclic aromatics and oxygen-containing functional groups. Vitrinous and fusinuous materials dominate over exinuous and amorphous materials.

All known oil shales are types I or II kerogen. Type III kerogen tends to produce mainly gas upon pyrolysis. In this study, kerogen type is being assessed by visual examination under the transmitted light microscope and by geochemical means including atomic H/C determinations and pyrolysate types (6).

Initial visual assessments of Whitby shales along the subcrop indicated a dominance of amorphous organic matter in the NW and a dominance of exinuous material in the SE. Less than 10% vitrinous and fusinuous material was found. H/C values ranged from 1.2 to 1.6. Both methods indicate the dominance of type I and type II kerogens in the Whitby Formation.

Generally, there is an increase in the ratio of aromatic to aliphatic hydrocarbon types in the sequence from type I, through type II to type III kerogen. The products of kerogen pyrolysis

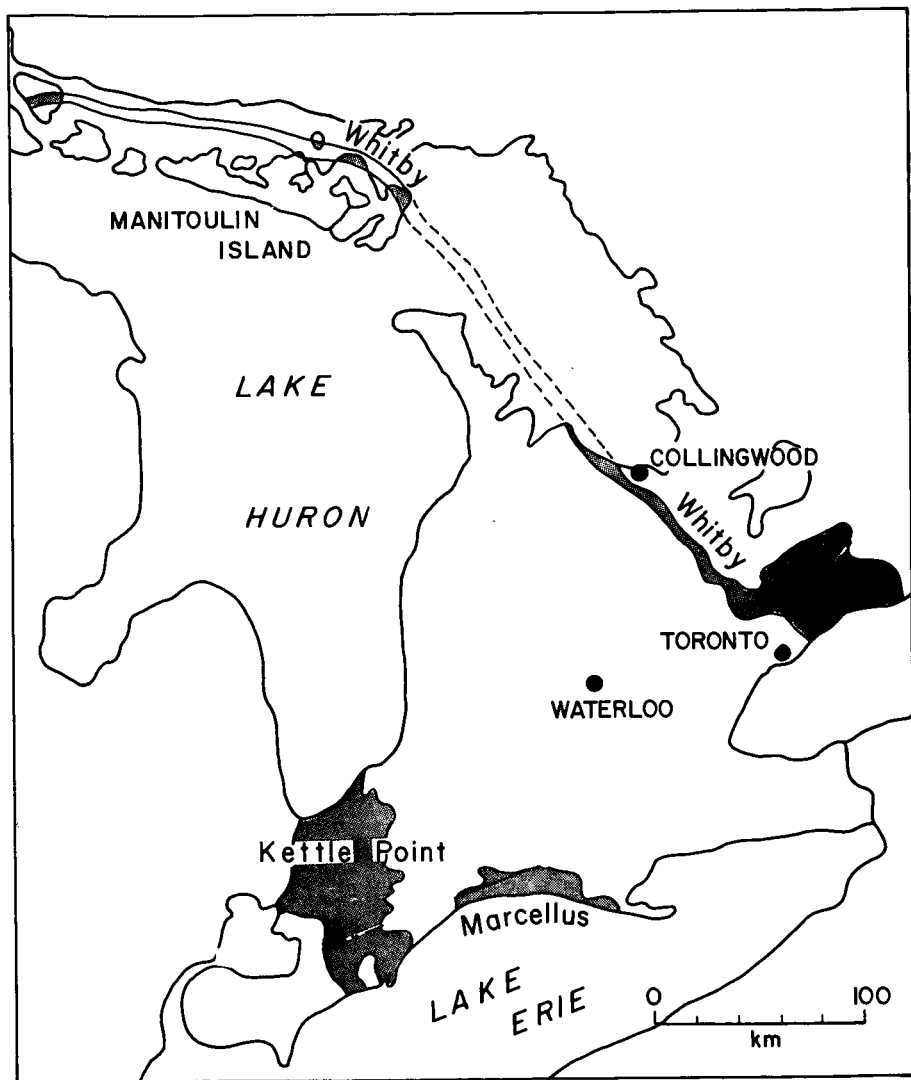


Figure 1. Outcrop and subcrop locations of the Whitby, Kettle Point and Marcellus shales in southern Ontario.

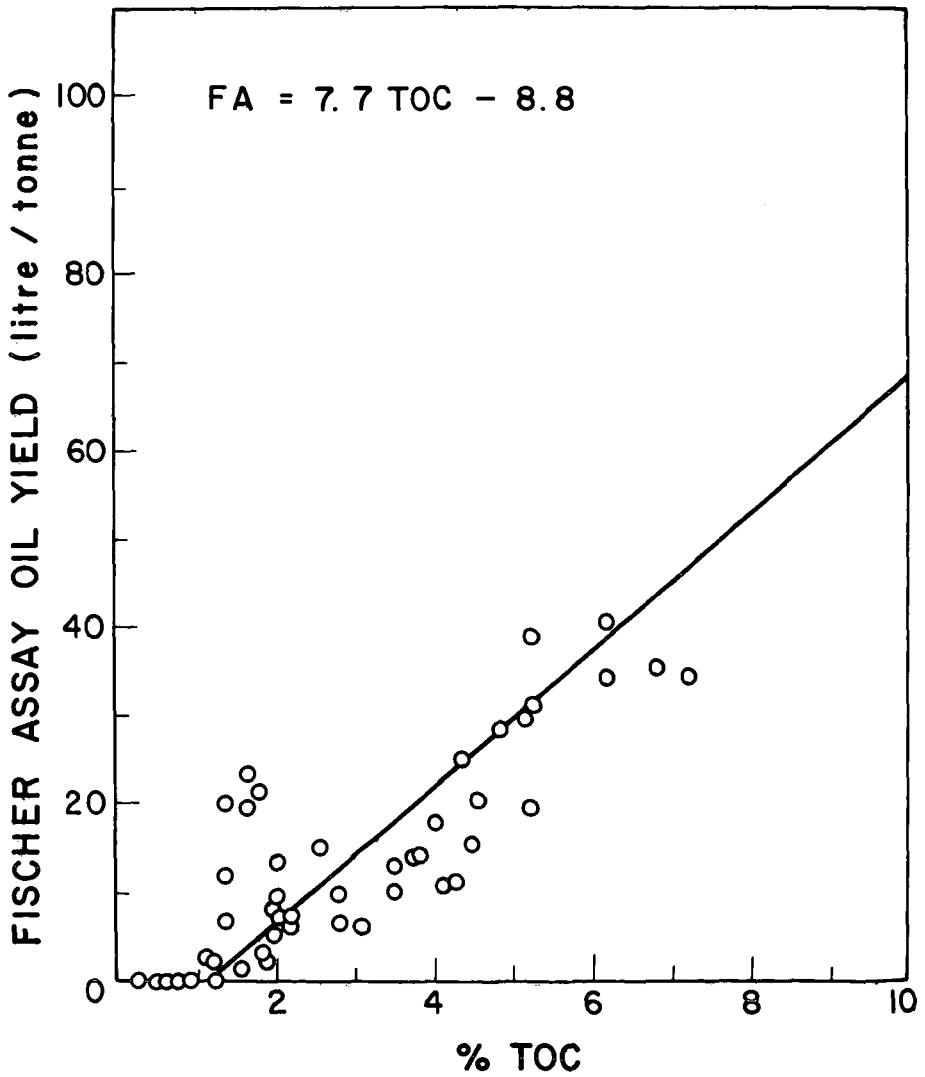


Figure 2. Relationship between oil yield by Fischer Assay and TOC for Whitby Formation samples.

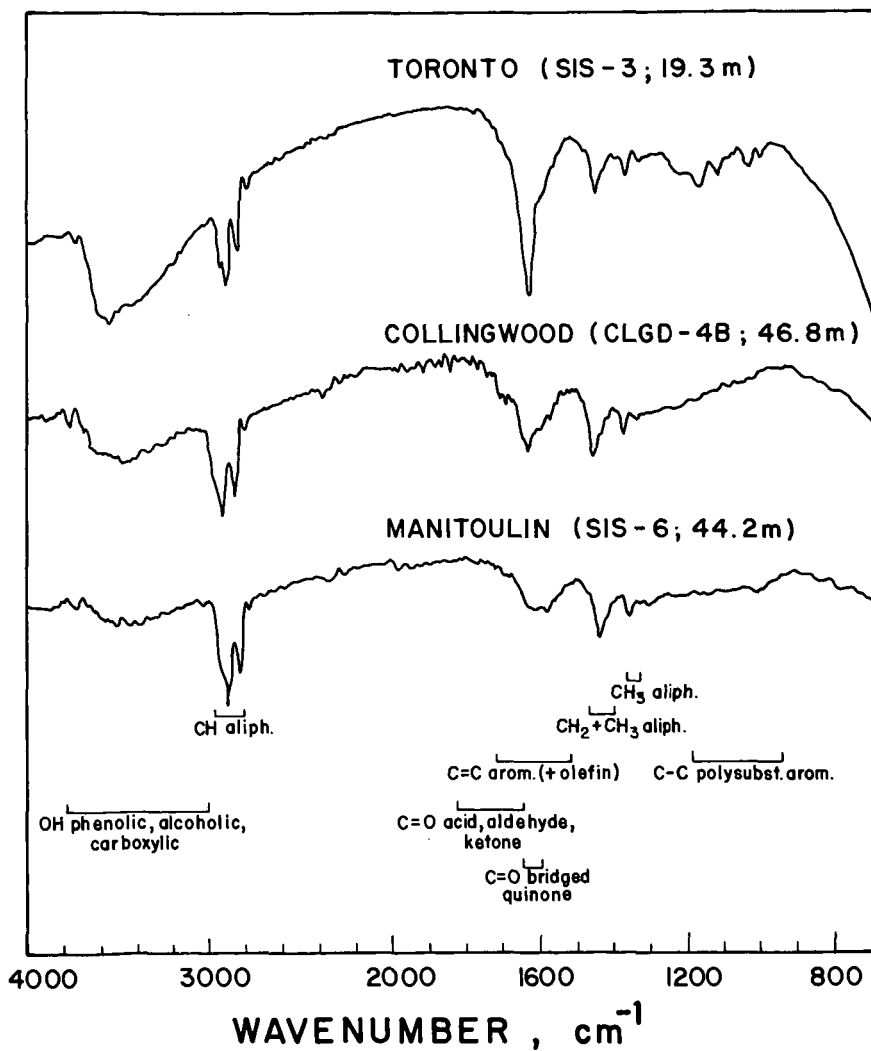


Figure 3. Typical I.R. spectra of kerogen isolated from the Whitby Formation.

also show this trend. Larter and Douglas (6) made use of this fact to establish a kerogen type index (R), which is the ratio of a selected aromatic (m- and p-xylene) to a selected aliphatic (n-octene) pyrolysis product. Type I kerogen has $R < 0.4$; type II has $0.4 < R < 1.3$; and type III has $R > 1.3$. Samples of Whitby shale and isolated kerogen have R values ranging from 0.28 to 0.7, again indicative of type I and type II kerogens.

Infrared (I. R.) spectra provide a qualitative indication of the types of organic structures present in the kerogen and their variation between samples (see Figure 3). In general, I. R. spectra from Manitoulin Island samples of Whitby shales are dominated by aromatic and aliphatic adsorption bands with a minor OH band. Shales from the Collingwood area also have only a minor OH band, but often have relatively larger C=C aromatic adsorption relative to aliphatic adsorption than Manitoulin samples. Many samples from the Toronto area show strong OH adsorption, C=O quinone adsorption and, perhaps, a more aromatic than aliphatic nature.

It seems that the Collingwood area shales are more aliphatic than the Manitoulin or Toronto area counterparts. This is reflected in higher H/C and higher FA/TOC for samples from Collingwood. The more aliphatic nature of Collingwood area spectra is also consistent with their greater proportion of amorphous organic matter. Clearly, more samples must be examined to assess the controls of the organic matter types and richness.

Isolated kerogen pyrolysates have been characterized by gas chromatography and mass spectrometry for clues as to the structural components of the kerogen itself. Horsfield and Douglas (7) found that mineral matrices increased the relative yield of low molecular weight pyrolysis products relative to high molecular weight products and also increased the proportion of aromatic to aliphatic pyrolysis products. Such secondary reactions were minimized by isolation from mineral catalysts. The gas chromatograms of kerogen pyrolysate are dominated by alkene-alkane pairs up to at least C₁₅ imposed on a background of polysubstituted benzenes. Above C₁₅, mono-substituted n-alkyl benzenes dominate.

The general view of kerogen structure presented by Tissot and Welte (5) is nuclei of stacked polyaromatic rings with some heterocycles containing O, N and S. Attached to these nuclei are alkyl chains, naphthenic rings and some oxygen-containing functional groups (hydroxyl, carboxyl, etc.). Bridges between nuclei include aliphatic chains and oxygen- and sulfur-containing groups such as ketones, esters and quinone. Almost all of these structural groups are indicated in the I. R. spectra. The pyrolysates clearly show the alkane-alkene chains, some of which may be breakdown products of the nuclei. The nuclei remnants are evident as higher molecular weight alkyl-substituted aromatics and as the lower molecular weight polysubstituted benzenes. No evidence of oxygen- or sulfur-containing heterocycles or bridges is found; however, CO₂ and H₂S are significant products of kerogen pyrolysis and could represent these components.

SUMMARY

In summary, the Upper Ordovician Whitby Formation represents an episode of deposition of fine-grained material on a shallow carbonate shelf. The Lower member - the Collingwood member - has the most potential for shale oil production, with TOC values ranging up to 9.2%. Fischer Assay oil yields of 40 l/t have been found. Yields up to 60 l/t can be expected for high TOC intervals.

These kerogen-rich rocks are immature to marginally mature with considerable oil generation potential remaining. Amorphous and exinous kerogen material dominate. Geochemical parameters point to a type II - minor type I kerogen which has favorable implications for shale oil potential. Kerogen pyrolysates are dominantly alkene-alkane chains of less than C₁₈ with numerous substituted benzenes including large molecular weight n-alkyl benzenes. Both pyrolysis products and I. R. spectra support current concepts of kerogen structure.

LITERATURE CITED

- (1) Macauley, G., Geological Survey of Canada Open File Report OFR-754, p. 156 (1981).
- (2) Hutt, R. B., MacDougall, T. A. and Sharp, D. A., Can. Soc. of Petrol. Geol. Mem. 1, pp. 411-441 (1973).
- (3) Staplin, F. L., Bull. of Can. Petrol. Geol., 17, pp. 47-66 (1969).
- (4) Legall, F. D., Barnes, C. R. and Macqueen, R. W., Bull. of Can. Petrol. Geol., 20 pp. 492-539 (1981).
- (5) Tissot, B. P. and Welte, D. H., "Petroleum Formation and Occurrence, A New Approach to Oil and Gas Exploration", Springer-Verlag, New York, p. 538 (1978).
- (6) Larter, S. R. and Douglas, A. G., in Adv. Organic Geochemistry, A. G. Douglas and J. R. Maxwell, eds., pp. 579-583 (1980).
- (7) Horsfield, H. and Douglas, A. G., Geochim. Cosmochim. Acta, 1119-1131 (1980).

SYMPOSIUM ON GEOCHEMISTRY AND CHEMISTRY OF OIL SHALE
PRESENTED BEFORE THE DIVISIONS OF FUEL CHEMISTRY, GEOCHEMISTRY,
AND PETROLEUM CHEMISTRY, INC.
AMERICAN CHEMICAL SOCIETY
SEATTLE MEETING, MARCH 20 - MARCH 25, 1983

GEOLOGY OF THE DEVONIAN BLACK SHALES
OF THE APPALACHIAN BASIN

By

J. B. Roen
U. S. Geological Survey, Reston, Virginia 22092

ABSTRACT

Black shales of Devonian age in the Appalachian basin are a unique rock sequence. The high content of organic matter, which imparts the characteristic lithology, has for years attracted considerable interest in the shales as a possible source of energy. Concurrent with periodic and varied economic exploitations of the black shales are geologic studies. The recent energy shortage prompted the U. S. Department of Energy through the Eastern Gas Shales Project of the Morgantown Energy Technology Center to underwrite a research program to determine the geologic, geochemical, and structural characteristics of the Devonian black shales in order to enhance the recovery of gas from the shales. Geologic studies produced a regional stratigraphic network that correlates the 15-foot sequence in Tennessee with 3,000 feet of interbedded black and gray shales in central New York. The classic Devonian black-shale sequence in New York has been correlated with the Ohio Shale of Ohio and Kentucky and the Chattanooga Shale of Tennessee and southwestern Virginia. Biostratigraphic and lithostratigraphic markers in conjunction with gamma-ray logs facilitated long range correlations within the Appalachian basin and provided a basis for correlations with the black shales of the Illinois and Michigan basins. Areal distribution of selected shale units along with paleocurrent studies, clay mineralogy, and geochemistry suggests variations in the sediment source and transport directions. Current structures, faunal evidence, lithologic variations, and geochemical studies provide evidence to support interpretation of depositional environments. In addition, organic geochemical data combined with stratigraphic and structural characteristics of the shale within the basin allow an evaluation of the resource potential of natural gas in the Devonian shale sequence.

SYMPOSIUM ON GEOCHEMISTRY AND CHEMISTRY OF OIL SHALE
PRESENTED BEFORE THE DIVISIONS OF FUEL CHEMISTRY, GEOCHEMISTRY,
AND PETROLEUM CHEMISTRY, INC.
AMERICAN CHEMICAL SOCIETY
SEATTLE MEETING, MARCH 20 - MARCH 25, 1983

THE DISTRIBUTION AND REGIONAL CORRELATION OF DEVONIAN OIL
SHALES IN THE EASTERN UNITED STATES

By

R. D. Matthews and H. Feldkirchner
Institute of Gas Technology, IIT Center, Chicago, Illinois 60616

RESOURCE STUDIES

The Devonian-Mississippian black shales of the Eastern United States contain varying amounts of organic carbon that can range up to nearly 25 percent by weight or as much as 40 percent by volume (1) and when they are retorted they will yield shale oil. The Fischer Assay yield is typically less than 10 gallons of oil per ton of rock. Such a yield by conventional retorting methods has been low enough when compared to Western oil shales to have limited interest in Eastern shale until new retorting technology enabled the Eastern shales to assume a competitive position. Eastern oil shales having levels of organic carbon similar to those of Western shales react comparably when a hydrogen retorting method is used (Table I).

TABLE I
U. S. OIL SHALES

	<u>Eastern</u>	<u>Western</u>
Ultimate Analysis, (dry basis) wt%		
Organic Carbon	13.7	13.6
Hydrogen	1.6	2.1
Sulfur	4.7	0.5
Carbon Dioxide	0.5	15.9
Ash	78.3	66.8
Fischer Assay Analysis		
Oil Yield, wt%	4.6	11.4
Assay, gal/ton	10.3	29.8
HYTORT Yields		
Oil Yield, wt%	9.1	--
Assay, gal/ton	23.2	--

The Eastern shales occur over a wide expanse from New York to Oklahoma and from Iowa to Alabama as shown on Provo's 1971 map (2), (Figure 1), yet as rocks that must be mined to be retorted, the shales of greatest potential are those near, or at the surface. A study of the Devonian-Mississippian Shales by the Institute of Gas Technology (IGT) to test them as feedstocks for the HYTORT[®] process (3) included an intensive sampling of the shales. IGT has sampled more than 180 locations from 15 Eastern and Western states and has taken more than 600 shale samples for analysis. Included in these were large-tonnage samples (10 to 50 tons) of shale from seven Eastern shales and from four Western geologic basins to provide the quantity necessary for a process development unit (PDU) having a 1 ton/h shale capacity which has been operating in Chicago since 1976 (4). Four criteria for resource assessment were imposed by IGT (5) in calculating resource estimates:

- . Organic carbon at least 10 percent by weight
- . Shale at least 10 feet thick
- . Stripping ratio less than 2.5 to 1, and
- . Maximum overburden thickness less than 200 feet.

The results of the sampling and testing program suggest a resource base in excess of 420 billion barrels of shale oil (Table II) from shale near the surface. The map (Figure 2) shows the area in square miles considered accessible in each of the several states studied, along with thickness

and richness data. The most important areas are in the States of Kentucky, Tennessee, Indiana, and Ohio, where nearly flat-lying beds, averaging 30 to 40 feet thick, are exposed at the surface in an outcrop belt nearly a thousand miles long.

TABLE II
ESTIMATED RESOURCES OF SHALE OIL RECOVERABLE BY THE HYTORT
PROCESS IN THE APPALACHIAN, ILLINOIS, AND MICHIGAN BASIN AREAS

<u>State</u>	<u>Total Area Suitable for Surface Mining, sq. mi.</u>	<u>Resources Recoverable by Aboveground Hydroretorting</u>	
		<u>billion bbl</u>	<u>bbl/acre</u>
Ohio	980	140	222,000
Kentucky	2650	190	112,000
Tennessee	1540	44	44,000
Indiana	600	40	104,000
Michigan	160	5	49,000
Alabama	300	4	21,000
Total	6230	423	

The shales have been studied for many years by many people and for many reasons. They are the source of a natural shale gas, a resource that has seen the development of over 9000 gas wells and is the subject of active research interest today (6). The shales are potential ores for uranium, some as high as 0.033 percent of that metal (7), and they are relatively high in other metals (8). They are likely source rocks for conventional crude oil and natural gas where they have been buried deeply enough to have matured. The variety and widespread nature of the black shales has led to a complex local nomenclature (Figure 3). The units named have been identified and used by stratigraphers because they are mappable, visibly recognizable in outcrop or from drill-hole data, and not because of any uniform geochemical characteristics. The stratigraphic framework based on color and natural radiation level that was available when Eastern shales became of recent interest proved inadequate to the understanding and prediction of retorting behavior and resource grade. The vertical and lateral variations within the rocks (9) were found to be great enough to require more detailed testing and correlation of shales from state to state as well as from basin to basin.

The manner of deposition of the black shales is still a subject of academic argument; it is complicated by the fact that organic matter in marine sediments can be preserved in a number of depositional environments, which share a common and necessary requirement of little or no oxygen (10).

One problem in developing a regional shale stratigraphy is the lack of fossils in the shale that can serve as time markers. A notable exception (Figure 4) is the fossil alga Foerstia, widely scattered across the Appalachian Basin but only found in a very narrow vertical range. Foerstia lived for a brief span of geological time and thus serves as a "time line" wherever found. As astronomical observations can be used to give precision and correlation to ancient history, so a fossil like Foerstia provides an accurate correlation of geologic events. The recent discovery by Kepferle (11) of the fossil alga in the Illinois Basin has changed the age relationship of rocks between that basin and the Appalachian Basin.

STRATIGRAPHIC INTERPRETATIONS

The Devonian rocks do not present as complete a record as many of the older, more deeply buried rocks, because there has been a loss by erosion of unknown thicknesses of Devonian section over the positive areas that separate the geologic basins. These positive areas, or arches, developed and were active at various times during the geologic past (Figure 5). The Algonquin Arch in southwestern Ontario existed as an early Upper Cambrian and Lower Ordovician feature (12), but was not sufficiently active during Late Devonian to prevent a continuous deposition of the Antrim/Kettle Point/Ohio Shales across Ontario. The Findlay Arch now separating northern Ohio from southeastern Michigan did not come into existence until after Devonian time (13) and thus would present no impediment to a complete deposition of black shales from Michigan through northwestern Ohio. These assumed rocks were lost by erosion as the arch lifted following the Pennsylvanian Age. Likewise, the Kankakee Arch now separating the modern Michigan and Illinois Basins in northwestern Indiana did not develop until after the Pennsylvanian and could not have been an obstacle to continuous black shale deposition of Antrim/New Albany from Michigan to Illinois; however, these shales no longer exist. The effect of the older Wisconsin-Illinois Arch on the deposition and survival of the Late Devonian shales can be seen in the composited Devonian shale map (Figure 6). In

east central Illinois, the shale thins to less than 100 feet over the arch, and the map trace of the outcrop is displaced to the south.

The inference that continuous and related deposition of shales did occur can be supported by the evidence of surviving lithofacies patterns and unit thicknesses. It is axiomatic that space must be available if sediments are to accumulate; thus, the preserved thickness of a sedimentary unit is one measure of the crustal subsidence. Downwarped "negative" areas will receive measurable thicknesses; however, when there is erosion of rock caused by crustal uplift in "positive" areas, the volume and thickness of rock lost cannot be determined easily. Where rocks are eroded, a gap in time occurs. Richter-Bernberg (14) holds a general principle that by far the greatest part of geologic time is unrepresented by remaining sediments; this would seem to be the case with Devonian Shales. The black shales of central Kentucky and Tennessee that are deposited (and preserved) over the positive areas southward of the Cincinnati Arch measure only a few tens of feet thick or may be absent. These few feet of shale resting on Silurian or older rock and overlain by Mississippian or younger rock are all that exists in that area to represent 50 million years of the Devonian; whereas, in the Appalachian Basin, more than 11,000 feet of Devonian sediments accumulated.

The thickness of Devonian Shale (15) (Figure 6) in northwestern Michigan establishes a depocenter some distance northwest of the center of the modern structural Michigan Basin. A similar area in west central Illinois received an unknown volume of Devonian sediments and has been called the Western Depocenter by Illinois stratigraphers (16). These two depocenters may have been related and joined as one across the line of the older Wisconsin-Illinois Arch. The Ellsworth equivalents in Illinois are not preserved in their original thickness, because they were eroded by uplift before being covered by the Burlington Limestone of Mississippian age (16). These shales thicken from about 100 feet to 160 feet in about 15 miles (4 feet/mile) as they approach the depocenter from the southeast, but the increase in thickness beyond 160 feet, whatever that may have been, was removed by erosional truncation. The Ellsworth of Michigan reached a thickness of about 800 feet (17) and probably was not eroded.

A striking feature of the upper Antrim in Michigan is the abrupt change in rock type from black, organic-rich shales in the east to greenish-gray, organic-poor shales in the west. These different shales were deposited contemporaneously and exist in a facies relationship to each other. The zone of lithofacies change is shown on Fisher's (17) map of the green-gray Ellsworth Shale, and a similar facies change has been noted in Indiana (18). The zero line from Hasenmueller's (19) Indiana Ellsworth map has been combined (Figure 7) into a regional composite with Fisher's as evidence of a single depositional control with a northwestern source for sediment and an environment of deposition unfavorable for the preservation of organics throughout a wide area of western Michigan and northern Illinois. A common feature of the Ellsworth/Antrim in Michigan and the Ellsworth/upper New Albany in the Illinois Basin is a similar overall shape. The configuration in cross section can be illustrated by a schematic drawing (Figure 8) depicting two episodes of deposition. The first (A) called the "lower black" shale here is widespread, carries a consistent internal gamma ray signature, and is relatively uniform in thickness. The second, composed of two facies, is widespread and is most apparent as a wedge of sediment having a black, organic-rich facies (B) that forms the thin side of the wedge and a green-gray, organic-poor shale (C) that forms the thick part of the wedge. The black shale (B) is here called the "upper black" shale, and the gray shales (C) are here called the "green-gray facies".

Applied to the Michigan Basin in east-west cross section, the "lower black" shale, (A) represents the Antrim of western Michigan and that part of the eastern Antrim identified by Subunits 1A, 1B, 1C, and 2. The "green-gray" facies (C) is the Ellsworth Shale, and the "upper black" is represented by all Antrim above Unit 2 and below the base of the Bedford Shale. The uniformity of the lower beds of the Antrim has been noted by several others (17, 20), and a westward source for the Ellsworth has been postulated by several (17, 20-22). Nevertheless, the westward source seems more applicable to those beds above the western Antrim, i. e., above the beds termed "lower black" in this paper.

The schematic black shale sequence (Figure 8) also can be applied to the upper New Albany of the Illinois Basin, where a facies relationship of the green-gray Hannibal/Saverton Shales with the Grassy Creek has been described by Lineback (23).

"The upper part of the Grassy Creek and its Indiana equivalents (the combined Morgan Trail, Camp Run, and Clegg Creek Members) grades laterally north-westward into a thickening wedge of greenish-gray shales and siltstone, the Saverton and Hannibal Shales in Illinois, the Ellsworth Member in Indiana."

Thus, the Hannibal/Saverton (C) and the upper part of the Grassy Creek (B) form the wedge in the sequence. The "upper black" can be postulated to be that part of the Clegg Creek Member of the New Albany in Indiana above the newly discovered Foerstia zone (11). If the lithologic and gamma ray correlations developed by the Illinois Geological Survey stratigraphers are correct (16), the Foerstia zone would appear to cut the Grassy Creek of Illinois into "upper black" and "lower black". If Foerstia extends into northwestern Illinois, it should be found just below the base of the Saverton in the top of the western Grassy Creek.

The sediment source for this great wedge would have been from the northwest, but the sediments below the presumed position of *Foerstia* in the Illinois Basin are not necessarily from that same source. Keperle's discovery of *Foerstia* on the eastern side of the Illinois Basin has established that the great bulk of black shale in Illinois predates much of the black shale in eastern Kentucky and Ohio (24).

The hypothetical black shale sequence is also applicable to various parts of the Sunbury Shale (Mississippian) in Michigan and Ohio. In eastern Michigan, the Sunbury increases from a typical thickness of 20 to 40 feet across most of the basin to over 140 feet in Sanilac County, where both cores and gamma ray logs document a local increase in thickness, that is shown on Fisher's 1980 isopach map of the Sunbury. The "normal" Michigan Sunbury represents the "lower black" (A); the unusual added thickness in the east becomes the "upper black" (B) with some part of the lower Coldwater Shale assumed to be a facies equivalent and representing part (C) of the upper wedge. The question of whether such a facies relationship exists between a part of the Sunbury and the Coldwater has not been answered, and to date no evidence can be advanced to support a division within the lower Coldwater Shale of central Michigan. Unfortunately, the Coldwater Shale, over 800 feet thick, is a unit of no economic interest and has drawn little investigation.

A similar geometry exists in the Sunbury of Ohio and can be illustrated on a section from the 1954 publication (25) by Pepper et al. (Figure 9). An abrupt increase in thickness of dark shales, logged as Sunbury by drillers, lies over a "normal" widespread Sunbury over most of Ohio. The widespread unit represents the "lower black" (A), the abnormal thickness of dark shale becomes the "upper black" (B), and the organic-poor facies (C) is represented by a part of the Orangeville Shale at the base of the Cuyahoga Group. The demonstration of a facies relationship and a division within the lower Cuyahoga is not available at this time; thus, as in Michigan, a two-part Sunbury based on shape must be considered as conjecture.

That two genetic types of Sunbury exist in the Appalachian Basin has been recognized by Van Beuren (26), who attempted to explain the geometric relationships between black shales and laterally adjacent gray/green shales and siltstones by means of a cycle of transgression and regression. His transgressive unit is "characteristically thin and widespread", and his regressive black shale is thicker, more laterally restricted and represents the distal facies of laterally adjacent non-black clastics. Related to the hypothetical black shale sequence (Figure 8), Van Beuren's transgressive unit is the "lower black" (A), the regressive Sunbury unit is the "upper black" (B), and the clastics represent the green-gray facies (C). The shape of the wedge of "upper black" (B) and its green-gray facies (C) requires that clastics came from the direction of the thick end and that the "upper black" was a deeper water deposit formed a greater distance from the source. The upper wedges are relatively local as compared with the "lower black" units, which are regional; the Lower Antrim/Kettle Point/Ohio (in part) is continuous and is representative of the black shales to be deposited over the arches between the three basins. The source of the lower unit is not as apparent as for the upper unit (B/C). If the "lower black" is cyclic as Van Beuren advocated for the lower Sunbury, it should have a source similar to the overlying wedge.

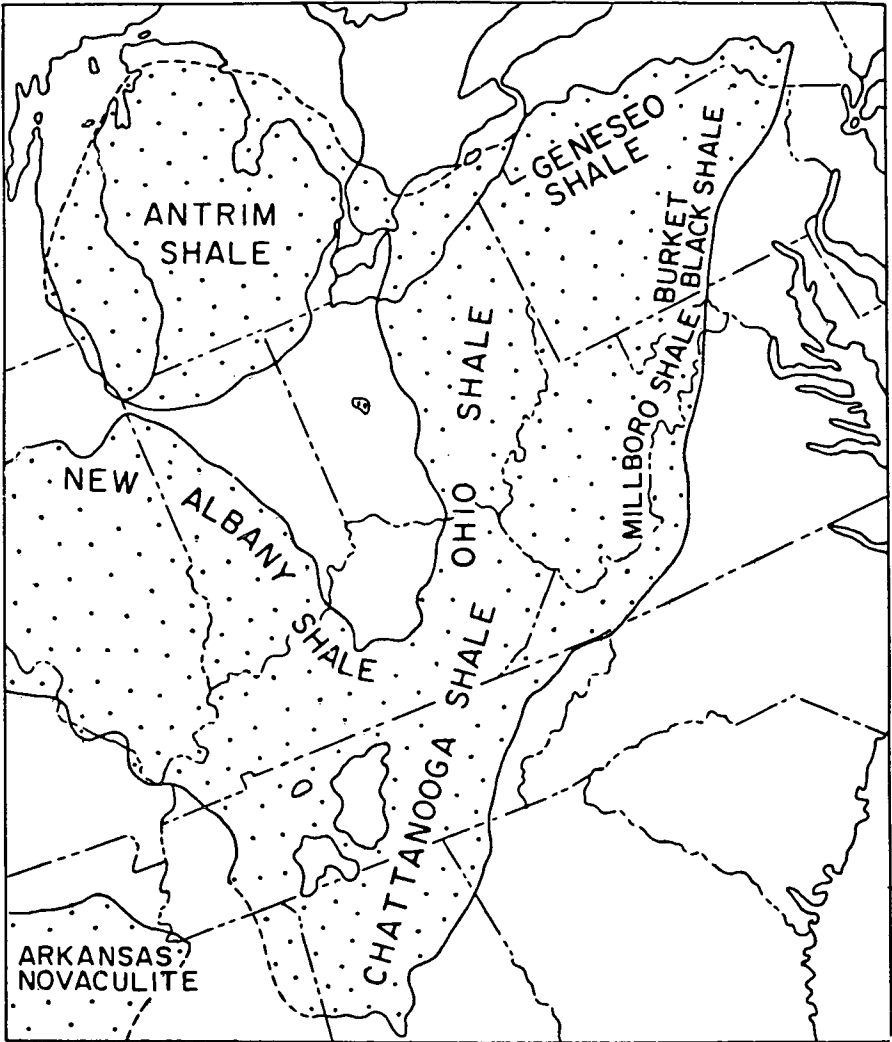
A westward or northwestward source for Ellsworth/Upper Antrim and for Hannibal-Saverton/upper Grassy Creek is appropriate for the overall geometry of an "upper shale" body. It is clear that great volumes of clastic material in the Appalachian Basin came from the east and that some of the black shale sequence also applies east of the Cincinnati Arch (in mirror image), I believe that some of the black shales in the basin will prove to be more regional in nature and of the "lower shale" type (A).

The pulses of increased clastic influx reflect tectonic activity, as has been suggested by Ettensohn and Barron (27, 28), but with the addition of a northwestern landmass to provide material west of the general line of the Algonquin and Cincinnati Arches. These pulses are represented by the upper wedges (C/B). Between pulses, there is widespread deposition of the "lower black" type of shales which, for the lower Antrim and Sunbury equivalents, were little influenced by arches. The southwestern source suggested by Ettensohn and Barron (27) seems very plausible for the lower shales (A) of the Illinois and Appalachian Basin and of Michigan as well.

The 50 million years of the Devonian Age is sufficient for tectonic control of a series of local wedges alternated with periods of truly regional deposition, with each episode spaced apart by great periods of little or no deposition (unconformities) within the Devonian-Mississippian Shales of the Eastern United States.

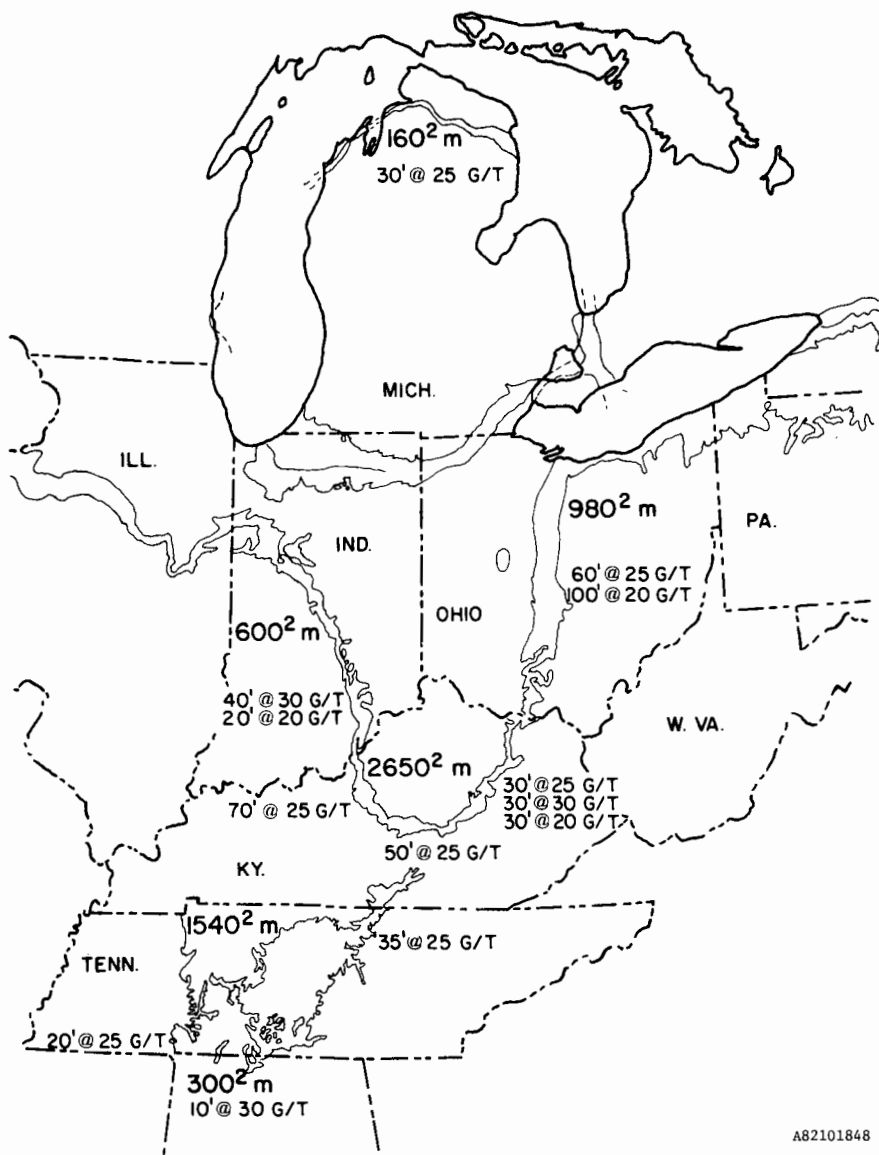
ACKNOWLEDGMENTS

The acquisition of large shale samples described here was funded most recently by the U. S. Department of Energy; earlier it was funded by the American Gas Association and later by the Gas Research Institute. The authors wish to express their appreciation to these organizations for permission to publish this paper. We also wish to thank personnel of the various state and federal agencies who assisted us in obtaining oil shale samples for testing and provided a considerable amount of geological information.



A82101849

Figure 1. Principal Devonian Oil Shale Deposits of the Eastern United States



A82101848

Figure 2. Map Showing Outcrop Areas and Resource Data for the Devonian-Mississippian Oil Shales of the Eastern United States

Outcrop is shown by line where narrow.

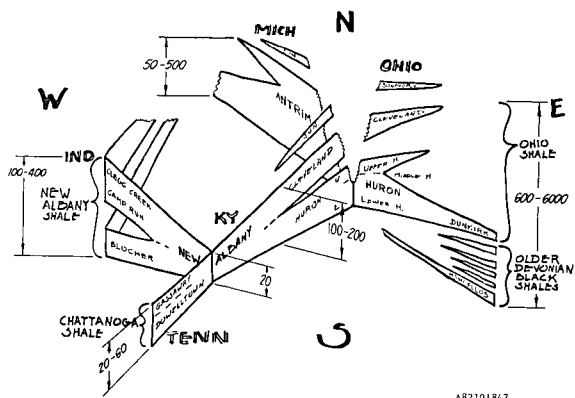


Figure 3. Fence Diagram Showing Black Shale Nomenclature and Thickness in Feet

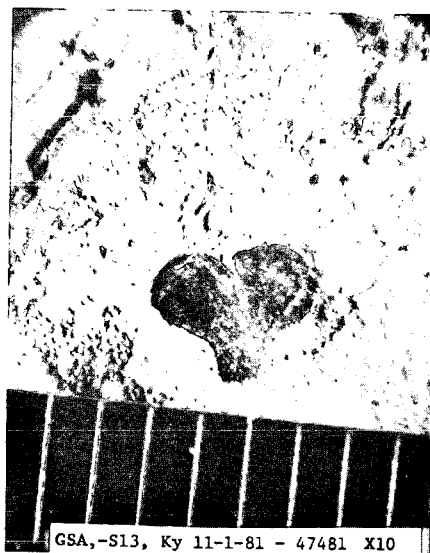
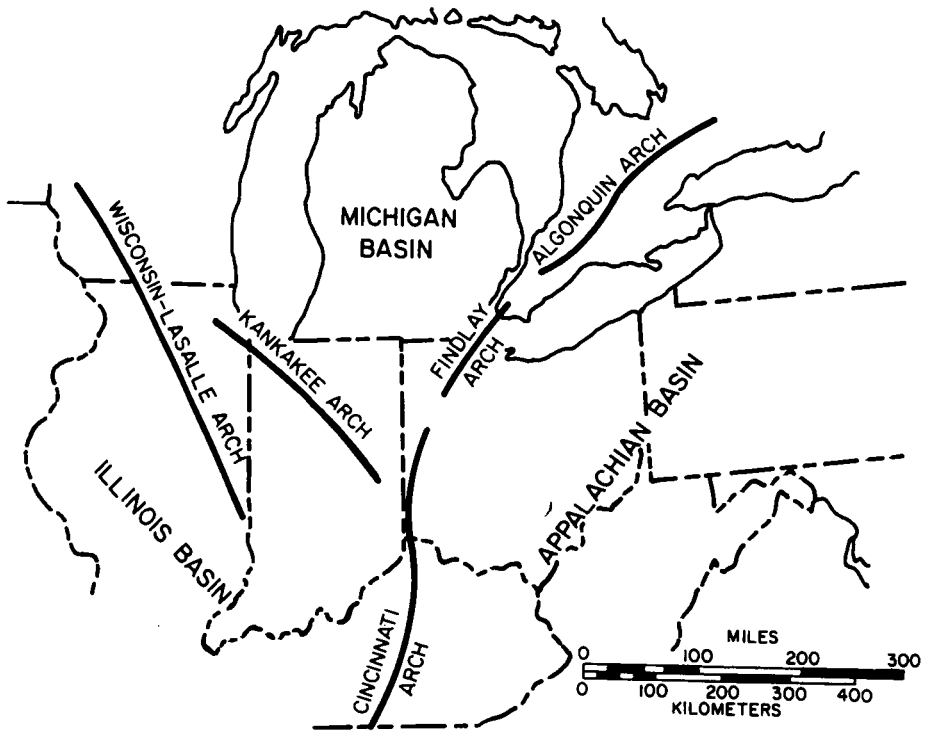
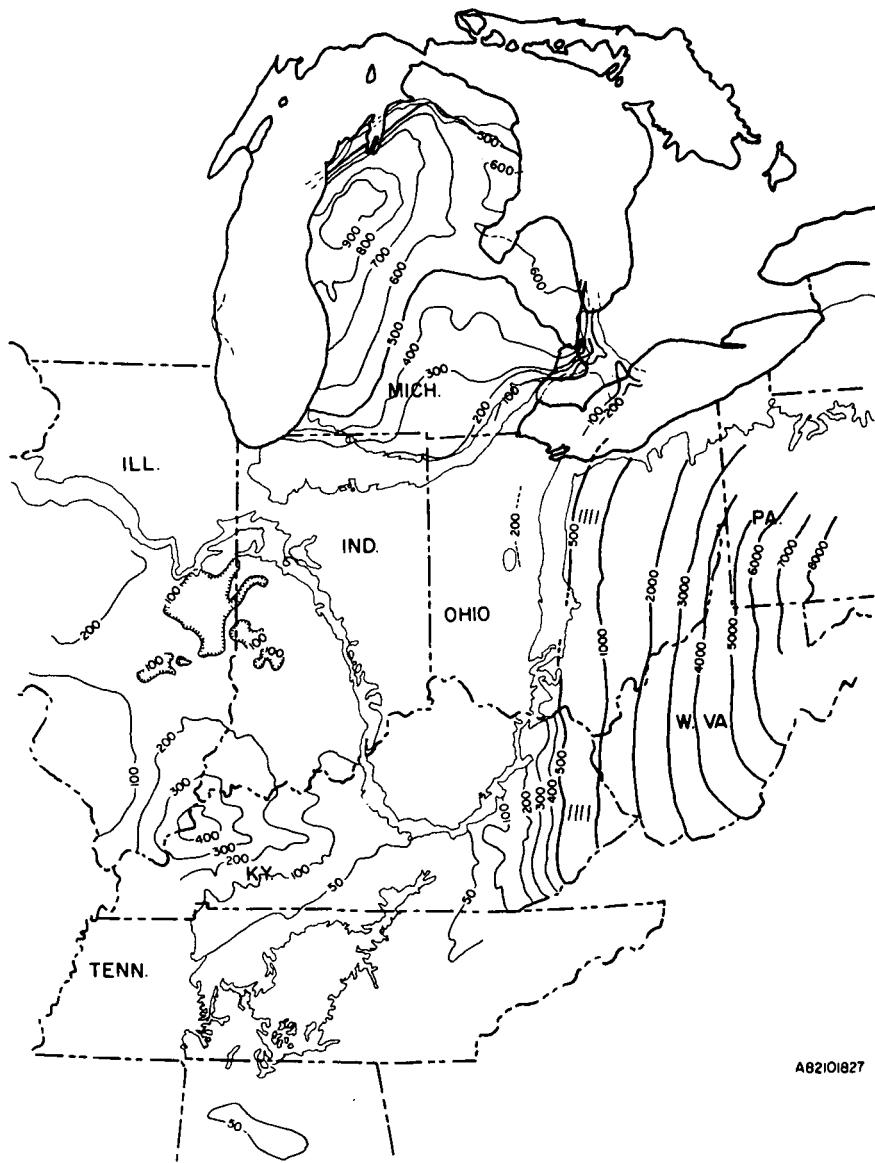


Figure 4. Photomicrograph of *Foerstia* From the Huron Member of the Ohio Shale Near Vanceburg, Kentucky (Millimeter Scale in Figure.)



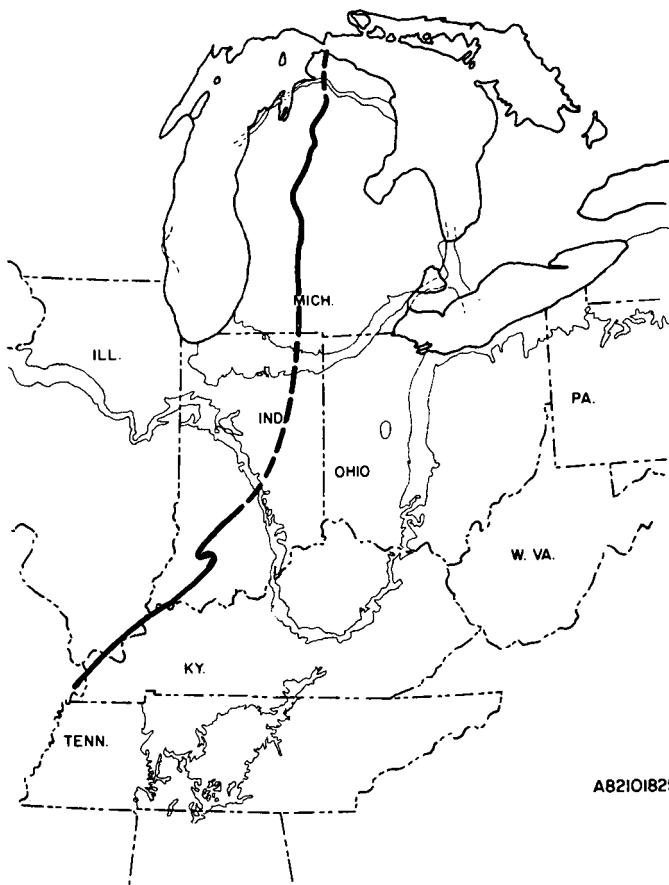
A82101824

Figure 5. Major Structural Features
Mentioned in the Text



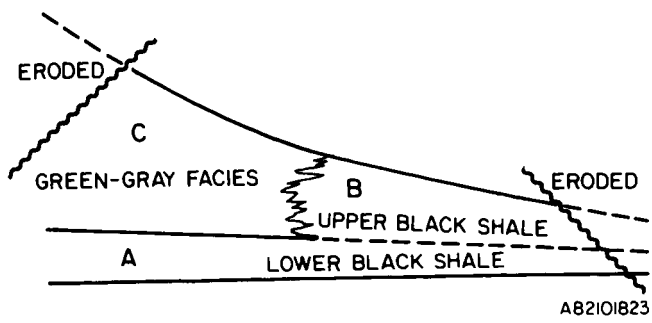
AB2101827

Figure 6. Isopach Map of Total Devonian Shale Composited From Numerous Literature Sources



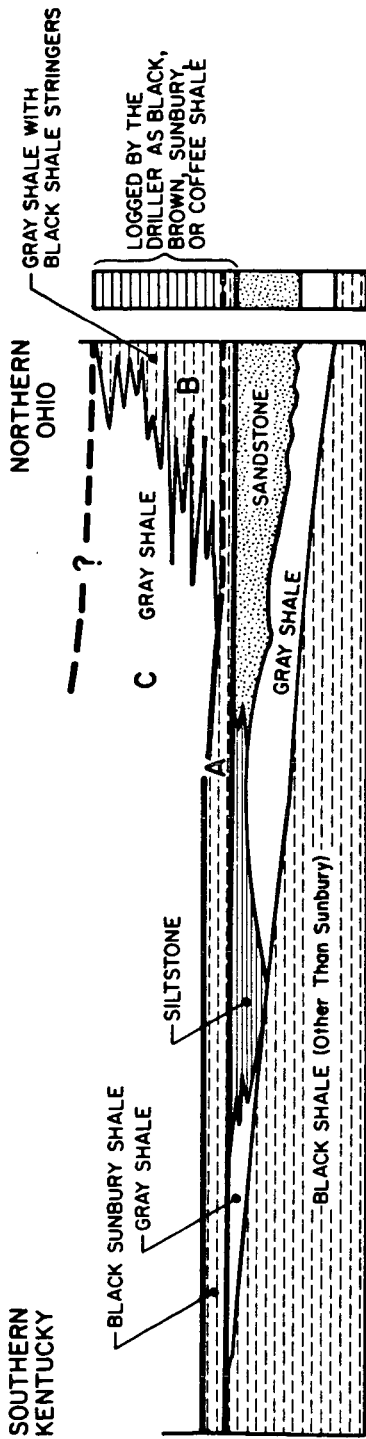
A82101825

Figure 7. Regional Map of the Ellsworth Shale Zero Line, Green-Gray Ellsworth-Type Shales to the West and Black Antrim-Type Shales to the East



A82101823

Figure 8. Hypothetical Black Shale Sequence



A82101826

Figure 9. Generalized Cross Section From Southern Kentucky to Northern Ohio Showing the Abnormal Thickness of Sunbury Shale as Recorded by Drillers — After Pepper (25)

LITERATURE CITED

- (1) Leifinger, R. K. , "Inorganic Geochemistry", pp. 53-61, in "Studies of the New Albany Shale (Devonian and Mississippian) and Equivalent Strata in Indiana", Hosenmueller, N. R. , and Woodard, G. S. , Eds, prepared for U.S. DOE, Morgantown, W. Va. , September, 1981.
- (2) Provo, L. J. , Kepferle, R. C. , and Potter, P. E. , Am. Assoc. Pet. Geol. Bull. , 62, 1703 (1978).
- (3) Matthews, R. D. , Janka, J. C. , and Dennison, J. M. , presented at Amer. Assn. of Petroleum Geologist-Eastern Section Meeting, Evansville, Indiana, October 2, 1980. (IGT preprints available.)
- (4) Feldkirchner, H. L. , and Janka, J. C. , Symposium Papers: Synthetic Fuels from Oil Shale, 489-524, Institute of Gas Technology, Chicago, April 1980.
- (5) Janka, J. C. , and Dennison, J. M. , Symposium Papers: Synthetic Fuels from Oil Shale, 21-116, Atlanta, Institute of Gas Technology, Chicago, April, 1980.
- (6) Potter, P. E. , Maynard, J. B. , and Pryor, W. A. , Oil Gas J. , 290-318, January 25 (1982).
- (7) Conant, L. C. , and Swanson, V. E. , U. S. Geol. Surv. Prof. Pap. 327 (1961).
- (8) Silverman, M. E. , and Spiewak, L. , Sep. Sci. Technol. , 16 (9), (1981).
- (9) Leventhal, J. S. , and Shaw, V. E. , J. Sediment. Petrol. , 77-81 (1980).
- (10) Tourtelot, H. A. , Clays Clay Miner. (5) 313-219 (1979).
- (11) Kepferle, R. C. , "Correlation of Devonian Shale Between the Appalachian and Illinois Basins Facilitated by *Foerstia (Protosalvinia)*", in Roberts, T. G. , Ed. , Geol. Soc. Amer. Cincinnati '81 Field Trip Guidebooks, Vol. II: Economic Geology Structure Field Trip No. 3, 35, 334-35, Amer. Geol. Inst. , 1981.
- (12) Sanford, B. V. , and Quillian, R. G. , Paper Geol. Surv. Canada, Canada Dept. of Mines and Techn. Surv. , Ottawa 1959.
- (13) Levorsen, A. I. , Paleogeologic Maps, 174, Freeman, W. H. , San Francisco, 1960.
- (14) Richter-Bernburg, Salt Deposits, p. 41, in Borchert, H. , and Muir, R. O. , D. Van Nostrand, Linden, 1964.
- (15) Oliver, W. A. , deWitt, Wallace, Jr. , Dennison, J. M. , and others, "Devonian of the Appalachian Basin", Oswald, D. H. , Ed. Int. Symp. Devonian System Proc. , Vol. 1, 1001-40, Pet. Geol. , Calgary, Alberta, 1967.
- (16) Bergstrom, R. E. , Shimp, N. F. and Cluff, R. M. , Illinois State Geol. Surv. Final Report prepared for U. S. Dept. Energy, Morgantown Energy Technology Center, 1980.
- (17) Fisher, J. H. , U. S. DOE Report No. FE-2346-80, 1980.
- (18) Lineback, J. A. , Illinois State Geol. Survey Final Report prepared for U. S. DOE, Morgantown Energy Technology Center, 1980.
- (19) Hasenmueller, N. R. , and Bassett, J. L. , Illinois State Geol. Survey for U. S. DOE Report Morgantown, W. Va. , September, 1981.
- (20) Eils, G. D. , U. S. DOE Report No. FE-2346-30, 1978.
- (21) Cohee, G. V. , Macha, C. , and Holk, M. , U. S. Geol. Surv. Oil and Gas Inv. Ser. , Chart OC-41, 1951.
- (22) Cross, A. , and Bordner, M. A. , U. S. DOE Report No. FE-2346-81, September 1980.
- (23) deWitt, W. , Jr. , U. S. Geological Survey, Ref. 18, p. 11, letter of August 27, 1982.
- (24) Linebach, J. A. , op. cit. , p. 11.
- (25) Pepper, J. F. , de Witt, W. , Jr. , and Demarest, D. F. , U. S. Geol. Surv. Prof. Pap. , 259 (1954).
- (26) Van Beuren, V. V. , "The Sunbury Shale of the Central Appalachian Basin - A Depositional Model for Black Basinal Shales" (Abstract only), in Prior, W. A. , et al. Eds. , "Energy Resources of Devonian-Mississippian Shales of Eastern Kentucky, Ann. Field Conf. , April 9-11, 1981", Kentucky Geological Survey, Lexington, 1981.
- (27) Ettensohn, F. R. , and Barron, L. S. "Depositional Model for the Devonian-Mississippian Black Shale Sequence of North America: A Tectonic-Climatic Approach", in Blackburn, W. H. , Compiler, Final Report, "Black Shale Studies in Kentucky", Univ. of Kentucky Research Group, Dept. of Geology and Kentucky Geological Survey, 1980.
- (28) Ettensohn, F. R. , and Barron, L. S. , "Depositional Model for the Devonian-Mississippian Black Shales of North America: A Paleoclimatic-Paleogeologic Approach", in Roberts, T. G. , Ed. , "Geol. Soc. Amer. Cincinnati '81 Field Trip Guidebooks, II: Economic Geology, Structure, Field Trip No. 3", 1980.

SYMPOSIUM ON GEOCHEMISTRY AND CHEMISTRY OF OIL SHALE
PRESENTED BEFORE THE DIVISIONS OF FUEL CHEMISTRY, GEOCHEMISTRY
AND PETROLEUM CHEMISTRY, INC.
AMERICAN CHEMICAL SOCIETY
SEATTLE MEETING, MARCH 20-25, 1983

GEOCHEMISTRY OF OIL SHALES IN EASTERN KENTUCKY

By

T. L. Robl, A. E. Bland, D. W. Koppelaar and L. S. Barron
Institute for Mining and Minerals Research, University of Kentucky, P. O. Box 13015
Lexington, Kentucky 40512

INTRODUCTION

Recent resource assessment studies of eastern Kentucky oil shales have established that this resource is a potential economic synthetic fuel feedstock (1). Extensive geochemical characterization of this resource has been carried out by the Institute for Mining and Minerals Research (University of Kentucky) with support from the Commonwealth of Kentucky Energy Cabinet, the U. S. Department of Energy and private industry. This effort will eventually culminate in the characterization of the entire oil shale resource within the Commonwealth; this particular study addresses the results gained from the first two drilling and sampling phases of the overall effort. The sampling and analysis program was initiated in Lewis and Fleming Counties, Kentucky, resulting in 10 cores being drilled with those core samples being designated as the "K-series" samples in this report. The second phase of the program produced an 11 additional cores in Rowan, Bath, Montgomery, Powell and Estill Counties; these samples are given the "D-series" designation. The location of these core sites as well as current drilling sites are depicted in Figure 1. This paper summarizes the geochemistry of the Devonian and Mississippian age oil shales of the K- and D-series study areas.

GENERAL GEOLOGY AND STRATIGRAPHY

In Kentucky, black shales rich in organic matter (OM) in the Devonian and Mississippian systems crop out in a roughly semi-circular pattern on the flanks of the Lexington Dome. The dome is a structural prominence on the Cincinnati Arch, which stretches between Nashville, Tennessee and southern Ohio. The black-shale outcrops occur in the outer Bluegrass and Knobs from Jefferson and Bullitt Counties on the west to Lewis and Fleming Counties on the east as shown in Figure 1. From the southern end of the semi-circle south into Tennessee, the black shale crops out in river valleys where the overburden is relatively shallow in the Cumberland Saddle, a structural col between the Lexington and Nashville domes on the Cincinnati Arch.

West of the Cincinnati Arch, the black shale dips into the subsurface of the Eastern Interior Basin where it becomes over 450 feet thick in Hardin County, Illinois and Union County, Kentucky (2). On the eastern flank of the Cincinnati Arch, the black shale dips eastward into the Appalachian Basin where it becomes over 1700 feet thick. To the south, the overall section thins to 30 or 40 feet along the crest of the arch.

In each of the three areas described above, the black-shale sequence differs in overall aspect from each of the other areas when viewed in outcrops. This difference has led to three sets of stratigraphic nomenclature having been applied to the black Devonian-Mississippian Shales. The general distribution of the usages of stratigraphic nomenclature is shown in Figure 2.

In eastern Kentucky, the Ohio Shale terminology has been used where the Mississippian Sunbury Shale and the underlying Bedford Shale can still be recognized. A typical stratigraphic section along with down-core carbon distribution is shown in Figure 3. Typically the overburden is a mixture of claystone and siltstone in the Borden Formation. This unit directly overlies the Sunbury Shale which is a black, laminated, siliceous shale rich in organic matter with some pyrite. The Sunbury thins to the south from 20-25 feet in Lewis County to four feet in Estill County.

The Mississippian Sunbury Shale is separated from the underlying OM-rich Devonian Ohio Shale by the Berea Sandstone and Bedford Shale in Lewis County and by the Bedford Shale in the remaining counties. This interburden unit thins to the south from over 100 feet in Lewis County to only a few inches in Estill County. The Ohio Shale is divided into three units as shown in Figure 3. The Cleveland Member is the upper unit. Its lower contact is marked at the upper greenish-gray (OM-deficient) shale of the Three Lick Bed. The lower greenish-gray shale marks the top and the angular unconformity at the base of the black shale, the underlying unit may be the Middle

Devonian Boyle Dolomite, the Silurian Crab Orchard Shale, or the Silurian Bisher Limestone.

The Cleveland Member consists primarily of black to brownish-black laminated siliceous shale. It contains minor amounts of calcareous laminae and cone-in-cone limestone. Pyrite is present as nodules, framboids and irregular forms. Other primary minerals include illite clay and clay- and silt-size quartz.

The Three Like Bed is a regional stratigraphic marker bed traceable throughout eastern Kentucky, Ohio, West Virginia and Tennessee (3). The bed contains three greenish-gray shales deficient in OM interbedded with two brownish-black, OM-rich shales. The greenish-gray shales contain *Lingula*, abundant trace fossils and pyritized micro fossils (4, 5).

The lower unit of the Ohio Shale which is present in the outcrop area of eastern Kentucky is the Huron Member. Primarily, the Huron consists of black to brownish-black to gray-black, laminated, siliceous, OM-rich shales. Calcareous laminae, cone-in-cone limestone, dolomitic gray shales, dolomite beds and bioturbated greenish-gray shales occur as interbeds and laminae in the lower parts of the member.

DEFINITION OF ECONOMIC ZONES

For the resource assessment studies, it was necessary to define potentially mineable oil shale zones. The resulting nomenclature has subsequently been carried over into the geochemical studies. For the purposes of the resource assessment, only surface mineable oil shale having an overburden plus interburden to shale ratio of less than 2.5:1 was considered economical. Economic zones were further defined as those resources with greater than 8% carbon (1). In the study area, this included all of the Sunbury shale and a High Grade Zone (HGZ) of the Upper Cleveland Member of the Ohio shale. This zone extends from the top of the member to a depth where the carbon content drops below 8%. This 8% level also corresponds to a point at which the carbon concentration is rapidly decreasing with depth (see Figure 3). A zone of +8% carbon also occurs in the lower Huron, but this oil shale is also high in sulfur, mineral carbon and is separated from the other economic zones by a thick sequence of lean oil shales.

The two defined economic zones (Sunbury shale and the HGZ of the Cleveland Member) are separated by interburden units of the Bedford Shale throughout the study area and the Berea Sandstone in Lewis County. Thickness histograms of the economic zones and their associated interburden units are presented in Figure 4, which shows that the Sunbury Shale decreases in thickness to the south while the Cleveland HGZ remains fairly constant at 25-30' thick. The Bedford and Berea units decrease in thickness rapidly toward the south with less than a foot of interburden separating the two economic zones in Montgomery County.

ORGANIC GEOCHEMISTRY

General

The organic geochemistry of the study samples is summarized by the elemental analysis data in Table I. Extensive detailed data on these samples on a core-by-core basis are available in previous reports (1, 6, 7).

TABLE I
ORGANIC ELEMENTAL ANALYSIS DATA FOR K- AND D-SERIES OIL SHALES

	K-Series				D-Series			
	Sunbury Shale	Cleveland Shale		Huron Shale	Sunbury Shale	Cleveland Shale		Huron Shale
		Total	HGZ			Total	HGZ	
C ^a	11.42(3) ^b	9.04(2)	11.11(3)	5.61(3)	13.12(10)	9.61(4)	11.08(3)	6.57(15)
H	1.20(4)	.99(2)	1.21(7)	.66(6)	1.47(14)	1.09(5)	1.25(5)	.76(12)
N	.41(5)	.39(4)	.39(3)	.22(7)	.44(10)	.32(10)	.36(10)	.23(16)
S	3.54(8)	2.42(6)	2.51(8)	3.15(3)	3.70(12)	2.79(12)	2.93(10)	3.61(7)

a. Wt % raw shale; H corrected for surface moisture.

b. Numbers in parentheses are coefficients of variation x 100.

Carbon data presented and discussed herein are given as total carbon unless specified otherwise. Mineral carbon contributions from calcite and dolomite are typically insignificant in comparison to total carbon values. Average mineral carbon contents for the K-series stratigraphic units are as follows: Sunbury, 0.01%; Cleveland, 0.06%; and Huron, 0.13%. Comparative data

from the D-series are: Sunbury, 0.14%; Cleveland, 0.10%; and Huron, 0.44%. A general trend toward increasing mineral carbon in the southerly samples of the study area is evident. Distinct calcitic bands in the cores do occur but were removed and analyzed separately and, thus, are not accounted for in the above data.

Hydrogen is present in these shales as surface moisture, mineral-bound hydration water, and organically-bound hydrogen. Surface moisture was determined for each sample; consequently, this hydrogen contribution is corrected for in the presented data. Mineral-bound hydrogen, being difficult to determine directly, is included in the hydrogen data presented. However, positive intercepts of H vs. C plots indicate approximately 0.2 wt% hydrogen from mineral origins. The consistency of these data for general assignment to mineral-bound hydrogen contributions is under current investigation.

Nitrogen occurs almost exclusively as organic nitrogen and N vs. C plots are linear and possess relatively constant slope values indicating a uniform geochemical presence of this element in these shales. Sulfur occurrence in these shales is composed of organic, sulfide and sulfate contributions. Our data indicate that >80% of the sulfur occurs in sulfide minerals, predominantly as pyrite (FeS₂). Current research is aimed at refinement of the sulfur forms data, primarily to assess the organic sulfur content of these shales.

Based on present data, the overall stoichiometry of the raw oil shale organic material is given by the empirical formula CH_{1.3}N_{0.31}. This can be compared to formulas given for western oil shales, e.g. CA_{1.5}N_{0.032} (8) and CH_{1.7}N_{0.27} (9). These data indicate that the eastern oil shales of Kentucky are more aromatic in character than the Western oil shales. This characteristic manifests itself in a slight hydrogen deficiency which ultimately limits oil yield. The remarkably similar N/C ratios between the two oil shales is also notable.

Stratigraphic and Regional Trends

Strong stratigraphic trends are evident in the distribution of carbon in the study cores, as Figure 3 illustrates. In general, the carbon content increases from top to bottom in the Sunbury Shale, with carbon values of approximately 9-10% at the top to 15% at the base. This pattern is reversed in the underlying Cleveland Member of the Ohio Shale. The top of the Cleveland has a carbon content similar to the base of the Sunbury, with values decreasing to 4-6% toward its base. The Three Lick Bed of the Ohio Shale shows erratic distribution of carbon, which is as expected, as this unit is defined on the basis of three barren, bioturbated green shales. The pattern of carbon distribution in the Huron Member of the Ohio Shale is the inverse of the Cleveland; the carbon content increases toward the base of this unit, reaching values of 9-10%. This pattern is somewhat broken up by the presence of burrowed and bioturbated green shale intervals toward the base of the Huron.

When the data of Table I are compared, the intra-core organic geochemistry of the individual shale units is relatively consistent considering the variance within each unit. A slight average decrease toward the lower units is evident, however. Intra-core H/C ratios for these data are essentially constant, but slightly higher H/C ratios in the upper Cleveland shales relative to the Sunbury have been observed. Intra-core N/C ratios are generally higher for the leaner Huron Shales; this correspondence has also been noted for Western oil shales (8, 9).

Regional trends in the study area are illustrated for carbon, hydrogen and sulfur in Figure 5. The carbon-hydrogen contents of the Sunbury shale are 11 and 1.1%, respectively, in the northern (Lewis County) cores and peak at 15 and 1.8% in the Powell County core sites before decreasing slightly again toward the south of the study area. The most rapid increase in carbon and hydrogen occurs as this unit thins and may be reflective of slower depositional rates. Regional C-H trends for the Cleveland HGZ are also illustrated but are not as distinct as those of Sunbury Shale. Shale variability as determined by the coefficients of variation in Table I is generally 2-3 times greater for the D-series as compared to the K-series samples. This is accounted for by the greater regional change within the D-series area. Region trends for sulfur generally follow carbon for both units, but levels of the element are noticeably lower in the Cleveland unit relative to the Sunbury.

Organic Geochemistry - Fischer Assay Relationships

Conventional and modified Fischer Assay analyses have been performed on many Sunbury and Cleveland HGZ oil shale samples. The meaning of Fischer Assay results when applied to Eastern U. S. oil shales is somewhat ambiguous. Such results do provide a basis for comparison among the study samples but probably underestimate the amount of extractable oil from the shale and, consequently, do not provide an accurate method for assessing the total recoverable energy from these shales. Comments concerning the applicability of the Fischer Assay test to eastern shales have been made in previous reports by our colleagues (10, 11) and generally indicate that these oil shales are much more sensitive to heating rate, product removal and retort atmosphere variables. Our data also indicate that Fischer Assay data for the same samples among different

performing laboratories is quite variable and is probably indicative of both laboratory and oil shale characteristics.

When the body of Fischer Assay data on the K-series samples is evaluated, mean values for the weighted averages of these cores are 10.3 and 11.9 gal/ton for Sunbury and Cleveland HGZ, respectively. Coefficients of variation of 8.2% (Sunbury) and 6.9% (Cleveland HGZ) were observed with a total range of assay values ranging from 5.4 to 18.4 gals/ton. Current data for some D-series samples are given in Figure 6, which illustrates the Fischer Assay-raw oil shale carbon content relationship for the two oil shale units. It is evident that the Cleveland oil shale yields slightly more oil than the Sunbury oil shale, in spite of the fact that the Sunbury Shale averages more carbon per unit weight. This same relationship was observed for the two oil shale units from the K-series (6) and is assumed to be reflective of kerogen differences between the two oil shales. Correlation of Fischer Assay with hydrogen content yields slightly better correlations indicating again the criticality of the hydrogen content of these shales.

Illustrative Fischer Assay yields and associated oil and gas composition data are presented in Table II for both eastern (29) and western (8) oil shales of nominally similar organic carbon content. The eastern oil shales yield more gas and water and less oil than the western oil shale used for comparison. The major differences in the oil composition include comparatively lower nitrogen and higher sulfur contents for the Sunbury and Cleveland shale oils. The lower H/C ratio for the eastern oils indicate a more aromatic oil, as reported previously (30). Assay contents with less C_3-C_6 and CO_2 contents. The lower C_3-C_6 levels in the case of the eastern oil shales is due to a more efficient condensation of those gases to the liquid product in our assay procedures (10, 11). Gas cleanup would ultimately be expected to yield a higher BTU gas for the eastern oil shale-derived gas than a corresponding western gas due to elimination of H_2S in the former and high CO_2 levels and condensation of much of the C_4-C_6 range in the latter. Finally, it should be emphasized that the compositional information presented is based on Fischer Assay retorting procedures and may not be entirely representative of products produced under commercial scenarios.

INORGANIC GEOCHEMISTRY

Mineralogic Composition

The subject shales are designated silty shales due to their high quartz content. The mineralogic composition of these shales has been studied (12-16) and is summarized in Table III. Illite (2M), muscovite and/or illite/smectite are the predominant clays found in these shales.

Stratigraphic Distribution and Regional Trends

Major and trace element determinations were performed and are presented as weight percent or ppm of the 500°C ash fraction of the samples. This was done to eliminate the effect of variation in organic content and to facilitate comparisons.

When the major element chemistry for the various stratigraphic units are compared, no large differences are found (Table IV). The concentration of Al_2O_3 in the shales is less than what would be expected from a clay shale, which together with the SiO_2 content, substantiates its significant quartz content. The level of K_2O present (about 4%) indicates that the clays are primarily illite or muscovite-mica which agrees with mineralogic determinations made on the shales. The CaO concentration in all of the stratigraphic units is low (generally less than 1.0% (Table IV)), also in agreement with the previous observations made for mineral carbon. Calcium content is generally higher in the Huron, particularly in the D-5 through D-8 cores where the Duffin and Ravenna lithologies are present. There is also a slight geographic trend of increasing CaO concentrations from north to south in the study area.

The coefficients of variation determined among the cores for the major element oxides are generally very low (Table IV) and in many cases almost at the level of analytic uncertainty. Two exceptions to this are CaO and P_2O_5 which are associated with carbonate minerals and phosphate nodules. These are not part of the primary lithologies of the shale and are subject to being either locally abundant or absent.

Unlike the organic elements, the major element chemistry does not show large stratigraphic zonation compared to its lateral continuity. Coefficients of variation for the stratigraphic intervals are only slightly greater than those calculated for the average core data. However, the concentration and distribution of the determined trace elements are stratigraphically controlled. Highest concentrations are found in the Sunbury, followed by the Cleveland and the Huron. The elements which show the greatest zonation based on stratigraphic unit include Mo, Ni, V and Zn. Each of these elements is found to have concentrations in the Sunbury at levels of 2-3 times those of the other units (Table IV). As in the case of the major elements, the coefficients of variation calculated for the trace elements among the cores for the stratigraphic intervals are very low in most cases (Table IV). Unlike the majors, however, the stratigraphic variations are high. This is

reflective of zonation within the individual stratigraphic units.

TABLE II
FISCHER ASSAY YIELDS WITH OIL AND GAS COMPOSITION DATA FOR
EASTERN VS WESTERN OIL SHALES

Oil Shale Formation	Sunbury ^a	Cleveland ^b	Green River ^c
Yields			
Oil, gal/ton	14.4	13.4	29.8
Gas, ft ³ /ton	684	740	461
Water, gal/ton	9.8	16.6	3.8
Oil Composition			
C, wt %	83.25	82.41	84.80
H, wt %	10.35	10.11	11.60
N, wt %	0.86	0.77	1.96
S, wt %	2.38	2.75	0.60
Density	0.9197	0.9199	0.9180
Btu/lb	17,800	17,800	18,750 ^d
Gas Composition, Vol %			
H ₂	37.0	30.6	25.7
CH ₄	22.2	24.0	16.5
C ₂ H ₄	1.50	1.60	2.30
C ₂ H ₆	5.98	6.09	6.7
C ₃ -C ₆	4.34	3.88	11.7
CO ₂	5.53	7.16	31.1
CO	3.33	4.14	0.7
H ₂ S	20.4	15.2	1.0
Btu/SCF	743	740	776 ^d

- Data from (29), sample SUN-002, Lewis Co., KY, organic carbon = 13.85%.
- Data from (29), sample CLE-002, Lewis Co., KY, organic carbon = 14.54%.
- Data from (8), sample 482B 'B', Anvil Points, CO, organic carbon = 13.61%.
- Calculated by authors.

TABLE III
MODAL MINERALOGIC COMPOSITION OF DEVONIAN OIL SHALES

	Cleveland (12)	Chattanooga (14-16)
Quartz	30	20-25
Pyrite	5	10-15
Illite	39] -25-30
Illite/Muscovite] -20	
Illite/Smectite Mixed Layered		
Kaolinite	Trace	Minor
Chlorite	7	Trace
Carbonates	Minor	Variable
Feldspar	Minor	10
Organics	(on Ash Basis)	15-20

TABLE IV

INORGANIC COMPOSITION FOR K- AND D-SERIES OIL SHALES

	K-Series				D-Series			
	Sunbury	Cleveland Shale		Huron	Sunbury	Cleveland Shale		Huron
	Shale	Total	HGZ	Shale	Shale	Total	HGZ	Shale
SiO ₂ ^a	63.7(3) ^b	66.6(1)	66.5(1)	64.4(1)	64.18(3)	65.78(1)	68.16(2)	61.93(2)
TiO ₂	.8(5)	.9(1)	.8(1)	.9(1)	.76(6)	.85(3)	.82(2)	.85(4)
Al ₂ O ₃	16.7(6)	16.4(1)	16.2(1)	16.6(1)	15.58(2)	15.57(3)	15.15(4)	16.12(4)
Fe ₂ O ₃	8.7(5)	6.8(2)	7.0(3)	7.9(3)	8.12(11)	6.67(4)	6.83(6)	8.20(4)
CaO	.4(28)	.6(21)	.6(20)	.9(29)	.88(114)	.90(36)	.84(43)	1.33(64)
MgO	1.5(6)	1.3(3)	1.4(2)	1.3(3)	1.43(4)	1.37(5)	1.36(5)	1.78(22)
K ₂ O	4.4(7)	4.3(1)	4.2(2)	4.3(1)	4.11(3)	4.13(3)	4.08(3)	4.26(3)
Na ₂ O	.4(20)	.5(13)	.5(13)	.5(8)	.38(19)	.50(15)	.47(18)	.54(11)
P ₂ O ₅	ND	ND	ND	ND	.29(77)	.22(44)	.28(48)	.12(23)
Ba ^c	645(4)	619(3)	607(4)	633(3)	622(7)	570(4)	568(4)	564(5)
Co	24(3)	21(2)	20(2)	25(2)	24(6)	19(3)	19(4)	27(3)
Cr	200(3)	159(2)	195(4)	90(1)	175(10)	151(19)	185(4)	93(4)
Cu	113(3)	91(3)	111(4)	57(3)	134(9)	97(6)	114(5)	74(20)
Mo	281(5)	94(3)	89(8)	66(5)	248(15)	104(4)	92(7)	86(6)
Ni	272(3)	125(9)	141(2)	81(3)	288(14)	129(4)	139(3)	96(13)
V	1533(5)	760(5)	1024(5)	209(3)	1155(24)	677(4)	796(6)	216(5)
Zn	1126(6)	444(5)	622(7)	144(8)	1202(15)	412(8)	510(7)	173(9)
U	37(5)	20(7)	20(7)	ND	43(15)	21(4)	19(4)	22(6)

a. Wt % in 500°C Ash

b. Coefficients of variation x 100

c. ppm (wt) in 500°C Ash

The concentrations of certain trace elements also appear to show regional trends. As an example of these trends, Figure 7 presents the regional distribution of Mo, Ni, V and Zn. Each of these elements shows a slight overall decrease in concentration between Lewis County (K-9 or 8) in the north and Estill County (D-10) in the south for both the Sunbury and the Cleveland HGZ. However, the regional trends for the Sunbury are somewhat obscured by an increase in concentration for Mo, Ni and Zn and a decrease in concentration for V in the region between Montgomery and Powell Counties. The cause for these regional anomalies is presently unclear.

Trace Metal Affinities

Trace-element and major-element associations in the oil shales have been a subject of several studies (17, 18). In general, the trace elements can be divided into three groups: those which have an affinity for carbon (Cu, Cr, Ni, V), those which have an affinity for sulfur (Co, Zn), and those which have an affinity for the silicates and carbonates (Ba) (not reported here). The associations are also, to some degree, stratigraphically dependent. For example, in Lewis and Fleming Counties, Cr, Ni and V concentrations were found to be strongly correlated with carbon concentration (correlation coefficients = .95, .91 and .82, respectively) in the shales of the Cleveland Member, but not strongly correlated in the Huron and Sunbury (18). Zn is listed as having an affinity for sulfur, even though it did not have a significant correlation. It is often associated with its own mineral phase (sphalerite, ZnS) and the lack of correlations with total sulfur is not surprising. Correlation coefficients for the trace metal affinities found in the K-series is presented in Table V. The trace element affinities discussed are similar to the observations of Keogh (19) who studied the trace element chemistry of the organic matter separated from the shale.

Economic Implications of Trace Element Geochemistry

The regional trends in the stratigraphy and geochemistry of the defined economic units are relevant to mining, processing and by-product recovery potential. Trace metal data for the total economic zone are presented in Table VI; these data are weighted for the thickness of the Cleveland HGZ and Sunbury Shale and, therefore, are representative of potential feedstocks for a retorting system.

The high concentration of metals in the eastern oil shales has led to considerable

speculation concerning the potential for by-product metals recovery (20-24). Much of this interest has centered on the recovery of such metals as Mo, V, Ni, Cu, U, Th, and Al. At present, the potential for the recovery of these metals appears to be sub-economic (1).

TABLE V
CORRELATION COEFFICIENTS FOR METALS AFFINITIES OF EASTERN SHALES

Element	Lithologic Unit	K-Series Data	
		Carbon	Sulfur
Co	Sunbury	-.38	.85
	Cleveland	.23	.76
	Huron	.67	.90
Cr	Sunbury	.17	-.34
	Cleveland	.95	.51
	Huron	-.45	-.55
Cu	Sunbury	.81	-.12
	Cleveland	.95	.44
	Huron	.54	.49
Mo	Sunbury	.15	.08
	Cleveland	.11	-.12
	Huron	.90	.78
Ni	Sunbury	.40	.25
	Cleveland	.91	.37
	Huron	.40	.17
V	Sunbury	.07	.15
	Cleveland	.82	.10
	Huron	.01	-.17

Underlined coefficients considered significant.

TABLE VI
TRACE METAL CONTENT OF TOTAL ECONOMIC ZONES

	K-9 Lewis County	K-4 Fleming County	D-1 Rowan County	D-4 Bath County	D-6 Montgomery County	D-8 Powell County	D-10 Estill County	Study Area Mean
Mo	158	151	175	152	145	119	99	148
Ni	191	187	187	172	184	172	153	179
V	1226	1164	1058	911	891	795	738	1025
Zn	819	749	728	663	698	636	545	723

Several of the metals present in eastern oil shales are of importance from a processing standpoint, however. Certain elements, particularly those shown to be associated with carbon (Table V) may tend to concentrate in the oils produced during retorting. Of particular concern in process and oil upgrading are As, V and Ni. These elements are known to be a problem in upgrading oils due to cracking and reforming catalyst poisoning. During upgrading, these oils require processing to remove these elements. The high trace element concentrations of Ni and V in the eastern oil shales (Tables IV and VI) coupled with their organic affinity imply that they may partition to the oils during retorting. Although the As values for these oil shales are limited, preliminary data for the units are: Sunbury (5-300 ppm), Cleveland (1-80 ppm) and Huron (30-50 ppm). Arsenic also is expected to concentrate in the oils during retorting. These predictions are somewhat confirmed by preliminary data presented in Table VII for a single two stage retort produced oil (25). The metals composition of other crude oils are also presented for comparison.

TABLE VII

TRACE ELEMENT COMPOSITION OF AN EASTERN SHALE OIL (CHATTANOOGA),
A WESTERN SHALE OIL AND TWO PETROLEUM CRUDES

	Chattanooga		Paraho	Alberta Canada Devonian Crude	Venezuelan Crude	Nigerian Crude	Iranian Crude	California Terhasy Heavy Crude
	1st Stage	2nd Stage	(25)	(26)	(27)	(28)	(28)	(27)
As (ppm)	50	59	28	.111	.005	1.2	.095	.66
Ni (ppm)	5.0	5.9	1.8	9.4	117	5.9	12	94
V (ppm)	6.3	6.3	.2	13.6	1120	9.5	53	7.5

CONCLUSIONS

The principal form of carbon present in the oil shale is as organic matter. Mineral-bound carbon was found to be insignificant, with the exception of the Duffin zone, a localized dolomitic lithology present near the base of the Huron.

Carbon and hydrogen are strongly zoned stratigraphically, with highest levels present in the upper and lower portions of the oil shale section. The variability of the organic chemistry among the study cores is low in comparison.

The Fischer Assay yields of the two economic units were similar, averaging 10.3 gal/ton for the Sunbury shale and 11.9 gal/ton for the Cleveland HGZ. The Fischer Assay data underestimates the maximum potential oil yield of these shales, however.

The major element chemistry is found to be both stratigraphically and laterally consistent for the oil shales.

Trace element concentrations are found to be highest in the Sunbury Shale, followed by the Cleveland and Huron members of the Ohio Shale. Trace element concentrations were found to be strongly stratigraphically zoned, but relatively consistent, among the cores.

The major regional trends affecting mining, processing and by-product recovery (north to south and including Lewis and Fleming Counties) include:

1. the thinning and virtual disappearance of the stratigraphic intervals separating the Sunbury Shale and Cleveland HGZ;
 2. the thinning of the Sunbury Shale;
 3. an increase in carbon and hydrogen in the Sunbury Shale (concomitant with thinning);
- and
4. a decrease in trace element content for the total defined economic zone.

Trace elements exhibited three types of association: those having an affinity for carbon (Cu, Cr, Ni, V), those having an affinity for sulfur (Co, Zn) and those having a silicate and/or carbonate affinity (Ba).

Trace elements, particularly those associated with the oil shale kerogen, may be incorporated into the oil product and present subsequent processing problems.

ACKNOWLEDGMENTS

This study was funded by the U. S. Department of Energy in cooperation with the Kentucky Department of Energy. This work is part of a large effort by the Institute for Mining and Minerals Research to characterize the Devonian-Mississippian oil shales of Kentucky and their economic potential for oil and by-product metals recovery for the Kentucky Department of Energy. The support of both the U. S. Department of Energy and the Kentucky Department of Energy is greatly appreciated.

Special acknowledgments are extended to the staff of IMMR at the Kentucky Center for Energy Research Laboratory for their timely contributions to the analytics and their invaluable suggestions and contributions to the substance of this project.

LITERATURE CITED

- (1) Vyas, K. C. , Aho, G. D. , Robl, T. L. , Synthetic Fuels from Eastern Oil Shale, Vols. I and II, Final Report, Project NC-5477, Federal Grant No. DE-FG-4480R410185, prepared for the Buffalo Trace Area Development District, Maysville, KY (1981).
- (2) Schwab, H. R. , Norris, R. L. , Studies of the New Albany Shale in Western Kentucky, Final Report, DOE/METC/8215-1, Morgantown Energy Technology Center, Morgantown, WV (1980).
- (3) Provo, L. J. , Kepferle, R. C. and Potter, P. E. , Amer. Assoc. Petr. Geol. Bull. , 62, 9, 1703 (1978).
- (4) Barron, L. S. and Ettenson, F. R. , Geol. Soc. Amer. Abstracts with Programs, 12, 218 (1980).
- (5) Barron, L. S. and Ettenson, F. R. , Paleocology of the Devonian-Mississippian Black-Shale Sequence in Eastern Kentucky with an Atlas of Some Common Fossils, DOE/ET/12040-151, Morgantown Energy Technology Center, Morgantown, WV (1981).
- (6) Barron, L. S. , Bland, A. E. , Robl, T. L. , Koppenaal, D. W. and Thomas, G. A. , Symp. Papers Synthetic Fuels from Oil Shale II, Oct. 26-29, 1981, Institute of Gas Tech. Chicago, IL (1982).
- (7) Bland, A. E. , Robl, T. L. and Koppenaal, D. W. , Proceedings--1981 Eastern Oil Shale Symp. , Nov. 15-17, 1981, Insti. for Mining and Minerals Research, Lexington, KY (1981).
- (8) Singleton, M. F. , Koskinas, G. J. , Burnham, A. K. and Raley, J. H. , Assay Products from Green River Oil Shale, Report UCRL-53273, Lawrence Livermore Laboratory, Livermore, CA (1982).
- (9) Larson, O. A. and Wen, C. S. , 14th Oil Shale Symp. Proceedings, April 22-24, 1981, Colorado School of Mines, Golden, CO (1981).
- (10) Rubel, A. M. and Coburn, T. T. , Proceedings--1981 Eastern Oil Shale Symp. , Nov. 15-17, 1981, Insti. for Mining and Minerals Research, Lexington, KY (1981).
- (11) Coburn, T. T. and Rubel, A. M. , Fuel Processing Tech. , submitted 1982.
- (12) Hosterman, J. W. and Whitlow, S. I. , USGS Open File Report 81-585, U. S. Geological Survey, Denver, CO (1981).
- (13) Markowitz, G. , Masters Thesis, Dept. of Geology, Univ. of Kentucky, Lexington, KY (1979).
- (14) Bates, T. F. , Geol. Soc. Amer. Bull. , 68, 1305 (1957).
- (15) Miller, M. L. , Masters Thesis, Dept. of Geology, Univ. of Kentucky, Lexington, KY (1978).
- (16) Conant, L. C. and Swanson, V. , USGS Prof. Paper No. 357, U. S. Geological Survey, Denver, CO (1961).
- (17) Bland, A. E. , Robl, T. L. and Koppenaal, D. W. , Amer. Assoc. Petrol. Geol. Bull. , 65, 903 (1981).
- (18) Bland, A. E. , Barron, L. S. and Robl, T. L. , Geol. Soc. Amer. Abstracts with Programs, 13, 7, 411 (1981).
- (19) Keogh, R. A. , Chapter IX, Geologic and Geochemical Studies of the New Albany Shale Group (Devonian-Mississippian) in Illinois, Illinois State Geological Survey, Univ. of Illinois, Urbana, IL (1980).
- (20) Krouse, C. S. , Chapter II, Oil Shales of Kentucky, Series VI, Vol. 24, Kentucky Geological Survey, Lexington, KY (1925).
- (21) Robeck, B. C. and Conant, L. C. , USGS Trace Element Investigations Report No. 64, U. S. Geological Survey, Denver, CO (1951).
- (22) Chase, C. K. , Symp. Papers Synthetic Fuels from Oil Shale , Dec. 3-6, 1979, Insti. of Gas Tech. , Chicago, IL (1980).
- (23) Matschler, P. H. , Hill, T. T. and Williams, B. B. , U. S. Bureau of Mines Report JC 8700, Pittsburgh, PA (1976).
- (24) Gilliam, T. M. , Caron, R. M. , Ryan, A. D. and Watson, J. S. , Proceedings--1981 Eastern Oil Shale Symp. , Nov. 15-17, 1981, Insti. for Mining and Minerals Research, Lexington, KY (1981).
- (25) Sullivan, R. F. , Chevron Research Co. , personal communication (1982).
- (26) Hitchon, B. , Filby, R. H. and Shah, K. R. , in Role of Trace Metals in Petroleum, T. F. Yen, ed. , Ann Arbor Science Publishers, Ann Arbor, MI (1975).
- (27) Filby, R. H. , in Role of Trace Metals in Petroleum, T. F. Yen, ed. , Ann Arbor Science Publishers, Ann Arbor, MI (1975).
- (28) Filby, R. H. , Shah, K. R. and Yaghmaie, F. , in Ash Deposits and Corrosion Due to Impurities in Combustion Gases, R. W. Bryers, ed. , Hemisphere Publishing Corp. and McGraw-Hill Co. , New York, NY (1977).

- (29) Rubel, A. , Taulbee, D. , Coburn, T. , Thomas, G. and Yates, L. , Proceedings--1982 Eastern Oil Shale Symp. , Oct. 11-13, 1982, Inst. for Mining and Minerals Research, Lexington, KY (1982).
- (30) Fabry, D. A. and Moore, H. F. , Proceedings--1981 Eastern Oil Shale Symp. , Nov. 15-17, 1981, Inst. for Mining and Minerals Research, Lexington, KY (1981).

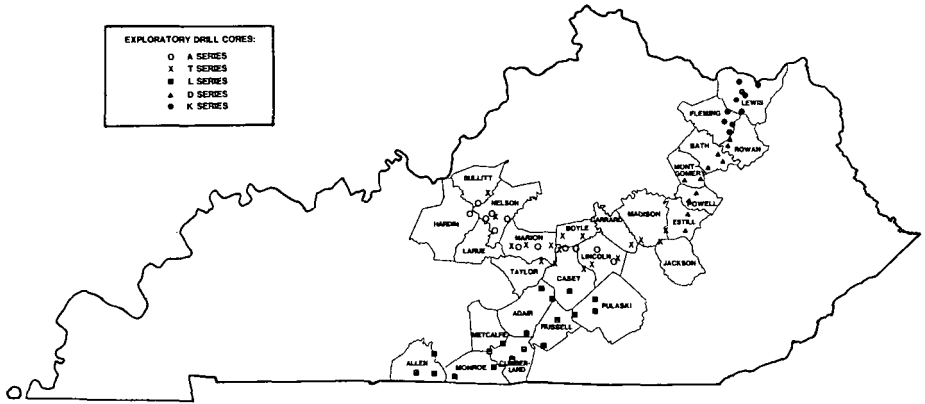


Figure 1. Depiction of oil shale resource exploration core sites in Kentucky. Devonian and Mississippian oil shales outcrop in the counties indicated. Drill cores designated as K- and D-series are the subject of this report.

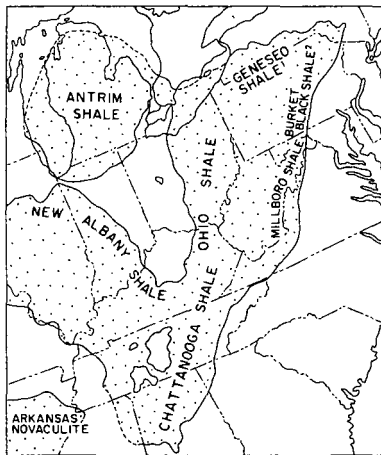


Figure 2. Geographic distribution of Devonian-Mississippian oil shale in the Eastern United States.

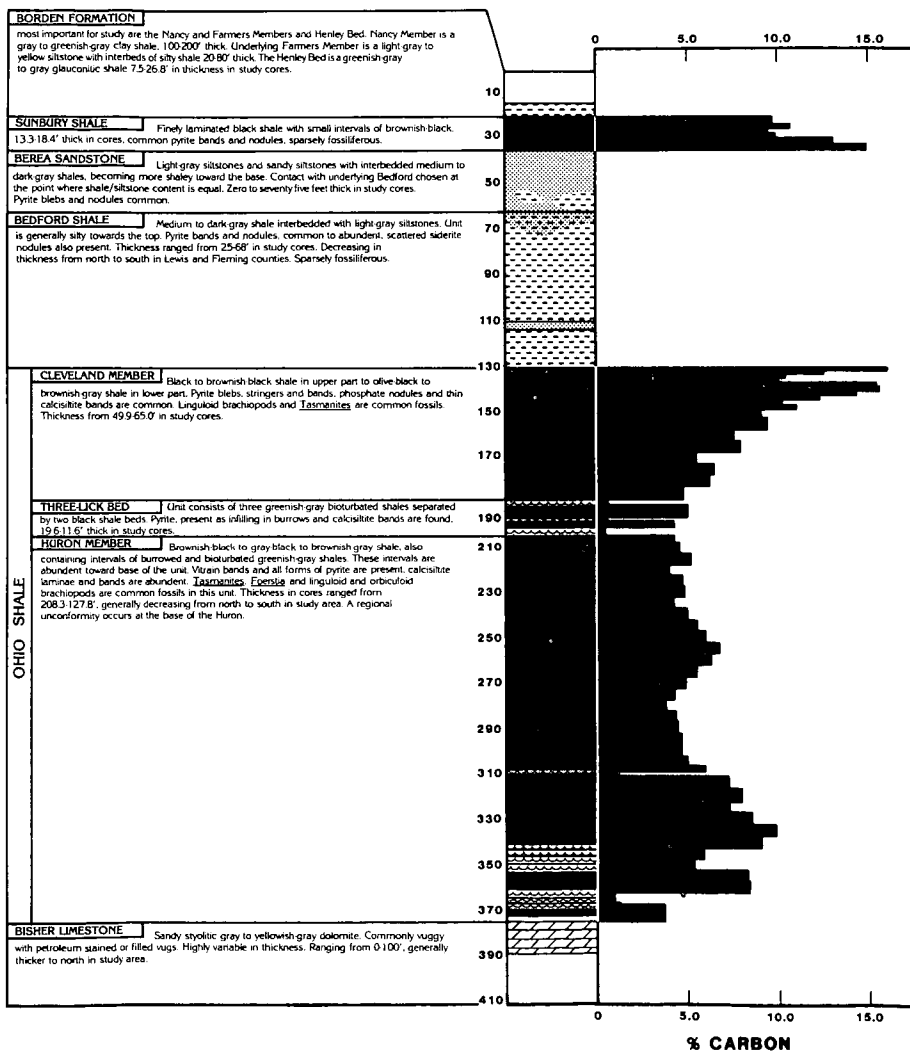


Figure 3. General stratigraphic column for the Devonian-Mississippian black shales in Eastern Kentucky.

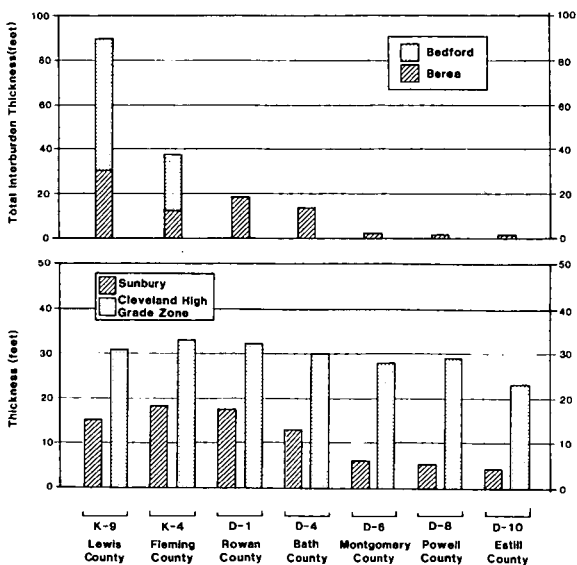


Figure 4. Thicknesses of economic oil shale units and their associated interburden units for selected cores in study area.

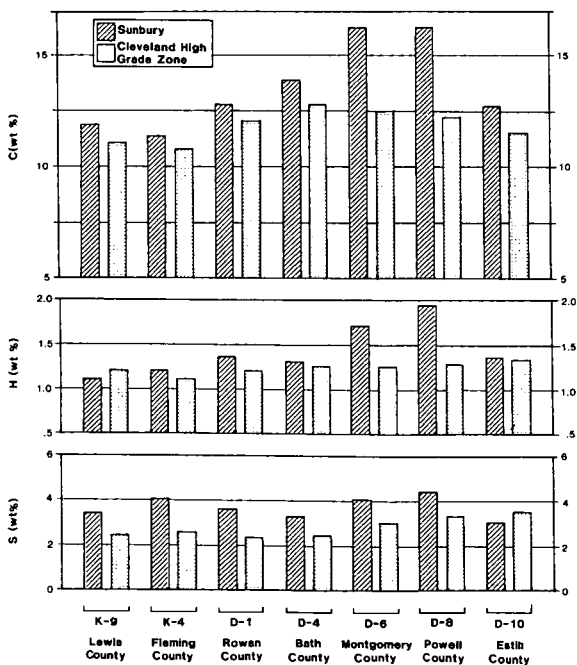


Figure 5. Regional trends for carbon, hydrogen, and sulfur in selected cores of study area.

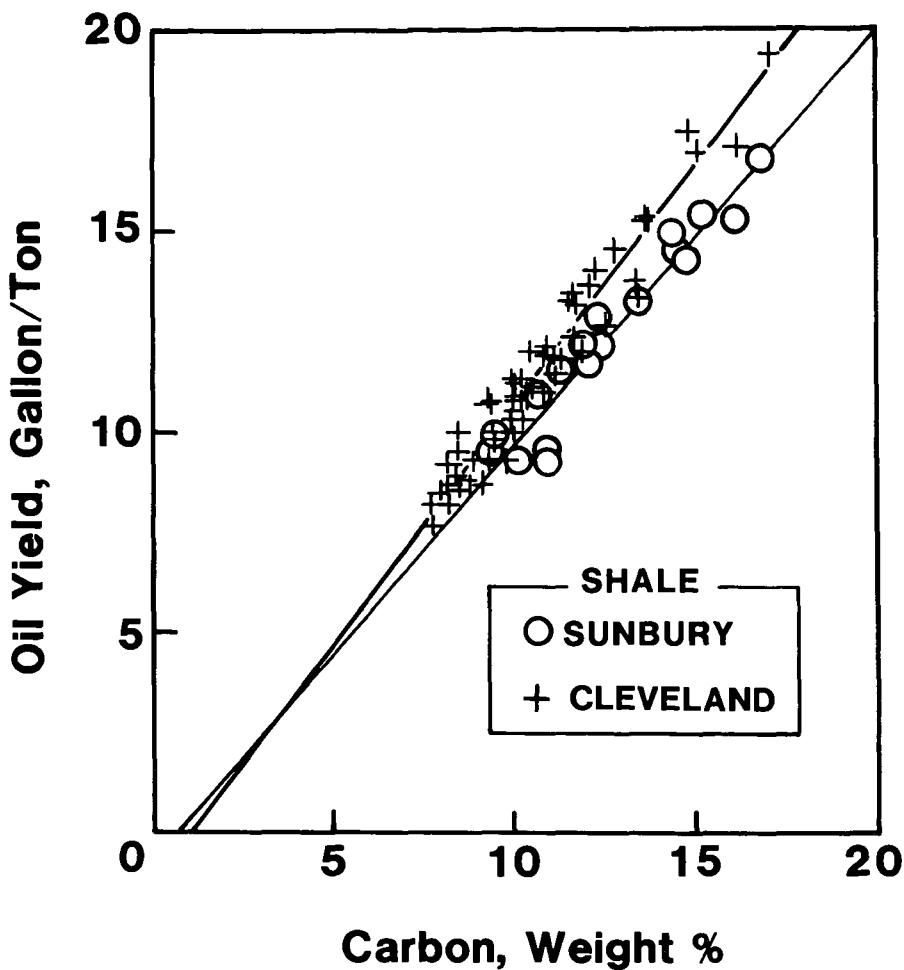


Figure 6. Plot of Fischer Assay yields and carbon content for D-series oil shales. Regression data are:

Sunbury Shale: Oil yield = 1.03 (%C) - 0.69 (r = .97)

Cleveland Shale: Oil yield = 1.18 (%C) - 1.16 (r = .97)

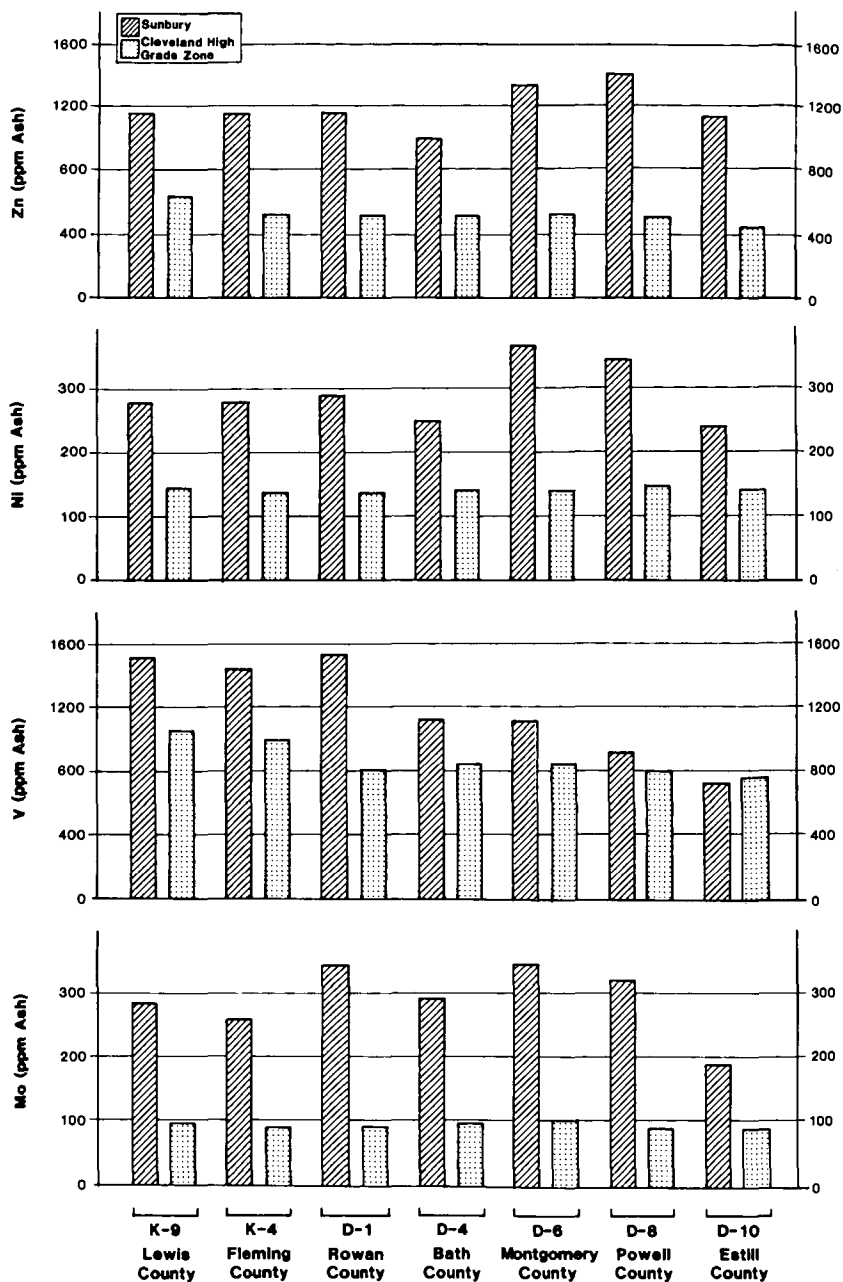


Figure 7. Regional trends for certain trace elements in selected cores of study area.

SYMPOSIUM ON GEOCHEMISTRY AND CHEMISTRY OF OIL SHALE
PRESENTED BEFORE THE DIVISIONS OF FUEL CHEMISTRY, GEOCHEMISTRY,
AND PETROLEUM CHEMISTRY, INC.
AMERICAN CHEMICAL SOCIETY
SEATTLE MEETING, MARCH 20 - MARCH 25, 1983

EASTERN DEVONIAN SHALES: ORGANIC GEOCHEMICAL STUDIES,
PAST AND PRESENT

By

I. A. Breger, P. G. Hatcher, L. A. Romankiw
U. S. Geological Survey, Reston, Virginia 22092
and
F. P. Miknis
Laramie Energy Technology Center, Laramie, Wyoming 82071

ABSTRACT

The Eastern Devonian shales are represented by a sequence of sediments extending from New York state, south to the northern regions of Georgia and Alabama, and west into Ohio and to the Michigan and Illinois Basins. Correlatives are known in Texas. The shale is regionally known by a number of names: Chattanooga, Dunkirk, Rhinestreet, Huron, Antrim, Ohio, Woodford, etc. These shales, other than those in Texas, have elicited much interest because they have been a source of unassociated natural gas. It is of particular interest, however, that most of these shales have no associated crude oil, in spite of the fact that they have some of the characteristics normally attributed to source beds. This paper addresses some of the organic geochemical aspects of the kerogen in these shales, in relation to their oil generating potential. Past organic geochemical studies on Eastern Devonian shales will be reviewed. Recent solid state ^{13}C NMR studies on the nature of the organic matter in Eastern Devonian shales show that Eastern Devonian shales contain a larger fraction of aromatic carbon in their chemical composition. Thus, despite their high organic matter contents, their potential as a petroleum source rock is low, because the kerogen in these shales is of a "coaly" nature and hence more prone to producing natural gas.

SYMPOSIUM ON GEOCHEMISTRY AND CHEMISTRY OF OIL SHALE
PRESENTED BEFORE THE DIVISIONS OF FUEL CHEMISTRY, GEOCHEMISTRY
AND PETROLEUM CHEMISTRY, INC.
AMERICAN CHEMICAL SOCIETY
SEATTLE MEETING, MARCH 20-25, 1983

GEOLOGICAL SETTING OF OIL SHALES IN THE PERMIAN PHOSPHORIA FORMATION
AND SOME OF THE GEOCHEMISTRY OF THESE ROCKS

By

Edwin K. Maughan
U. S. Geological Survey

SUMMARY

Recent studies of the Meade Peak and the Retort Phosphatic Shale Members of the Phosphoria Formation have investigated the organic carbon content and some aspects of hydrocarbon generation from these rocks. Phosphorite has been mined from the Retort and Meade Peak members in southeastern Idaho, northern Utah, western Wyoming and southwestern Montana. Organic carbon-rich mudstone beds associated with the phosphorite in these two members also were natural sources of petroleum. These mudstone beds were differentially buried throughout the region so that heating of these rocks has been different from place to place. Most of the Phosphoria source beds have been deeply buried and naturally heated to catagenetically form hydrocarbons. Deepest burial was in eastern Idaho and throughout most of the northeastern Great Basin where high ambient temperatures have driven the catagenesis to its limit and beyond to degrade or to destroy the hydrocarbons. In southwest Montana, however, burial in some areas has been less than 2 km, ambient temperatures remained low and the kerogen has not produced hydrocarbons (2). In these areas in Montana, the kerogen in the carbonaceous mudstone has retained the potential for hydrocarbon generation and the carbon-rich Retort Member is an oil shale from which hydrocarbons can be synthetically extracted.

The Phosphoria Formation was deposited in a foreland basin between the Cordilleran geosyncline and the North American craton. This foreland basin, which coincides with the area of deposition of the two organic carbon-rich mudstone members of the Phosphoria, has been named the Sublett basin (Maughan, 1979). The basin has a northwest-southeast trending axis and seems to have been deepest in central Idaho where deep-water sedimentary rocks equivalent to the Phosphoria Formation are exceptionally thick. The depth of the basin was increasingly shallower away from central Idaho toward the Milk River uplift -- a land area in Montana, the ancestral Rocky Mountains. The basin is composed of land areas in Colorado, the Humboldt highland in northeastern Nevada and intervening carbonate shelves in Utah and Wyoming. The phosphorites and the carbonaceous mudstones were deposited on the foreslope between the carbonate and littoral sand deposits on the shelf and the dominantly cherty mudstone sediments in the axial part of the basin.

Paleomagnetic evidence indicates that in the Permian the region would have been within the northern hemispheric trade wind belt; and wind-direction studies determined from studies of sand dunes, indicate that the prevailing winds from the Milk River uplift would have blown offshore across the Phosphoria sea. Offshore winds would have carried surface water away from the shore and generated upwelling in the sea in eastern Idaho and adjacent areas in Montana, Wyoming and Utah.

Prior to deposition of the Phosphoria, the region was the site of extensive deposition of shallow-water carbonate sediments. Equivalent rocks in the northern part of the basin are dominantly sandstone derived from the adjacent Milk River uplift and similar sandstone strata in the southeastern sector were derived from the ancestral Rocky Mountains uplift. Tectonic subsidence of the Sublett basin in part of the region seems to have provided a sea-floor profile favorable for upwelling circulation and the shift in deposition from regional carbonates and local sandstone into a more complex depositional pattern that included the accumulation of the mudstone-chert-phosphorite facies that comprises the Phosphoria Formation. High biological productivity and the accumulation of sapropel on the sea floor is associated with contemporary coastal upwelling (1) and similar environmental and depositional conditions are attributed to the rich accumulations of organic matter in the Phosphoria Formation.

Sapropelic mudstone and phosphorite composing the Meade Peak Member are approximately 60 m thick near the center of the Sublett basin. The Meade Peak thins to the north, east and south away from the area of maximum sapropel accumulation and towards areas of shoaling, which were unfavorable environments for depositional preservation of organic matter near the margin of

the Phosphoria sea. The Retort Member is thickest in southwestern Montana where it is approximately 30 m thick. The Retort closely resembles the Meade Peak except that its thickness is about half that of the Meade Peak and its shorelines and apparent depocenter are displaced northward from those of the Meade Peak.

Organic carbon content in the Meade Peak is greatest, averaging about 9 wt %, near the Wyoming border east of Pocatello, Idaho (3) and is offset northeastward from the central axis of the basin onto the flank of the area of thickest accumulation of organic carbon-rich mudstone. This offset position of the maximum organic carbon concentration is believed to approximately coincide with an area of upwelling marine currents from out of the deeper parts of the Sublett basin onto the submarine slope of fringing barrier island and carbonate bank deposits. Organic carbon content of the Retort is greatest, averaging about 10 wt %, near Dillon, Montana. The center of maximum organic carbon deposition in both the Meade Peak and the Retort approximately coincides with that of maximum Phosphorus concentration.

Traces of many metals, some of unusually high concentration (4), occur in the carbonaceous shale and phosphorite beds of the Phosphoria. The loci of the average concentration of several metals in the carbonaceous shale members also approximate the loci of organic carbon and phosphorus. It seems likely that the trace metals were concentrated from the sea water by the organisms living in the Phosphoria sea, as were the carbon and the phosphorus, but some metals have been diagenetically adsorbed onto the residual organic matter or are incorporated in the clay or other minerals in these rocks. The coincidence of the metallic concentrations, the phosphorus and the organic carbon in the Retort and the Meade Peak are believed to confirm the indicated location of centers of upwelling in southwest Montana and in the vicinity of the Idaho-Wyoming border.

Petroleum generation from the Phosphoria Formation has been investigated and a total yield of 30.7 tons is estimated by Claypool and others (2). Oil expelled from these rocks has been discovered and produced from the Pennsylvanian Tensleep Sandstone and the middle Permian Park City Formation in central Wyoming. Oil in the Lower Permian upper member of the Minnelusa Formation in northeastern Wyoming and adjacent areas as well as the probable Lower Permian part of the Weber Sandstone in northwestern Colorado has probably been derived from the Phosphoria Formation. Hydrocarbon generation has taken place in most of the region where burial has been in excess of about 2 km. In eastern Idaho, the critical depth of burial occurred as early as Late Triassic and regionally the maximum depth of burial of the Permian rocks is inferred to have been at the end of the Cretaceous Period, although sediments continued to accumulate in local, intermontane basins through the Paleocene and into early Eocene time (2). In southwest Montana, however, depth of burial has been less than 2 km, hydrocarbons have not been generated and the carbonaceous mudstones remain effective oil shales.

LITERATURE CITED

- (1) Brongersma-Sanders, Margeretha, The Importance of Upwelling Water to Vertebrate Paleontology and Oil Geology, K. Nederlandsche Akad. van Wetensch., afd. Naturk., Tweede Sect., Deel XLV, no. 4 (1948).
- (2) Claypool, G. E., Love, A. H. and Maughan, E. K., Organic Geochemistry, Incipient Metamorphism and Oil Generation in Black Shale Members of Phosphoria Formation, Western Inter. U.S.: Amer. Assoc. Petrol. Geologists Bull., v. 62, no. 1, 98-120 (1978).
- (3) Maughan, E. K., Organic Carbon in Shale Beds of the Permian Phosphoria Formation of Eastern Idaho and Adjacent States--A Summary Report, Wyoming Geological Assoc., 27th Annual Field Conf. Guidebook, p. 107-115 (1975).
- (4) _____, Organic Carbon and Selected Element Distribution in the Phosphatic Shale Members of the Permian Phosphoria Formation, Eastern Idaho and Parts of Adjacent States, U. S. Geological Survey Open-file Report 76-577 (1976).
- (5) _____, Petroleum Source Rock Evaluation of the Permian Park City Group in the Northeastern Great Basin, Utah, Nevada and Idaho, in Great Basin Guidebook, Rocky Mountain Assoc. of Geologists, Utah Geological Assoc., p. 523-530 (1979).

SYMPOSIUM ON GEOCHEMISTRY AND CHEMISTRY OF OIL SHALE
PRESENTED BEFORE THE DIVISIONS OF FUEL CHEMISTRY, GEOCHEMISTRY,
AND PETROLEUM CHEMISTRY, INC.
AMERICAN CHEMICAL SOCIETY
SEATTLE MEETING, MARCH 20 - MARCH 25, 1983

THE CHEMISTRY WHICH CREATED GREEN RIVER FORMATION OIL SHALE

By

J. W. Smith
Consultant, 1472 North Fifth Street, Laramie, Wyoming 82070

INTRODUCTION

The Green River Formation oil shales have been the object of only a limited amount of effort aimed at describing how they came to be. Much that has appeared looks at only one facet of a complex, integrated system. In 1925 Bradley (2) published an initial postulate which still has much strength although Bradley ultimately was moved away from this idea. Smith and Robb (16), Smith (13), and Smith and Lee (15) have extended Bradley's postulate to develop a comprehensive picture of the genesis of the Green River Formation deposits. These are summarized here.

GREEN RIVER FORMATION CHARACTERISTICS

The Eocene Green River Formation is unique in organic-rich sedimentary deposits. Nothing like it exists elsewhere. Although many collections of sedimentary rocks containing organic matter exist, the Green River Formation contains spectacularly large amounts making up much larger than average volume fractions of the total sediment. In addition this deposition persisted through literally millions of years. An excellent example of this is the oil shale sampled by the U. S. B. M. -A, E. C. Colorado Corehole No. 1 which demonstrated the existence of about 2100 feet (640 meters) of continuous oil shale (17). Average organic content through this section is nearly 25 volume percent of the total rock. This organic matter is remarkably uniform and relatively rich in hydrogen. The carbon-to-hydrogen weight ratio in organic matter throughout the Formation is about 7.7-7.8, similar to the high end of the petroleum spectrum and much lower than most other oil shales of the world. The only change in the nature of the organic matter through the 2100-foot section is decarboxylation with depth of burial (12,14). A study purporting to detect variations in organic matter through the oil shales in Colorado Corehole No. 1 (10) actually demonstrates the remarkable and persistent similarity of the organic matter in the Green River Formation thickness deposited over millions of years.

The lateral consistency of the Green River Formation deposition is also remarkable. Figure 1 compares oil yield histograms for about 500 feet (150 meters) of continuous oil shale at two locations in the Green River Formation (19). Figure 2 shows the locations of these two coreholes--about 85 miles apart. These histograms are deposition profiles correlated in time. They demonstrate the gross lateral persistence of oil shale deposition. This is also demonstratable on a much smaller scale. Figure 3 shows the stratigraphic variation across a 2-inch (5 cm) block. Trudell et al. (18) published a classic photograph indicating comparability of such markings over a 75-mile (120 km) span. A third level of persistence exists on a microscale. Annual depositional cycles produced varying. The varves are too small (~30 μ) to be photographed and reproduced here, but they couldn't even be located if they were not laterally persistent.

Associated with the lateral continuity of the formation is the lateral consistency of mineral composition. This might be startling except for the fact that the mineral suite in Green River Formation oil shale is uniform stratigraphically as well as laterally. This mineral suite is authigenic, formed by the chemistry of the lake. Two major mineral variations warrant mention, because they appear to belie mineral uniformity. One is the illite concentration deposited early in the formation's sedimentary history which was rather abruptly replaced by dolomite. The other is the appearance of truly remarkable minerals--nahcolite (NaHCO_3), dawsonite [$\text{NaAl}(\text{OH})_2\text{CO}_3$], shortite ($\text{Na}_2\text{CO}_3 \cdot 2\text{CaCO}_3$), and trona ($\text{Na}_2\text{CO}_3 \cdot \text{NaHCO}_3 \cdot 2\text{H}_2\text{O}$). These minerals are rare in the rest of the world but appear in billions of tons in the Green River Formation. An additional peculiarity is the formation of shortite and trona in the Wyoming deposits and the development of dawsonite and nahcolite in Colorado.

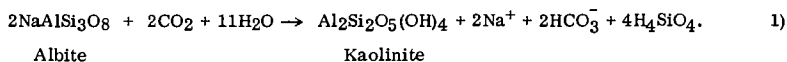
These characteristics pose a set of rather difficult problems in describing the genesis of the Formation. A geochemical postulate has been developed (15) to explain this genesis and its peculiarities. This pattern is outlined.

LAKE UINTA'S POSTULATED CHEMICAL HISTORY

Depositional conditions postulated for the Green River Formation must accommodate the major requirements described above. Colorado's deposits, formed in ancient Lake Uinta, offer the most complete example. Generalizations must be made in trying to evaluate briefly the conditions which formed Green River oil shale through perhaps six million years. Because the oil shale is virtually continuous, the conditions were also continuous. Consequently, generalization is appropriate.

The basic postulate for oil-shale genesis is a stratified lake, separating the lake waters into two non-mixing layers. Bradley (2) recognized this requirement in his early studies of the Green River Formation. A number of permanently stratified lakes, called meromictic lakes, exist currently in the United States (3) and several sets of conditions leading to stable stratification have been outlined by Hutchinson (6). Colorado's Lake Uinta probably began in the northwestern part of the present Piceance Creek Basin, where a long sequence of normal lacustrine sediment occurs. Thermal density differences probably produced the initial stratification. Three primordial lakes probably existed--the one in Colorado's Piceance Creek Basin, one in Wyoming north of the Uinta Mountains and one in Utah south of the Uinta Mountains. Since all three lakes did the same thing, the Green River Formation's development may have been due to minerals arising from the Uinta Mountains.

Hydrolysis of local silicates and aluminosilicates in the stratified lake's lower layer began to build up a chemical stratification. Garrels and Mackenzie (5, p. 175) give the following equation as an example of this hydrolysis, using albite as a simple specimen:



Albite

Kaolinite

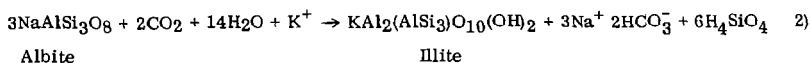
Notice that acid, represented here by CO_2 and water, is consumed and that sodium and bicarbonate ions are produced as albite alters to kaolinite. Decomposition of organic matter furnished carbon dioxide. Concentration of sodium carbonates and other dissolved salts in solution in water of the stratified lake's lower layer built up, raising the water density. The evolution from normal lacustrine sediments to oil shale in the northwestern part of the Piceance Creek Basin is continuous and without evidence of evaporative cycles (18). The acid-consuming hydrolysis indicated in Equation 1 probably was the primary mechanism which built up the water density. This created a remarkably stable chemical stratification in ancient Lake Uinta, lasting through the entire period of oil-shale deposition.

Permanent stratification of ancient Lake Uinta was accompanied by a limitation of the supply of materials reaching the lake's lower layer. Currents in the water of the lower layer had to be very slow or the organic matter deposited uniformly in the tiny varves would have accumulated unevenly. Currents in the water of the upper layer could not be strong because of the relatively small flow of water through a huge area. In slow currents larger clastic materials deposit near the lake shore. Only air-borne particles and water-borne particles small enough to remain suspended in slow currents could be distributed over the lake's huge area. Tiny particles, predominantly silicates, and organic debris plus the small amount of clastic material deposited on the edges of the lake made up the supply of material available to the lake. Both the amount and the composition of this supply was limited and continued to be so through much of the time oil shale was deposited.

Organic debris from the lake's upper layer fell into the lower layers. This organic matter made up a relatively large portion of the material reaching the lower layer of the stratified lake, not because the lake producing it teemed with life (it didn't) but because the lake strongly limited the available mineral matter. The organic matter chemically consumed the available oxygen. In the stratified lake no oxygen supply could reach the bottom layer which quickly became, and remained, a reducing environment. The reducing environment became powerful enough to continually hydrogenate organic matter, making the organic residue rich in hydrogen and poor in oxygen. Oil-shale deposition began.

Water of the lower layer must have been lethal to macrolife and probably also to microscopic life--bioturbation would have destroyed the varves and lamina. The upper or surface layer, however, must have been fresh enough for life to exist because organic matter was continuously deposited in the sediment. In its travel through the lake's lower layer, the organic matter was exposed to basic reducing solutions which digested it and homogenized it. Only particular chemical structures would survive exposure to the basic environment, automatically selecting similar materials. In addition, the strongly reducing environment in the lake and the sediment would hydrogenate the organic matter to produce the hydrogen-rich organic matter. This mode of deposition over a wide area explains the lateral uniformity observed in element composition of organic matter in Mahogany zone oil shale (11), and the similarity in properties of the oil-shale organic matter over the entire deposit. The paucity of microfossils in the oil shale, limited largely to an occasional gas scale and the like, illustrates the power of the lake's lower layer to digest organic matter.

As hydrolysis of the silicates and aluminosilicates continued (Equation 1), dissolved sodium and bicarbonate ions were continually produced, and acid was consumed. The pH of the water gradually increased. Formation of kaolinite was replaced by formation of montmorillonite and finally by production of illite. The reactions indicated by Equation 1 were replaced by the family of reactions indicated in Equation 2, written using the hydrolysis of albite as an example.



Loughnan (7) gives the above chemical composition for illite, pointing out that illite is characterized by substitutions in the silica sheet. As pH of the lake water increased, silica became more mobile than alumina. Formation of the relatively silica-poor illite resulted. Dehydration of the dissolved silica in the sediment's water (Equation 3) produced quartz. The large amounts of illite from the reactions represented by Equation 2 and the quartz from Equation 3 formed the major mineral constituents in the oil shales below the mineral change.



The illite-producing reaction in Equation 2 continued to consume acid, apparently in amounts greater than could be supplied by CO₂ from the organic matter. This made the water of the lower layer progressively more basic. When the pH of this water exceeded 10, alumina also became mobile. Solubility of both SiO₂ and Al₂O₃ increases dramatically as the solution pH increases past 10. The water of the lower layer was now primarily a sodium carbonate solution, strongly basic and strongly reducing. The protective layer of Al(OH)₃ which had continually formed around aluminosilicate particles now dissolved because of the amphoteric behavior of aluminum. Consequently, when the tiny clastic particles entered this water, they were destroyed, and the aluminate ion also began to accumulate in the lake's lower layer. Illite was no longer produced in quantity from the protected skeletons, and the mineralogy of the resulting oil shales changed abruptly.

The organic matter being deposited changed little across this major change in minerals, but the organic matter now became a major factor in the production of oil-shale minerals. As organic matter, produced seasonally in the lake's upper layer, collected on the lake bottom, it trapped water from the lake's lower layer. This water had a pH on the order of 11, was strongly reducing, and had continued to build up a supply of dissolved materials. Laboratory tests have shown that organic matter from the Green River oil shales has a large capacity for forming a water-retaining suspension (16). In addition, the sediment probably acted as an ionic filter, retaining ions as water was forced from the sediment. Reductive conditions in the sediment continued to operate on the organic matter which evolved CO₂ and some H₂S. These gases dissolved in the interstitial water, lowering its pH.

The limits of reduction potential and pH in the sediments which became oil shale of the Parachute Creek Member can now be defined. These are presented as the shaded area in Figure 4. The block's bottom boundary (4) represents the lower stability limit of water. At reductive potentials below this line, water breaks down to yield hydrogen, illustrating the strength of the hydrogenating environment in the sediment. The upper boundary, defined by the ratio of sulfate to sulfide ion, is drawn three orders of magnitude below the Eh values represented by equal parts of sulfate and sulfide ions because sulfate has not been observed in unweathered Parachute Creek sediments. The lower pH boundary is set because of strong bicarbonate (nahcolite) buffering at about pH 8.4. The upper boundary is set at a pH of 10 because of the sharp increase in silica and alumina solubility above this pH. The pH of the interstitial water probably averaged about 9.

With the sharp lowering of pH from perhaps 11 to 9 at the organic sediment interface, silicates began to form from the interstitial water trapped in the sediment. The solubility of both silica and alumina decreases sharply as pH changes from 11 down to 9. The resulting chemical conditions in the sediment encouraged development of authigenic feldspars and formation of quartz. Silicate precipitation should be enhanced by large amounts of organic matter producing larger amounts of CO₂. Silicate formation definitely increases with increasing organic matter in Colorado's Green River oil shales (9). Silicates generated in this manner should tend to concentrate in the organic layers and in the organic-rich (dark) fraction of the light-dark varve cycle.

Smith and Robb (16) describe the authigenic formation of dolomite, calcite, and aragonite in Lake Uinta. Calcite was formed in the lake's lower layer from the calcium released by chemical digestion of silicate and aluminosilicates. Calcium was released to a calcite-saturated sodium carbonate solution, immediately forming calcite. The calcite crystals settled to the lake bottom as a continuous and very dispersed shower of tiny calcite particles. The Mg⁺⁺ and Fe⁺⁺ released by dissolving particles precipitated as Mg(OH)₂ and Fe(OH)₂, also descending to the lake bottom.

When these hydroxides were enclosed in the sediment they dissolved, releasing Mg^{++} and Fe^{++} to form the Green River Formation's iron-bearing dolomite. Part of the iron was used to form pyrite. During deposition of the Mahogany zone, aragonite formed seasonally in the lake's upper layer, fell to the lake bottom, and was partially dolomitized and partially preserved (16). This generated the dolomite-rich light layers in Mahogany zone varves. Thus the chemical conditions in the stratified lake Uinta explain the lateral persistence of the tiny varves and the large laminations, which can be correlated over huge areas, reflecting area wide changes particularly in the growing conditions that produced the depositing organic matter.

One event in the life of Lake Uinta remains to be explained, the production of the unique saline mineral suite. The saline mineral suite consists of dawsonite [$NaAl(OH)_3CO_3$] with its accompanying nordstrandite [$Al(OH)_3$], nahcolite ($NaHCO_3$), and halite ($NaCl$), deposited in the Parachute Creek Member around the early depositional center. Two factors combined to produce the saline minerals: 1) the continual buildup of sodium carbonate and aluminate ion in the water of the lake's lower layer, and 2) the gradual loss of water from the lake's lower layer and the accompanying increase in concentration of the materials in solution. The hydrolysis mechanism continuously supplying sodium carbonate and aluminate ion to this water has been described (see Equation 2). The loss of water from the lake's lower layer had to be a mechanism at the lake's edges because the upper layer of Lake Uinta continued to supply organic matter to the lake bottom through the deposition of the saline minerals.

Dawsonite occurs in oil shale as a matrix mineral formed from the lake water as a precipitate in the sediment. Bader and Esch (1) synthesized dawsonite by bubbling CO_2 into a sodium aluminate solution at a pH of 11. As the pH of their solution dropped, dawsonite precipitated. Dawsonite was obtained only when the sodium carbonate to aluminate ratios were higher than 15 to 1. This synthesis method is almost an exact description of the natural mechanism which formed dawsonite in the sediment. Carbon dioxide from the deposited organic matter performed on the sodium carbonate and aluminate ion dissolved in the trapped water exactly as in the synthesis method, forming dawsonite.

Nahcolite crystallization was also produced by CO_2 from organic matter. Sodium carbonate in the interstitial water was converted to sodium bicarbonate by the reaction shown in Equation 4.



By this reaction 106 grams of sodium carbonate becomes 168 grams of sodium bicarbonate. Sodium bicarbonate is less soluble than sodium carbonate by a factor of 3 or 4. As the concentration of the salts that were dissolved in the lower layer gradually increased, a point was reached where nahcolite ($NaHCO_3$) began to crystallize in the sediment. These crystals grew as the sodium bicarbonate dissolved in the interstitial water migrated to them. Crystals that grew in sediment make up most of the nahcolite occurrence in the Piceance Creek Basin. As Milton and Eugster (8) point out, nahcolite is the solid phase expected at the relatively high CO_2 pressure in the unconsolidated sediment. None of the other sodium carbonate crystal forms known to occur in nature have been found in core from the Piceance Creek Basin. In Colorado the stratified lake persisted through saline mineral deposition. In Wyoming, however, the corresponding lake went nearly or completely to dryness, losing its protective top. When exposed to atmospheric levels of CO_2 , sodium carbonate solutions crystallize trona. Wyoming's lake did.

Smith and Lee (15) tested stability of the postulated chemical stratification. These tests indicated that the density stratification would persist largely unmixed through all possible stresses--earthquakes, seiches, tides, temperature variations, and even windstorms stronger than any known.

SUMMARY

The genesis pattern presented for Green River Formation oil shale explains the major observation. Deposition of relatively large quantities of hydrogen-rich organic matter in the oil shales is a natural consequence of the chemical conditions (basic water and reducing atmosphere) and the physical limitation of clastic materials developed in the stratified ancient Lake Uinta. Stability of the stratification produced the continuous deposition of the organic matter and its uniformity over the deposit. Authigenic formation of the oil-shale minerals proceeds naturally from the lake stratification, and the varve production stems from the seasonable development of organic matter. The lake's stratification produced uniform deposition over the entire area it covered, making the correlatable lateral persistence of the thin laminations a natural consequence. As the lake developed, the attack on aluminosilicates by sodium carbonate in the lake's lower layer produced a silicate skeleton protected by aluminum trihydroxide. On deposition, this aluminum-rich skeleton formed illite in quantity. As the lake became more basic, the protecting aluminum hydroxide coating dissolved amphoterically and illite production dropped at a specific point. Continual build-up of sodium carbonate and aluminate ion in the water of the lake's lower layer reached conditions which

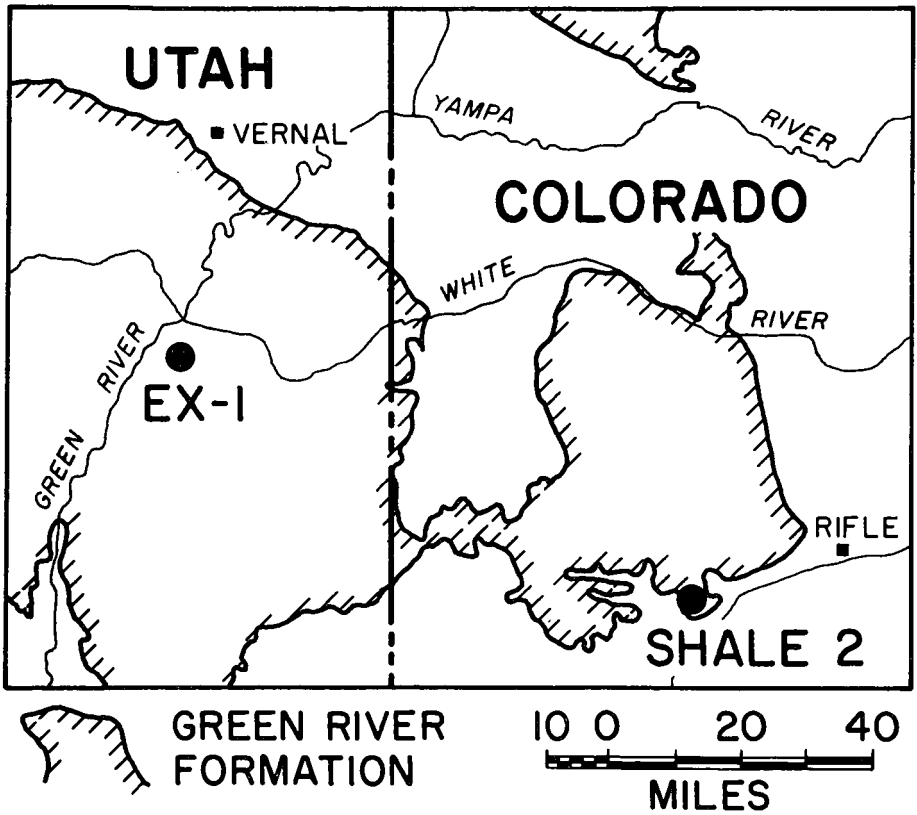


Figure 2. Oil Shale Locations compared in Figure 1.

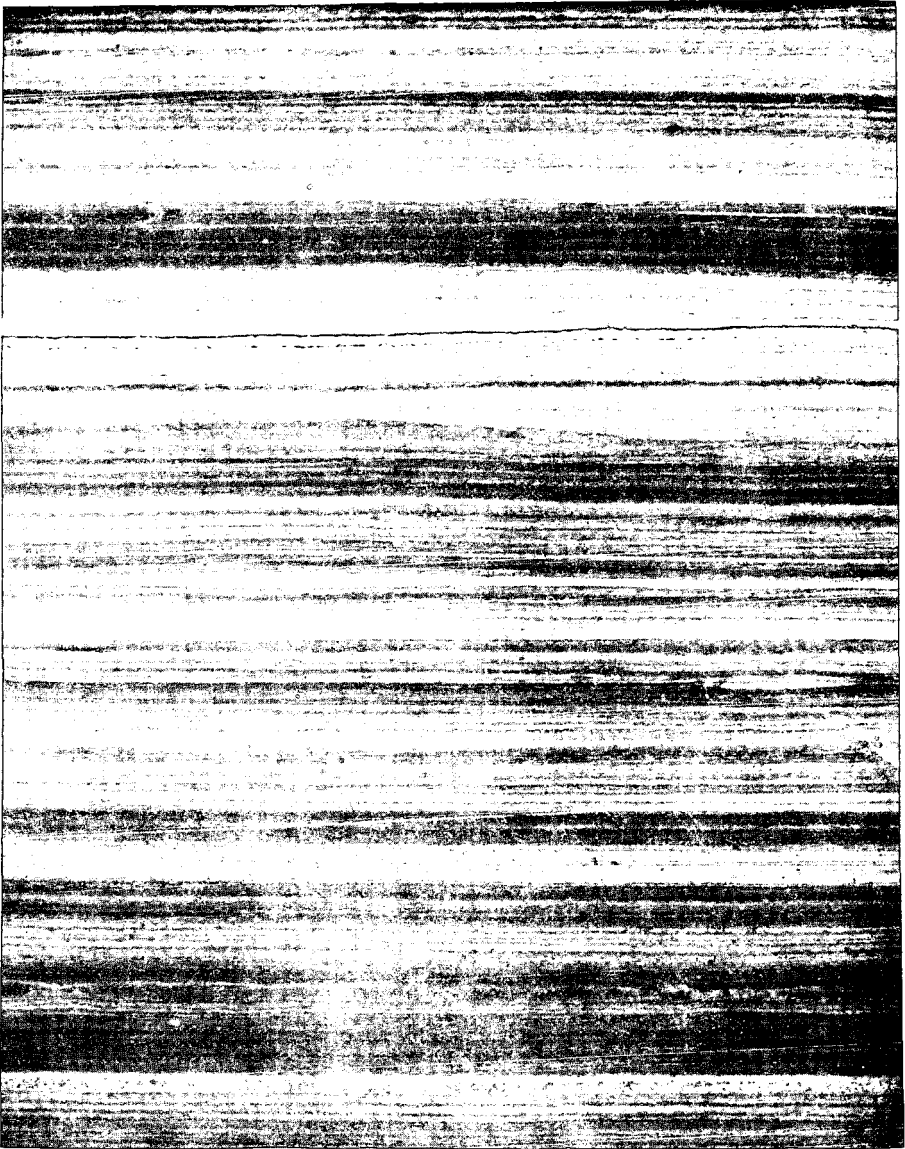


Figure 3. Oil Shale Laminations in a Two-Inch Block.

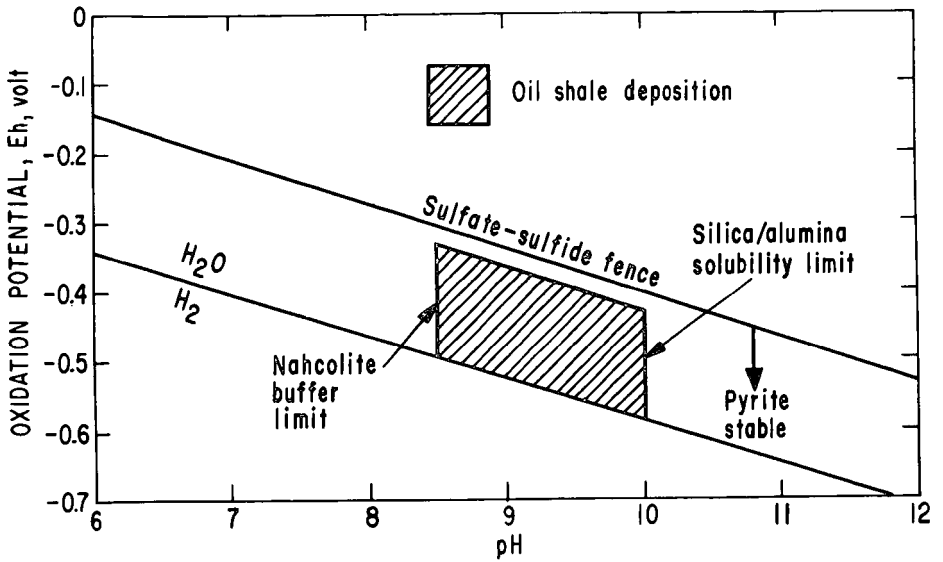


FIGURE 4 - Eh-pH limits in sediments which became Green River oil shale.

precipitated dawsonite and crystallized nahcolite in the sediment as a result of CO₂ production from organic matter.

LITERATURE CITED

- (1) Bader, E., and Esch, U., *Zeitschrift fur Elektrochemie*, 50, 266 (1944).
- (2) Bradley, W. H., *Am. Assoc. Petrol. Geol. Bull.*, 9 (2), 247 (1925).
- (3) Frey, D. G., *Limnology in North America*: University of Wisconsin Press, Madison, Wis., 734 p. (1963).
- (4) Garrels, R. M., "Mineral Equilibria", Harper and Brothers, New York, N. Y., 254 p. (1960).
- (5) Garrels, R. M., and Mackenzie, F. T., "Evolution of Sedimentary Rocks", W. W. Norton, New York, N. Y., 397 p. (1971).
- (6) Hutchinson, G. E., *Trans. Connecticut Acad. Arts Sci.*, 33, 47 (1937).
- (7) Loughnan, F. C., "Chemical Weathering of Silicate Minerals", American Elsevier, Inc., New York, N. Y., 154 p. (1969).
- (8) Milton, C., and Eugster, H. P., in Abelson, P. H., ed., "Researches in Geochemistry", 1, John Wiley and Sons, New York, N. Y., p. 118 (1959).
- (9) Robb, W. A., Smith, J. W., and Trudell, L. G., U.S.D.O. E. LETC RI-78/6, 39 p. (1978).
- (10) Robinson, W. E., and Cook, G. L., U.S. BuMines Rept. Inv. 7492, 32 (1971).
- (11) Smith, J. W., U.S. BuMines Rept. Inv. 5725, 16 (1961).
- (12) Smith, J. W., *Am. Assoc. Petrol. Geol. Bull.*, 47 (5), 804 (1963).
- (13) Smith, J. W., Twenty-fifth Field Conf. Guidebook, Rocky Mountain Assn. Geol., p. 71 (1974).
- (14) Smith, J. W., and Harbaugh, J. W., U.S. BuMines Rept. Inv. 6883, 11 (1966).
- (15) Smith, J. W., and Lee, K. K., *Proc. 15th Oil Shale Symp.*, Colorado School of Mines, pp. 101-114 (1982).
- (16) Smith, J. W., and Robb, W. A., U.S. BuMines Rept. Inv. 7727, 21 (1973).
- (17) Smith, J. W., Trudell, L. G., and Dana, G. E., U. S. BuMines Rept. Inv. 7071, 28 (1968).
- (18) Trudell, L. G., Beard, T. N., and Smith, J. W., U. S. BuMines Rept. Inv. 7357, 226 (1970).
- (19) Trudell, L. G., Smith, J. W., Beard, T. N., and Mason, G., U. S. D.O. E. LETC/RI-82/4, 32 p. (1982).

SYMPOSIUM ON GEOCHEMISTRY AND CHEMISTRY OF OIL SHALE
PRESENTED BEFORE THE DIVISIONS OF FUEL CHEMISTRY, GEOCHEMISTRY
AND PETROLEUM CHEMISTRY, INC.
AMERICAN CHEMICAL SOCIETY
SEATTLE MEETING, MARCH 20-25, 1983

MAJOR AND TRACE ELEMENTS IN MAHOGANY ZONE OIL SHALE IN TWO CORES
FROM THE GREEN RIVER FORMATION, PICEANCE BASIN, COLORADO

By

Michele L. Tuttle, Walter E. Dean and Nancy L. Parduhn
U. S. Geological Survey, Denver Federal Center, Denver, Colorado 80225

LONG ABSTRACT

The Parachute Creek Member of the lacustrine Green River Formation contains thick sequences of rich oil-shale. The richest sequence and the richest oil-shale bed occurring in the member are called the Mahogany zone and the Mahogany bed, respectively, and were deposited in ancient Lake Uinta. The name "Mahogany" is derived from the red-brown color imparted to the rock by its rich-kerogen content.

Geochemical abundance and distribution of eight major and 18 trace elements were determined in the Mahogany zone sampled from two cores, U. S. Geological Survey core hole CR-2 and U. S. Bureau of Mines core hole O1-A (Figure 1). The oil shale from core hole CR-2 was deposited nearer the margin of Lake Uinta than oil shale from core hole O1-A. The major- and trace-element chemistry of the Mahogany zone from each of these two cores is compared using elemental abundances and Q-mode factor modeling.

The results of chemical analyses of 44 CR-2 Mahogany samples and 76 O1-A Mahogany samples are summarized in Figure 2. The average geochemical abundances for shale (1) and black shale (2) are also plotted on Figure 2 for comparison. The elemental abundances in the samples from the two cores are similar for the majority of elements. Differences at the 95% probability level are higher concentrations of Ca, Cu, La, Ni, Sc and Zr in the samples from core hole CR-2 compared to samples from core hole O1-A and higher concentrations of As and Sr in samples from core hole O1-A compared to samples from core hole CR-2. These differences presumably reflect slight differences in depositional conditions or source material at the two sites.

The Mahogany oil shale from the two cores has lower concentrations of most trace metals and higher concentrations of carbonate-related elements (Ca, Mg, Sr and Na) compared to the average shale and black shale. During deposition of the Mahogany oil shale, large quantities of carbonates were precipitated resulting in the enrichment of carbonate-related elements and dilution of most trace elements as pointed out in several previous studies.

Q-mode factor modeling is a statistical method used to group samples on the basis of compositional similarities. Factor end-member samples are chosen by the model. All other sample compositions are represented by varying proportions of the factor end-members and grouped as to their highest proportion. The compositional similarities defined by the Q-mode model are helpful in understanding processes controlling multi-element distributions. The models for each core are essentially identical. A four-factor model explains 70% of the variance in the CR-2 data and 64% of the O1-A data (the average correlation coefficients are 0.84 and 0.80, respectively). Increasing the number of factors above 4 results in the addition of unique instead of common factors. Table I groups the elements based on high factor-loading scores (the amount of influence each element has in defining the model factors). Similar elemental associations are found in both cores. Elemental abundances are plotted as a function of core depth using a five-point weighted moving average of the original data to smooth the curve (Figure 3 and 4). The plots are grouped according to the four factors defined by the Q-mode models and show similar distributions for elements within the same factor.

Factor 1 samples are rich in most trace metals. High oil yield and the presence of illite characterize the end-member samples for this factor (3, 4) suggesting that adsorption of metals onto clay particles or organic matter is controlling the distribution of the metals. Precipitation of some metals as sulfides is possible (5).

Factor 2 samples are high in elements commonly associated with minerals of detrital or volcanogenic origin. Altered tuff beds and lenses are prevalent within the Mahogany zone. The CR-2 end-member samples for this factor contain analcime (3) which is an alteration product within the tuff beds of the Green River Formation. Those from O1-A contain much less analcime, but do contain dawsonite (4). The presence of dawsonite in the samples from core hole O1-A may be

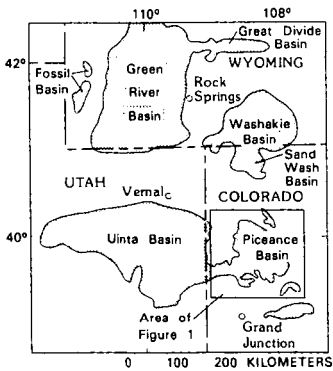
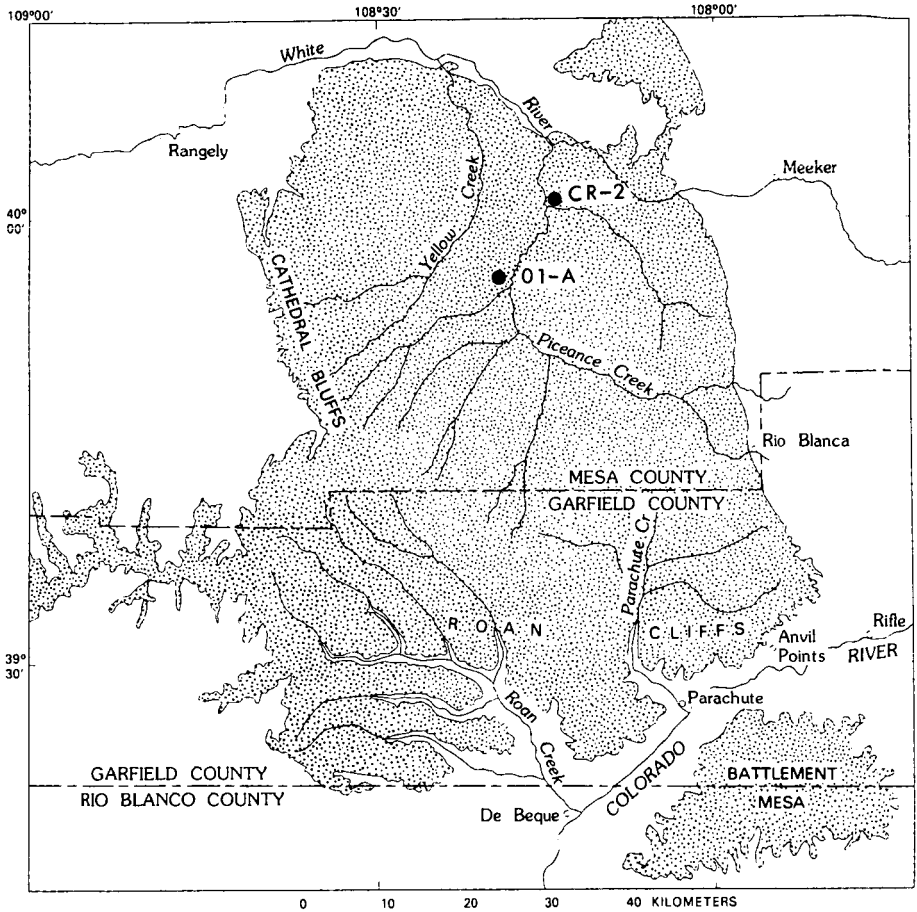


Figure 1. Index map of Piceance basin showing location of core holes CR-2 and O1-A.

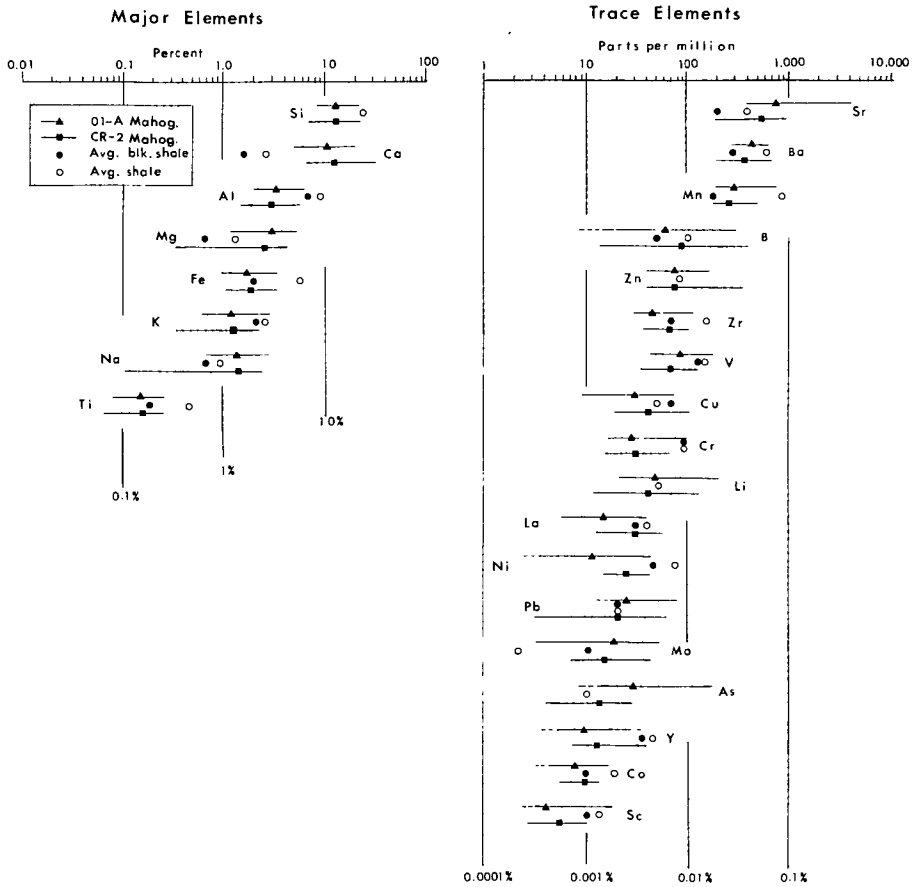


Figure 2. Observed ranges and geometric means for O1-A and CR-2 Mahogany zone core samples. Average shale (3) and average black shale (4) are also represented.

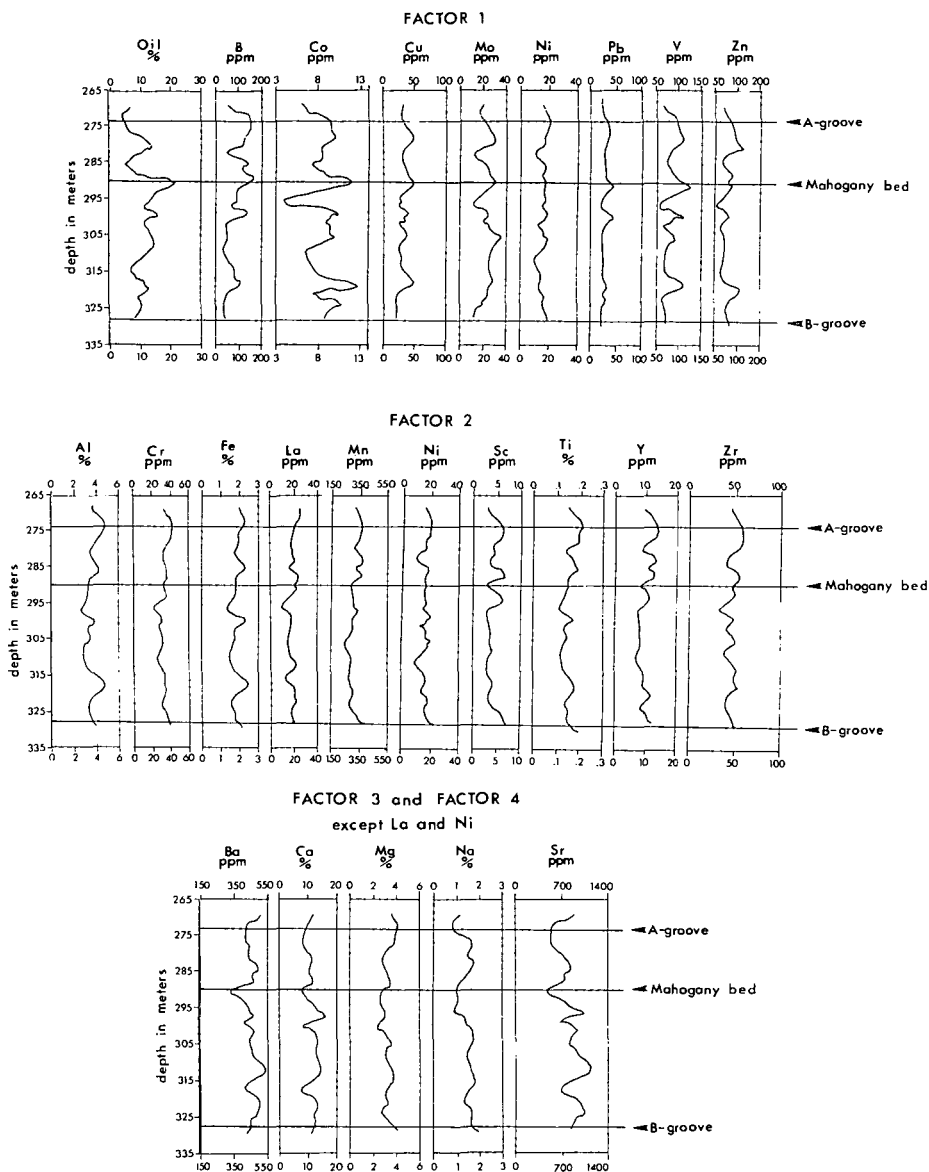


Figure 3. Distribution of elements in core O1-A as a function of core depth. Elements are grouped into the Q-mode model factors. Elements designated as excepted are plotted in a previous factor.

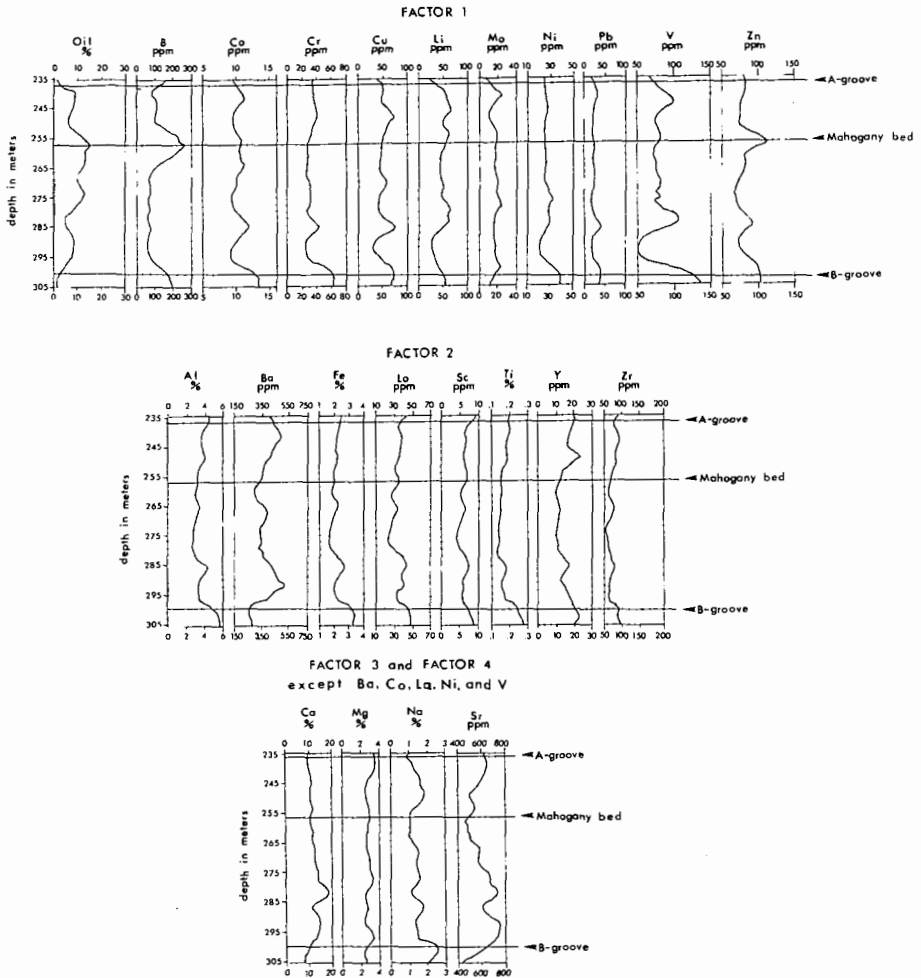


Figure 4. Distribution of elements in core CR-2 as a function of core depth. Elements are grouped into the Q-mode model factors. Elements designated as excepted are plotted in a previous factor.

due to the reaction of analcime with CO₂. The reaction consumes analcime and produces quartz and dawsonite (6).

Factor 3 and Factor 4 samples are similar in the sense that both are carbonate-type samples. The samples contain both dolomite and calcite (3, 4). Barium, Sr and La are enriched in Factor 3 samples. Lanthanum substitutes diadochically for Ca in carbonates (7); Ba and Sr probably precipitated as carbonates. Factor 4 samples contain Co, Ni and V. The importance of these metals in defining the carbonate-rich factor is not obvious. All three metals are known to form organometallic compounds (7) which may account for their concentration in these samples.

TABLE I
COMPOSITIONAL VARIABLES IN O1-A AND CR-2 MAHOGANY OIL SHALE
AS TO THEIR Q-MODE MODEL FACTOR

Factor 1		Factor 2		Factor 3		Factor 4	
O1-A	CR-2	O1-A	CR-2	O1-A	CR-2	O1-A	CR-2
B	B	Al	Al	Ba	Ba	Ca	Ca
Co	Co	Cr	Ba	Ca	Ca	Mg	Co
Cu	Cu	Fe	Fe	La	Mg	Na	La
Mo	Cr	La	K	Mg	Na	Ni	Ni
Ni	Li	Mn	La	Na	Sr	Sr	Sr
Pb	Mo	Ni	Sc	Sr			V
Zn	Ni	Sc	Ti				
V	Pb	Ti	Y				
	V	Y	Zr				
		Zr					

LITERATURE CITED

- (1) Krauskopf, K. B. , Introduction to Geochemistry, New York, McGraw-Hill Book Co. , p. 617 (1979).
- (2) Vine, J. D. and Tourtelot, E. B. , Geochemistry of Black Shale Deposits--A Summary Report, Economic Geology, v 65, pp. 253-272 (1970).
- (3) Dean, W. E. , Pitman, J. K. and Harrach, G. H. , Geochemical and Mineralogical analyses of U. S. Geologic Survey Oil-Shale Core CR-2, Piceance Creek Basin, Colorado, U. S. Geological Survey Open-file Report 81-596, pp. 1-25j (1981).
- (4) Robb, W. E. , Dept. of Energy, unpublished data.
- (5) Saether, O. M. , Runnells, D. D. and Meglen, R. R. , Trace Elements in Rich Oil Shales of the Mahogany Zone Concentrated by Differential Density Centrifugation, in Trace elements in oil shale progress report, U. S. Dept. of Energy Report COO-10298-1, p. 237-255 (1980).
- (6) Brobst, D. A. and Tucker, J. D. , X-Ray Mineralogy of the Parachute Creek Member, Green River Formation, in the Northern Piceance Creek Basin, Colorado, U. S. Geological Survey Professional Paper 803, p. 53 (1973).
- (7) Rankama, Kalervo and Sahama, Th. G. , Geochemistry, Chicago, The University of Chicago Press, p. 912 (1950).

SYMPOSIUM ON GEOCHEMISTRY AND CHEMISTRY OF OIL SHALE
PRESENTED BEFORE THE DIVISIONS OF FUEL CHEMISTRY, GEOCHEMISTRY,
AND PETROLEUM CHEMISTRY, INC.
AMERICAN CHEMICAL SOCIETY
SEATTLE MEETING, MARCH 20 - MARCH 25, 1983

MOLECULAR MECHANISM OF OIL SHALE PYROLYSIS
IN NITROGEN AND HYDROGEN ATMOSPHERES

By

F. Hershkowitz, W. N. Olmstead, R. P. Rhodes, and K. D. Rose
Exxon Research and Engineering Company, Linden, New Jersey 07036

ABSTRACT

This paper describes the changes in carbon functionality that occur during the pyrolysis and hydrolypyrolysis of Green River (Colorado) oil shale. This paper is different from earlier work in that shale and product characterization is combined with highly mass-balanced reactions to allow a mechanistic discussion of the role of functionalities in the generation of oil during shale pyrolysis. We identify some important factors in maximizing the conversion of kerogen to oil.

Green River Oil Shale was pyrolyzed under conditions of slow heatup ($6^{\circ}\text{C}/\text{min}$) and short gas residence times (2-10 sec) in a nitrogen or hydrogen atmosphere at 2600 kPa. Product characterization was by elemental analysis, GC, and NMR (solid and liquid).

The aliphatic portion of the shale either cracks to give oil and gas or aromatized to give aromatics in the oil or spent shale. The aromatic portion of the kerogen either cracks to give oil or ends up in the spent shale. Mineral carbonates, rather than organic functionalities, are the source of almost all the CO_2 . Hydrogen is effective at inhibiting the reactions which lead to aromatization and formation of residual carbon. Molecular hydrogen in the system also reduces carbonates to methane and water.

SYMPOSIUM ON GEOCHEMISTRY AND CHEMISTRY OF OIL SHALE
PRESENTED BEFORE THE DIVISIONS OF FUEL CHEMISTRY, GEOCHEMISTRY,
AND PETROLEUM CHEMISTRY, INC.
AMERICAN CHEMICAL SOCIETY
SEATTLE MEETING, MARCH 20 - MARCH 25, 1983

GEOCHEMISTRY AND PYROLYSIS OF OIL SHALES

By

B. P. Tissot and M. Vandenbroucke
Institut Français du Pétrole, BP 311, 92506, Rueil-Malmaison, France

There is no geological or chemical definition of an oil shale. Any rock yielding oil in commercial amount upon pyrolysis may be considered as an oil shale. The composition of the inorganic fraction may vary from a shale where clay minerals are predominant, such as the Lower Jurassic shales of Western Europe (particularly France and West Germany), to carbonates with subordinate amounts of clay and other minerals, such as the Green River shales of Colorado, Utah and Wyoming.

The organic fraction is mainly an insoluble solid material, kerogen, which is entirely comparable to the organic matter present in many petroleum source rocks (1,2). Figure 1 shows the elemental composition of the Green River shales, the Lower Toarcian shales of the Paris Basin and West Germany and also various oil shales from different origins. A large number of core samples from the Green River and the Paris Basin shales was taken at various burial depths. They cover the diagenesis, catagenesis and metagenesis stages of thermal evolution (1) (the latter stage was available from the Green River shales only). The diagram shows that these two shales series constitute typical evolution paths of type I and type II kerogens according to the definition of Tissot et al. (3). Furthermore, other oil shale kerogens belong either to type I, such as Coorongite and Keroseene shales (Australia), Torbanite (Scotland and S. Africa) and bogheads; or to type II, such as Kukersite (USSR), Irati (Brazil) and Messel (W. Germany) shales; Tasmanite (Australia) shows an intermediate elemental composition. The evolution path of humic coals is also shown in Figure 1 for comparison. It has obviously a lower hydrogen content than any of the oil shale kerogens, unless they have been deeply altered by thermal evolution.

Infrared spectroscopy (Figure 2 and Table I) of the kerogens (4) from oil shales shows that all of them are rich in aliphatic bands at 2900 and 1450 cm^{-1} related to chainlike and cyclic saturated material. However, kerogens of type I, such as Green River shales and Torbanite, contain a larger proportion of long aliphatic chains, marked by the absorption bands at 720 cm^{-1} .

TABLE I
RELATIVE IMPORTANCE OF ALIPHATIC BANDS IN INFRARED SPECTROSCOPY
OF SOME KEROGENS FROM SELECTED OIL SHALES (ARBITRARY UNITS)

Type	Sample	IR Aliphatic bands (cm^{-1})			
		K ₂₉₀₀ C-H	K ₁₄₅₀ CH ₂ +CH ₃	K ₁₃₇₅ CH ₃	K ₇₂₀ (CH ₂) _n n>4
I	Green River shale	136.6	11.2	1.5	1.3
	Torbanite	103.5	10.8	2.1	1.1
II	Toarcian shales	73.0	10.0	2.5	0
	Kukersite	72.7	11.5	2.8	0.4
	Messel shales	76.0	9.6	3.7	0.2

The total oil yield obtained from the shale upon pyrolysis is usually measured by the standard Fischer assay. However, it is possible to obtain a fast and accurate measurement of the oil yield by using the Rock Eval. source rock analyzer (5), which operates on small quantities of rock, such as 50 or 100 mg. Figure 3 shows the comparison between the value obtained from the Rock Eval pyrolysis and the yield of the Fischer assay on the Toarcian shales of the Paris Basin.

A series of experiments has been carried out to observe the generation of the different classes of oil constituents. Aliquots of two kerogens from the Green River Shales (type I) (6) and the Lower Toarcian shales of the Paris Basin (type II) (7) were heated at a constant heating rate of 4°C min^{-1} to different final temperatures ranging from 375°C to 550°C. A humic coal from Indonesia

(type III) was also used for comparison (8). These various samples have experienced a comparable thermal history in geological conditions: they belong to the final stage of diagenesis (1) (vitrinite reflectance between 0.4 and 0.5%). The mass balance of the organic fraction is shown in Figure 4 as a function of the final temperature. At 375°C, most of the organic material is still made of kerosene. With increasing final temperature an increasingly large fraction is converted to oil which condenses in a cold trap, leaving a solid residue or char. The non-recovered fraction is assumed to be mainly carbon dioxide, water and light hydrocarbons non-condensable in the cold trap.

A somewhat different behavior is observed according to the type of kerogen: the Green River shale (type I) requires higher temperatures, as the maximum rate of conversion occurs ca. 475°, versus 425-450°C for the Paris Basin shale (type II) and the humic coal (type III). Furthermore, the conversion ratio and the composition of the products are different: the total conversion ratio (condensate plus non-recovered products) decreases from over 80% for type I, to 55% for type II and only 35% for coal. The amount of oil (condensate) generated is relatively high in kerogens from oil shales: 62% for type I and 47% for type II, whereas it is low (less than 12%) for coal. This is partly due to an important generation of carbon dioxide and water from humic coals. The relative proportion of hydrocarbons (saturated, unsaturated, aromatics) compared to N, S, O - compounds also decreases from type I to type III.

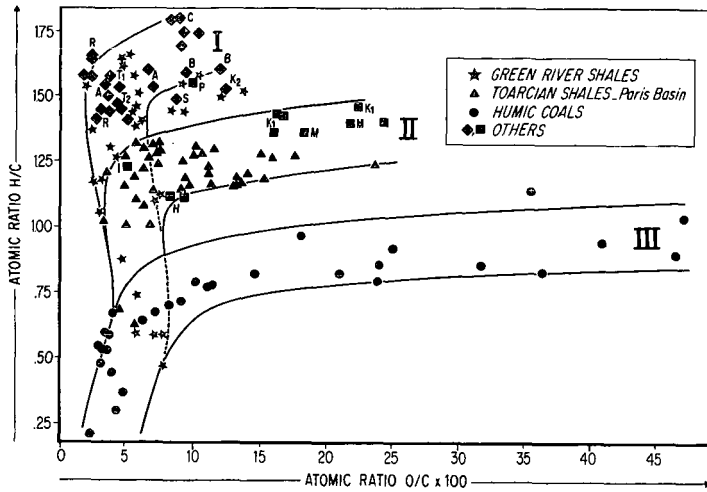
The total amount and composition of the hydrocarbons generated is shown in Figure 5. The Green River oil shale (type I) produces mainly linear or branched hydrocarbons, whereas the Paris Basin shale (type II) generates mainly cyclic - particularly aromatic - hydrocarbons. The percentage of aromatics is also important in coal pyrolysis, but the absolute amount is much smaller. The bottom part of Figure 6 shows the distribution of n-alkanes in shale oils: it is regularly decreasing from C17 to C30 in the oil derived from type II kerogen, which is a fluid synthetic oil; it is relatively flat up to C30 (type I) or even increasing towards a C25-C29 maximum (type III) in the two other synthetic oils which have a waxy character. Furthermore, a slight predominance of the odd-numbered molecules (C25, C27, C29) noted in the oil derived from humic coal points to a contribution of natural waxes from higher plants to the organic material.

A direct pyrolysis-gas chromatography of the kerogens was also performed and is presented in Figure 7 (9). The chromatograms taken at pyrolysis temperature of 475°C show the total distribution of hydrocarbons, with the relative importance of long chain molecules up to C30 in types I and III. It also shows the importance of low-boiling aromatics (B: benzene; T: toluene; X: xylenes) generated from humic coal (type III) as compared to those generated from oil shales (types I and II).

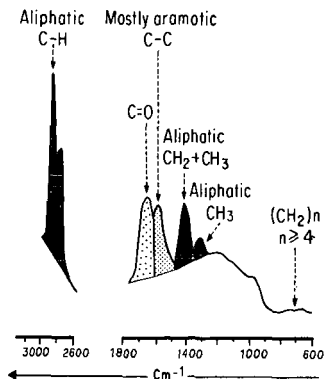
Composition of the solid organic residue of pyrolysis was also analyzed in order to follow the progressive change from the immature kerogen to the final char. Figure 8 presents the elemental composition of the solid organic fraction corresponding to the experiments reported in Figure 4. Artificial evolution of the two types of oil shale kerogen and the humic coal is represented by the elemental composition and the final temperature of pyrolysis. The artificial evolution paths corresponding to types I and II are reasonably comparable to the natural evolution paths observed in geological situation (10, 11), where the Green River and Paris Basin shales are buried at depth (this path is marked by bands I and II, respectively, in Figure 8). The major loss of hydrogen occurs ca. 475-500°C for type I and ca. 400-475°C for type II kerogen; this remark is in agreement with a comparable delay in their respective conversion ratio reported in Figure 4. The behavior of coal is somewhat different from that of oil shale kerogen: its artificial evolution does not duplicate the natural evolution path of humic coals. This is possibly due to the higher oxygen content of the initial sample and to its preferential elimination as water (a hydrogen consuming process) during pyrolysis, as compared to geological situations, where oxygen is mostly eliminated as carbon dioxide.

A confirmation of the inadequacy of pyrolysis to simulate the natural evolution of coal is provided in Figure 9, where two parameters of the Rock Eval pyrolysis are presented. The hydrogen index (5) is plotted as a function of a thermal evolution parameter T_{max} (temperature of pyrolysis corresponding to the maximum rate of release of organic compounds). The hatched bands marked I, II and III correspond to the natural evolution paths (under burial in geological situation) of the Green River Shales (10), the Paris Basin and W. Germany Toarcian (11), and humic coals (12), respectively. Again, the artificial evolution paths of type I and type II oil shale kerogens are reasonably comparable to the natural evolution paths, whereas the deviation is important for coal. The graph points to an early loss of hydrogen, possibly used for oxygen elimination through water generation; thus the hydrogen index, which measures the potential for further hydrocarbon generation, is lowered at an early stage of thermal evolution as compared to its behavior in geological situation.

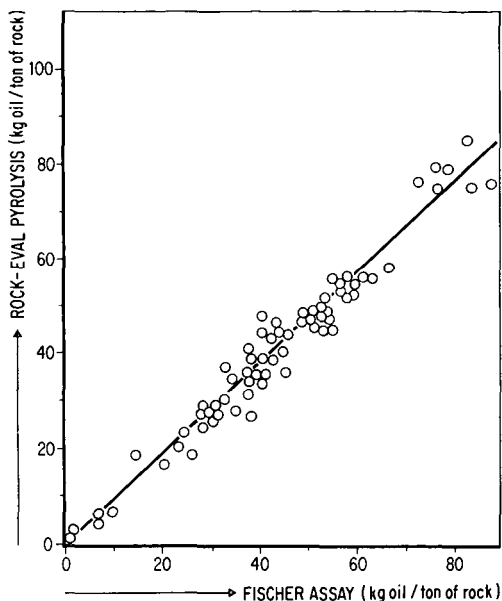
Another aspect of the comparison between pyrolysis and natural evolution of the organic matter is shown in Figure 10. In the Paris Basin, Lower Jurassic shales have been mined as oil shales where they are outcropping, whereas in the central part of the basin they were submitted to sufficient burial to generate bitumen in large amounts (11); in turn, a small fraction of that bitumen migrated to form small oil fields. Figure 10 presents the global composition of a) shale oil generated by laboratory pyrolysis, b) natural bitumen generated at depth in the shale acting as a source rock, and c) crude oil accumulated in a small field. The global composition of shale oil (non-aromatic



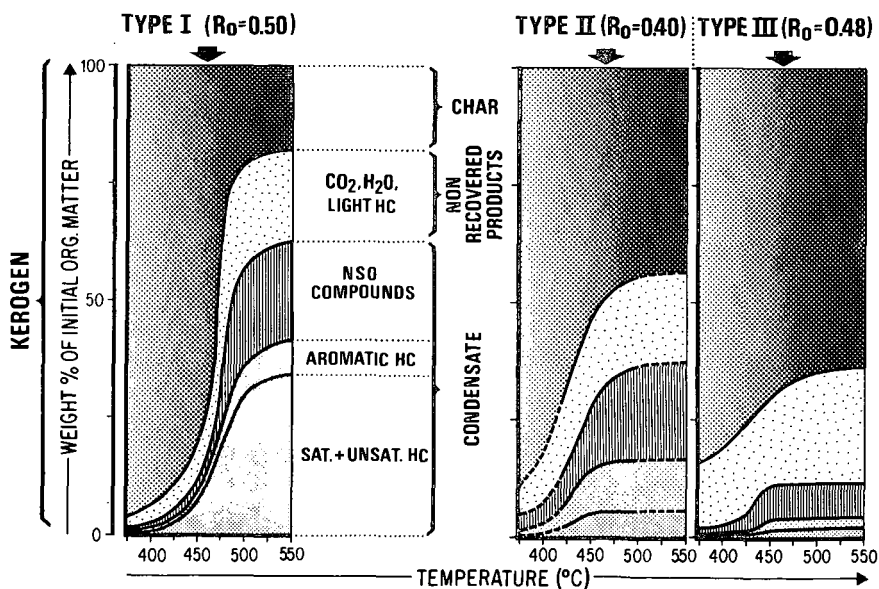
1. Van Krevelen diagram showing the elemental composition of oil shale kerogens. The organic constituents of the Green River shales and the Toarcian shales of the Paris Basin are typical kerogens of Types I and II, respectively. Other oil shales belong to either Type I (★) or II (▲) or III (●); A: Autun boghead, Permian, France; B: Moscow boghead, Permian, USSR; C: Coorongite, Recent, Australia; H: Marahunite, Tertiary, Brazil; I: Irati shales, Permian, Brazil; K₁, K₂: Kukersite, Paleozoic, USSR; M: Messel shale, Eocene, W. Germany; R: Kerosene shale, Permian, Australia; S: Tasmanite, Permian, Australia; T₁: Torbanite, Carboniferous, Scotland; T₂: Torbanite, Permian, Australia. The evolution path of humic coals (type III) is shown for comparison.



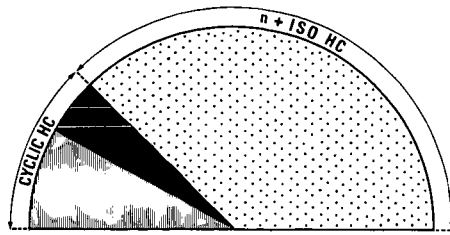
2. Typical infra-red spectrum of the kerogen isolated from lower Toarcian shales, Paris Basin.



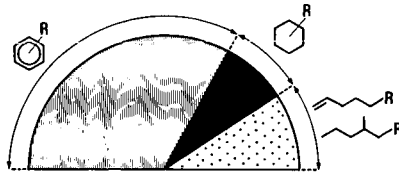
3. Correlation between oil content obtained by Fischer assay and by Rock-Eval pyrolysis.



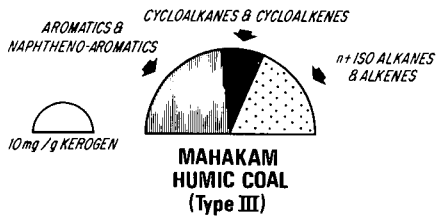
4. Pyrolysis of kerogens at a standard heating rate of $4^{\circ} \text{ min}^{-1}$ up to different final temperatures. Mass balance of recovered and non recovered products plus residual char.



GREEN RIVER SHALE (Type I)

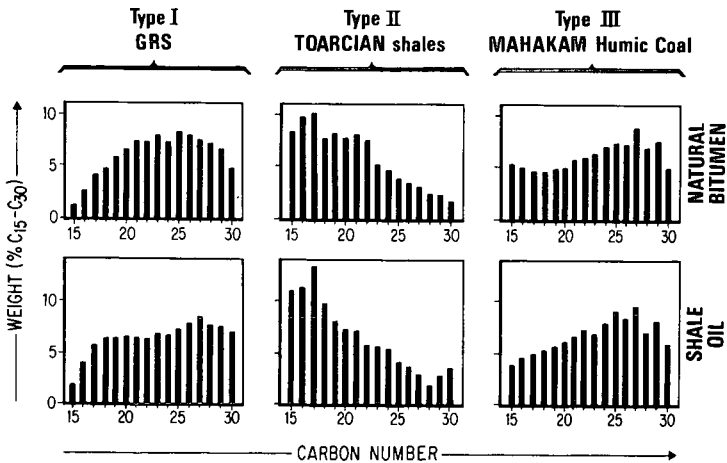


TOARCIAN SHALE (Type II)

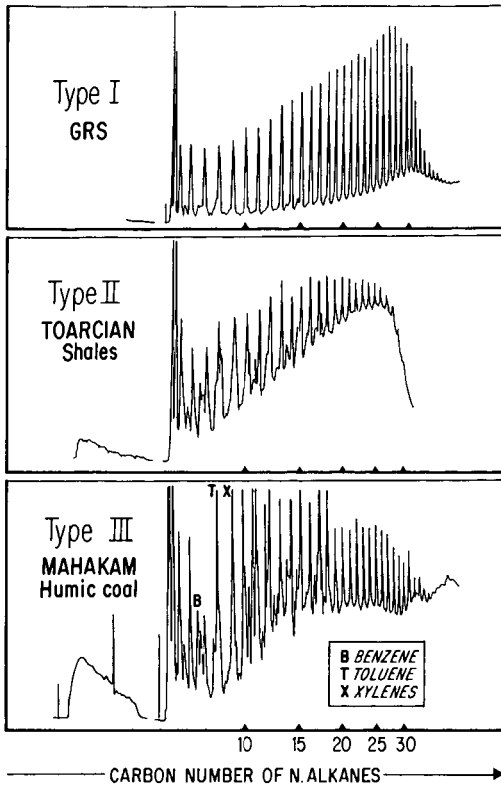


MAHAKAM HUMIC COAL (Type III)

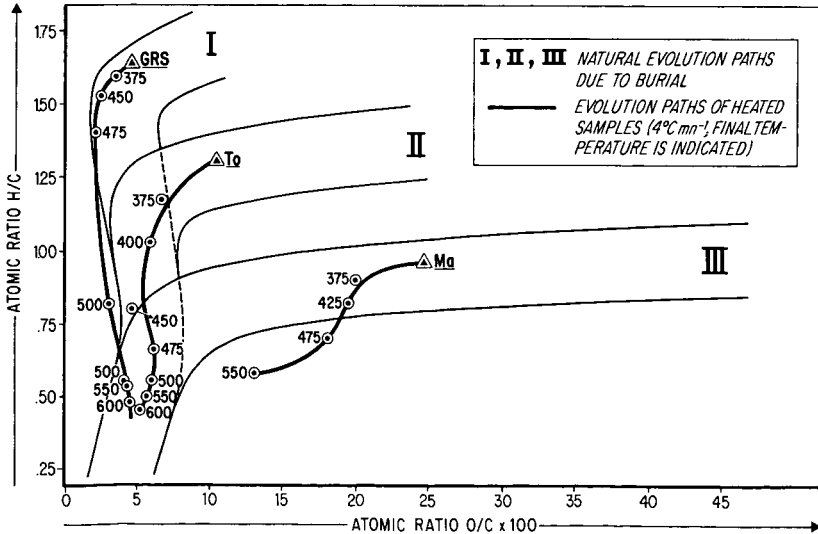
5. Hydrocarbons generated from the two main types of oil shales by pyrolysis at $4^{\circ} \text{ min}^{-1}$ rate up to 500° C . Hydrocarbons generated from a humic coal (type III) are shown for comparison.



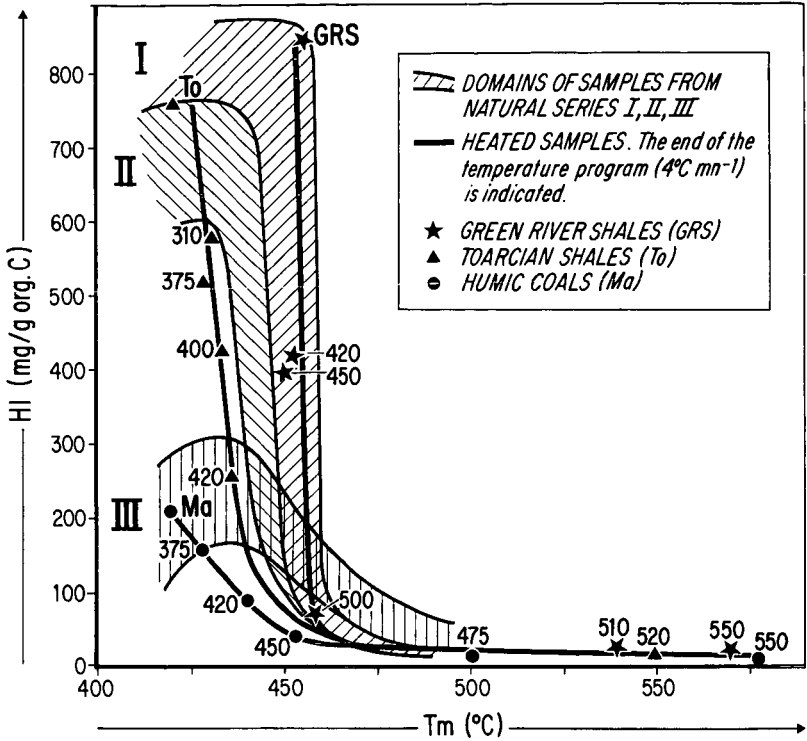
6. Comparison of the normal alkane distribution in shale oil generated by pyrolysis and in bitumen from geological samples with an equivalent stage of thermal evolution.



7. Pyrolysis — Gas chromatography at 475° C. The chromatogram shows total hydrocarbons.



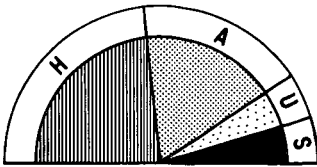
8. Evolution paths of heated samples compared to natural evolution paths of series I, II, III.



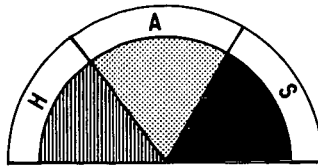
9. Evolution of hydrogen index versus T_{max} of Rock-Eval pyrolysis in natural series I, II, III (hatched) and in heated samples (identified by final temperature of pyrolysis).

Type II ORGANIC MATTER

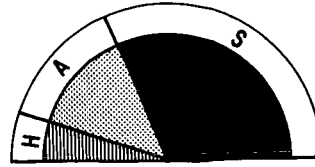
H NSO COMPOUNDS
 U UNSATURATES
 A AROMATICS
 S SATURATES



SHALE OIL



NATURAL BITUMEN



POOLED OIL

10. Composition of shale oil, natural bitumen present at depth and pooled oil, all derived from lower Jurassic shales, Paris Basin.

hydrocarbons, aromatic hydrocarbons, N,S,O - compounds) shows some similarities with that of natural bitumen, especially the high content of N,S,O - compounds, as compared to the content in pooled oil. This similarity is also observed in Figure 6 where the n-alkanes distribution of three shale oils is compared with that of three natural bitumens of comparable stage of thermal evolution.

There are two major causes for the differences observed between shale oil and crude oil. One is due to generation by pyrolysis of compounds unusual in natural bitumens and crude oils, such as unsaturated hydrocarbons (olefins): Figure 10. Nitrogen hetero-compounds are also much more abundant than they are in natural bitumen or crude oils. The other difference is due to the migrated character of pooled oil which results in a preferential migration of hydrocarbons, especially saturates, and a retention of most of the N,S,O - compounds in the source rock (1). Thus natural bitumen has an intermediate composition, separated from shale oil by the conditions of pyrolysis and from pooled oil by migration across sedimentary beds.

LITERATURE CITED

- (1) Tissot, B. P. and Welte, D. H., *Petroleum Formation and Occurrence*, Springer-Verlag, Berlin-Heidelberg, New York, 538 p. (1978).
- (2) Durand, B., in "Kerogen, Insoluble Organic Matter from Sedimentary Rocks", edited by B. Durand, Editions Technip, Paris, p. 13, 113 (1980).
- (3) Tissot, B., Durand, B., Espitalie, J., and Combas, A., *Am. Assoc. Petrol. Geol. Bull.*, **58**, 499 (1974).
- (4) Rouxhet, P. G., Robin, P. L., and Nicaise, G., in "Kerogen", edited by B. Durand, Editions Technip, Paris, p. 163 (1980).
- (5) Espitalié, J., Madec, M., Tissot, B., Menning, J. J., and Leplat, P., *Offshore Technology Conference, Preprint OTC 2935*, 439 (1977).
- (6) Vandenbroucke, M., Durand, B., and Hood, A., in "8th International Meeting on Organic Geochemistry, Moscow, (1977), in press.
- (7) Huc, A. Y., Thesis, University of Strasbourg, (1978).
- (8) Monin, J. C., Durand, B., Vandenbroucke, M., and Huc, A. Y., in "Advances in Organic Geochemistry 1979", ed. by A. G. Douglas and J. R. Maxwell, Pergamon Press, Oxford, p. 517 (1980).
- (9) Saint-Paul, C., Monin, J. C., and Durand, B., *Rev. Inst. Fr. Pétrole*, **XXXV-6**, 1065 (1980).
- (10) Tissot, B., Deroo, G., and Hood, A., *Geochim. et Cosmochim. Acta*, **42**, 1469 (1978).
- (11) Tissot, B., Califfet-Debyser, Y., Deroo, G., and Oudin, J. L., *Am. Assoc. Petrol. Geol. Bull.*, **55-12**, 2177 (1971).
- (12) Durand, B., Nicaise, G., Roucache, J., Vandenbroucke, M., and Hagemann, H. W., in "Advances in Organic Geochemistry 1975", ed. R. Campos and J. Goni, Enadimsa, Madrid, p. 6C1 (1977).

SYMPOSIUM ON GEOCHEMISTRY AND CHEMISTRY OF OIL SHALE
PRESENTED BEFORE THE DIVISIONS OF FUEL CHEMISTRY, GEOCHEMISTRY,
AND PETROLEUM CHEMISTRY, INC.
AMERICAN CHEMICAL SOCIETY
SEATTLE MEETING, MARCH 20 - MARCH 25, 1983

THE GEOLOGY, GEOCHEMISTRY, AND PYROLYSIS KINETICS
OF SEVERAL KEY WORLD OIL SHALES

By

H. E. Nuttall, T.-M. Guo, S. Schrader, and D. S. Thakur
Department of Chemical and Nuclear Engineering
The University of New Mexico, Albuquerque, New Mexico 87131

INTRODUCTION

International oil shales vary widely in age and geological genesis and thus there are great differences in their behavior under pyrolyzing conditions. Our purpose is to understand and quantify how these differences in world oil shales may influence their future recoverability.

Emphasis is on a comparative study of several key international oil shales. Information is presented on the geology, organic and inorganic chemistry, and pyrolysis kinetics. To study and compare the thermal decomposition behavior of the oil shales, a series of nonisothermal gravimetric tests was performed. The thermal data were analyzed using several different kinetic models (Coats-Redfern, Nuttall-Chen, and Anthony-Howard). Results are presented for oil shales from Australia (Rundle), Brazil (Iratí), China (Fushun and Maoming), USA (Green River Formation), Israel, Morocco, Sweden (Naerke), and Yugoslavia.

SUMMARY

This study addresses the measurement, analysis, and comparison of pyrolysis kinetics and other characteristic parameters for several key international oil shales. Geologic and chemical information about each of the oil shale samples is presented to illustrate the widely varying nature of oil shale.

A summary of the kinetic models and data analysis methods is presented below along with the more significant kinetic results.

I. The weight loss data were first treated using the two parameter models (Coats-Redfern and Nuttall-Chen). The calculated activation energies were physically very low, thus leading to the evaluation of more sophisticated treatment methods and kinetic models.

II. Next, the TGA data were treated using the models mentioned in 'I', but the temperature range was divided into two regions (i. e., a region above and below 375°). This approach gave a better fit to the single heating rate data, but was not satisfactory for correlating the full multiple heating rate data.

III. The three parameter model, by Anthony and Howard, was best for correlating the full range of nonisothermal data. This is the first time that the Anthony-Howard model has been used to treat nonisothermal oil shale pyrolysis data. The calculated activation energies were physically more reasonable and the overall fit to the data was improved as compared to the two parameter models. This model gave satisfactory results for the full range of heating rates tested. Of course, a different set of model parameters was required for each sample.

IV. The Moroccan shale exhibited the highest kinetic rate constant.

V. Colorado oil shale showed the highest activation energy.

VI. The pyrolysis results clearly show that oil shales differ greatly in their thermal decomposition behavior and that some process modifications or new reactor designs may be needed to optimally treat a specific oil shale. Since oil shales are from widely different physical locations and were formed at greatly different geological times, it is not surprising that the pyrolysis kinetics and other properties vary widely.

ACKNOWLEDGMENT

This study is made possible by a research grant from Texaco, Inc. We wish to acknowledge the assistance of Texaco and express our thanks to their Bellaire Research Laboratories, in Bellaire, Texas, for the chemical analysis work they have done.

SYMPOSIUM ON GEOCHEMISTRY AND CHEMISTRY OF OIL SHALE
PRESENTED BEFORE THE DIVISIONS OF FUEL CHEMISTRY, GEOCHEMISTRY,
AND PETROLEUM CHEMISTRY, INC.
AMERICAN CHEMICAL SOCIETY
SEATTLE MEETING, MARCH 20 - MARCH 25, 1983

ASPECTS OF THE CHEMICAL AND RETORTING PROPERTIES
OF SELECTED AUSTRALIAN OIL SHALES

By

A. Ekstrom, H. J. Hurst and C. H. Randall
CSIRO Division of Energy Chemistry, Lucas Heights Research Laboratories,
Private Mail Bag 7, Sutherland, NSW, 2232, Australia

INTRODUCTION

Much of the present understanding of the chemical processes occurring during the heating and retorting of oil shales is based on work carried out with shales from the American Green River deposit (1-3). However, this shale is not typical of oil shales found in other deposits, and comparative studies of the chemical properties and retorting chemistry of a variety of shales might provide further insights into the undoubtedly very complex chemistry of these materials.

This paper presents results of some laboratory scale studies of the chemical and retorting properties of representative samples from five Australian oil shale deposits. In general terms, the results obtained indicate that these shales differ significantly in their chemical properties both from each other and from the shale of the Green River deposit.

EXPERIMENTAL

The kinetics of the oil and gas formation during the retorting of the shales were determined using an apparatus essentially identical to that described by Campbell et al. (2). Heating rates of 3°C/min were used and the argon carrier gas flow rates were 130 cc/min for the determination of the oil formation, and 30 cc/min for the determination of the rates of gas evolution. The shale samples used in these studies were sized, and dried at 120°C for 12 hours prior to use.

Demineralization of the shale was carried out using HCl/HF digestion on -90 µm sized samples. Solvent extraction studies on the demineralized shale were carried out using conventional Soxhlet extractors. TGA studies were carried out using a computer controlled Cahn thermobalance (Model No. RG2050) of conventional design.

RESULTS AND DISCUSSION

The samples of shale used in this work all originated in the various shale deposits located near the coastal areas of central Queensland. These deposits are believed to be of tertiary age and of lacustrine origin, and in contrast to the Green River deposit contain only small amounts of mineral carbonates. As summarized in Table I, the chemical composition of these shales differ widely, ranging from the Nagoorin carbonaceous shale with an organic carbon content of 65%, to the more conventional Duarina shale with an organic carbon content of 11%. The precise origin and nature of the black or carbonaceous shales found in the Nagoorin and Condor deposits are not understood at present, but from a chemical viewpoint significant differences between the black and conventional shales are readily apparent. Thus, the black shales are generally characterized by a high kerogen content, a significantly lower H/C ratio and a markedly lower oil yield per unit kerogen content. As will be shown below, the kinetics of the gas evolution from the black shales also differ from those of the normal shales.

The results of extraction of the kerogens isolated from the Stuart and Nagoorin shales with solvents of increasing polarity (Table II) indicate that these kerogens contain significant proportions of relatively low molecular weight, and presumably polar compounds. The fraction of kerogen extractable with a given solvent appears to be comparable with the results of similar studies on the Green River kerogen (4) and indeed with those obtained for bituminous coals (5,6). The appearance of the extract ranged from pale waxes for the less polar solvents to black, lustrous solids for pyridine, dimethyl formamide and dimethyl sulfoxide. The nature of extracts are not known at present, but elemental analysis on the dimethyl sulfoxide extracts showed these to have a lower H/C and higher O/C, S/C and N/C ratios than the original kerogen. This result would suggest that these extracts are composed of heteroatom-containing aromatic compounds. This very tentative conclusion

is supported by TGA results which showed that the pyrolysis of the extracts results in a significantly higher proportion of involatile residues when compared to the original kerogen.

TABLE I
PROPERTIES OF OIL SHALES

Sample	Fischer Assay (Litres/Tonne)	Assay (a)						Kerogen Content (wt %)	Ash in Kerogen (wt %)	Oil Yield/g Kerogen (cc/g)
		%C	%H	%N	%S	%O	H/C			
Nagoorin Carbonaceous (16998C)	232	65.2	4.94	2.74	0.1	17.9	0.91	72	0.2	0.32
Condor Carbonaceous (13338C)	69	28.3	2.43	1.29	0.4	11.0	1.03	33	0.4	0.21
Condor (19541C)	93	12.3	1.59	0.66	0.7	8.5	1.55	12	3.9	0.75
Stuart (18313C)	178	19.3	2.20	0.52	3.1	12.3	1.38	25	0.3	0.72
Duaringa (5363C)	86	11.0	1.93	0.40	0.1	8.3	2.09	14	4.7	0.61

(a) Based on shale dried at 120°C for 12 hours.

TABLE II
EFFECT OF SOLVENT POLARITY ON THE EXTRACTION OF KEROGEN

Solvent	% Kerogen Extracted	
	Stuart	Nagoorin
Hexane	2.4	2.0
Acetone	4.4	5.8
Chloroform	6.0	6.2
Methanol	7.9	3.2
Pyridine	9.9	16.4
Dimethylformamide	19.5	25.6
Dimethylsulfoxide	27.2	30.2

The retorting properties of the various oil shales heated at a linear rate of 3°C/min in an inert gas atmosphere are summarized in Table III. The most notable features of these data are firstly the relatively high water content of these shales, particularly for the two carbonaceous shales, and secondly the poor oil yield (relative to the Fischer assay) obtained by this technique. This latter effect appears to be related to the heating rate, and recent work (7) has shown that at a heating rate of 15°C/min, an oil yield equivalent to the Fischer assay can be obtained for the Condor (19541C) shale. In this respect, the shales studied in the present work appear to differ significantly from the Green River shale, for which it has been shown (8,9) that the oil yields decrease significantly only at heating rates below 1°C/min. It is possible therefore that the much greater effect observed for the present shales is a reflection of the greater tendency of the oil produced to undergo coking reactions.

Typical results of kinetic studies on the rates of oil formation from various shales (Figure 1, Table IV) show some differences in kinetic behavior amongst the various shales, although the general appearance of the curves and the temperatures at which the oil yields are maximum are similar to those reported for the Green River Shale (2). The results of the least squares analysis of these data in terms of the Anthony-Howard model (3,10) for non-isothermal kinetics (Table IV) showed that the results of the Nagoorin, Condor, Stuart and Duaringa shales could be reproduced quite well by a single process with activation energies in the range 200-232 kJ mol⁻¹ and relatively small (20-5 kJ mol⁻¹) standard deviation parameters. By comparison, the activation energy for the evolution of oil from the Green River shale heated at 2°C/min has been determined (3) as 219 kJ mol⁻¹. Only in the case of the Condor Carbonaceous shale was it necessary to consider two distinct processes

for the oil formation, in which the first process was responsible for 54% of the total oil yield and the second process for the remainder.

TABLE III
SUMMARY OF RETORTING CHARACTERISTICS^(a)

Sample	Fischer Assay Litres/Tonne	Wt Loss on Drying (b) %	Oil %	Product Yields ^(c)			Oil Yield (% of Fischer Assay)
				Water %	Char %	Gas + Losses %	
Nagoorin Carbonaceous 16998C	232	20.1	12.8	9.7	62.4	15.1	62
Condor Carbonaceous 13338C	69	14.3	6.1	8.0	79.9	6.0	99
Condor 19541C	93	3.4	6.0	3.8	82.3	7.9	75
Stuart 18313C	179	6.2	12.7	4.7	75.9	6.7	85
Duaringa 5363C	86	10.3	5.5	2.9	83.6	8.0	73

(a) Heating rate of 3°C/min in helium flowing at 130 cc/min. Particle size: - 3.3 mm + 1.4 mm

(b) Samples dried at 120°C for 12 hours

(c) Expressed as % of weight of dried shale.

TABLE IV
SUMMARY OF ACTIVATION PARAMETERS FOR OIL FORMATION^(a)

Sample	Preexponential Factor	Activation Energy kJ Mole ⁻¹	σ ^(b) kJ Mole ⁻¹	(°C)	
				Temperature at which rate of oil formation is maximum	
Nagoorin Carbonaceous (16998C)	2.5 x 10 ¹²	201	5.1	420	
Condor Carbonaceous (13338C)	Process (1)	1 x 10 ¹²	195	1.0	420
	(2)	1 x 10 ¹²	206	8.0	480
Condor (19541C)	1.0 x 10 ¹⁴	232	0.05	455	
Stuart (18313C)	1 x 10 ¹³	215	5.0	445	
Duaringa (5363C)	1 x 10 ¹⁴	225	5.0	430	

(a) Heating rate of 3°C/min, carrier gas flow rate of 130 cc/min. Values determined by least squares fit of data to Equation 1.

(b) Standard deviation of activation energies.

The effects of temperature on the rates of hydrogen, methane, carbon monoxide and carbon dioxide evolution from the five oil shales are shown in Figures 2-6, the integrated gas yields summarized in Table V, and the activation parameters for various representative contributing processes determined by analysis of the data in terms of the Anthony-Howard equation compiled in Table VI. The accuracy with which the gas evolution curves could be described by this procedure is illustrated in Figure 7, which compares the calculated and observed rates of methane evolution from the Condor carbonaceous shale. However, other cases, e.g., the H₂ evolution from Duaringa shale, were much more complex, and fits of the Anthony Howard equation only to the major contributing processes were attempted.

TABLE V
TOTAL GAS YIELDS TO 850°C^(a)

Sample	Gas Yields (cc/g) ^(b)			
	H ₂	CH ₄	CO	CO ₂
Nagoorin Carbonaceous (16998C)	46.9 (72.2)	19.8 (30.5)	73.5 (113.1)	22.6 (34.7)
Condor Carbonaceous (13338C)	28.0 (100.0)	14.0 (49.5)	17.1 (60.4)	7.3 (58.4)
Condor (19541C)	13.5 (109.7)	3.5 (28.5)	21.3 (173.1)	19.6 (159.3)
Stuart (18313C)	< 1	7.0 (36.2)	16.5 (85.5)	12.9 (66.8)
Duaringa (5363C)	11.4 (102.7)	3.2 (29.0)	5.7 (51.8)	6.9 (62.7)

(a) Heating rate:- 3.0°C/min

(b) At 0°C and 0.1 MP a pressure. Figures in brackets are the gas yields expressed as cc/g of organic carbon.

TABLE VI
SUMMARY OF REPRESENTATIVE PARAMETERS DETERMINED BY FITTING THE
ANTHONY-HOWARD EQUATION TO THE RATES OF GAS EVOLUTION

Sample	Gas	Process	Temp. at which rate of process is maximum °C	A S ⁻¹	E kJ mol ⁻¹	σ kJ mol ⁻¹	Fraction
Nagoorin Carbonaceous (16998C)	H ₂	1	570	1 x 10 ¹⁷	318	20	0.14
		2	700		384	31	0.86
	CO ₂	1	280	1 x 10 ⁸	110	8	0.23
		2	400		140	8	0.57
		3	600		182	8	0.20
	Condor Carbonaceous (13338C)	CO ₂	1	300	1 x 10 ⁸	120	18
2			430	148		6	0.60
CH ₄		1	500	1 x 10 ¹⁵	256	12	0.36
		2	570		287	14	0.42
		3	700		330	20	0.22
H ₂		1	600	6 x 10 ¹⁵	297	23	0.26
	2	730	361		29	0.74	
Condor (19541C)	CO ₂	1	460	5 x 10 ⁹	178	0.05	1.00
		2	580		249	21	0.60
	CH ₄	1	500	9 x 10 ¹²	223	10	0.40
		2	580		249	21	0.60
Stuart (18313C)	CO	1	450	5 x 10 ⁹	174	11	1.00
Duaringa(c) (5363C)	H ₂	1	460	1 x 10 ⁹	165	0.05	1.00

(a) Standard deviation of activation energies.

(b) Fractional contribution of the process considered to the total gas yield.

(c) Only the process with a maximum rate at the indicated temperature was considered in the analysis of the data.

Hydrogen

Examination of the hydrogen evolution profiles shows a striking difference between those observed for the carbonaceous shales and those of the normal shales. For the two carbonaceous shales, hydrogen evolution reaches a maximum in the temperature range 700–720°C with a minor contribution from a process having a maximum of $\sim 600^\circ\text{C}$. As summarized in Table VI, the activation energies for the 600°C process are in the range 300–320 kJ mol⁻¹, and 360–380 kJ mol⁻¹ for the 700°C process. The hydrogen evolution from these samples thus occurs in a temperature range in which the secondary pyrolysis reactions of the residues which remain after the primary bitumen decomposition is complete are thought to take place (2). In contrast, the hydrogen evolution rates from the Condor and Duaringa deposit resemble those observed for the Green River Shale (2) and show a sharp peak at 460°C, close to the temperature at which the oil formation is maximum. For the Duaringa shale this process is associated with an activation energy of ~ 165 kJ mole⁻¹ and is followed by further hydrogen evolution obviously comprising many processes occurring in the secondary pyrolysis region.

Methane

The methane evolution profiles for all five shale samples are surprisingly similar, but occur at significantly higher temperatures than have been observed (2) for the Green River shale. Although some methane evolution accompanies the oil formation, the major part is formed in the secondary pyrolysis region. At least three major processes with maxima at 500, 580 and 700°C appear to contribute to the total methane formation. Typical activation energies for these processes were determined for Condor carbonaceous shale and are summarized in Table VI.

Carbon Dioxide

The carbon dioxide evolution profiles for the Nagoorin, Duaringa and Condor carbonaceous shales are characterized by significant contributions commencing at temperatures as low as 150°C. It is unlikely that these processes are the result of mineral decomposition reactions, and their presence must reflect a contribution from thermally very labile components of the kerogen. A further major contribution to the CO₂ yield from these shales was found at temperatures corresponding to the maximum oil formation, but little CO₂ was formed in the secondary pyrolysis temperature range. In this respect, the behavior of these shales differs significantly from the American Green River Shale which shows (2) a negligible CO₂ evolution rate accompanying the oil release, but a very large rate at temperatures above 550°C resulting from the decomposition of the carbonate minerals.

The CO₂ evolution from the Condor and Stuart shales show sharp peaks at 500°C superimposed on a peak corresponding to the temperature at which the oil evolution occurs. These sharp peaks are probably associated with the decomposition of mineral constituents of the shale, but further work with acid washed shales would be required to confirm this conclusion.

Carbon Monoxide

All shale samples showed a significant peak in the CO evolution rates in the temperature range over which oil evolution occurs. At these relatively low temperatures it is unlikely that the reaction between CO₂ and residual char could be a significant source of carbon monoxide (2), and it appears that for these shales and in contrast to the Green River shale (2) the decomposition of the kerogen results in the formation of CO. In the case of the Stuart shale, the processes leading to the formation of the CO in the low temperature range are characterized by a mean activation of ~ 174 kJ mol⁻¹ and a distribution of 11 kJ mol⁻¹ (Table VI).

CONCLUSION

In conclusion, it appears that the shales examined in this study are characterized by the significant evolution of both carbon dioxide and carbon monoxide at temperatures near or below that at which oil evolution occurs. This effect is particularly pronounced for the two carbonaceous shales which also show hydrogen evolution in a temperature range normally associated with secondary pyrolysis reactions. These properties are more characteristic of brown and even bituminous coals, and it is possible that the carbonaceous shales and to a lesser extent the normal shales contain varying proportions of lignin-derived materials in addition to the more conventional oil shale kerogen (11). A detailed comparison of the composition of the oil produced from the carbonaceous and normal shales may provide further confirmation of this hypothesis, as would a petrographic comparison of these materials.

ACKNOWLEDGMENTS

We wish to thank Mr. John Gannon of Southern Pacific Petroleum Pty Ltd for the samples of oil shale used in this work and Mr. Jack Kristo for his assistance in the experimental work.

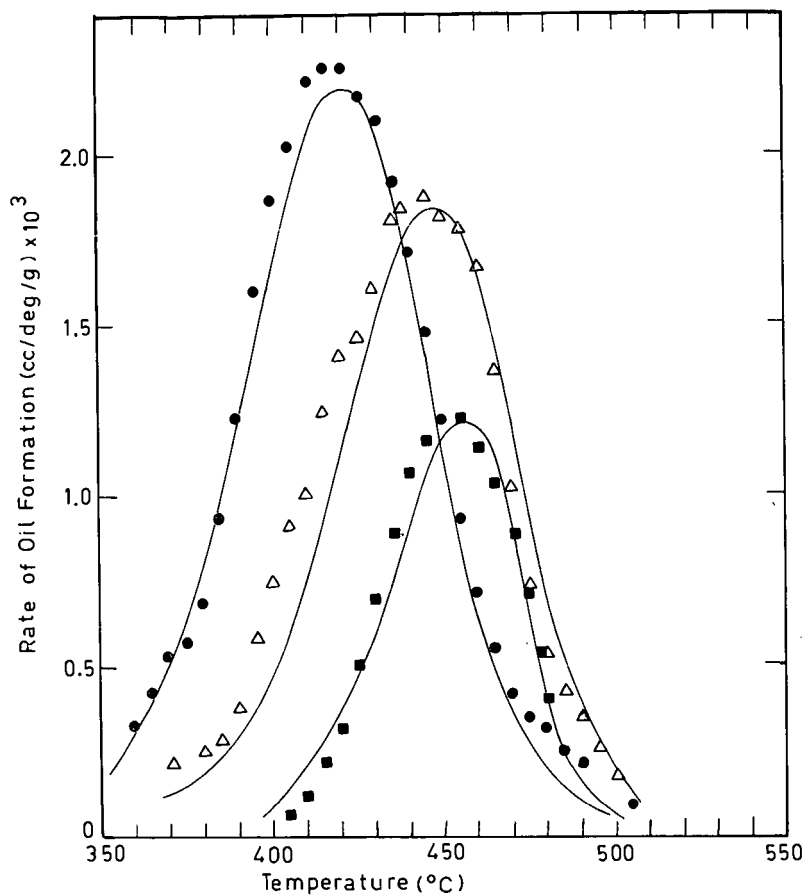
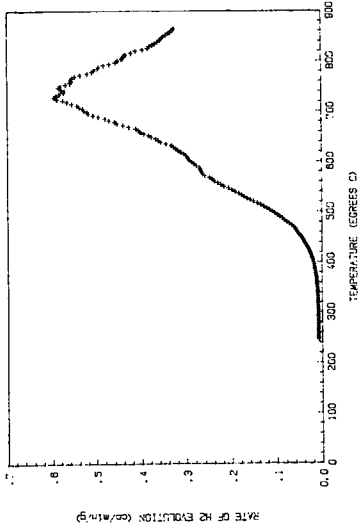
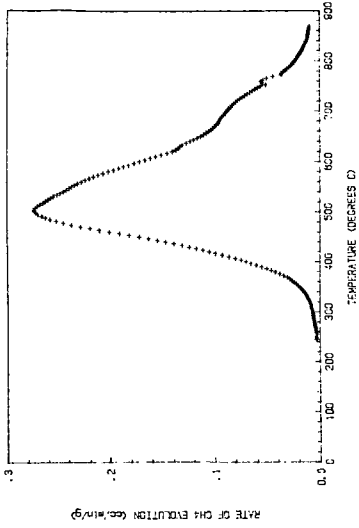


Figure 1. Effect of temperature on the rate of oil evolution. Heating rate $3^{\circ}\text{C}/\text{min}$, Argon flow rate $130 \text{ cc}/\text{min}$. Points are experimental data, solid line was calculated by Anthony-Howard equation using the parameters summarized in Table IV. ● Nagoorin carbonaceous, Δ Stuart, \square Condor carbonaceous.

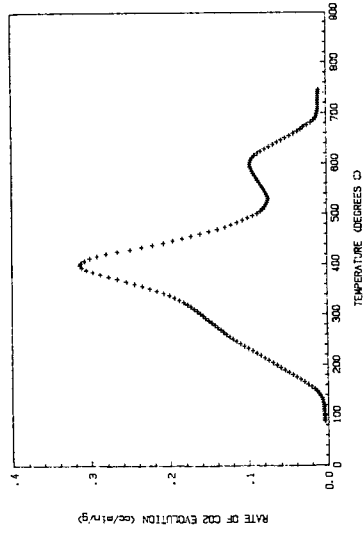
HAGGORN: (16998C) H₂



HAGGORN: (1998C) CH₄



HAGGORN: (16998C) CO₂



HAGGORN: (16998C) CO

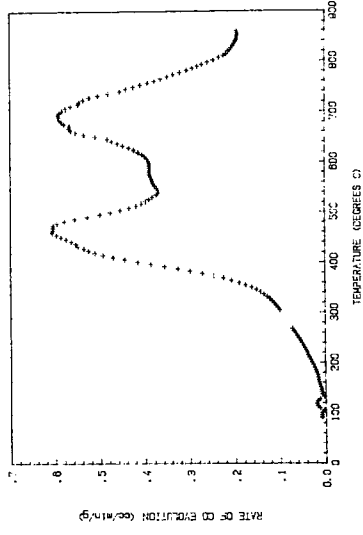
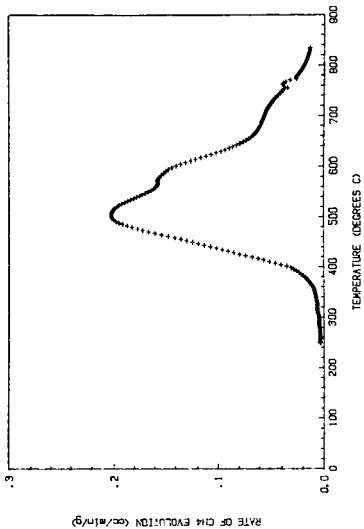
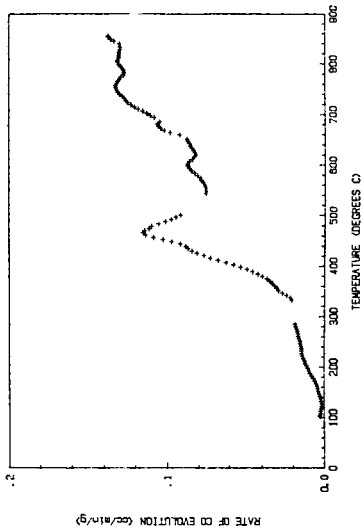


Figure 2. Effect of temperature on the H₂, CH₄, CO₂ and CO evolution rates from Nagoorin shale.

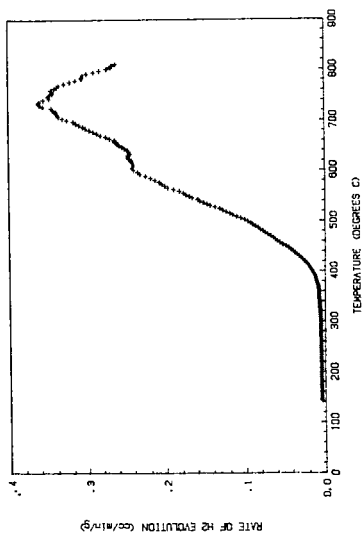
CONDOR CARBONACEOUS (1333BC) CH₄



CONDOR CARBONACEOUS (1333BC) CO



CONDOR CARBONACEOUS (1333B C) H₂



CONDOR CARBONACEOUS (1333BC) CO₂

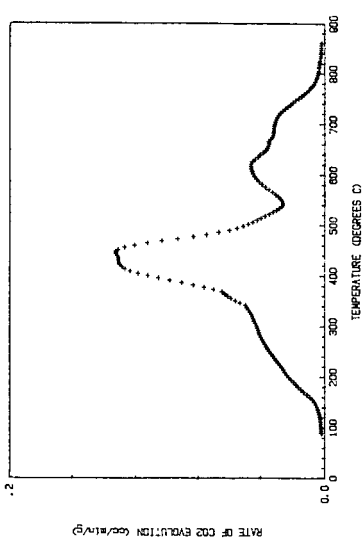
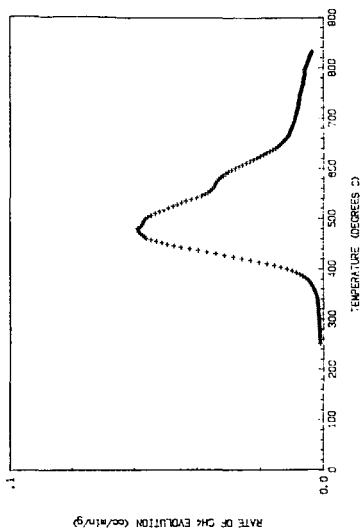
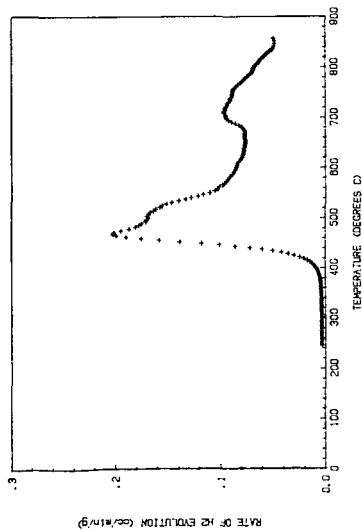


Figure 3. Effect of temperature on the H₂, CH₄, CO₂ and CO evolution rates from Condor carbonaceous shale.

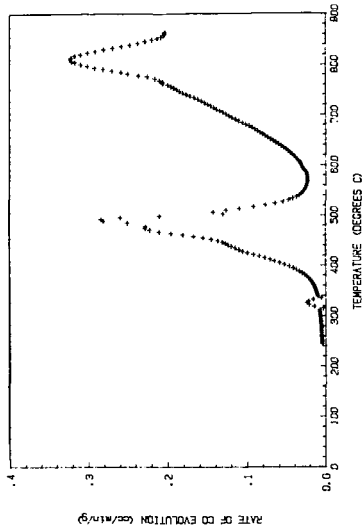
CONDOR (19541C) CH4



CONDOR (19541C) H2



CONDOR (19541C) CO



CONDOR (19541C) CO2

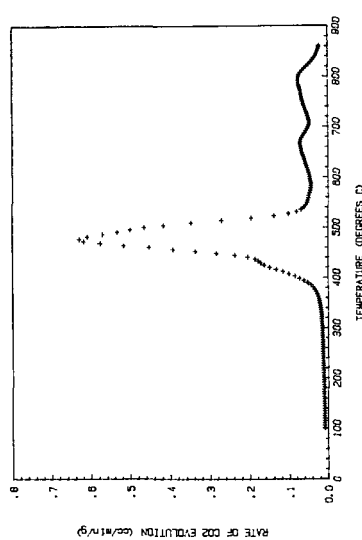
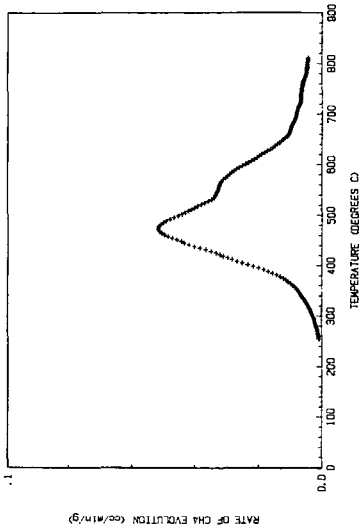
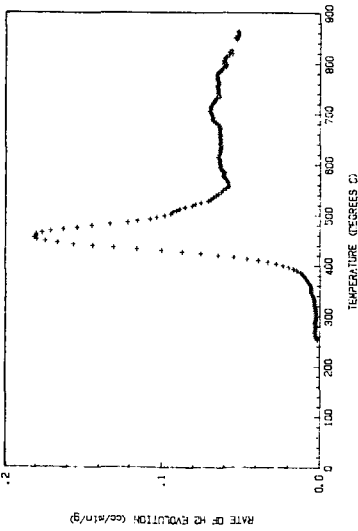


Figure 4. Effect of temperature on the H₂, CH₄, CO₂ and CO evolution rates from Condor shale.

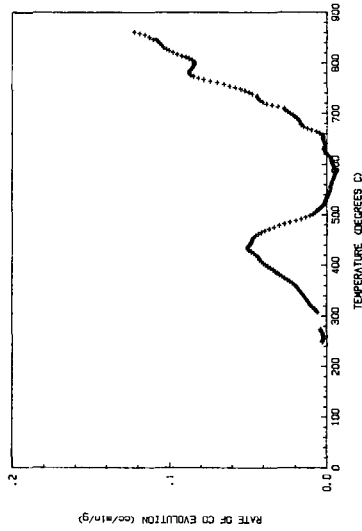
DUARINGA (5363C) CH4



DUARINGA (5363C) H2



DUARINGA (5363C) CO



DUARINGA (5363C) CO2

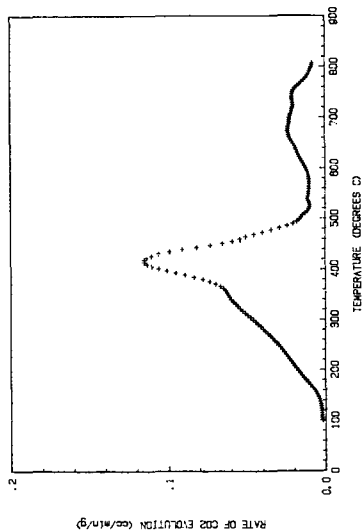
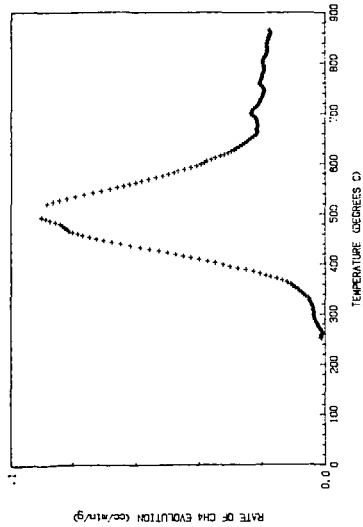
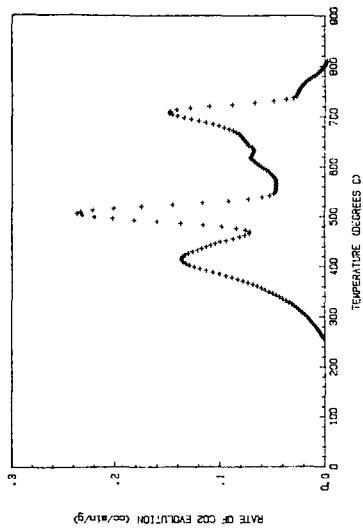


Figure 5. Effect of temperature on the H₂, CH₄, CO₂ and CO evolution rates from Duaringa shale.

STUART (18913C) CH₄



STUART (18913C) CO₂



STUART (18913C) CO

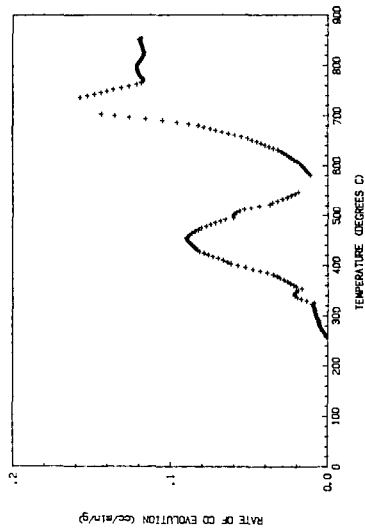


Figure 6. Effect of temperature on the CH₄, CO₂ and CO evolution rates from Stuart shale.

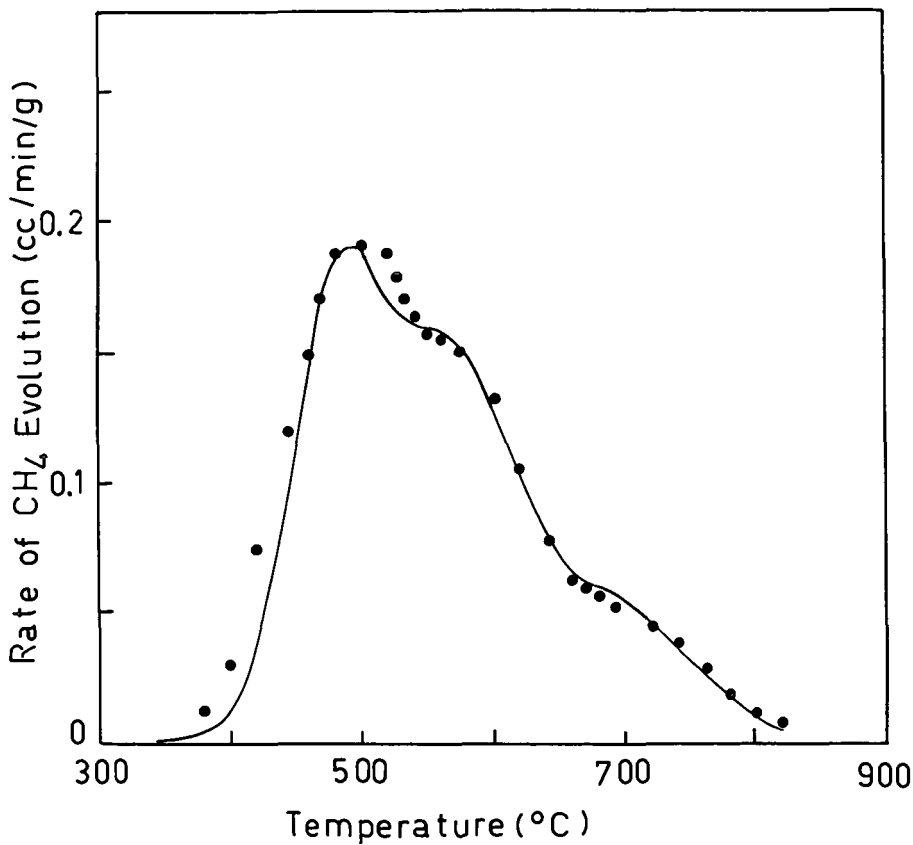


Figure 7. Comparison of the observed and calculated rate of methane evolution from Condor Carbonaceous shale. Solid line — calculated from Anthony-Howard equation using the parameters summarized in Table XI, ● - experimental data.

LITERATURE CITED

- (1) Campbell, J. H., Koskinas, G. J., and Stout, N. D., *Fuel*, 57, 376 (1978).
- (2) Campbell, J. H., Koskinas, G. J., Galligos, G., and Gregg, M., *Fuel*, 59, 718 (1980).
- (3) Campbell, J. H., Galligos, G., and Gregg, M., *Fuel*, 59, 727 (1980).
- (4) Robinson, W. E., "Kerogen of the Green River Formation", Chpt. 26 in "Organic Geochemistry, Methods and Results", G. Eglinton and M. J. J. Murphy ed. Springer-Verlag Berlin (1969).
- (5) Marzec, A., Juzwa, M., Betley, K., and Sobkowiak, M., *Fuel Process. Technol.*, 2, 35 (1979).
- (6) Marzec, A., Juzwa, M., and Sobkowiak, M., in "Gasification and Liquefaction of Coal". Symposium on the Gasification and Liquefaction of Coal, Katowice, Poland, April 1979. Coal/Sem. 6/R. 62 United Nations, Economic Commission for Europe (1979).
- (7) Ekstrom, A., and Randall, C. H., unpublished observation.
- (8) Campbell, J. H., Koskinas, G. J., Stout, N. D., and Coburn, T. T., *In-Situ*, 2, 1 (1978).
- (9) Evans, R. A., and Campbell, J. H., *In-Situ*, 3, 33 (1979).
- (10) Anthony, D. B., and Howard, J. B., *AIChEJ.*, 22, 625 (1976).
- (11) The authors thank Dr. J. Saxby for drawing their attention to this interpretation.

SYMPOSIUM ON GEOCHEMISTRY AND CHEMISTRY OF OIL SHALE
PRESENTED BEFORE THE DIVISIONS OF FUEL CHEMISTRY, GEOCHEMISTRY
AND PETROLEUM CHEMISTRY, INC.
AMERICAN CHEMICAL SOCIETY
SEATTLE MEETING, MARCH 20-25, 1983

HIGH-PRESSURE PYROLYSIS OF COLORADO OIL SHALE

By

Alan K. Burnham and Mary F. Singleton

Lawrence Livermore National Laboratory, P. O. Box 808, L-207, Livermore, California 94550

INTRODUCTION

Studies of pyrolysis of kerogen-rich rocks under pressure are valuable for evaluating potential oil shale processing schemes (1-5) as well as understanding the formation of petroleum (6, 7). The great variety of experimental techniques has led to a variety of results. None of the existing studies are sufficiently broad ranged to properly separate the effects of temperature (or heating rate), pressure, residence time and gas atmosphere on oil yield and composition.

In the work we present here, we have pyrolyzed Green River oil shale in a low porosity reactor where the products are allowed to escape as produced. This self-purging design results in the pyrolysis occurring in a nearly autogenous atmosphere. One application of pyrolysis results for the conditions considered here is the estimation of oil yield from radio-frequency in-situ processing (8). This report is a preliminary analysis of work in progress.

EXPERIMENTAL

The sample used in the study was a 94 L/Mg (22.4 gal/ton) Green River oil shale from the Anvil Points mine near Rifle, CO. The particle size was 0.42 to 0.84 mm (-20 +40 mesh). It contained by weight 10.88% org C, 4.76% min C, 1.64% H, 0.42% N and 0.59% S. It was a byproduct of a large-scale sample preparation for other experiments and, thereby, represents an average composition over a broad stratigraphic section of the Mahogany zone.

The apparatus used is shown schematically in Figure 1. The sample is compressed into 3.2 cm diam. pellets using a pressure of 24,000 psi. Two of these pellets, weighing a total of about 110 g, are welded into the sample can (3.3 cm diam.) along with quartz sand above and around the pellets to reduce porosity. We determined the porosity of the pellets to be about 24% from the helium buoyancy density of the raw shale and the weight and dimensions of the pellets. Total porosity in the reactor averaged 29%, or equivalently, the total void volume was about 20 cm³.

For the near-atmospheric pressure experiments, a thermocouple in a well measured the temperature near the center of the oil shale sample. Previous experience in similar experiments indicates that the difference in temperature across the sample is less than 5°C. A second thermocouple measured the temperature outside the reactor near the furnace wall. For the high-pressure experiments, the sample thermocouple was omitted and the sample temperature was estimated from the furnace thermocouple and the difference between the sample and furnace thermocouples in the atmospheric-pressure experiments.

The sample and oil collection system is prepressurized with argon and the pressure is maintained approximately constant during the experiment by a back-pressure regulator. In fact, the pressure in the reactor increased by nearly 1 atm over the course of the experiment as the gas collection system filled. Sufficient steam is produced at temperatures below 250°C to purge the argon from the reactor. We believe that the diffusion of argon back into the reactor is sufficiently slow that the pyrolysis occurs in an atmosphere close to the composition of the pyrolysis products. At the end of the experiment, all the gas in the system is pumped into the gas collection bottle by a bellows pump. The second trap is cooled to -77°C during pumping. Other analytical procedures are the same as those described previously (9).

RESULTS AND DISCUSSION

The material balance, oil yields and distribution of organic carbon are shown in Table I. Oil properties are given in Table II. A few observations are in order. The density of the oil changes sufficiently that the yield depends strongly on whether it is calculated on a weight or volume basis, so comparisons of yields under various conditions should be made cautiously.

At near-atmospheric pressure, the oil yield decreases with a decrease in heating rate.

The volumetric yields are in excellent agreement with those previously reported by Campbell (10, 11). The slow-heating-rate oils have a lower nitrogen content due to coking of nitrogen-rich aromatics. Nearly four times as much organic carbon is converted to coke as to gas during coking reactions and the principal gaseous products are H_2 and CH_4 (Table III). Both these results are consistent with those of Campbell et al. (10). The slow-heating-rate oil has lower density and nitrogen content, in agreement with Stout et al. (12) and a lower boiling-point distribution, in agreement with Jackson et al. (13).

TABLE I
PRODUCT DISTRIBUTION

Heating rate (°C/h)	Pressure (atm)	Mass balance (%) ^a	Condensed Oil Yield		Organic Carbon Distribution ^b				
			Wt % FA	Vol % FA	Condensed Oil	Total Oil ^c	Gas ^d	Shale ^e	Total
720	1.0	99.56	100	100	65.0	66.4	5.9	22.7	95.0
110	1.5	99.73	97	98	63.5	64.6	6.1	25.2	95.9
11	1.5	99.29	86	89	56.1	57.5	7.6	29.0	94.2
1	1.5	99.18	77	81	49.6	51.0	6.2	31.9	89.0
108	27	99.34	78	84	50.3	50.5	9.1	31.5	91.1
9	27	99.41	73	80	46.3	46.4	8.6	35.4	90.4
1	26	99.36	72	79	45.7	45.9	6.6	33.8	86.2

- Oil + water + gas + retorted shale/raw shale; sample size ~110 g.
- Percent of the raw shale organic carbon in products.
- Includes C_5+ compounds in gas.
- CO , CO_2 and C_1 - C_4 hydrocarbons.
- Includes a very minor contribution from coke deposited in the sand surrounding the cores.

TABLE II
OIL PROPERTIES

Heating rate (°C/h)	Pressure (atm)	Density (g/cm ³) ^a	Elemental Analysis (Wt %)				Simulated Distillation ^b				
			C	H	N	S	10%	25%	50%	75%	90%
720	1.0	0.906	83.3	11.2	2.7	0.66	175	258	361	450	504
110	1.5	0.888	84.0	11.2	2.8	0.69	155	238	340	429	485
11	1.5	0.872	83.9	11.6	2.3	0.70	151	226	319	403	459
1	1.5	0.862	82.6	12.3	1.6	0.56	155	225	303	381	440
108	27	0.842	82.4	11.4	2.6	0.57	104	168	250	332	403
9	27	0.823	81.5	11.7	2.2	0.43	111	169	241	317	385
1	26	0.826	81.6	12.9	1.5	0.36	122	178	256	330	395

- 23°C
- Temperature (°C) at which the given percentage has distilled - ASTM-D-2887.

The yields from all the pyrolysis experiments at 27 atm are lower than the lowest oil yield from the atmospheric pressure experiments. The oil yield at 27 atm also decreases with a decrease in heating rate, but the effect is much smaller than at atmospheric pressure. As in the case of yield loss caused by slow heating, most of the yield loss caused by high pressure goes into coke production. This conclusion must be qualified with the caution that the carbon balances on the high pressure experiments are significantly lower than what we normally consider satisfactory. We are not sure of the reason for this problem, but the most likely source of loss is in gas, especially light hydrocarbons. Besides the possibility of leakage, which we were not able to detect, gas collection is complicated by the high gas solubility in the oil at 27 atm. About 1.5 cm³ of "liquid" boils away when the pressure is released at the end of an experiment. The original plan was to pump the oil collection system down to several Torr, in which case C_3 and C_4 hydrocarbons would be transferred to the gas collection bottle, while C_5 and higher compounds would be captured in the dry ice trap if pumped from the oil receiver. Unfortunately, the bellows pump only reached a pressure of about 200 Torr, in which case most of the butane and some of the propane was probably retained in the dry ice trap, then lost during warmup and before weighing. This would not have been

a problem during the atmospheric pressure experiments because most of the C₃ and C₄ hydrocarbons would already be in the gas collection system prior to cooling the trap.

TABLE III
GAS PRODUCTION

(M Moles of Product/g of Raw Shale Organic Carbon)

Heating rate (°C/h)	Pressure (atm)	H ₂	CH ₄	C ₂ H _x	C ₂ H ₄		C ₃ H ₆	
					C ₂ H ₆	C ₃ H _y	C ₃ H ₈	C ₄ H _z
720	1.0	1.47	0.98	0.47	0.30	0.34	0.88	0.21
110	1.5	2.02	1.17	0.46	0.20	0.32	0.68	0.19
11	1.5	2.98	1.69	0.60	0.12	0.40	0.45	0.23
1	1.5	3.36	1.88	0.90	0.08	0.35	0.28	0.21
108	27	1.14	2.26	0.85	0.05	0.38	0.23	0.20
9	27	0.82	3.36	1.00	0.01	0.38	--	0.05
1	27	0.39	2.87	0.61	0.003	0.21	--	0.03

There are some other interesting results from the high pressure experiments. The nitrogen content of the oil is only slightly less than that at the same heating rate at atmospheric pressure. This indicates that the principal mechanism of coke deposition at high pressure is probably different from that at atmospheric pressure, although our oil characterization is too incomplete yet to be more definitive. In contrast, the sulfur content is approximately independent of heating rate at atmospheric pressure, but is significantly reduced at high pressure, especially at slow heating rates. A similar effect of pressure on nitrogen and sulfur contents was observed by Wise et al. (2). The high pressure oil is also substantially lighter as reflected in density, boiling point distribution and color. In fact, the product from the 27 atm pyrolysis experiments at 1 and 9°C/h is a clear amber rather than the usual opaque brown. A similar observation was made many years ago by McKee (14). Apparently the highly light absorbing chromophores, presumably aromatic heterocycles, are not being formed or are being hydrolyzed by the pyrolysis gas. In this regard, we note that the H₂ production is decreased at high pressures.

At the present time, we have just begun our characterization of the liquid product. Analysis by capillary column chromatography has produced some interesting results, a few of which are shown in Figure 2 and in Table IV. Alkene/alkane ratios, as exemplified by 1-dodecene/n-dodecane, decrease with both a decrease in heating rate and an increase in pressure as expected. We have noted previously that ratios involving sums of alkenes and alkanes are nearly independent of heating rate (oil coking) (15). The ratio of phytane to n-octadecene plus 1-octadecene (C₁₈s) is nearly constant. Also, the pristane+enes/phytane ratio is approximately constant although the prist-1-ene/pristane and prist-2-ene/phytane ratios vary dramatically with conditions.

TABLE IV
VALUES OF INDICATOR RATIOS DETERMINED BY
CAPILLARY COLUMN GAS CHROMATOGRAPHY

Heating rate (°C/h)	Pressure (atm)	1-dodecene		phytane C ₁₈ s	pristane+enes phytane	Sterane content
		n-dodecane	n-dodecane			
720	1.0	0.84	0.53	2.2	high	
110	1.5	0.60	0.47	2.1	medium	
11	1.5	0.34	0.45	1.9	medium	
1	1.5	0.22	0.43	1.8	medium	
108	27	0.21	0.38	1.9	low	
9	27	0.09	0.34	1.7	low	
1	26	0.03	0.31	1.9	low	

However, high temperatures that cause thermal cracking of long-chain hydrocarbons can cause the phytane/C₁₈s ratio to decrease. In Figure 3, we show a reanalysis of old data on shale oil cracking (16). The phytane/C₁₈s ratio decreases because longer chain normal alkanes can crack to n-C₁₈s, but there are no longer-chain isoprenoids to produce phytane. A comparison of

the results in Table IV and Figure 2 indicates that oil yield loss at 27 atm by cracking long-chain hydrocarbons to (primarily) hydrocarbon gases ranges from about 5% at 108°C/h to about 10% at 1°C/h. This is also reflected in the lower boiling point distribution given in Table II. We also note that the high pressure pyrolysis almost completely eliminates the sterane and pentacyclic triterpane content of the oil.

The destruction of steranes and triterpenes caused by the oil cracking may be less in a solid core of material having essentially no initial porosity. The residence time of the biomarker compounds in the reactor would be substantially lower with a smaller initial porosity because they are the first compounds to be evolved (15). The later-evolving products would be affected less by the decreased initial porosity because this grade of shale produces about 25% porosity during oil evolution (17) which would only result in a two-fold change in residence time. The overall yield for a lower porosity reactor might be 5% or so higher at our slowest heating rate and highest pressure.

Finally, we note that high pressure appears to delay evolution (not necessarily generation) of oil. This effect has been previously noted by Noble et al. (3). The temperature for ~99% completion of oil evolution is compared in Table V with that predicted by the kinetic expressions of Campbell et al. (18) and Shih and Sohn (19), both of which were derived at atmospheric pressure. In all cases, a higher temperature is required than calculated. The disagreement is greatest at slow heating rates and high pressures, although the effect of pressure itself appears to be lowest at the slowest heating rates. A more complete comparison of time-dependent oil yield is given in Figure 4 using the kinetic expression of Campbell (18) for the calculated value. Pressure would be expected to affect the oil evolution rate if the rate of evaporation is comparable or slower than the rate of generation.

TABLE V

EXPERIMENTAL ($\pm 5^\circ\text{C}$) AND CALCULATED TEMPERATURES FOR 99% OF OIL EVOLUTION

Heating rate ($^\circ\text{C}/\text{h}$)	Pressure (atm)		Calculated	
	1.5	27	Campbell (18)	Sohn (19)
110	465	495	460	465
10	430	455	415	415
1	400	410	380	375

SUMMARY

Rates of oil evolution and oil yields and compositions have been reported for heating rates from 1 to 100°C/hr and pressures up to 27 atm. Pyrolysis occurred in an autogenous atmosphere and generated products were allowed to escape the pyrolysis region continuously. We found that both higher pressures and lower heating rates cause a decrease in oil yield, although the effects are not additive. The lowest oil yield was approximately 72 wt % or 79 vol % of Fischer assay. Lower oil yield is generally accompanied by lower boiling-point distribution, nitrogen content and density and higher H/C ratios. The high-pressure/slow-heating rate oils are a clear amber color instead of the usual opaque brown. We demonstrated the effect of pyrolysis conditions on biological markers and other diagnostic hydrocarbons. Finally, we showed that the rate of oil evolution is retarded by pressure and that existing kinetic expressions for oil evolution overestimate the rate at slow heating rates and high pressures.

ACKNOWLEDGMENTS

We appreciate the design of the apparatus by E. Huss, W. Miller and R. Taylor and the construction and continuing support by J. Taylor and C. Hall. We also thank L. Gregory, J. Clarkson, J. Cupps, C. Otto and R. Ryan for analytical support and R. Taylor for numerous helpful discussions.

Work was performed under the auspices of the U. S. Department of Energy by the Lawrence Livermore National Laboratory under contract number W-7405-ENG-48.

APPARATUS FOR PYROLYSIS UP TO 27 ATM

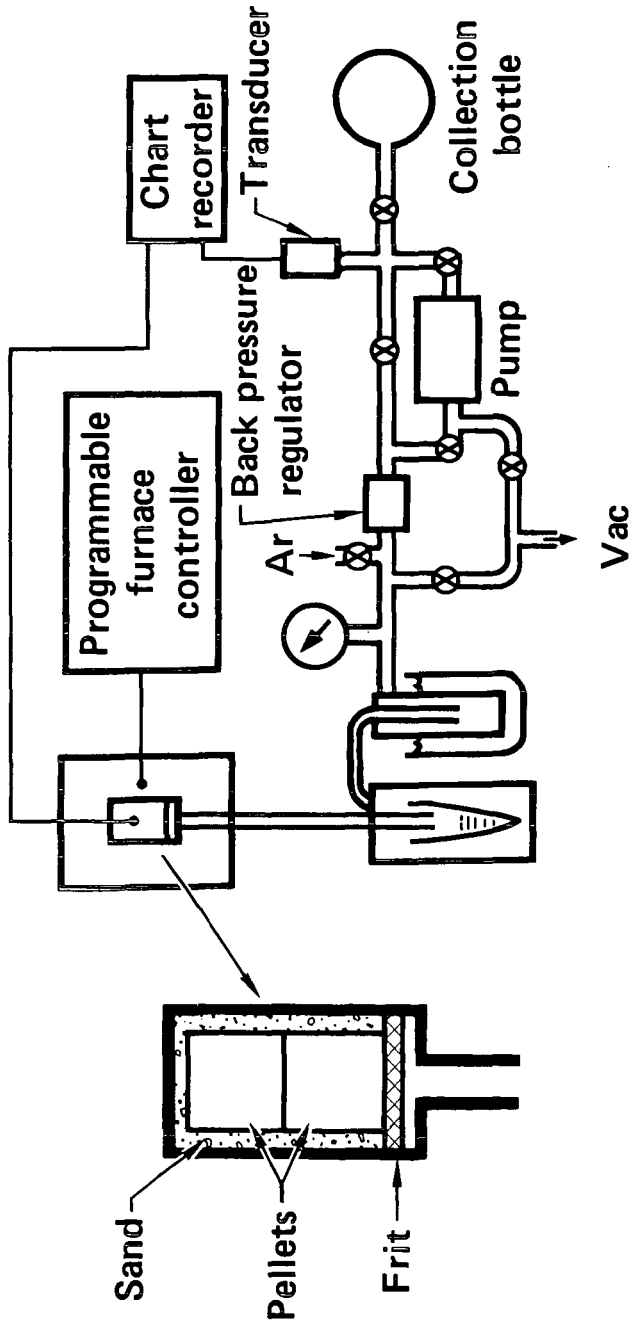


Figure 1. Apparatus for pyrolysis under an autogenous atmosphere.

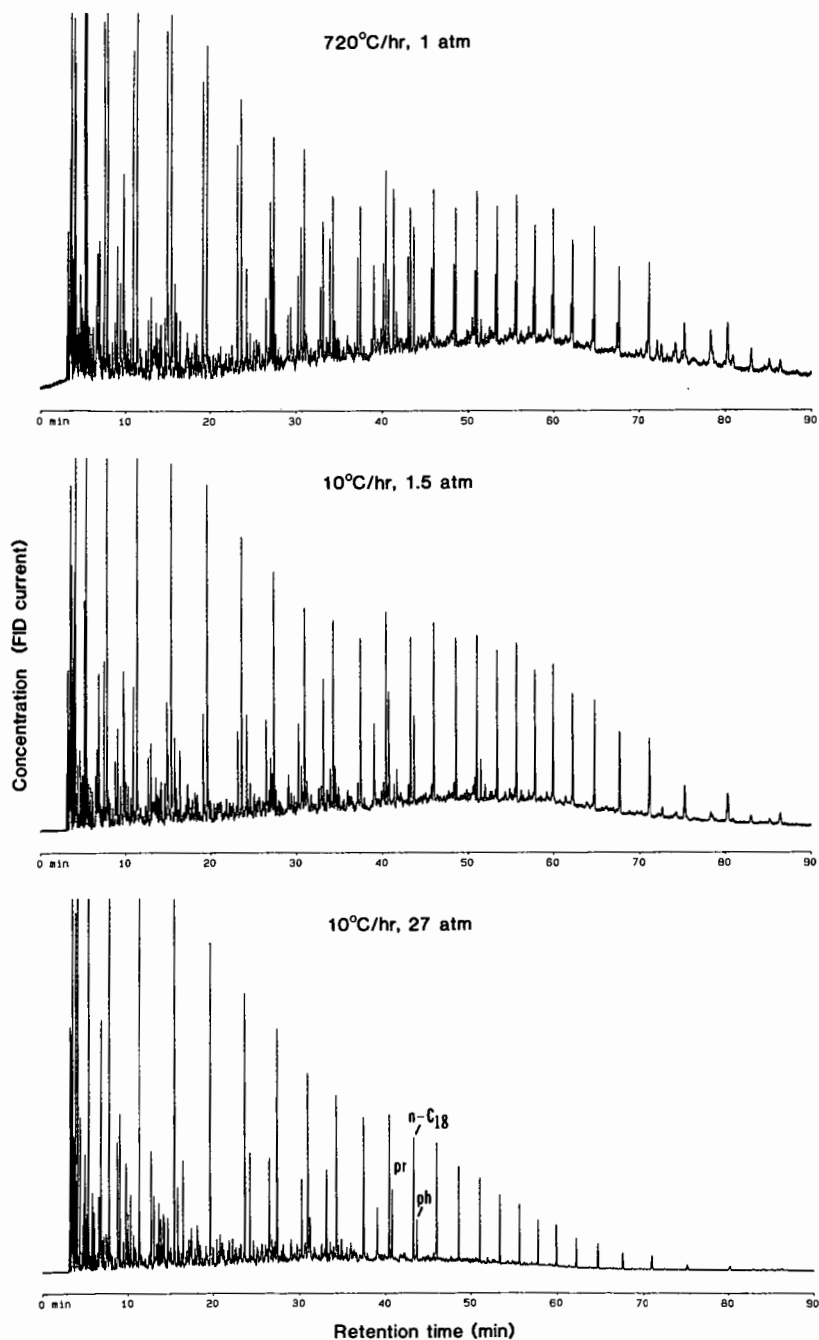


Figure 2. Capillary column gas chromatograms of three oil samples produced during this work. For reference, pristane (pr) phytane (ph) and $n\text{-C}_{18}$ are labeled in the bottom chromatogram.

PHYTANE CONCENTRATION IS DECREASED BY CRACKING

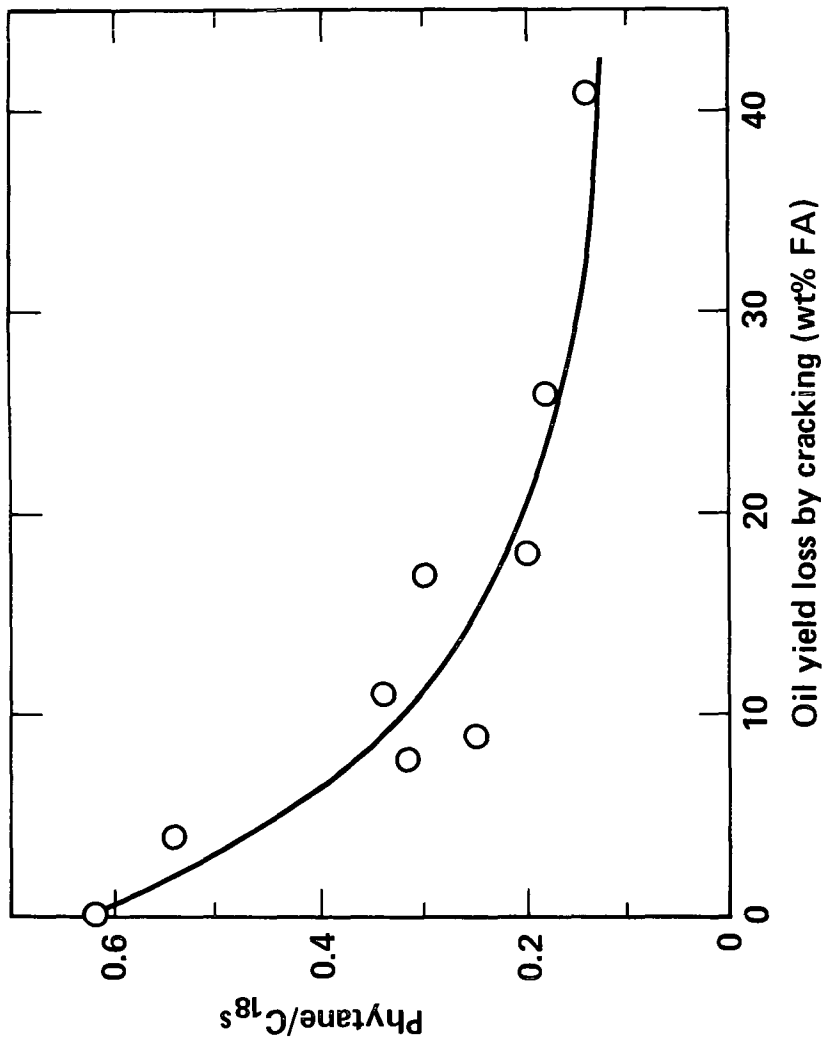


Figure 3. Relationship between phytane content and oil cracking determined from previously reported results (16).

COMPARISON OF MEASURED AND CALCULATED OIL EVOLUTION



○ 1.5 atm
△ 27 atm

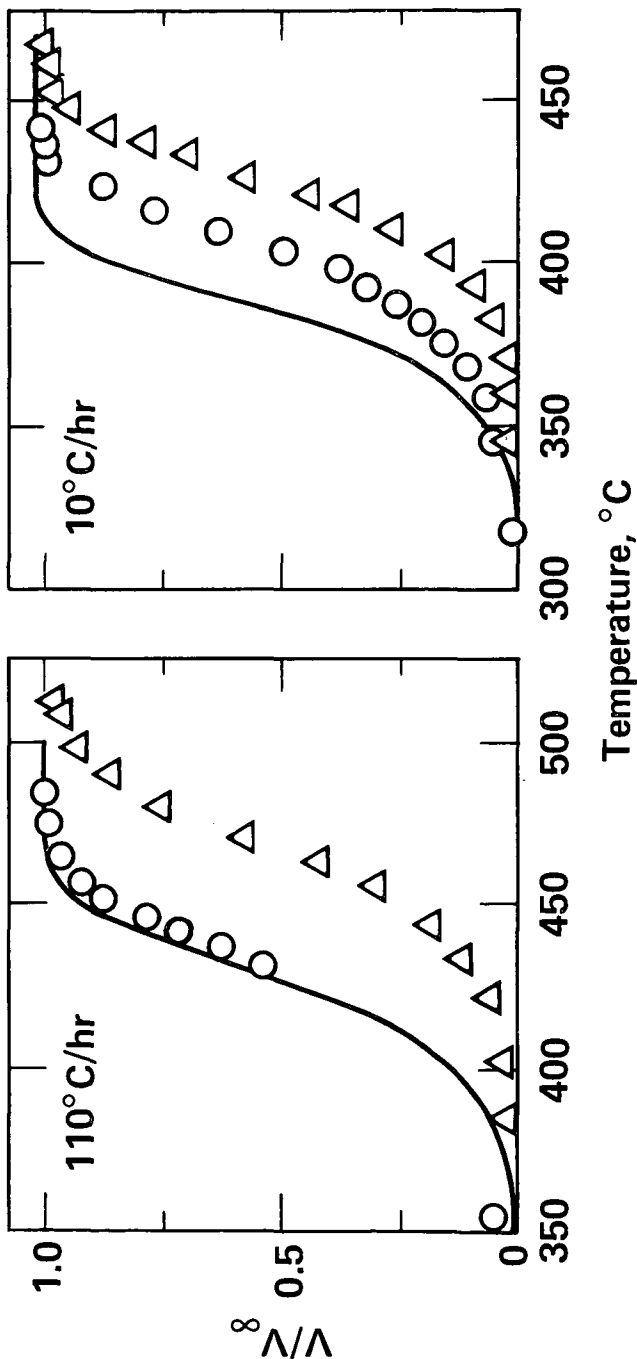


Figure 4. Experimental (points) and calculated (lines) volumes of oil evolved as a function of temperature as the sample is heated at the indicated heating rate.

LITERATURE CITED

- (1) Bae, J. H., "Some Effects of Pressure on Oil-Shale Retorting", Soc. Petrol. Eng. J., 278-292 (1969).
- (2) Wise, R. L., Miller, R. C. and George, J. H., "A Laboratory Study of Green River Oil Shale Retorting Under Pressure in a Nitrogen Atmosphere", Preprints, ACS, Div. Fuel Chem., 21 (6), 87 (1979).
- (3) Noble, R. D. and Wang, C. -C., Kerogen Decomposition Under Elevated Pressures, Rept. DOE/LC/01761-T2 (1981).
- (4) Weil, S. A., "Oil Shale Hydrotreating Laboratory Studies at IGT", in Symp. Papers, Synthetic Fuels from Oil Shale, Inst. Gas Technol., 353-376 (1980).
- (5) Sresty, G. C., Dev, H., Snow, R. H. and Bridges, J. E., "Kinetics of Low Temperature Pyrolysis of Oil Shale by the IITRI RF Process", 15th Oil Shale Symp. Proceedings, Colorado School of Mines Press, 411-423 (1982).
- (6) Lewan, M. D., Winters, J. C. and McDonald, J. H., "Generation of Oil-Like Pyrolysates from Organic-Rich Shales", Science, 203, 897-899 (1979).
- (7) Bandurski, E., "Structure Similarities Between Oil-Generating Kerogens and Petroleum Asphaltenes", Energy Sources, 6, 47-66 (1982).
- (8) Mallon, R. G., Economics of Shale Oil Production by Radio Frequency Heating, Lawrence Livermore Natl. Laboratory Rept. UCRL-52942 (1980).
- (9) Singleton, M. F., Koskinas, G. J., Burnham, A. K. and Raley, J. H., Assay Products from Green River Oil Shale, Lawrence Livermore Natl. Laboratory Rept. UCRL-53273 (1982).
- (10) Campbell, J. H., Koskinas, G. J., Stout, N. D. and Coburn, T. T., "Oil Shale Retorting: Effects of Particle Size and Heating Rate on Oil Evolution and Intraparticle Oil Degradation, *In situ*, 2, 1 (1978).
- (11) Evans, R. A. and Campbell, J. H., "Oil Shale Retorting: A Correlation of Selected Absorbance Bands with Process Heating Rates and Oil Yield", *in situ*, 3, 33 (1979).
- (12) Stout, N. D., Koskinas, G. J., Raley, J. H., Santor, S. D., Opila, R. J. and Rothman, A. J., "Pyrolysis of Oil Shale: Effects of Thermal History on Oil Yields", Colorado School of Mines Quart., 71, 153 (1976).
- (13) Jackson, L. P., Allbright, C. S. and Poulson, R. E., "Olefin Analysis in Shale Oils", in Anal. Chem. Liq. Fuel Sources, Avd. Chem. Ser. 170, 232-42 (1978).
- (14) McKee, R. H., Shale Oil, Chemical Catalog Co., 1, 82 (1925).
- (15) Burnham, A. K., Clarkson, J. E., Singleton, M. F., Wong, C. M. and Crawford, R. W., "Biological Markers from Green River Kerogen Decomposition", Geochim. Cosmochim. Acta, 46, 1243-1251 (1982).
- (16) Burnham, A. K., "Chemistry of Shale Oil Cracking", Oil Shale, Tar Sands and Related Materials, ACS Symp. Series No. 163, 39-60 (1981).
- (17) Slettevold, C. A., Biermann, A. H. and Burnham, A. K., A Surface-Area and Pore-Volume Study of Retorted Oil Shale, Lawrence Livermore Natl. Laboratory Rept. UCRL-52619 (1978).
- (18) Campbell, J. H., Koskinas, G. J. and Stout, N. D., "Kinetics of Oil Generation from Colorado Oil Shale", Fuel, 57, 372 (1978).
- (19) Shih, S. M. and Sohn, H. Y., "Nonisothermal Determination of the Intrinsic Kinetics of Oil Generation from Oil Shale", I and EC, Process Design and Develop., 19, 420-426 (1980).

SYMPOSIUM ON GEOCHEMISTRY AND CHEMISTRY OF OIL SHALE
PRESENTED BEFORE THE DIVISIONS OF FUEL CHEMISTRY, GEOCHEMISTRY
AND PETROLEUM CHEMISTRY, INC.
AMERICAN CHEMICAL SOCIETY
SEATTLE MEETING, MARCH 20-25, 1983

PROTON NMR THERMAL SCANNING METHODS FOR THE STUDY OF OIL SHALE PYROLYSIS

By

Leo J. Lynch and David S. Webster
CSIRO Physical Technology Unit, 338 Blaxland Road, Ryde. 2112. Australia

INTRODUCTION

Dynamic experimental techniques by which non-equilibrium states of a system can be observed during thermally induced transformations allow the kinetics of pyrolysis mechanisms to be directly studied. This paper reports on the novel use of simple low resolution Proton nuclear magnetic resonance (^1H NMR) measurements as a reaction time probe to monitor the state of oil shales during heating from room temperature to $\sim 870\text{K}$. The method involves the observation of the ^1H NMR transverse relaxation transient at regular intervals during heating. Similar studies of coal pyrolysis (1-6) and a description of the apparatus (7) used have been previously reported. In these reports, the ability to obtain non-equilibrium data during fossil fuel pyrolysis despite the limited scope for signal averaging and the deterioration of signal-to-noise of the ^1H NMR signal with rise in temperature was demonstrated.

The experiments reported here involved measurements of the ^1H NMR during pyrolysis of shale specimens contained in open tubes and flushed with dry nitrogen gas so that volatile pyrolysis products were quickly removed. A number of different parameters extracted from the data are investigated for their usefulness in monitoring changes that occur in the properties of the specimen. These parameters relate to the loss of hydrogen from the specimen and changes that occur in the molecular structure and mobility as a consequence of chemical and physical transformations.

The results presented are not part of a systematic study of oil shale pyrolysis but rather those of various experiments selected to demonstrate the utility and potential of the method.

EXPERIMENTAL

The shale samples used here were obtained from CSIRO Division of Fossil Fuels and CSIRO Division of Energy Chemistry in a finely ground form. The specimens for measurement consisted of 300-500 mg of material predried under nitrogen at 105°C and contained in open glass tubes. The ^1H NMR measurements were made at 60 MHz or 90 MHz using high temperature specimen probes and temperature control apparatus described previously (7). The specimens were positioned within the inner 2/3 of the measurement radio-frequency coil of the NMR probe so that at all stages during an experiment the ^1H NMR signal of all the residual material was recorded. The specimen tubes were continuously flushed with a stream of dry nitrogen gas throughout the heating cycles which rapidly removed volatile products formed from the measurement zone.

The $90^\circ\text{-}\tau\text{-}90^\circ$ NMR pulse sequence (8) was used to stimulate the solid-echo ^1H NMR transverse relaxation signal as shown in Figure 1. This method of observing the signal is preferred to the simpler single 90° pulse method to overcome the receiver dead-time problem which is significant for many of the rapidly relaxing ^1H NMR transients observed. Receiver dead-time was $\sim 4\mu\text{s}$ and a pulse spacing, τ , of $15\mu\text{s}$ was used.

Measurements were recorded dynamically at regular intervals while the specimens were heated at a uniform rate of $4\text{K}/\text{minute}$ from room temperature to temperatures greater than 850K . Temperatures were recorded with an accuracy of $\pm 1\text{K}$ and care was taken to maintain tuning of the NMR probe during the changing conditions of the experiment. A Bruker BC-104 transient digitizer carefully compensated for spurious signals was used to record the ^1H NMR solid-echo signals.

RESULTS AND ANALYSIS

A typical ^1H NMR solid-echo signal recorded during heating is shown in Figure 1. For a rigid-lattice pair-wise dipolar coupled population of proton spins, the solid-echo signal is a full representation of the transverse relaxation and the peak of the echo, i_T , a measure of the total hydrogen content of the specimen (8). The extent to which the proton populations of the heated oil shales deviate from such a model will vary in a complex way during pyrolysis and we expect a

corresponding variation in the recorded ^1H NMR signals which, therefore, cannot be strictly considered in terms of the theory for a pair-wise dipolar coupled solid. It is expected that deviations from the model will occur because of multiple proton dipolar interactions, the variable degree of molecular mobility that occurs and the occurrence of dipolar interactions with paramagnetic species during pyrolysis. Details of how these factors affect the solid-echo experiment have been considered to some extent by others (8, 9).

The experimental echo peaks that are clearly visible for pulse spacings of $\tau = 15\mu\text{s}$ (Figure 1), however, occur 2-3 μs earlier than the 3 μs predicted if the systems behaved ideally. This discrepancy is consistent with the facts that when the specimens exhibit purely 'rigid-lattice' behavior, the condition $\tau \ll T_2$ does not hold, where T_2 is the transverse relaxation time and that under other conditions the specimens are not ideally dipolar coupled solids.

In this analysis, we interpret the experimental results as true solid-echoes but discuss implications of deviations from the assumed model where appropriate.

The echo peak height, i_T , is chosen as a measure of the total hydrogen remaining in the residue at any given time during pyrolysis. Because the sensitivity of the ^1H NMR signal of a population of spins is inversely related to some power of the temperature (10), it is necessary to apply an amplitude correction to the measured values of i_T . An empirical temperature calibration of the experimental probe was made using a coal char specimen sealed in a glass ampoule. This material had been previously pyrolysed at a temperature of greater than 950K and besides having a constant hydrogen content, appears relatively constant in its ^1H NMR properties over the temperatures of the calibration (i. e. 300-770K). The ^1H NMR signals for a Glen Davis oil shale observed dynamically at four temperatures during heating are shown in Figure 2. These ^1H NMR data have been compensated for temperature dependence using the coal char calibration so that the echo peak amplitudes, therefore, represent the apparent hydrogen contents. This calibration has been found qualitatively successful when applied to the data of a number of coal pyrolysis experiments (5, 6) but when used for most oil shale experiments, an anomaly occurs in that there is an initial increase in the apparent hydrogen content on heating above room temperature. This anomaly can be seen in the plots of the temperature dependencies of the apparent hydrogen content for both a whole and a demineralized Julia Creek oil shale (Figures 4 and 5) and for a Glen Davis oil shale (Figure 3). This anomaly is not so apparent if the magnetic field is made inhomogeneous so that the transient ^1H NMR signals are always rapid and independent of the specimen's nature. However, we suspect this anomaly is related to the presence of paramagnetic species in the specimens and the fact that it occurs greatly reduces the quantitative usefulness of this method of hydrogen content determination. It, nonetheless, is very useful for at least qualitatively defining the main pyrolysis regions at higher temperatures, where there is a rapid loss of hydrogen. Numerical differentiations of these data (Figures 3-5) show the temperature region of maximum rate of '% hydrogen loss'. These 'hydrogen loss' scans are analogous to thermogravimetric analysis and in the several instances where parallel measurements have been performed, similar temperature regions have been observed for the maximum rates of 'hydrogen loss' and weight loss, respectively.

Besides detecting thermal decomposition of the specimen, these ^1H NMR signals clearly indicate changes that occur in the state of the specimen during pyrolysis. It is useful to postulate that, at all stages of pyrolysis, the organic material contains both 'rigid' hydrogen with a rapidly relaxing ^1H NMR transient and 'mobile' hydrogen with a relatively slower relaxing transient. We have attempted to make such a distinction by resolving the observed transients into two components. The procedure for doing this is to a large extent arbitrary and the accuracy to which a particular method can be applied varies greatly with the condition of the specimen. The method we have used is to fit an exponential - $i_m \exp(-t/T_2^*)$ - to the tail of the transients where it is assumed only the 'mobile' slowly relaxing protons are represented. This method of analysis is outlined in Figure 1. From this analysis, two parameters are obtained: (i) the percentage of the residual hydrogen in the 'rigid' state - i. e.

$$i_R \% = \left(\frac{i_T - i_m}{i_T} \right) \times \frac{100}{1}$$

and (ii) the time constant T_2^* of the 'mobile' hydrogen component of the ^1H NMR transient. The results of such analyses of pyrolysis data for Glen Davis, Julia Creek and Julia Creek demineralized shale specimens are shown in Figures 6, 7 and 8, respectively.

A parameter that has been widely used in the study of the structure and thermal properties of solid organic materials (11-13) and particularly coals (12, 14) is the ^1H NMR second moment. To compute such a parameter from our solid echo data requires its Fourier transformation from the time domain to obtain a complex frequency domain ^1H NMR spectrum, i. e. $g'(\omega) = u'(\omega) + iv'(\omega)$. The quadrature components of this spectrum represent linear combinations of the pure absorptive ($u(\omega)$) and dispersive ($v(\omega)$) modes of the true spectrum, i. e. ,

$$u'(\omega) = v(\omega)\cos\theta + u(\omega)\sin\theta$$

$$v'(\omega) = v(\omega)\sin\theta + u(\omega)\cos\theta$$

where θ (ω) is a frequency dependent phase shift nominally resulting from an error in the zero of time in the time domain data. For our data, its value is determined by the time selected for the solid-echo peak which is uncertain to varying degrees. It is usual to empirically adjust the phase relationship to separate the absorptive and dispersive modes. However, because the usual second moment parameter is critically dependent on this adjustment, we have instead computed the power spectrum given by

$$a(\omega) = u'(\omega)^2 + v'(\omega)^2$$

which is independent of the phase error. Such power spectra computed for the Glen Davis solid echo transients shown in Figure 2 are shown in Figure 6. Echart and Wroblewski (15) have demonstrated the validity of using this power spectrum rather than the absorption spectrum for line shape analysis in high resolution spectroscopy. We have, therefore, computed a second moment parameter, M_2^* , of the power spectrum defined as

$$M_2^* = \int_{\omega_0}^x a(\omega)\Delta\omega^2 d\omega / \int_{\omega_0}^x a(\omega) d\omega$$

where ω_0 is the central resonance frequency, $\Delta\omega = (\omega - \omega_0)$ and the limit of integration, x , is chosen to be at a frequency where $a(\omega) = a(\omega_0)/10$. Truncation at this value of x has been chosen by trial as a compromise between increased random errors that accrue for smaller values and the increase in systematic errors that result from greater truncation. We have found that the temperature dependence of M_2^* computed for this truncation is qualitatively the same as for lesser truncations and most of the quantitative features are relatively the same.

Examples of the temperature dependence of M_2^* are shown in Figures 10, 11 and 12 for Julia Creek, Julia Creek demineralized shales and Glen Davis shale, respectively.

DISCUSSION

^1H NMR results presented here are unique in that they were obtained under the non-equilibrium conditions of temperature controlled pyrolytic decomposition of the shales. We have established experimental techniques that ensure good reproducibility of the changes manifest in these dynamically recorded ^1H NMR solid echo signals. By these techniques, it is possible to obtain a set of data characterizing a shale which we choose to call a ^1H NMR thermal scan¹.

The analysis of the ^1H NMR thermal scan data has been in three parts:

(i) An intensity parameter, i_T , directly related to the hydrogen content of the residual, has been used to monitor the loss of volatile products and, thereby, detect the main region of pyrolytic decomposition.

(ii) The ^1H NMR signals have been resolved into two components according to a model that distinguishes two phases differing in molecular mobility. It should be emphasized that this division is, to a large extent, arbitrary and that although these analytical components are referred to as 'rigid' and 'mobile', respectively, the distinction is only relative and, in fact, the so called 'rigid' component need not be that of a truly rigid-lattice structure. Also obtained by this method of analysis is a parameter, T_2^* , which is the time constant of the 'mobile' component of the ^1H NMR transient. This is a measure of the average molecular mobility of the 'mobile' material - the greater the average mobility, the greater the value of T_2^* . It is expected that, as the temperature is raised, a number of different factors would, therefore, influence the value of T_2^* - (a) the rate of transformation of material from the 'rigid' to the 'mobile' state, (b) thermal activation and/or breakdown of the 'mobile' molecules, (c) the rate of loss by volatilization of presumably the smaller and more mobile of the molecules and (d) at higher temperatures, the formation of the rigid residue from the 'mobile' material.

(iii) The second moment of the power spectrum, M_2^* , has been derived as a parameter which monitors the changes in the structural composition and mobility of the material that are manifest in the total line shape function of the ^1H NMR signals. Low temperature ($\sim 70\text{K}$) ^1H NMR second moments, measured for the frequency spectrum rather than for the power spectrum, have been used to estimate the chemical composition of coals (14). This is because the second moment of the coal can be defined as the weighted average of the second moments of all the constituent groups. For a rigid-lattice solid, each chemical group can be assigned a characteristic second moment

which is a measure of the dipolar interactions and, therefore, critically dependent on the interproton distances. Of particular significance is the fact that the second moment values for rigid lattice aliphatic structures are about three times those typical of aromatic structures (12, 14). The dipolar interactions of reorienting molecular groups are greatly reduced by the motion so that the groups no longer significantly contribute to the overall second moment of the specimen. Thus, by monitoring this normally used second moment of the frequency spectrum or the closely related parameter, M_2^* , used by us, we witness the thermally induced changes both in the chemical composition of the shale and the net molecular mobility of the constituent groups. It should be noted, that to the extent that his parameter is a measure of the average molecular mobility of the total specimen, its value is dominated by the more rigid components.

Although each of the three methods of analysis is subject to uncertainty in interpretation and precision of measurement, they separately and in combination provide much novel information on the processes involved in shale pyrolysis.

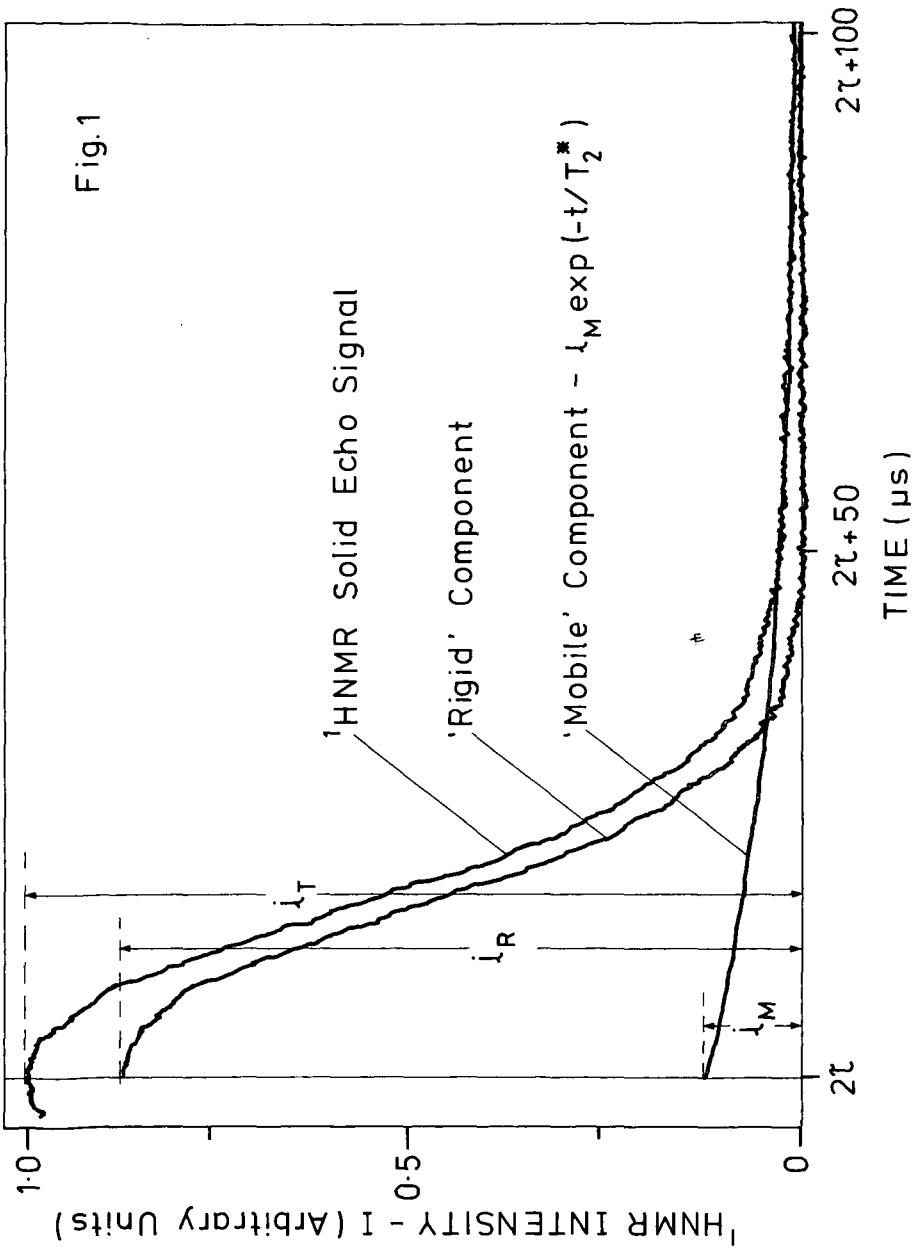
From the apparent hydrogen content and differential hydrogen content data for the Glen Davis shale (Figure 3), it is seen that rapid thermal decomposition and loss of volatile material occurs during a clearly defined period between 700 and 800K. In the course of heating, it is seen that there is a steady conversion of hydrogen from the 'rigid' to the 'mobile' state (Figure 7) and that this process seems to occur in two stages. The first stage occurs between room temperature and 660K and the second and more rapid conversion between 660K and 720K by which time all of the material is in the 'mobile' state. This is reflected in the temperature dependence of M_2^* (Figure 12). At 720K, M_2^* attains a very small value consistent with the absence of any significant amount of rigid-lattice hydrogen. Between 720K and 800K and accompanying the rapid loss of volatile hydrogen from the specimen, a rigid residue is formed which contains more than 10% of the total hydrogen and has a M_2^* value consistent with it being a rigid-lattice, aromatic material. Beyond 800K, the decrease in M_2^* is evidence of molecular 'softening' in this residue. We have observed this same phenomenon for bituminous coals and more particularly in an inertinite concentrate but not for a vitrinite concentrate.

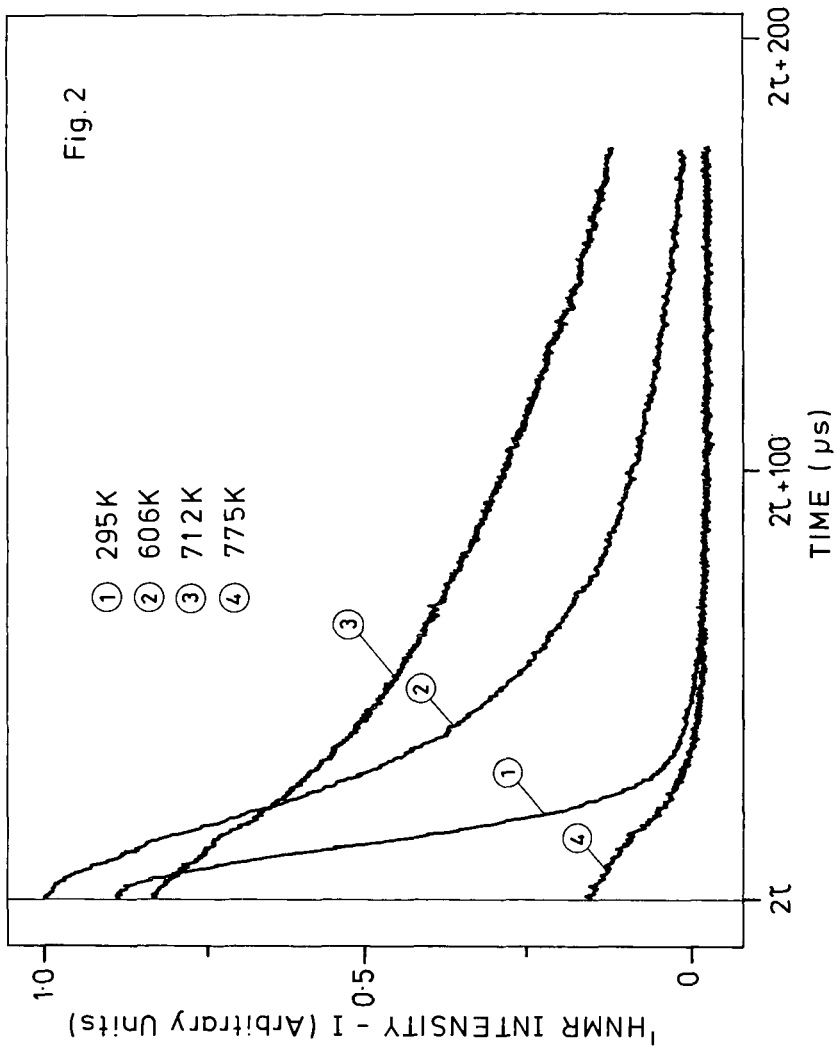
The behavior of the T_2^* parameter reflects its rather complex nature but the well defined maximum which occurs near the temperature of maximum rate of hydrogen loss (Figures 3 and 7) is the result of the competing processes of molecular breakdown and thermal activation on the one hand and the loss of mobile material by volatilization and conversion to the rigid residue on the other.

The ^1H NMR thermal scanning data for the Julia Creek shale and demineralized shale are similar to each other but are quite different from those of the Glen Davis shale. Compared to the data for the Glen Davis shale, we note the following general differences for the Julia Creek materials. (a) The onset of thermal decomposition is not as sudden (Figures 4 and 5) and the major zones of thermal decomposition as indicated by the apparent hydrogen loss and differential hydrogen loss occur at significantly lower temperatures. Also, the temperatures of maximum rate of percentage hydrogen loss occur at significantly lower temperatures and these rates are significantly less. (b) There is little change in the molecular mobility of the Julia Creek specimens below 450K as indicated by changes in either M_2^* (Figures 10 and 11) or the proportion of 'rigid' hydrogen (Figures 8 and 9) but beyond 450K, the rate of molecular 'mobilization', as revealed by these parameters, proceeds more rapidly. Whereas M_2^* reaches a very small minimum value indicating the absence of any rigid lattice component in the materials at a lower temperature than for the Glen Davis shale, the minimum in the 'rigid' hydrogen content (Figures 8 and 9) only reaches 30-40% as compared to ~0% for the Glen Davis shale. This apparent contradiction can be explained by reference to the ^1H NMR solid echo signals which are not shown here. The ^1H NMR relaxation rates of the so called 'rigid' hydrogen fraction in this temperature region indicate that, although this material is considerably less mobile than the 'mobile' fraction, it is not, in fact, a rigid structure. (c) The formation of the rigid residues occur earlier and again in parallel with the loss of volatile material but a much greater fraction of the hydrogen remains in the residue (Figures 10 and 11 and Figures 4 and 5).

In comparing the ^1H NMR thermal scanning data of the whole and demineralized Julia Creek materials, we note the following. (a) A general similarity in the apparent hydrogen loss behavior but that the maximum rate of percentage hydrogen loss occurs sooner for the demineralized shale although the maximum rates are the same (Figures 4 and 5). (b) There is little difference in the behavior of M_2^* except that the demineralized shale acquires 'mobility' at a slightly earlier period. The same small minimum values of M_2^* are attained indicating the absence of rigid components in either structure (Figures 10 and 11). (c) The proportion of 'rigid' hydrogen falls to a lower value for the demineralized shale and there is a major difference in the variations of the T_2^* parameter. This parameter shows that a much greater molecular mobility is acquired by the 'mobile' fraction of the demineralized shale (Figures 8 and 9).

This comparison of the whole and demineralized Julia Creek shales shows that, although the degree of molecular mobility of the material 'softened' during the heating, is greatly inhibited





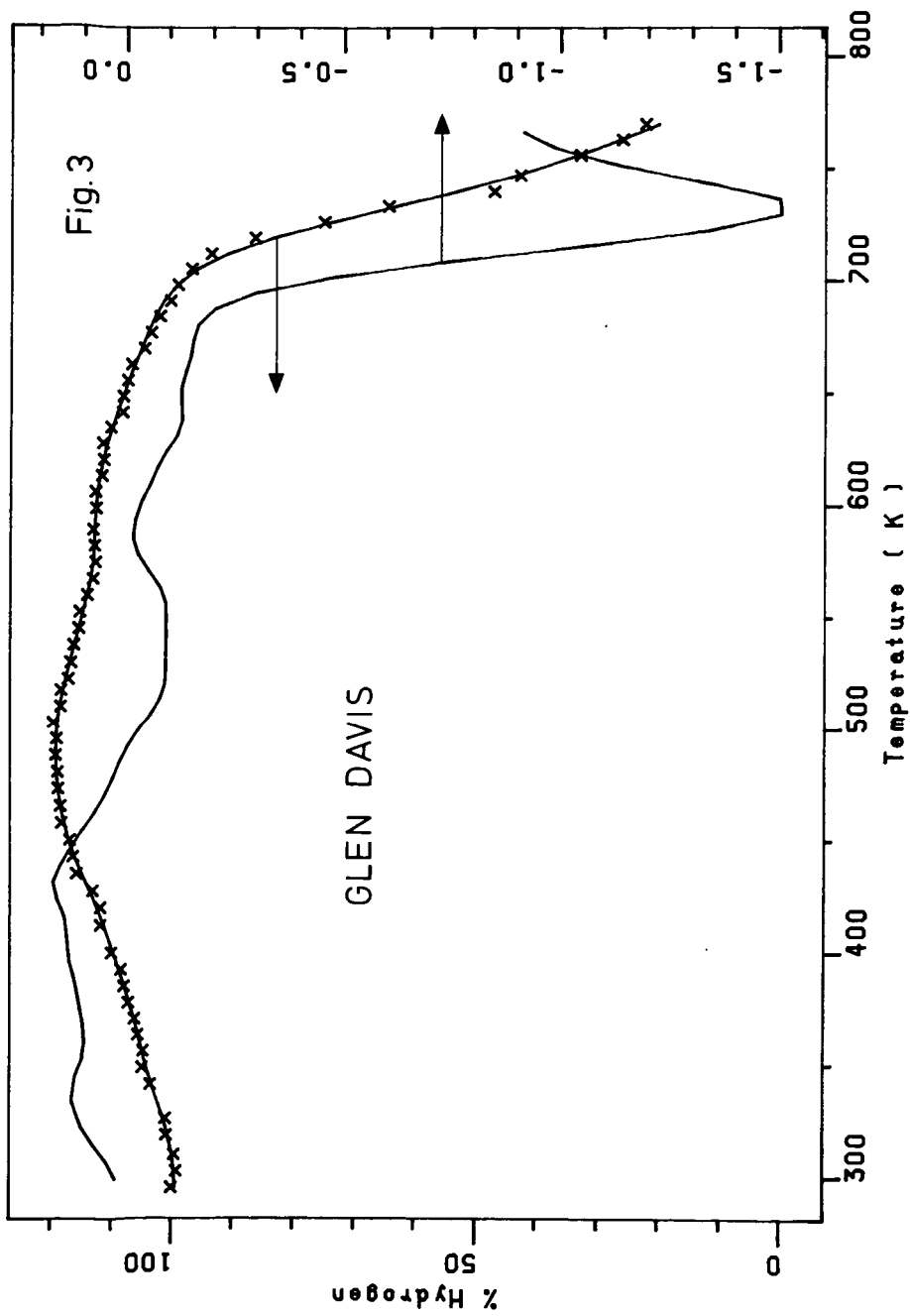
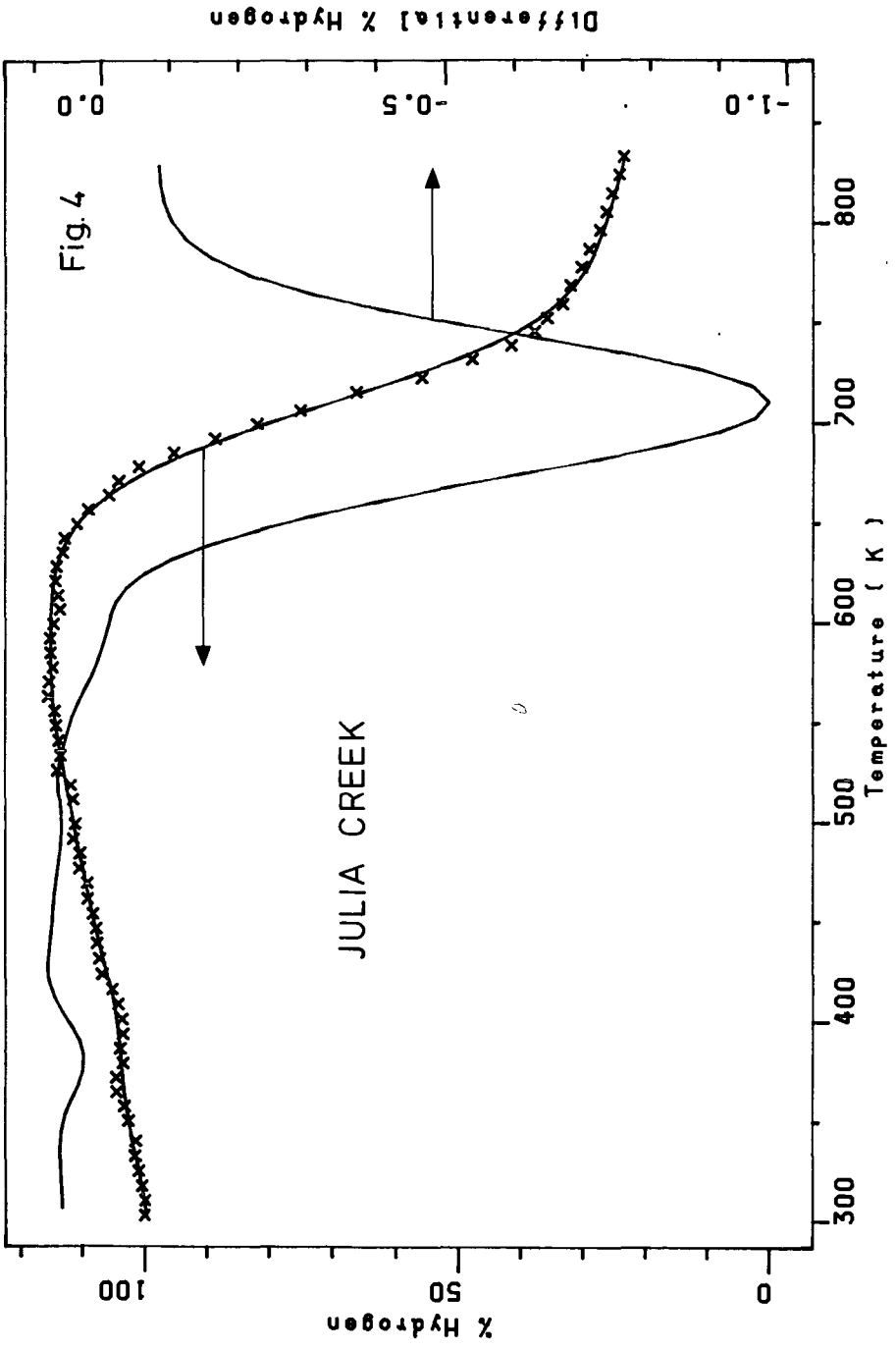


Fig. 3

GLEN DAVIS



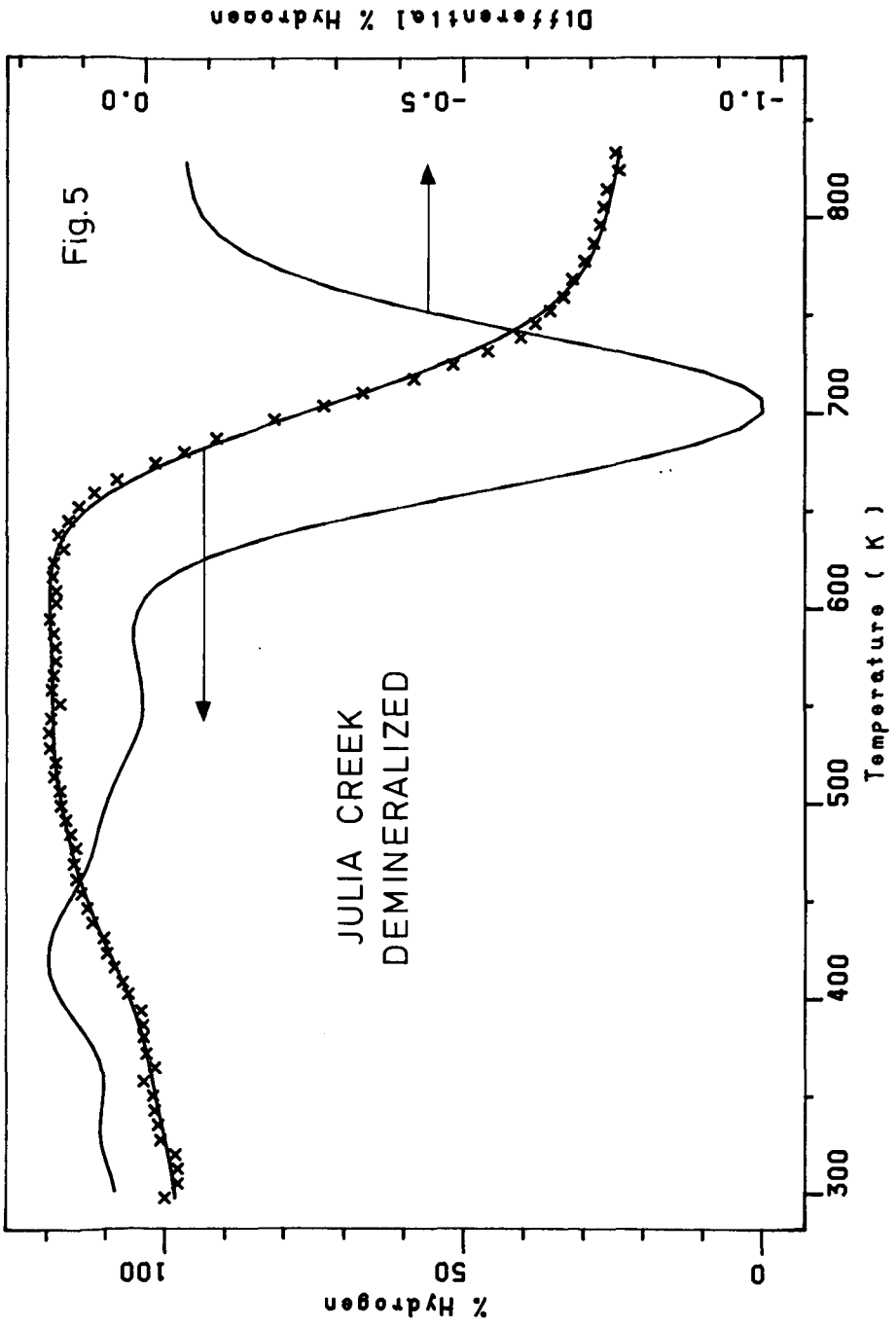
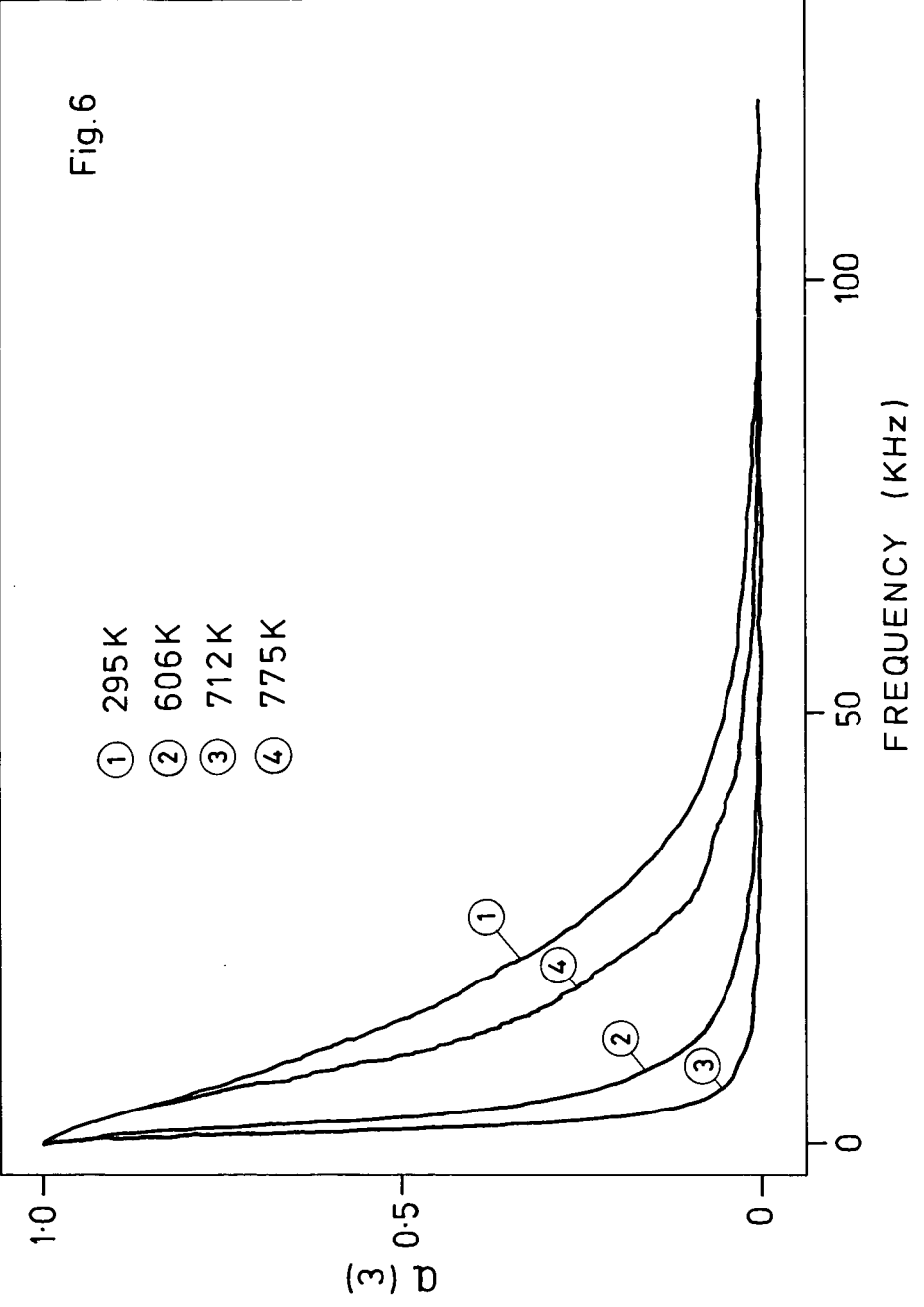
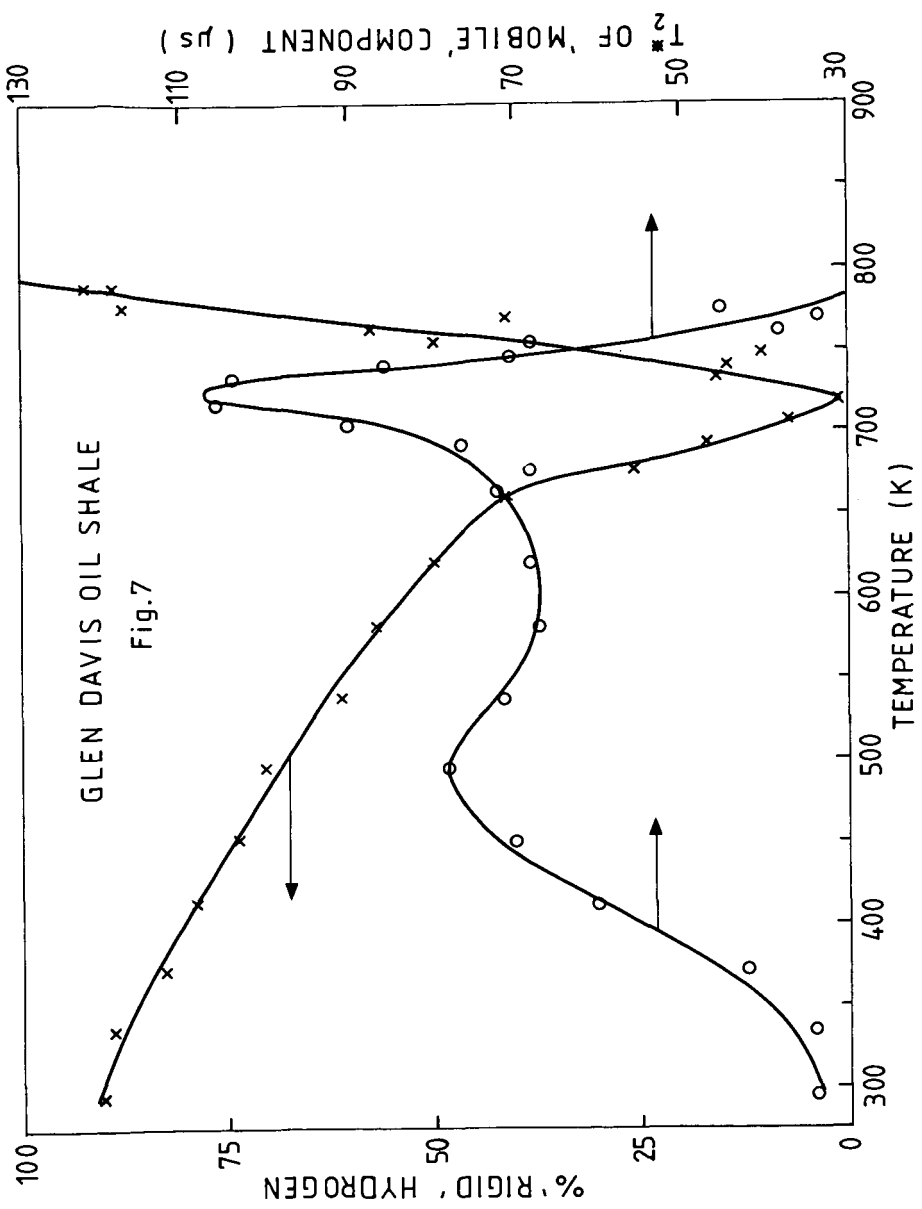
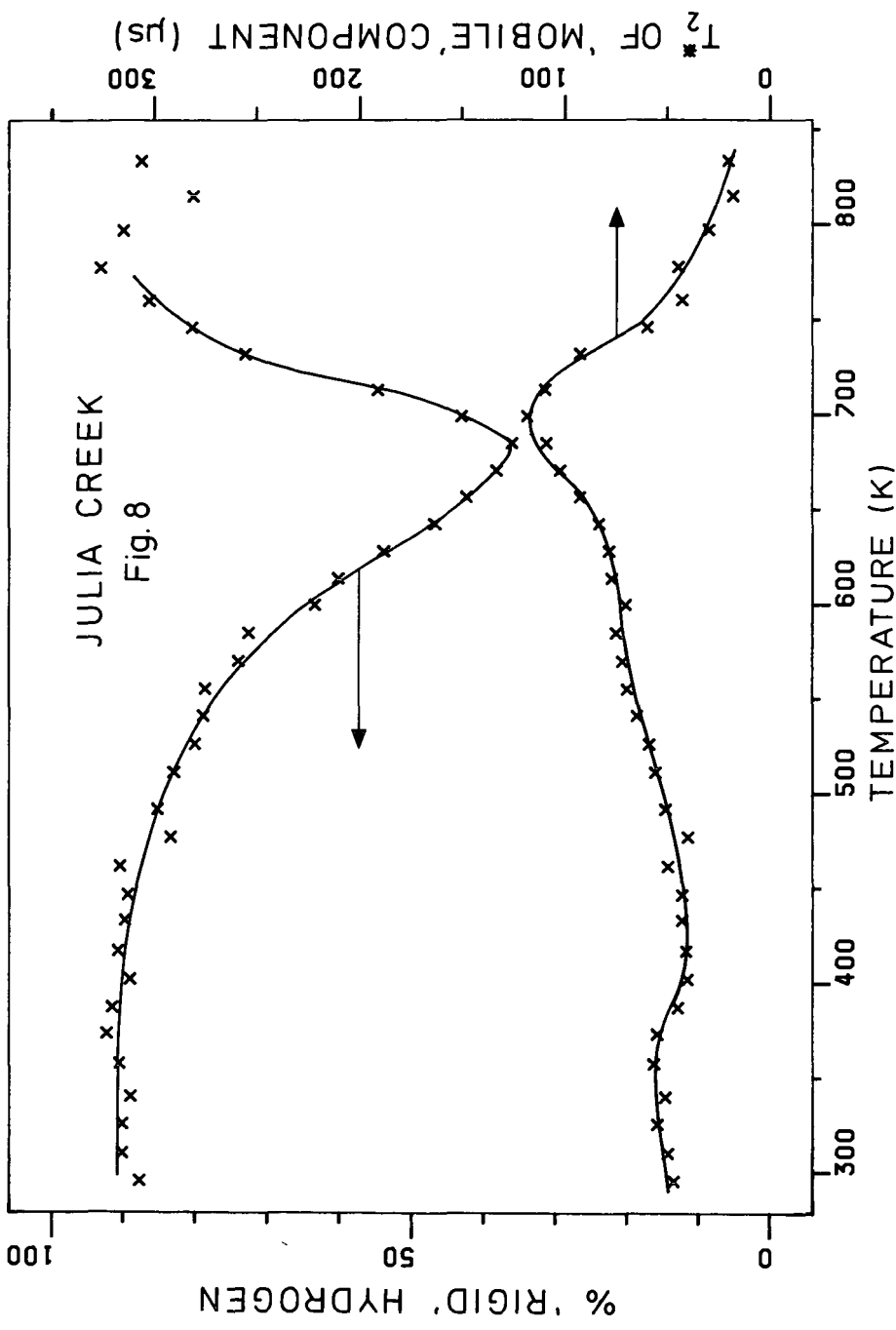
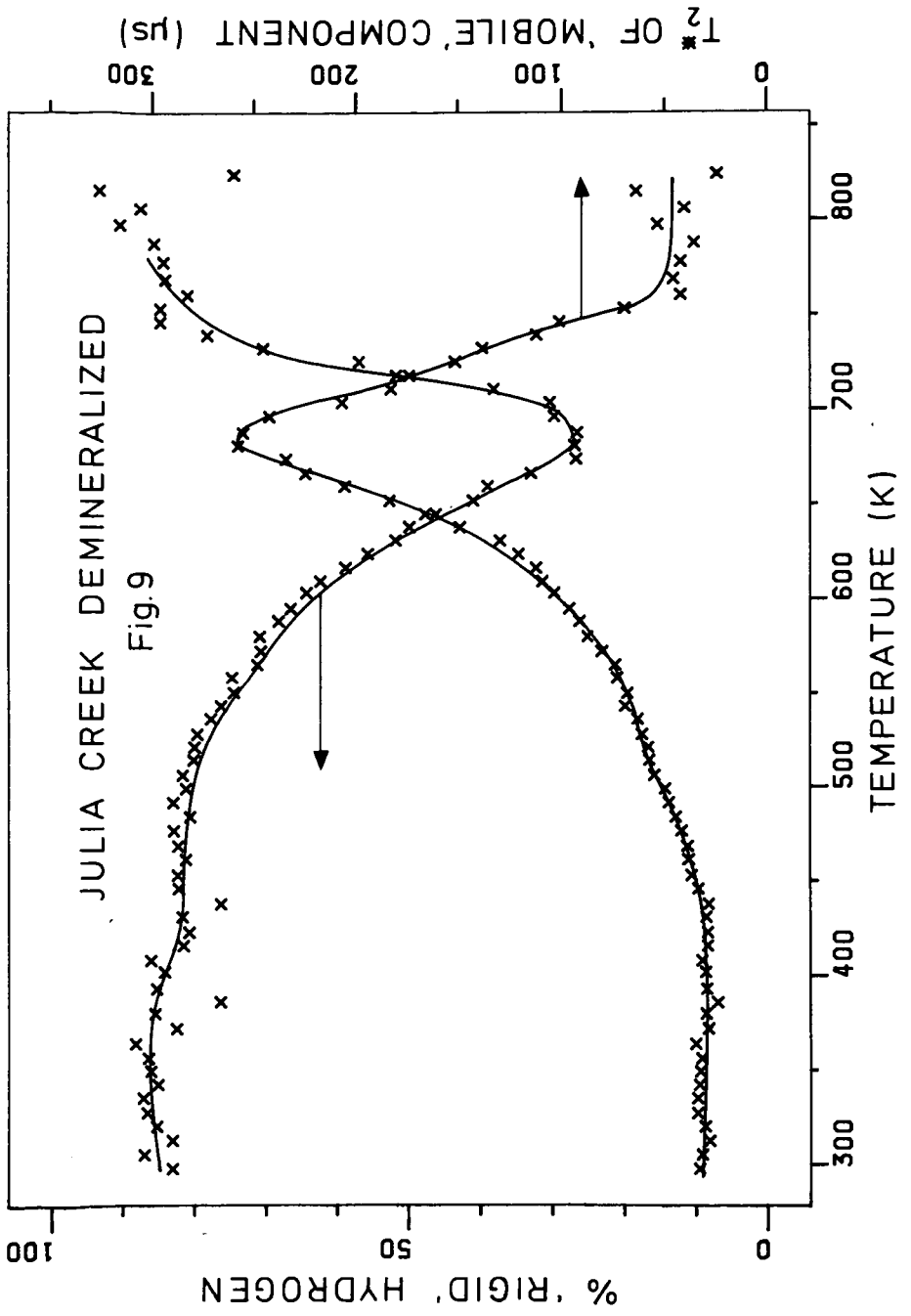


Fig.6



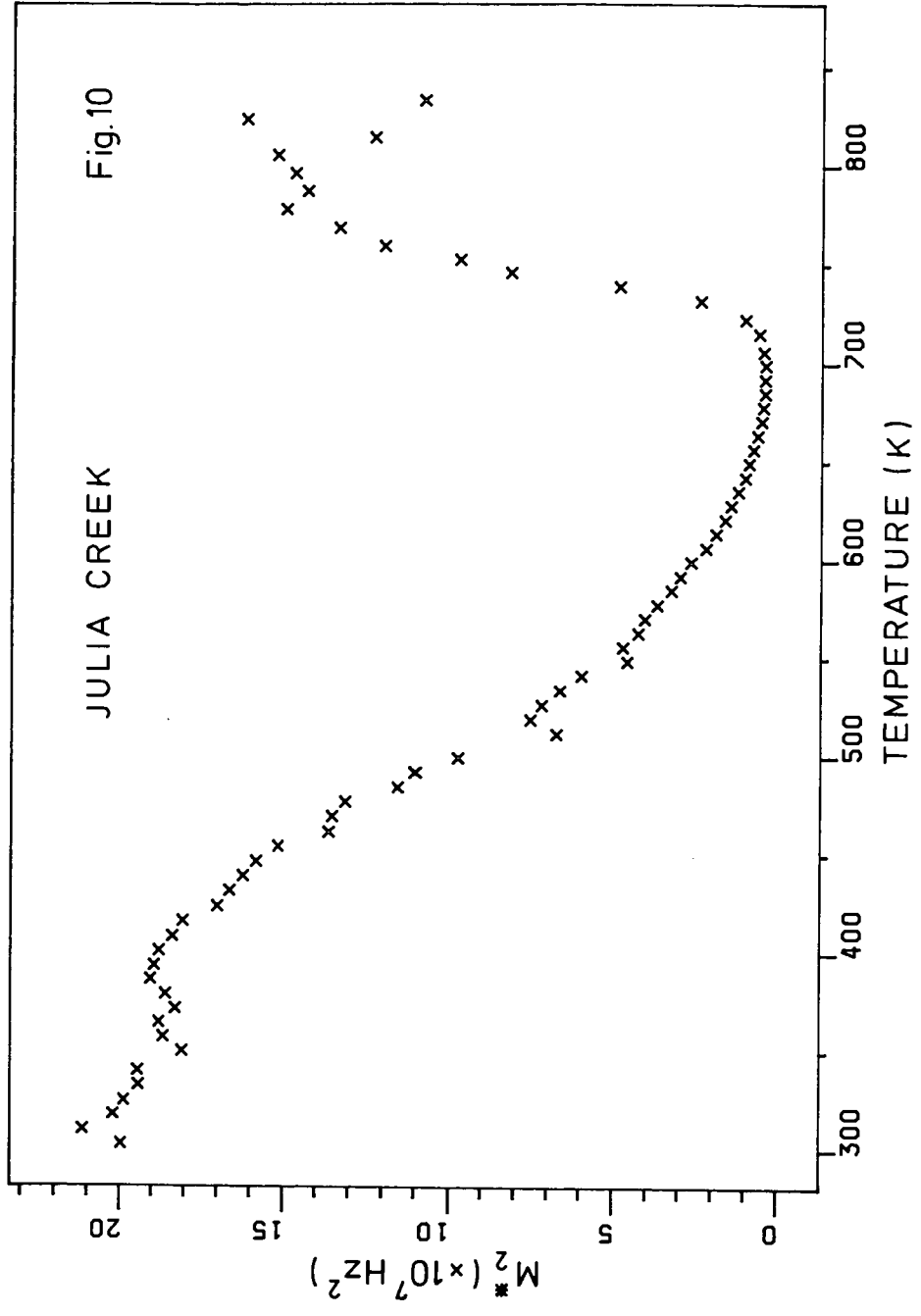




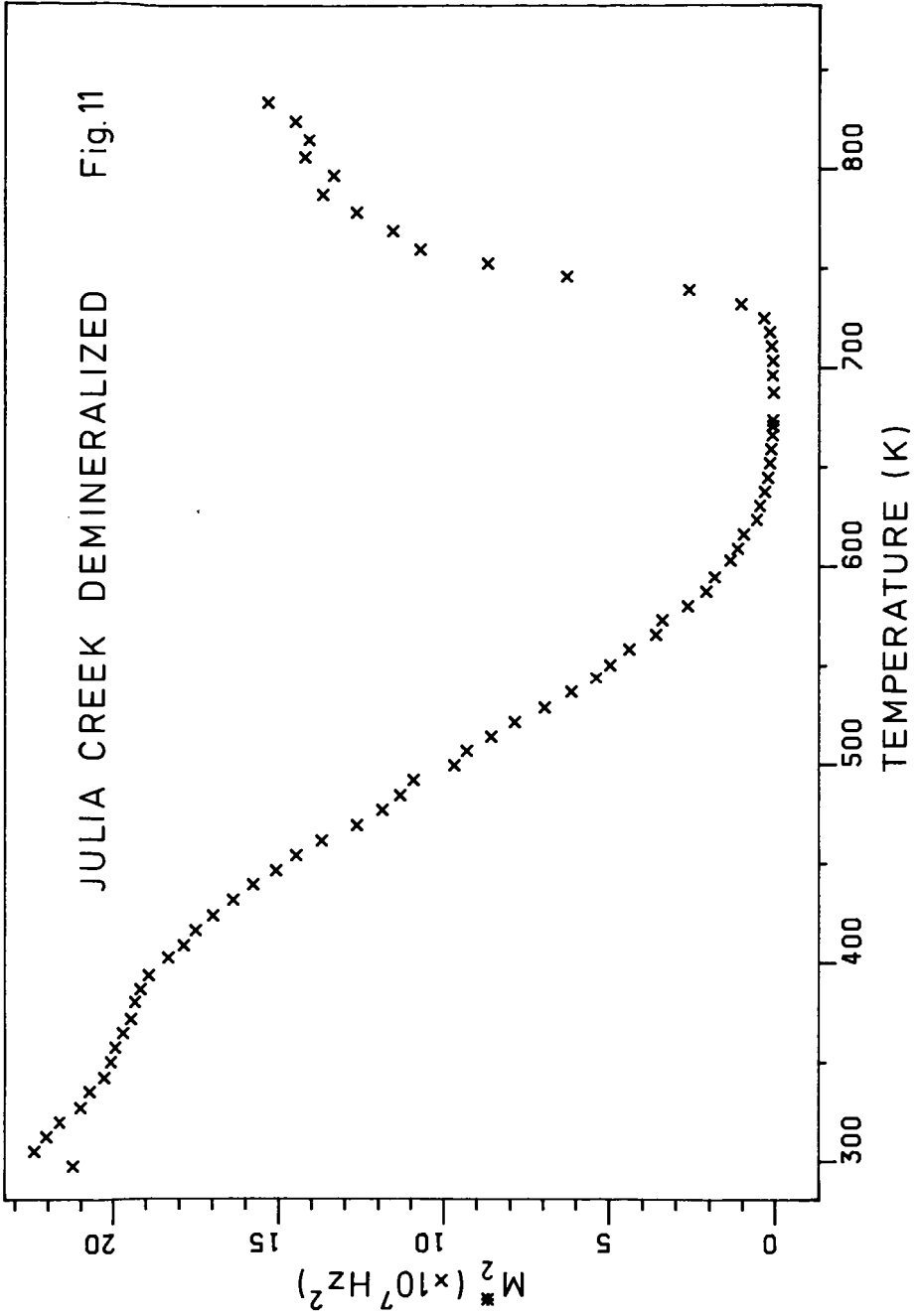


JULIA CREEK

Fig.10

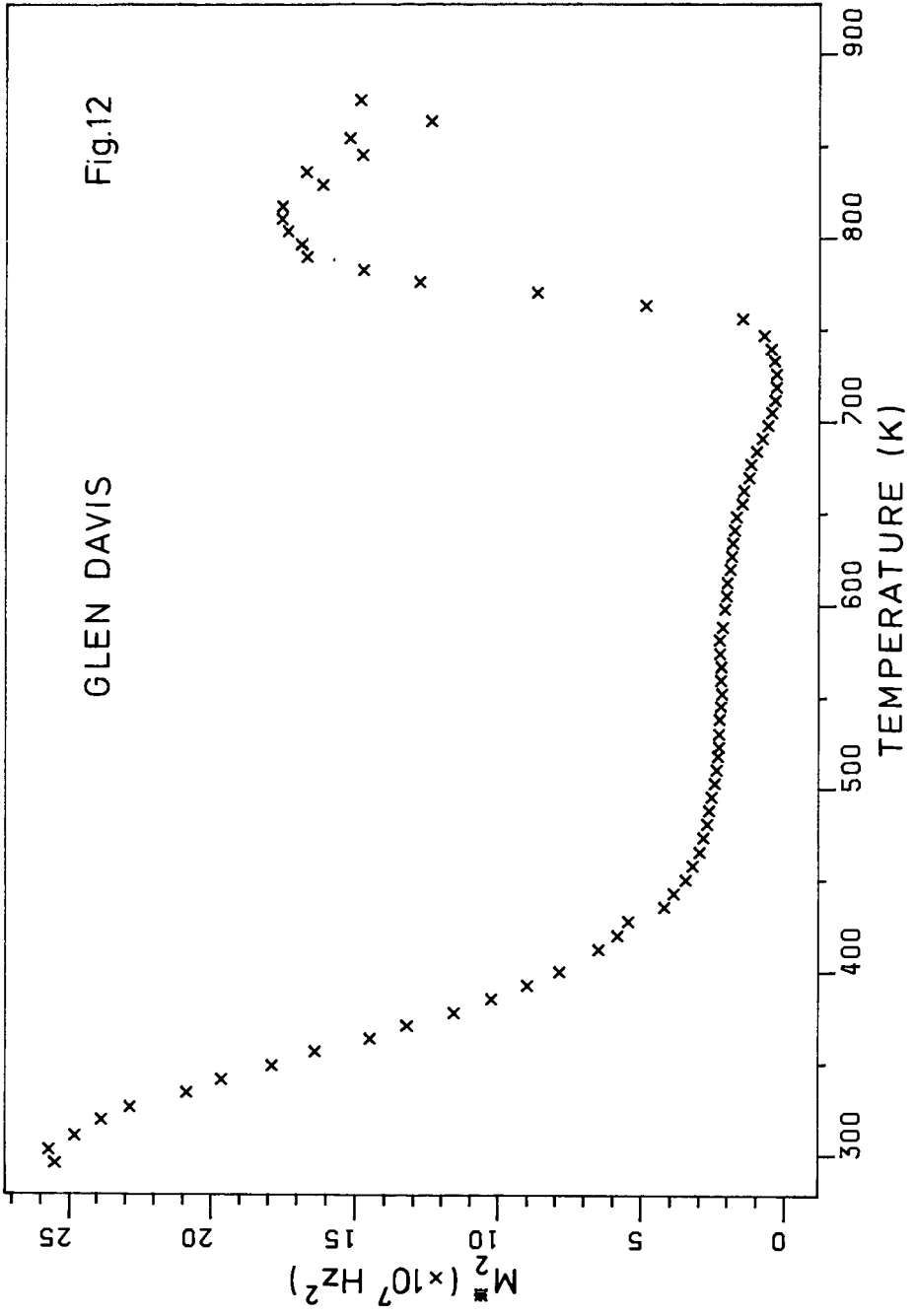


JULIA CREEK DEMINERALIZED Fig.11



GLEN DAVIS

Fig.12



by the presence of the inorganic material it does not have much effect on the eventual thermal decomposition of the organic material.

The observations of Miknis et al (16) that the aromatic component of oil shales remain inert during pyrolysis does not appear to be the case for the shales studied here. This is apparent from the transient behavior of the molecular mobilities as indicated by the parameter M_2^* . The very low values of M_2^* achieved prior to the main pyrolysis zone clearly show that all significant components of the organic hydrogen in both the Julia Creek and Glen Davis shales pass through a highly mobile stage before a residual rigid lattice component is formed during the main pyrolysis periods. It is unlikely that the original aromatic materials in these shales could undergo the transient softening observed here without the occurrence of at least some chemical change as well as the obvious physical changes.

ACKNOWLEDGMENTS

Mr. Neil A. Bacon contributed to the development of the software used for the analyses. This work has been in part supported by the Department of National Development and Energy of the Commonwealth of Australia under NERDDC Project No. 80/0384.

LITERATURE CITED

- (1) Lynch, L. J. and Webster, D. S., *Fuel*, 58, 235 (1979).
- (2) Webster, L. J. and Lynch, L. J., *Fuel*, 60, 549 (1981).
- (3) Lynch, L. J. and Webster, D. S., 4th Australian Workshop on Coal Hydrogenation, Richmond, Victoria, Abstracts and Papers, Paper 15 (1979).
- (4) Lynch, L. J. and Webster, D. S., *Proc. Intern. Conf. on Coal Sci.*, Dusseldorf, D14, p. 675 (1981).
- (5) Lynch, L. J. and Webster, D. S., 6th Australian Workshop on Coal Hydrogenation, Clayton, Victoria, Abstracts and Papers, 5A-6 (1981).
- (6) Lynch, L. J., Webster, D. S. and Bacon, N., *Symp. on Characteristics of Australian Coals and Their Consequences per Utilization*, North Ryde, N.S.W., Australia, Abstracts and Papers, 33-1 (1982).
- (7) Webster, D. S., Cross, L. F. and Lynch, L. J., *Rev. Sci. Instrum.*, 50, 390 (1979).
- (8) Powles, J. G. and Strange, J. H., *Proc. Phys. Soc. (London)* 82, 6 (1963).
- (9) Cosgrove, T. and Barnett, K. G., *J. Magn. Resonance* 43, 15 (1981).
- (10) Abragam, A., "The Principles of Nuclear Magnetism", p. 39, Oxford Univ. Press (Clarendon), London (1961).
- (11) Andrew, E. R. and Eades, R. G., *Proc. Roy. Soc. (London) Series A*, 216, 398 (1953).
- (12) Ladner, W. R. and Stacey, A. E., *Fuel*, 42, 75 (1963).
- (13) Sircar, R. and Gupta, R. C., *Indian J. Phys.*, 56A, 55 (1982).
- (14) Sharkey, A. G., McCartney, J. T., in "Chemistry of Coal Utilization", 2nd Suppl. Vol., M. A. Elliot, Ed., John Wiley and Sons, New York, p. 159 (1981).
- (15) Ejchart, A. and Wroblewski, K., *J. Magn. Resonance* 40, 469 (1980).
- (16) Miknis, F. P., Szeverenyl, N. M. and Maciell, G. E., *Fuel*, 61, 341 (1982).

SYMPOSIUM ON GEOCHEMISTRY AND CHEMISTRY OF OIL SHALE
PRESENTED BEFORE THE DIVISIONS OF FUEL CHEMISTRY, GEOCHEMISTRY,
AND PETROLEUM CHEMISTRY, INC.
AMERICAN CHEMICAL SOCIETY
SEATTLE MEETING, MARCH 20 - MARCH 25, 1983

PYROLYSIS OF SHALE OIL VACUUM DISTILLATE FRACTIONS

By

R. N. Hazlett and E. Beal
Naval Research Laboratory, Washington, D. C. 20375

INTRODUCTION

The freezing point of U. S. Navy jet fuel (JP-5) has been related to the amounts of large n-alkanes present in the fuel (1,2). This behavior applies to jet fuels derived from alternate fossil fuel resources, such as shale oil, coal, and tar sands, as well as those derived from petroleum. In general, jet fuels from shale oil have the highest and those from coal the lowest n-alkane content. The origin of these n-alkanes in the amounts observed, especially in shale-derived fuels, is not readily explained on the basis of literature information. Studies of the processes, particularly the ones involving thermal stress, used to produce these fuels are needed to define how the n-alkanes form from larger molecules. The information developed will significantly contribute to the selection of processes and refining techniques for future fuel production from shale oil.

Carbon-13 nmr studies indicate that oil shale rock contains many long unbranched straight chain hydrocarbon groups (3). The shale oil derived from the rock also gives indication of considerable straight chain material with large peaks at 14, 23, 30 and 32 ppm in the C-13 nmr spectrum.

Previous pyrolysis studies stressed fractions of shale crude oil residua, measured the yields of JP-5, and determined the content of potential n-alkanes in the JP-5 distillation range (4).

In this work, a shale crude oil vacuum distillate (Paraho) was separated into three chemical fractions. The fractions were then subjected to nmr analysis to estimate the potential for n-alkane production and to pyrolysis studies to determine an experimental n-alkane yield.

EXPERIMENTAL

Separation

Paraho shale oil was distilled at atmospheric pressure to an end point of 300°C. A second cut was obtained by continuing the distillation at reduced pressure, 40 mm Hg. This vacuum distillate, with an end point of 300°C, was used in the studies described in this paper.

The vacuum distillate was separated on silica gel into saturate, aromatic, and polar fractions by the procedure described earlier (4). The vacuum distillate comprised 33% of the crude shale oil and contained 1.82% (W/W) of nitrogen. The three chemical classes represented 36% saturates, 22% aromatics, and 42% polars of the vacuum distillate and contained < 0.01, 0.23 and 3.0% nitrogen, respectively. The mass recovery from the silica gel separation was 94%, but the nitrogen recovery was only 67%. The vacuum distillate contained 7.8% n-alkanes and 1.3% 1-olefins (21.5% and 3.5% of saturate fraction), respectively.

Carbon-13 nmr Analysis

Samples of the three compound classes were submitted to analysis by C-13 nmr. The C-13 spectrum affords a distinct separation of the aromatic and aliphatic absorption regions plus a good resolution of many peaks due to specific molecular structure. Thus, a good amount of useful information can be obtained even for a complex mixture such as a fuel fraction. With respect to the present study, the aliphatic region of the spectrum is of particular importance. A spectrum for the aliphatic region of the polar fraction is shown in Figure 1. The distinctive peaks at 14, 23, 32, and 30 ppm demonstrate the presence of significant amounts of long unbranched groups in this fuel fraction. Quantitation of the spectral information using the methanol internal standard gives the data listed in Table I. As expected, the content of long unbranched alkyl groups is greatest for the saturate fraction. Further, the straight chain alkyl groups in the saturate fraction are longer on the average than those in the aromatic and polar fractions. We conclude that there is a definite potential for making n-alkanes and 1-olefins in the jet fuel distillation range by cracking compounds found in the shale oil vacuum distillate.

TABLE I
CARBON-13 NMR EXAMINATION OF SHALE OIL
VACUUM DISTILLATE FRACTIONS

Fraction	Wt. % Carbon in Aliphatic Region	Wt. % Unbranched Alkyl Groups ^(a)	Average Carbon Chain Length ^(b)
Saturate	100	58	19
Aromatic	48	15	13
Polar	55	36	13

- (a) Sum of areas of absorption peaks at 14, 23, 30 and 32 ppm.
(b) For unbranched alkyl groups: based on ratio of 30 ppm peak area to average of 14, 23 and 32 peak areas.

Precision: $\pm 10\%$

Pyrolysis

The vacuum distillate fractions have been stressed at conditions corresponding to the petroleum refining process known as delayed coking (5). These conditions are 450°C and about 90 psi pressure. Each thermal stress was conducted in a 1/4 inch o. d. 316 s. s. tube fitted with a stainless steel valve via a Swagelok connection. The tube, with a weighed amount of sample (approximately 0.1 g), was attached to a vacuum system, cooled to -78°C, and pumped to remove air. The tube was then thawed and the cooling/pumping process repeated. The tubes were heated by inserting them into 9/32-inch holes in a six-inch diameter aluminum block fitted with a temperature controller.

Complete details of sample workup and analysis can be found in Literature Cited (4). One gas chromatographic (GC) technique determined the JP-5 yield from the pyrolysis by summing the total FID area for carbon numbers 9 through 16. A second GC analysis determined the individual n-alkanes and 1-alkenes with a fused silica capillary column.

The saturate fraction of the vacuum distillate contained about 25% n-alkanes plus p-alkenes (Table II). In keeping with the distillation characteristics of this fraction, the bulk (82%) of these compounds contained 17 or more carbons. However, this saturate material did contain significant amounts of the C14, C15 and C16 n-alkanes and 1-alkenes, compounds which fall within the JP-5 distillation range.

TABLE II
n-ALKANES AND 1-ALKENES IN UNSTRESSED SATURATE FRACTION

Carbon Number	Percent Concentration		
	n-Alkane	1-Alkene	n-Alkane + 1-Alkene
11	0.172	--	0.172
12	0.161	0.036	0.197
13	0.282	0.076	0.358
14	0.647	0.187	0.834
15	0.936	0.379	1.315
16	1.244	0.377	1.621
17	1.895	0.533	2.428
18	1.665	0.521	2.186
19	2.076	0.388	2.464
20	1.698	0.412	2.110
21	1.872	0.189	2.061
22	1.516	0.192	1.708
23	1.589	0.119	1.708
24	1.168	0.046	1.214
25	1.306	0.049	1.355
26	0.859	0.021	0.880
27	0.939	0.029	0.968
28	0.75	--	0.75
29	0.75	--	0.75
Totals (11-29)	21.53	3.55	25.08
Totals (9-16)	3.44	1.06	4.50
JP-5 range			

Pyrolysis of the saturate fraction for 30 minutes at 450°C gave the n-alkane and 1-alkene product distribution shown in Figure 2. Comparison between Figure 2 and Table II indicates a net loss in concentration for the n-alkanes C₁₆ and larger, and a net gain for those with 14 or less carbons. The 1-alkenes exhibit a similar relationship with carbon number. For this pyrolysis time, the yield of small olefins equals or exceeds the yield of small n-alkanes.

The effect of stress time on yield for the saturate fraction is illustrated in Figure 3. The n-alkane plus 1-alkene sum for each carbon number is plotted. The combined alkane/alkene yields for carbon numbers above 16 decrease with increasing stress time and are almost depleted at 180 minutes. The yields for carbon numbers below 13 increase with stress time through 120 minutes but exhibit a drastic reversal at 180 minutes. Thus, the larger n-alkanes and 1-alkenes are undergoing single-step Fabuss-Smith-Satterfield pyrolysis (6) to smaller hydrocarbons. The smaller alkanes and alkenes are initially products but, at the longer stress times, these compounds fragment also. The 1-alkenes are less stable than the n-alkanes; consequently, the latter predominate at the longer stress times.

Yields for the polar fraction pyrolyses are depicted in Figure 4. The combined n-alkane/1-alkene yields for carbon numbers less than 15 were reasonably good for a 15-minute pyrolysis but secondary fragmentation sharply reduced the yields for longer stress periods. The olefins were more reactive in the polar environment than the saturate environment and were generally minor products at all stress times. The low yield of alkanes and alkenes for carbon numbers above 14 corroborates the average chain length of 13 found by carbon-13 nmr analysis.

Limited experiments with the aromatic fraction from the vacuum distillate indicated this material resembled the polar fraction much more than the saturate in pyrolysis behavior. This would be consistent with the carbon-13 nmr results.

A summary of the JP-5 yield data for all fractions stressed for various times at 450°C is presented in Table II. The saturate fraction affords the highest yield of JP-5 but the polar fraction also gives good yields. The maximum yields for these two fractions came at 60-minutes stress but the overall effect of time on yield was moderate. The results for the aromatic fraction were inconclusive because of limited amount of starting material. The general pattern of JP-5 yield for the vacuum distillate fractions was similar to that found for shale oil residual fractions (4).

TABLE III
PRODUCT YIELD^(a)

Pyrolysis Time (min.)	JP-5 Yield (Percent)		
	Saturate	Aromatic	Polar
15	24.0	--	17.8
30	25.6	11.8	17.9
60	27.0	25.8	21.7
120	24.8	--	20.4
180	15.7	--	20.2

(a) Pyrolysis Temperature - 450°C

The potential n-alkane yields in the JP-5 cut are listed in Table IV. These values were obtained by summing the capillary GC yields of n-alkanes and 1-alkenes for carbon numbers 9 through 16. This total was divided by the corresponding JP-5 yield in Table III to give the potential n-alkane yield.

TABLE IV
POTENTIAL n-ALKANE YIELD FROM VACUUM DISTILLATE FRACTIONS

Pyrolysis Time (min.)	Potential n-Alkane Yield ^(a)		
	Saturate	Aromatic	Polar
15	31.0	--	12.7
30	31.0	4.2	11.4
60	33.0	15.5	10.3
120	24.8	--	11.5
180	18.5	--	9.4

(a) Pyrolysis Temperature - 450°C; yield in percent is sum of n-alkanes + 1-alkenes for C₉ to C₁₆ hydrocarbons divided by JP-5 yield from Table III.

C-13 NMR-ALIPHATIC REGION
SHALE VACUUM DISTILLATE
POLAR FRACTION

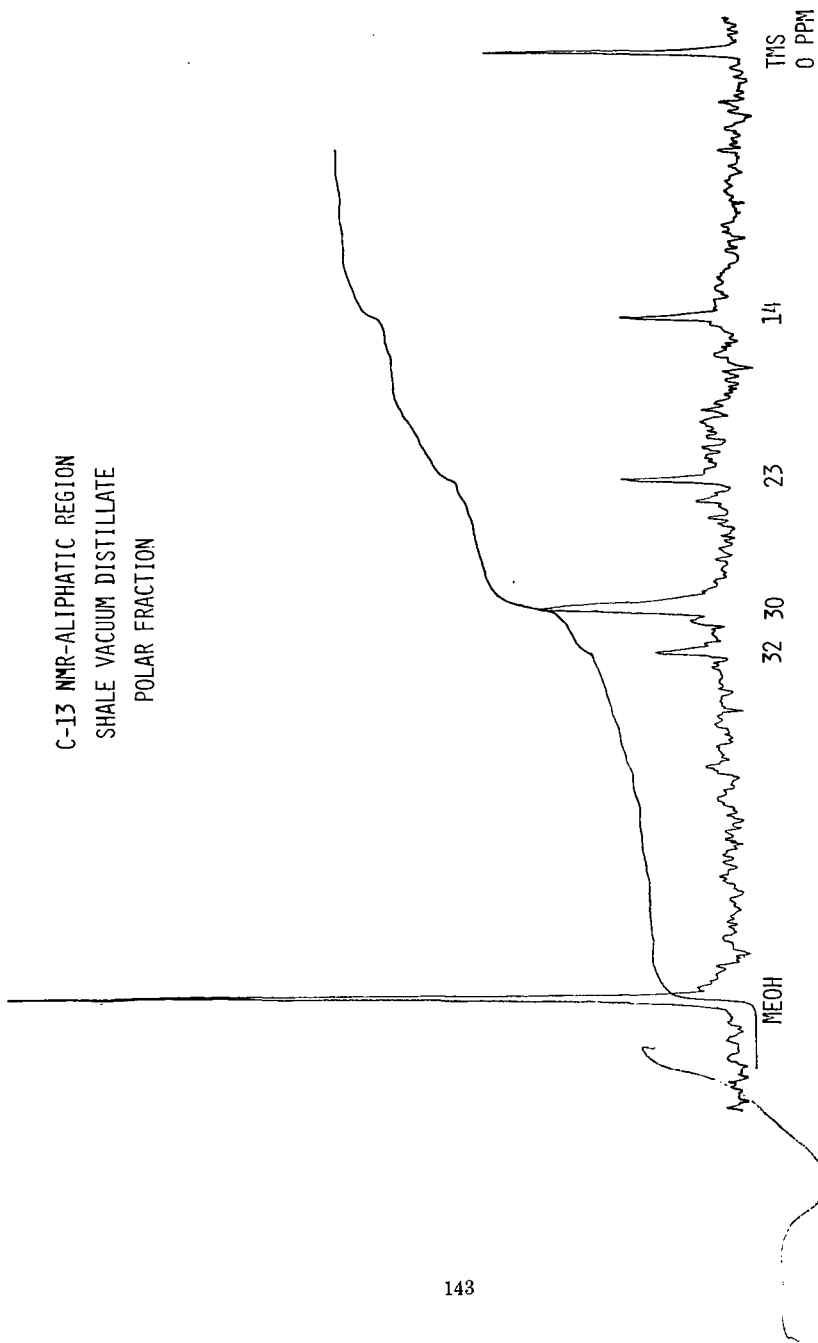


Figure 1. C-13 nmr spectrum of shale oil vacuum distillate polar fraction, aliphatic region, TMS reference, methanol internal standard, integration trace (upper curve).

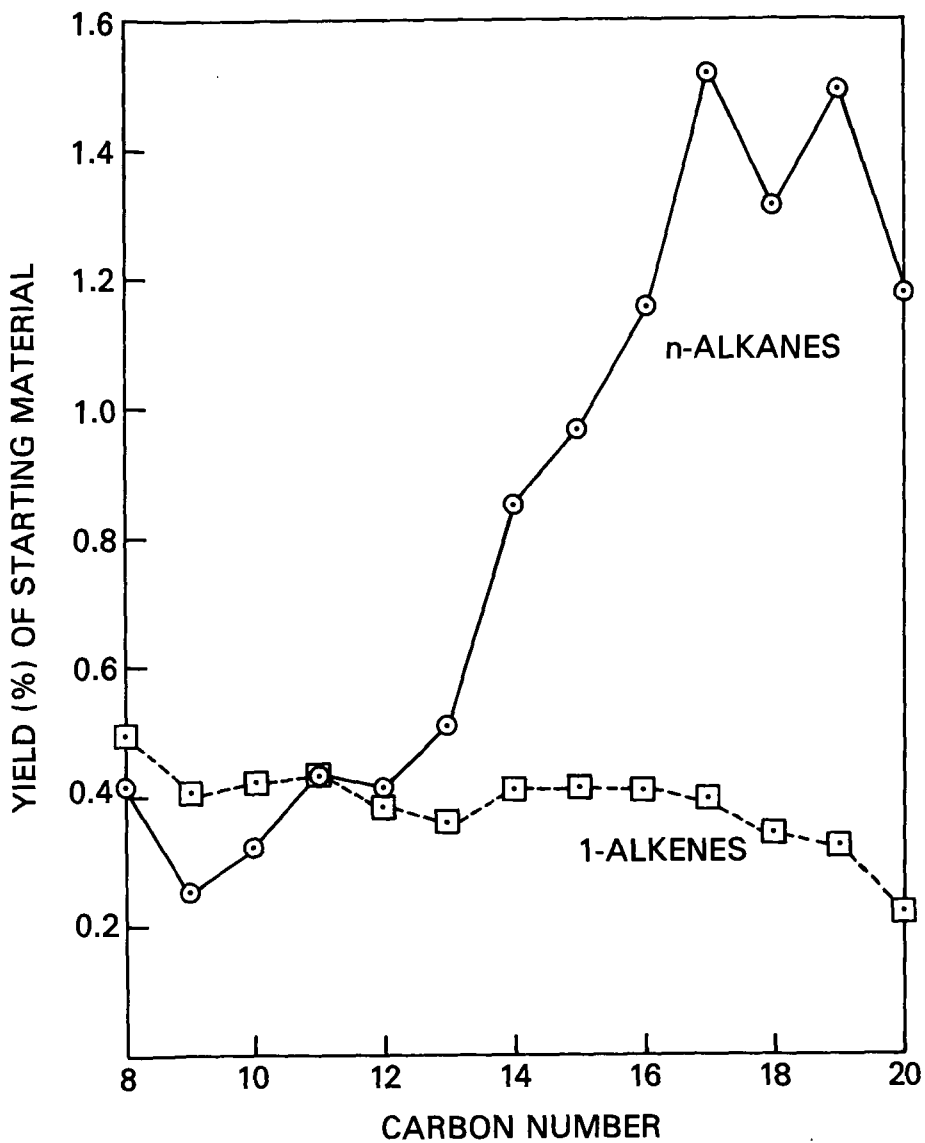


Figure 2. Pyrolysis of shale oil vacuum distillate saturate fraction at 450°C, for 30 minutes.

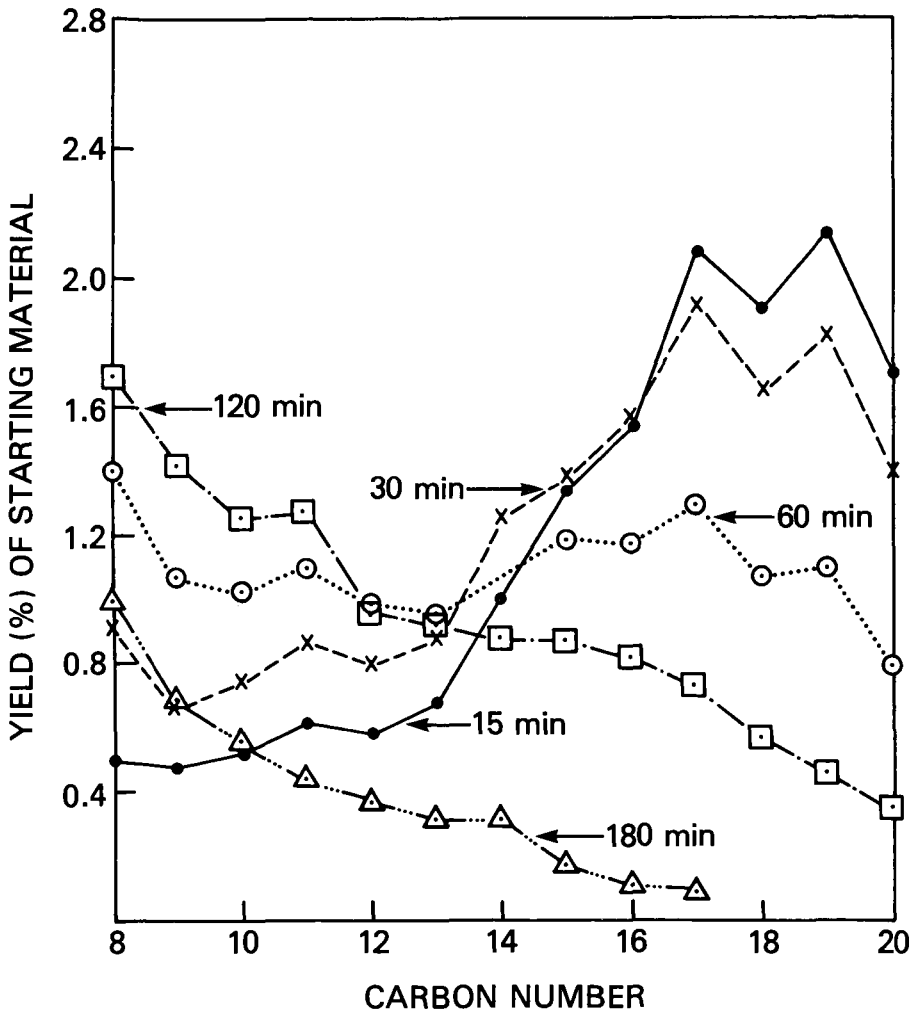


Figure 3. Pyrolysis of shale oil vacuum distillate saturate fraction at 450°C. The yield is the sum of n-alkane plus 1-alkene for the indicated chain length.

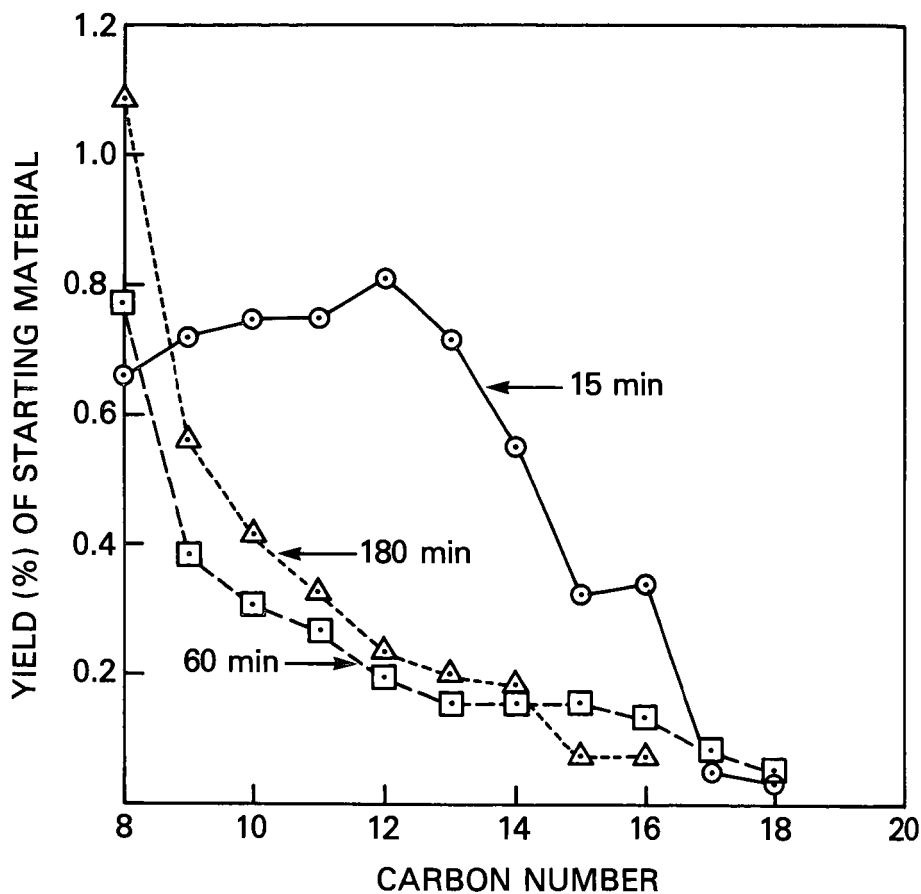


Figure 4. Pyrolysis of shale oil vacuum distillate polar fraction at 450°C. The yield is the sum of n-alkane plus 1-alkene for the indicated chain length.

The saturate fraction gave substantial yields of potential n-alkanes in the JP-5 range at all stress times. The highest yields were for shorter stress times, however, and the maximum of 33% was found at 60 minutes.

The potential n-alkane yield for the aromatic and polar fractions fell much below that of the saturates. This is consistent with the much lower wt. % unbranched alkyl group and average chain length data found by nmr.

DISCUSSION AND CONCLUSIONS

Over 50% of unbranched alkyl groups in the saturate fraction can be converted to potential n-alkanes in the JP-5 distillation range. This indicates that the average chain length of 19 is fragmenting during the pyrolysis to give substantial amounts of n-alkanes and l-alkenes with carbon numbers in the 9 to 16 range. Single step Fabuss-Smith-Satterfield breakdown would explain this behavior. The potential n-alkane yields in excess of 30% approach those of 37% found for JP-5 made from shale oil by a delayed coking operation (1). Thus, the saturate molecules in the vacuum distillate portion of Paraho shale oil seem to be significant contributors to JP-5 and n-alkane production in the delayed coking process.

The aromatic and polar fractions in the shale oil vacuum distillate contribute much less than the saturate fraction to n-alkane production. This is consistent with studies on model compounds (7). Substituted benzenes and pyridines preferentially fragment to give n-alkanes and l-alkenes with one and two fewer carbons than the length of the side chain. For the average side chain of 13 for the polar fraction, which contains large amounts of pyridines, the alkane/alkene fragment would be primarily 11 or 12 carbons. Figure 4 illustrates a sharp increase in yield near these carbon numbers at the longer stress times for the polar fraction.

Highest yields of JP-5 come at 60 minutes for the various fractions. Unfortunately, this time also gives the highest yield of potential n-alkanes for the saturate fraction. Thus, differentiation between a good yield of JP-5 and a low yield of n-alkanes cannot be made on the basis of pyrolysis time.

ACKNOWLEDGMENT

The authors thank Dr. Hyman Rosenwasser of the Naval Air Systems Command for funding support.

LITERATURE CITED

- (1) Solash, J., Hazlett, R. N., Hall, J. M., and Nowack, C. J., *Fuel*, 57, 521 (1978).
- (2) Affens, W. A., Hall, J. M., Holt, S., and Hazlett, R. N., *Preprints, Am. Chem. Soc. Div. of Fuel Chem.*, 26 (3), 178 (1981).
- (3) Resing, H. A., Garroway, A. N., and Hazlett, R. N., *Fuel*, 57, 450 (1978).
- (4) Hazlett, R. N., Beal, E., Vetter, T., Sonntag, R., and Moniz, W., "Pyrolysis of Shale Oil Residual Fractions", Chap. 19 in *ACS Symp. Ser. No. 163*, ed. H. C. Stauffer, p. 285 (1981).
- (5) Gary, J. H., and Hardwerk, G. E., *Petroleum Refining*, Chap. 5, Marcel Dekker, Inc., New York, N. Y., 1975.
- (6) Fabuss, B. M., Smith, J. O., and Satterfield, C. N., *Adv. Pet. Chem. and Refin.*, 9, 157 (1964).
- (7) Hazlett, R. N., and Mushrush, G. W., *Preprints, Am. Chem. Soc. Div. of Fuel Chem.*, 27 (3-4), 214 (1982).

SYMPOSIUM ON GEOCHEMISTRY AND CHEMISTRY OF OIL SHALE
PRESENTED BEFORE THE DIVISIONS OF FUEL CHEMISTRY, GEOCHEMISTRY,
AND PETROLEUM CHEMISTRY, INC.
AMERICAN CHEMICAL SOCIETY
SEATTLE MEETING, MARCH 20 - MARCH 25, 1983

CHARACTERIZATION OF SHALES USING SINK FLOAT PROCEDURES

By

C. J. Vadovic
Exxon Research and Engineering Company, Baytown, Texas 77520

INTRODUCTION

The analysis of the organic fraction in shale leads to important processing insights. However, the analysis is complicated by the presence of a substantial fraction of rock. The rock often contains carbon, as carbonates, and hydrogen, as water of hydration, which make it extremely difficult to obtain a true organic analysis. The route used most often to obtain organic analyses is to isolate the kerogen by acid removal of the inorganics. This poses numerous problems in that the acids used, HCl and HF, can interact with and be incorporated into the organic matrix. Also basic nitrogen compounds are easily extracted from the shale. It has been observed that up to 20% of the organic carbon and up to 50% of the total nitrogen may be removed by acid extraction. To obviate these difficulties a procedure has been developed which utilizes the analyses of raw sink float shale samples to calculate the ratios of organic hydrogen and nitrogen to organic carbon. In addition an estimate of the hydrogen and nitrogen content of the mineral matter is obtained. (Table I)

SINK FLOAT PROCEDURE

The starting point for the procedure outlined here is the floating of material containing rock and mineral matter at a predetermined specific gravity. The principles involved are depicted in Figure 1. At a low media specific gravity essentially all of the material will sink. As the specific gravity increases more of the material floats. At a sufficiently high specific gravity all of the material will float.

In the procedure described here a method analogous to the collection of distillation cuts was employed. The shale was subjected to a low specific gravity and the float fraction collected. The sink fraction was subjected to an incrementally higher specific gravity and the float fraction collected. The procedure was repeated until very little material remained. In this manner a series of samples, differing primarily by organic to rock ratio, was collected.

The nature of the shale plays a role in the selection of the media. Heavy hydrocarbon media may be used on dry, impervious shales such as Colorado. For wet shales, such as Rundle, it is more practical to use an aqueous based heavy media system. The judicious selection of media prevents contamination of the shale and allows accurate analysis.

TABLE I
SINK FLOAT PROCEDURES OFFER ALTERNATIVES
IN SHALE CHARACTERIZATION

- Gravity Separation Analogous to Distillation
- Samples fractionated by weight fraction
of rock and organic
- Characterization Procedure Eliminates Need for
Acid Extraction to Obtain Kerogen
- Atomic ratios determined by analyses of
rock containing samples
- ◆ H and N Content of Rock Determined

PROCEDURAL DETAILS AND RESULTS

The basis for the procedure presented here is an element balance of the form

$$X_i^{\text{total}} = X_i^{\text{organic}} + Y_i \cdot X_{\text{mineral}}$$

where X_i^{total} and X_i^{organic} are the total and organic weight percent of component i in the raw shale, respectively, X_{mineral} is the weight percent of minerals in the shale, Y_i is the weight percent of component i in the minerals and i is hydrogen or nitrogen.

By algebraic manipulation of the above equation, the details of which are shown in Table II, an equation of the form below is obtained.

$$\frac{100 X_i^{\text{total}}}{\text{Ash} + \text{CO}_2} = \frac{12 X_i^{\text{organic}}}{\text{MW}_i \text{C}_{\text{org}}} \frac{100 \text{C}_{\text{org}} \text{NW}_i}{(\text{Ash} + \text{CO}_2) 12} + Y_i$$

TABLE II
ELEMENT BALANCES KEY TO SINK FLOAT ANALYSES

$$X_i^{\text{total}} \text{ (wt\% of shale)} = X_i^{\text{organic}} \text{ (wt\% of shale)} + X_i^{\text{inorganic}} \text{ (wt\% of shale)}$$

$$X_i^{\text{inorganic}} = Y_i^{\text{minerals}} \text{ (wt\% of minerals)} \times \text{minerals (wt\% of shale)} / 100$$

Assume: Minerals = Ash + CO₂

$$X_i^{\text{total}} = X_i^{\text{organic}} + Y_i^{\text{minerals}} \times (\text{Ash} + \text{CO}_2) / 100$$

Rearranging Yields

$$\frac{100 X_i^{\text{total}}}{\text{Ash} + \text{CO}_2} = \frac{100 \times \text{MW}_i \times \text{C}_{\text{organic}}}{(\text{Ash} + \text{CO}_2) 12} \left(\frac{X_i^{\text{organic}} \times 12}{\text{C}_{\text{organic}} \times \text{MW}_i} \right) + Y_i^{\text{minerals}}$$

where Y_i^{minerals} = Content of i th element in minerals

$$\frac{X_i^{\text{organic}} \times 12}{\text{C}_{\text{organic}} \times \text{MW}_i} = \text{Atomic } i/\text{C ratio}$$

A simplifying assumption in this derivation is that the mineral content of the shale can be represented by the sum of the ash and carbonate CO₂. The total component X_i and the organic carbon are determined by elemental analyses. To effectively use the above equation, a series of samples containing varying amounts but similar compositions of both organic and inorganic constituents must be obtained.

The sink float procedure yields a series of samples which contain various levels of organic and inorganic material. It is assumed that in these samples variations in both organic and inorganic composition are minimal (Table III). The variation in ash elements for Brazil and Rundle shale are shown in Figure 2. The variations observed in sink float samples from these clay-containing shales are slight. By plotting $100 X_i^{\text{total}} / \text{Ash} + \text{CO}_2$ vs $100 \text{C}_{\text{org}} \text{MW}_i / 12 (\text{Ash} + \text{CO}_2)$ two results are achieved. The slope is the atomic $X_i / \text{C}_{\text{org}}$ ratio and the intercept is the inorganic content of the element i . The results of such a plot for Brazil and Rundle shales are shown in Figure 3. As can be seen, straight lines with high correlation coefficients result.

The mineralogy of the Colony sink float samples is illustrated in Figure 4. Colorado shale is made up of primarily non-hydrated minerals: calcite, dolomite and quartz. There are, however, measurable quantities of clays which do contain water of hydration. Also there is more variation in mineralogy with specific gravity than has been observed for the Rundle and Brazil samples. The plot of $100 H_{\text{total}} / (\text{Ash} + \text{CO}_2)$ vs. $100 \text{C}_{\text{organic}} / 12 (\text{Ash} + \text{CO}_2)$ for Colony shale is shown in Figure 5. Again a straight line with a high correlation coefficient results.

TABLE III
IMPLICIT ASSUMPTIONS DO NOT LIMIT TECHNIQUE APPLICABILITY

- Sink float samples are generated based on organic content of rock only
- Organic content is uniform
- Inorganic content is uniform

The method, as outlined here, is also applicable to nitrogen. The approach was applied to Rundle, Brazil and Colony shale samples and the results are plotted in Figure 6. The resultant plots are linear for these three shales. At zero organic content all shales exhibit some nitrogen content. An unexpected result is that the calculated nitrogen content of the mineral matrix of both Rundle and Colony shale is similar. It has been postulated in the literature that compounds composed of ammonia (NH₃) may be present in clay minerals. There are also other naturally occurring ammonia minerals that have been identified. However, the reason for similar levels of inorganic nitrogen in both Rundle and Colony is unclear.

The calculated atomic ratio of H/C and N/C are compared in Table IV with values calculated from analytical results on acid extracted kerogens. The results for raw shale calculated from the procedure suggested here compare quite favorably with the kerogen values. The results show that the H/C ratio for the Rundle shales tested (1.68) is greater than that calculated for Colony (1.55), which in turn is higher than that of Brazil. The N/C ratio for Colony is almost double that of Rundle, 0.029 vs. 0.019. The slight differences between the sink float and the kerogen values suggest that the kerogen extraction procedure is valid despite the loss of both organic carbon and nitrogen during acid extraction.

TABLE IV
H/C AND N/C RATIOS COMPARE FAVORABLY WITH
EXTRACTED KEROGEN VALUES

	H/C, Atom/Atom		N/C, Atom/Atom	
	<u>Sink-Float</u>	<u>Kerogen</u>	<u>Sink-Float</u>	<u>Kerogen</u>
Rundle	1.68	1.63	0.017	0.016
Brazil	1.32	1.30	0.024	0.023
Conoly	1.55	1.56	0.029	0.027

The amount of mineral hydrogen and nitrogen relative to the total amount of hydrogen and nitrogen present is shown in Table V. The total levels are representative of the average yield of the shales analyzed. The average yields for Rundle, Brazil and Colony are 25, 20 and 35 gpt respectively. The mineral hydrogen content ranges from 3 to 15% of the total hydrogen, and the mineral nitrogen content ranges from 4 to 31% of the total. Two potential sources of inorganic hydrogen and nitrogen are water of hydration and ammonia. It is obvious that the release of these compounds during retorting can have a measurable effect on retorting yields.

TABLE V
H AND N CONTENT OF MINERALS ARE SMALL BUT SIGNIFICANT

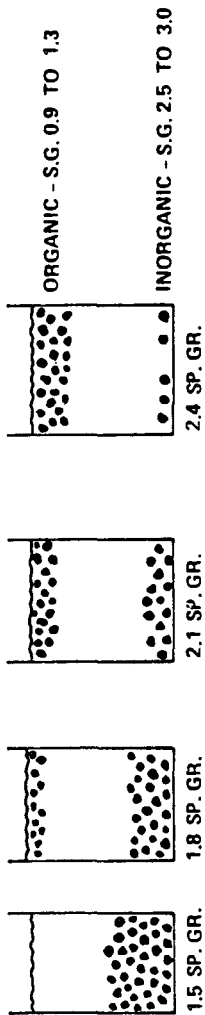
Shale	Levels Representative of Average of Deposit					
	Min, Wt%	Hydrogen		Min, Wt%	Nitrogen	
		Total, Wt%	Min/Total		Total, Wt%	Min/Total
Rundle	0.25	2.16	0.11	0.13	0.42	0.31
Brazil	0.28	1.86	0.15	0.02	0.41	0.04
Colony	0.08	2.83	0.03	0.10	0.83	0.12

EXTENSION TO SULFUR AND OXYGEN

The method developed here is only applicable to hydrogen and nitrogen. This is primarily because it assumed that the mineral form is uniform and the H and N in the mineral matter are proportional to the amount of mineral matter present. These assumptions are not true for sulfur and oxygen (Table VI). A major source of sulfur is pyrite, which seems to be randomly distributed through the sink float fractions. Consequently, a procedure to back out pyrite prior to mathematical analysis would be desirable. However, an accurate method for pyrite analyses in shales is not yet

FIGURE 1
HOW PHYSICAL SHALE BENEFICIATION WORKS

NOTE: EACH PARTICLE CONTAINS SOME ROCK OR MINERAL MATTER



LABORATORY FLOAT / SINK TESTS

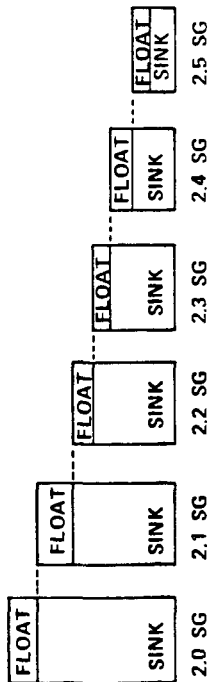


FIGURE 2
ASH ELEMENTS ARE UNIFORM IN SINK FLOAT FRACTIONS

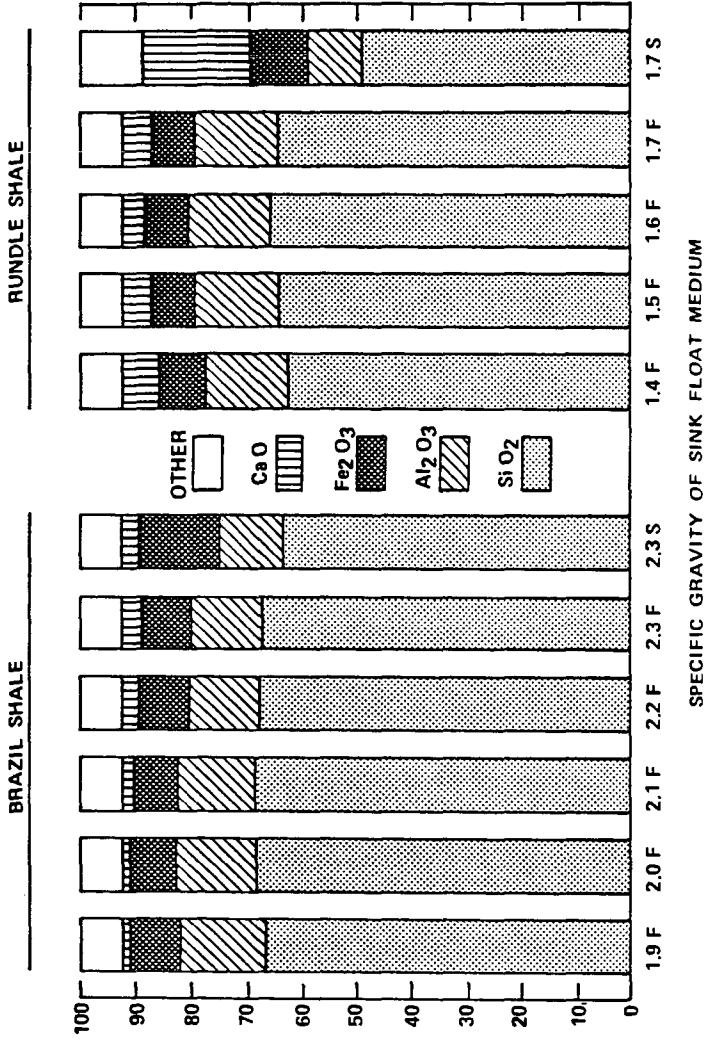


FIGURE 3
HYDROGEN ANALYSIS FOR CLAY CONTAINING SHALES

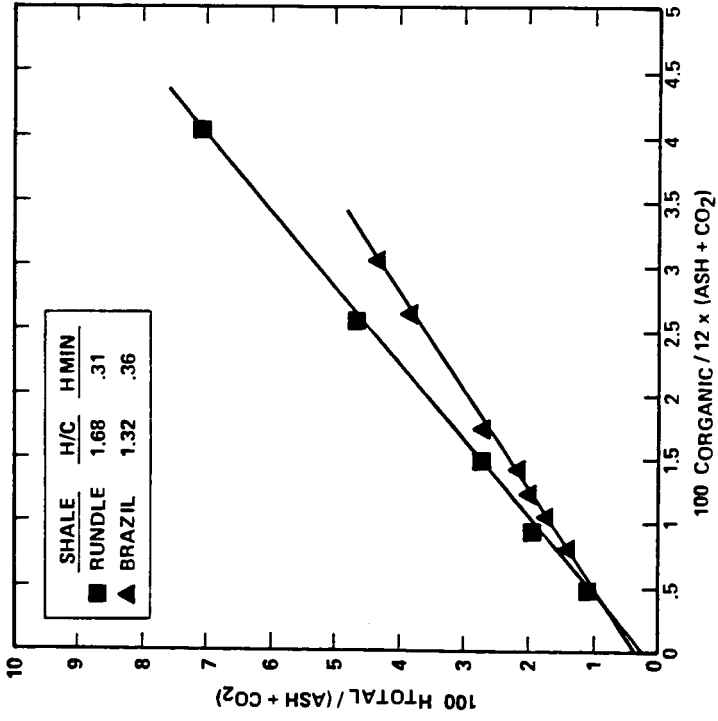
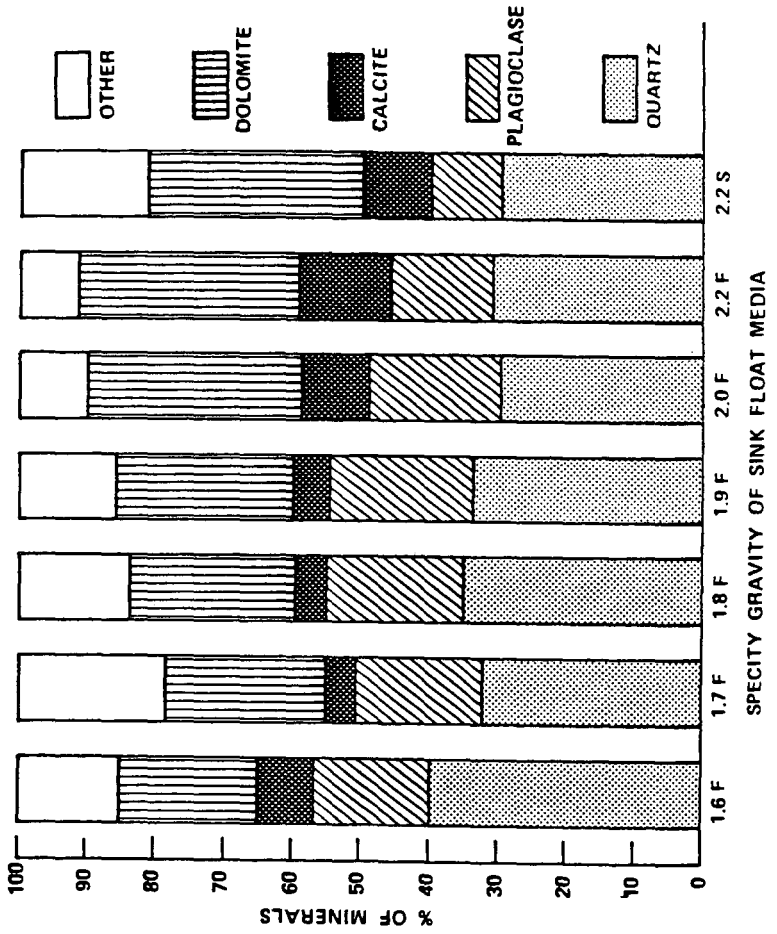


FIGURE 4
MINERALOGY OF COLONY SINK FLOAT SAMPLES



HYDROGEN ANALYSIS FOR COLONY SHALE

FIGURE 5

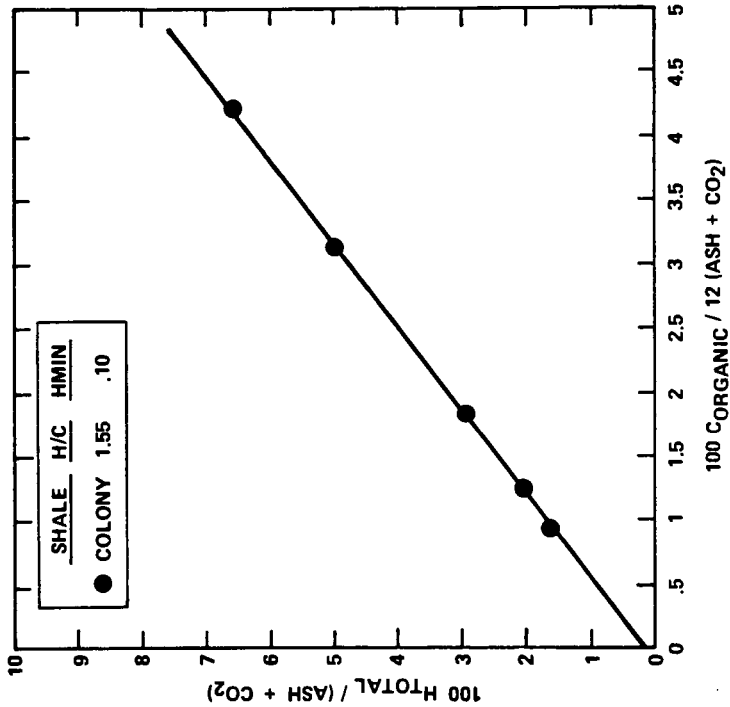
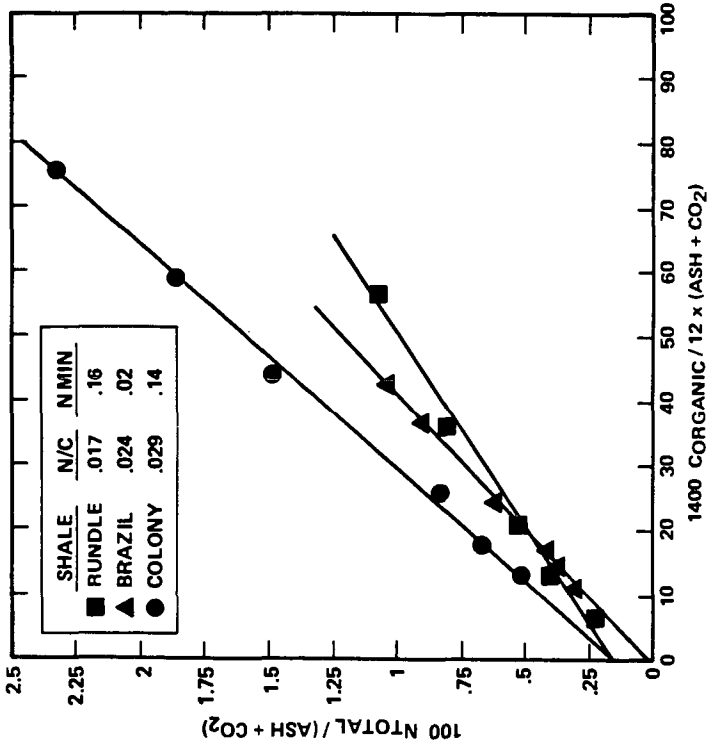


FIGURE 6
**SHALE NITROGEN DISTRIBUTION ALSO DETERMINED
 FROM SINK/FLOAT ANALYSIS**



available. A similar situation exists for oxygen. There are three major sources of oxygen: organic, carbonate, and metal oxides. The carbonate can be analyzed and backed out. It is not clear, however, that the high level of oxygen as metal oxides will allow the accurate calculation of either the slope or the intercept. The extension of the procedure to sulfur and oxygen must be evaluated as more accurate data become available.

TABLE VI
TECHNIQUE APPLICABLE TO SULFUR AND OXYGEN

- Overall Balances Slightly Different
 - $O_{total} = O_{organic} + O_{Ash} + O_{CO_2}$
 - $S_{total} = S_{organic} + S_{SO_4} + S_{pyrite}$
- Analyses Complicated by Analytical Difficulties
 - Pyritic and sulfate sulfur difficult to measure in shale
 - Oxygen analyses not straightforward
- Extension to Spent Shale also Possible

TABLE VII
ALTERNATIVE CHARACTERIZATION PROCEDURE INITIATED

- Sink Float Techniques Useful as Characterization Tool
- H/C and N/C Atomic Ratios Calculated
 - Good agreement with extracted kerogen values achieved
- H and N Content of Mineral Matter Calculated
 - Inorganic H and N are significant fractions of total element
- Procedure Applicable to other Elements

CONCLUSIONS

A method has been developed, utilizing sink float procedures, which:

- calculates the H/C and N/C ratios in raw shales
- eliminates the need for acid extraction
- estimates the H and N content of the mineral matrix.

The procedure has been tested on several shales with good results.

SYMPOSIUM ON GEOCHEMISTRY AND CHEMISTRY OF OIL SHALE
PRESENTED BEFORE THE DIVISIONS OF FUEL CHEMISTRY, GEOCHEMISTRY,
AND PETROLEUM CHEMISTRY, INC.
AMERICAN CHEMICAL SOCIETY
SEATTLE MEETING, MARCH 20 - MARCH 25, 1983

REDUCTION AND PHENOL ACID DEPOLYMERIZATION OF
WESTERN U.S. OIL SHALE KEROGEN

By

J. Solash, D. C. Cronauer, and T. P. Kobylinski
Gulf Research & Development Company,
P. O. Drawer 2038, Pittsburgh, Pennsylvania 15230

INTRODUCTION

The chemical structure of U.S. Western oil shale kerogen is not known with certainty. Many structure studies employed strong oxidants to degrade kerogen (1-4). Acidic products are isolated and analyzed. In most cases, relatively small amounts of material are analyzed. Structural inferences from analysis of small quantities (generally less than 20% of kerogen) of degraded material are apt to be misleading.

The literature is in conflict regarding even basic structural features of kerogen. Yen and coworkers have used X-ray analysis to deduce that kerogens contain very little aromatic material (5). However, ^{13}C CP/MAS nmr measurements show that Western kerogens are 20-30% aromatic (6,7). The structure of nitrogen containing moieties is also in doubt. It has been suggested (8) that tetrapyrroles in kerogen pyrolyze to yield pyridines, quinolines, and other classes of nitrogenous compounds found in shale oil. No quantitative data were given. Pyrolysis of simple pyrroles was found to give low yields of pyridines (9). Pyridines and quinolines are the major nitrogen-containing species in distillate shale oils.

Our approach has been to attempt to degrade Western U.S. oil shale kerogen under mild conditions. There has been a report of reducing kerogen using dissolving metals (10). Jones and Dickert reported that treating Colorado oil shale kerogen with lithium aluminum hydride, HI, or lithium in ethylene diamine were all ineffective in increasing kerogen solubility (10). Interestingly, HI has been reported to convert kukersite to 100% ether and benzene solubles (11). No data were reported on the possible extent of reduction with lithium in ethylene diamine.

We would like to report our results of treating kerogen with several well-known reagents. We decided to reinvestigate reductively alkylating kerogen using sodium in hexamethylphosphoric triamide (Na/HMPA). This reagent has been reported to be a superior medium to produce solvated electrons (12). Na/HMPA is capable of reducing isolated double bonds (13); reducing the solvent or adding an electron transfer agent to the substrate can be avoided using Na/HMPA (14). There is a rich literature dealing with similar reduction of coal and model compounds (15-18). Treating kerogen with Na/HMPA and a variety of alkylating agents resulted in only small increases in solubility. Treating kerogen with known ether and ester cleavage reagents ($\text{FeCl}_3/\text{Ac}_2\text{O}$; $\text{Me}_3\text{SiCl}/\text{NaI}$) resulted in very little increase in kerogen solubility. Kerogen is rapidly but incompletely oxidized by trifluoroperoxyacetic acid (TFPA). The oxidized products show evidence of pyridines and quinolines. Phenol-toluenesulfonic acid treatment results in solubilizing large fractions of kerogen.

EXPERIMENTAL

General Methods

The kerogens used in this study were derived from Colorado oil shale. The oil shales used are: R351, a 25 gal/ton (gpt) shale; Rio Blanco, a 22 gpt shale; and Hazen, a 52 gpt pretreated shale. These oil shales were all mined from the Gulf C-a tract. R-351 is a Mahogany Zone oil shale of unknown geographic origin. The Rio Blanco and Hazen samples were both from the MDP-1 core; Rio Blanco is a core composite sample while Hazen is a homogeneous G-level oil shale sample. The Hazen sample was beneficiated by gravity methods (1.60 sp. gr. float) prior to our treatment. Minerals were removed from the oil shales by sequential HCl then HF treatment. Bitumen was removed from the kerogens by extracting with benzene-methanol (7:3). The elemental analysis of the three kerogens used is presented in Table I. Others at our laboratories are investigating the nature of residual mineral matter in kerogen after beneficiating in various ways.

Elemental analyses were determined by Microanalysis Inc., Wilmington, Delaware; oxygen was directly determined by a modified Unterzaucher technique. IR spectra were recorded on a Digilab Model 15C Interferometer using KBr pellets. NMR spectra were recorded on a Varian XL-200.

TABLE I
ELEMENTAL ANALYSES OF KEROGEN CONCENTRATES

Sample	C	H	Elemental Analysis, wt%				Cl	Ash
			N	S	O	F		
R351	69.35	8.75	1.61	4.84	5.90	1.16	---	6.44
Rio Blanco	65.12	8.15	2.10	4.59	10.21	0.77	1.03	11.03
Hazen	65.40	8.79	2.05	3.24	5.37	1.49	0.22	13.57

Dissolving Metal Reduction

A typical experiment follows: a 100 ml round bottom flask, equipped with pressure equalizing addition funnel, efficient condenser, and gas addition tube was used. The apparatus was oven dried, assembled hot, and allowed to cool under dry N₂. The flask was charged with 15 ml of freshly distilled HMPA. Sodium (about 1.5 g) was freshly cut into small pieces. Several pieces of sodium were added to the HMPA with stirring. After several minutes, the solution turned blue. About 1 g of kerogen was added; 5 ml of HMPA were used to rinse any kerogen adhering to the sides of the flask. The blue color disappeared upon adding kerogen. After solvated electrons reappeared, the addition funnel was charged with the calculated quantity of quencher (methanol or alkyl iodides). The quencher was added dropwise until the blue color was removed; when solvated electrons reappeared more quencher was added. Sodium was added as required. The quantity of quencher was calculated on the basis of the aromatic content (assume fa = .25) and the oxygen content. After all quenching agent was added, the mixture was poured into 50 ml of water and filtered. The solids were washed with large volumes of water, dried in vacuo (85°C, 24-48 hr, 300-400 torr), and weighed. The solids were then Soxhlet extracted with toluene and submitted for elemental analysis. Incorporated ¹³C (from ethyl iodide-1-¹³C) was determined by Global Geochemistry, Inc., Canoga Park, California, using a combustion method.

Phenol-p-Toluene Sulfonic Acid Depolymerization

The kerogens were treated with phenol and tosyl acid according to literature methods (24). After reacting, excess phenol was removed by steam distilling. The products were filtered, washed with water, and dried in vacuo. The products were then Soxhlet extracted with toluene, methanol, and finally pyridine. Extracts were isolated, weighed, and analyzed as outlined in the text. Product recoveries are outlined in Figure 1. For instance, for the Rio Blanco (RB) kerogen, 3.87 g of solids were recovered from 2.00 g of starting kerogen (193% yield). From the recovered (phenolated) product, 46% was soluble in toluene.

The toluene soluble products from each reacted kerogen were subjected to SARA analysis (saturates, aromatics, resins, asphaltenes). The Rio Blanco toluene solubles gave almost 91% asphaltenes. The Hazen kerogen toluene solubles were almost 81% asphaltenes. The Hazen toluene solubles were more difficult to handle; 14.5% of the material was unrecovered from the chromatographic column.

RESULTS AND DISCUSSION

Reductive Alkylatton

The kerogens described in the experimental section were reductively alkylated by continually quenching the intermediate anions. The method requires that the dark blue solution (solvated electrons) be stoichiometrically quenched with alkylating agent. When the dark blue solution reappears, more alkylating agent is added. The results of reductively alkylating three kerogens with methanol (protonate) and ethyl-, butyl-, and octyl iodide are presented in Table II.

Table II presents the recovery and elemental analysis data of the solids recovered after reductively alkylating. In a number of cases, the recovery of material was greater than 100% based on starting kerogen. Using the elemental analysis data in Tables I and II, we calculated the number of alkyl (or proton) groups added to the kerogens. The R351 and Rio Blanco kerogens incorporated more protons and alkyl groups than the Hazen kerogen. In two experiments (Table II, Runs 6 and 12) we used ¹³C labelled ethyl iodide as alkylating agent and measured incorporated ¹³C in the product solids. We found that the Rio Blanco kerogen incorporates almost twice the number of ethyl groups as the Hazen kerogen (2.44 vs. 1.25 ethyl groups/100 atoms C) based on ¹³C labelling data. This compares fairly well with the elemental analysis data in Table II (Runs 6 and 12).

While we can alkylate kerogen, the alkylated products were only slightly (<5%) soluble in toluene. These results must be compared to those found for reductive alkylates of coal (15,16). Reductively alkylating coal generally results in very large increases in benzene or toluene solubility of the alkylated coal product. Dissolving metals are very effective for reductively cleaving many kinds of ethers and esters. Some carbon-carbon bonds are also cleaved by reductive alkylation.

The lack of increased alkylated-kerogen solubility implies that ether linkages are not important in holding kerogen together. To confirm this, kerogen was treated with $\text{FeCl}_3/\text{Ac}_2\text{O}$ (19) and $(\text{H}_3\text{C})_3\text{-SiCl}/\text{NaI}$ (20). These known ether-cleavage reagents failed to increase the toluene solubility of our kerogens. Ethers and ester linkages can be ruled out as important crosslinks of kerogen "monomers".

TABLE II
ELEMENTAL ANALYSES FOR Na/HMPA TREATED KEROGENS

Sample	Elemental Analysis, wt%					AA ^a	#Gp/ 100 C	Recovery
	C	H	N	S	O			
R351 (1)	65.35	8.97	2.94	--	--	M	14 ^b	97.6%
(2)	71.22	9.4	12.34	2.59	9.61	O	3.3	105
Rio Blanco								
(3)	63.79	8.40	2.15	4.32	11.45	M	8	93.5
(4)	64.95	8.36	2.50	5.88	8.75	M	4	83.5
(5)	64.08	8.37	2.34	2.14	--	E	2.8	88.3
(6)	66.67	8.82	2.34	3.04	7.95	E- ¹³ C	3.6	97.4
(7)	65.76	8.75	2.35	3.60	8.94	B	4.4	106
(8)	66.61	8.95	2.45	2.31	8.24	B	4.9	95
Hazen								
(9)	64.96	8.75	2.48	1.51	5.75	M	0.0	91.8
(10)	62.45	7.95	2.30	2.54	9.10	M	-8	88.7
(11)	66.24	9.01	3.40	1.93	--	E	0.8	108
(12)	65.61	8.89	2.12	2.66	5.10	E- ¹³ C	0.4	97
(13)	63.54	8.85	3.00	1.79	--	B	2.7	108

- a. AA = alkylating agent; M = methanol, E = ethyl iodide, B = butyl iodide, O = octyl iodide.
b. All entries in this column refer to the calculated number of alkyl groups incorporated per 100 atoms C of substrate (see test for details).

TFPA Treatment of Kerogens

We treated our kerogen with TFPA. We found that all kerogens lost weight after exposure to TFPA but to varying extents. These results will be published elsewhere (21).

Phenol-Tosyl Acid Depolymerization

The use of phenol-p-toluenesulfonic acid to dissolve coal is well-known (22-25). This method apparently has not been applied to oil shale kerogens (26).

In Figure 1, an outline of the product recovery results from phenol-tosyl acid treatment of kerogen is shown. Product recoveries are high (183-193%). Kerogen is much more reactive toward phenol than is coal (23,24). The recovered products were sequentially extracted with toluene, methanol, and pyridine. The extracts were isolated and weighed. As shown in Figure 1, the depolymerized products are 42-46% soluble in toluene. This wt% solubility in toluene assumes a fairly uniform distribution of phenol in all the products. We will confirm this assumption using labelled phenol. In Tables III and IV are shown the results of elemental analyses and some molecular weight measurements on the toluene-soluble material from depolymerized Rio Blanco and Hazen kerogen.

The results shown in Tables III and IV reveal some interesting features of these kerogens. The elemental analyses of the extracts from both kerogens are remarkably similar. There is a partitioning of nitrogen and sulfur heteroatoms among the solvents according to solvent polarity. The oxygen content of the extracts remains approximately constant. The H/C atomic ratio of the various solvent extracts also does not vary much ($\text{H/C} = 1.00 \pm .08$) for the Rio Blanco kerogen extracts (Table III). The H/C average value of 1.00 shows that much less hydrogen is present in the products. This is consistent with large amounts of incorporated phenol. The H/C atomic ratio varies more for the solvent extracts of phenol-reacted Hazen kerogen; H/C is 0.86 for toluene solubles, 1.0 for methanol solubles, and 1.26 for pyridine solubles. If we assume that the toluene-soluble fraction of the Hazen kerogen should have an oxygen content of about 5.4% (assume uniform elemental distribution among solvent extracts), then 11.6% oxygen found represents oxygen from incorporated phenol. The amount of phenol incorporated in the toluene solubles on this basis is 33% for the Rio Blanco kerogen ($(12-6.4) \times \frac{24}{16}$) and 36% for the Hazen kerogen ($(11.6 - 5.4) \times \frac{24}{16}$).

Large quantities of incorporated phenol are also evident from the ¹H and ¹³C spectra of the toluene solubles (Figure 2). The sharp bands in the aromatic regions of the ¹H and ¹³C spectra are due to substituted phenol moieties. The ¹³C spectrum integral can be used to calculate how

much phenol was incorporated in the Rio Blanco toluene solubles. Using the data shown in Figure 2 (first correcting for small amounts of residual toluene), we calculate that the toluene solubles from the Rio Blanco depolymerized kerogen contain about 46 wt% (incorporated) phenol.

TABLE III
DEPOLYMERIZATION OF RIO BLANCO OIL SHALE KEROGEN
VIA PHENOL-TsOH

Kerogen	Soxhlet ^b Solvent	Elemental Analysis, wt%					MW ^a
		C	H	N	S	O	
Unreacted		64.5	8.4	2.1	5.6	6.4	
C-a, Rio Blanco	Tol. Sol.	78.4	6.0	0.13	1.7	12.0	272(VPO) 334(GPC)
	MeOH Sol.	73.0	6.1	1.3	5.2	13.3	494(VPO) 343(GPC)
	Pyridine Sol.	77.2	6.7	2.3	2.9	10.0	

- a. Wt. Aver. MW by GPC for Tol. Extr. and MeOH Extr. are less than 1000.
b. Solvent soluble fraction of crude, isolated phenol kerogen product.

TABLE IV
DEPOLYMERIZATION OF HAZEN OIL SHALE KEROGEN
VIA PHENOL-TsOH

Kerogen	Soxhlet ^b Solvent	Elemental Analysis, wt%					MW ^a
		C	H	N	S	O	
Unreacted		65.4	8.8	2.1	3.2	5.4	
C-a, Hazen	Tol. Sol.	80.6	5.8	0.25	1.5	11.6	276(VPO) 370(GPC)
	MeOH Sol.	73.4	6.1	1.2	4.1	12.8	
	Pyridine Sol.	61.2	6.4	2.8	8.0	16.3	

- a. Wt. Aver. MW by GPC for Tol. Extr. and MeOH Extr. are less than 1000.
b. Solvent soluble fraction of crude, isolated phenol kerogen product.

The data in Tables III and IV also reveal that individual "monomeric" units of oil shale kerogen are of very low molecular weight. For instance, the major toluene-soluble fraction of each depolymerized kerogen has an average molecular weight of about 300-400. If almost half the carbons of toluene-soluble depolymerized Rio Blanco kerogen are from reagent phenol, then the molecular weights of "monomeric" kerogen units shown in Table III should be decreased by one or two incorporated phenol molecules (94-188 units).

The molecular weight data for the toluene-soluble fractions of both depolymerized kerogen products was confirmed by field ionization mass spectroscopy (FIMS). A FIMS spectrum for the depolymerized Rio Blanco kerogen toluene solubles is shown in Figure 3. The number average molecular weight calculated from Figure 3 is 401. Figure 3 shows that much of the ion intensity is concentrated in a relatively small number of peaks. The FIMS data cannot be compound-class analyzed using hydrocarbon classes only since the toluene solubles for this fraction contain about 12% oxygen. We do not want to assume that all oxygen in the toluene solubles is from incorporated phenol (the data do not support this assumption). Thus, assigning our FIMS data to specific hydrocarbon classes is not possible. We are applying low voltage-high resolution mass spectroscopy methods to these samples. We are also further fractionating our depolymerized samples to allow for simpler structure analysis.

The elemental analysis data (Tables III and IV) and the nmr spectra (Figure 2) of the depolymerized kerogen are surprising. The alkyl carbon portion of the ¹³C nmr spectrum is dominated by long chain saturates (chain length ≈ 15 carbons). There is little saturated cycloalkyl carbon present. Recently it was proposed that kerogens are composed primarily of saturated condensed cycloalkanes (27). The depolymerized products also appear to be "too aromatic". For instance, on the basis of the ¹³C nmr spectrum, we calculated that the depolymerized Rio Blanco kerogen toluene solubles had 46 wt% incorporated phenol. The atomic H/C ratio of the original Rio Blanco kerogen (Table I) is 1.49. After correcting for incorporated phenol (and residual toluene) by nmr, the calculated atomic H/C for the toluene-soluble Rio Blanco products is 0.95. This is much lower than

Figure 1
PHENOL-TsOH REACTION WITH KEROGEN

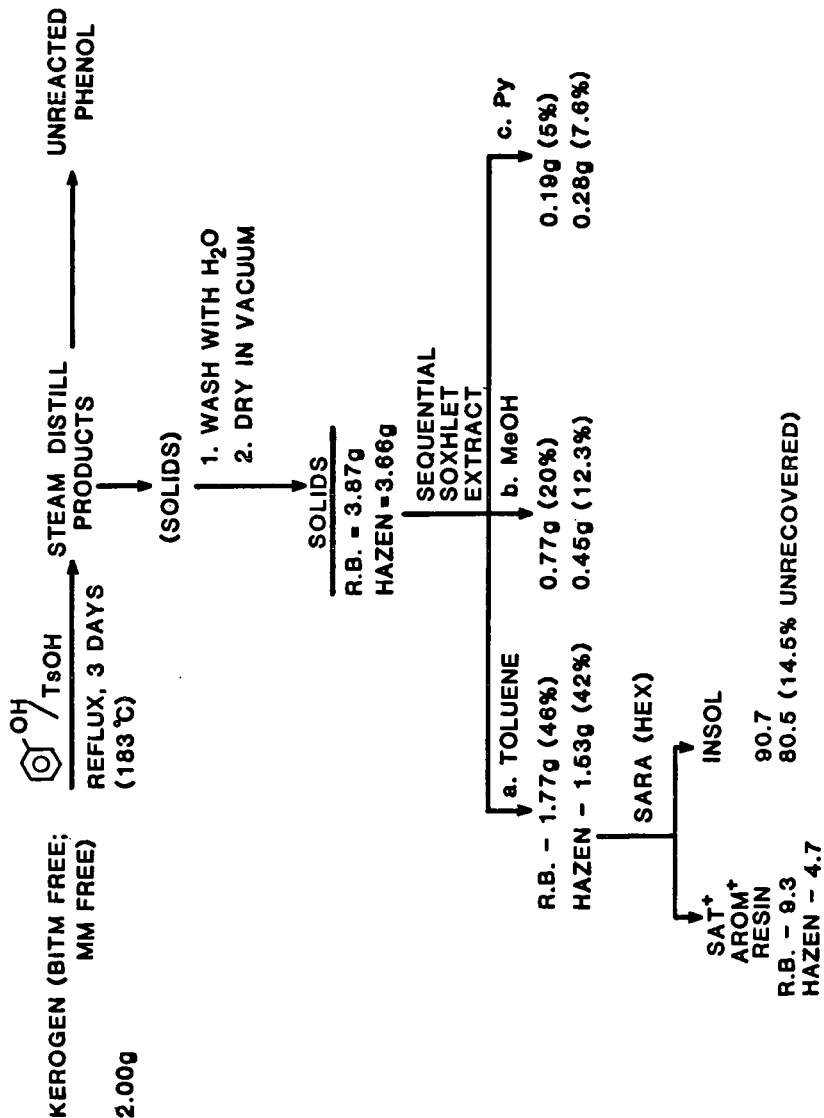
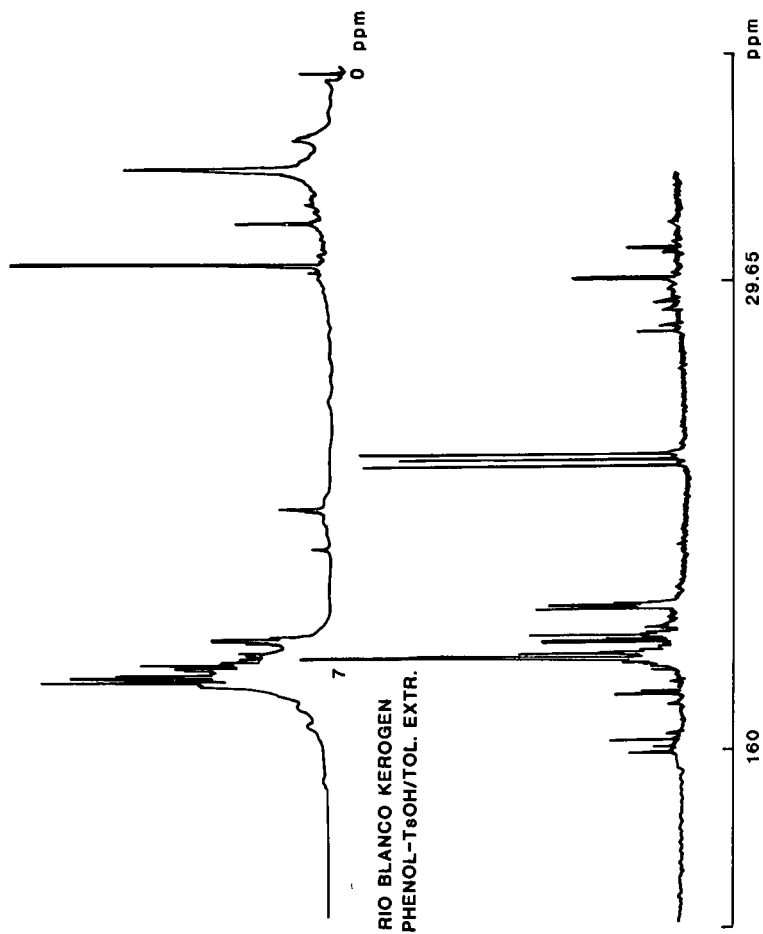


Figure 2
NMR Spectra of Depolymerized Rio Blanco
Kerogen; Toluene Solubles.
Top: $^1\text{H-NMR}$ Spectrum.
Bottom: $^{13}\text{C-NMR}$ Spectrum



R06004. SUM

GULF R&D, 1100-028-E2

1-10

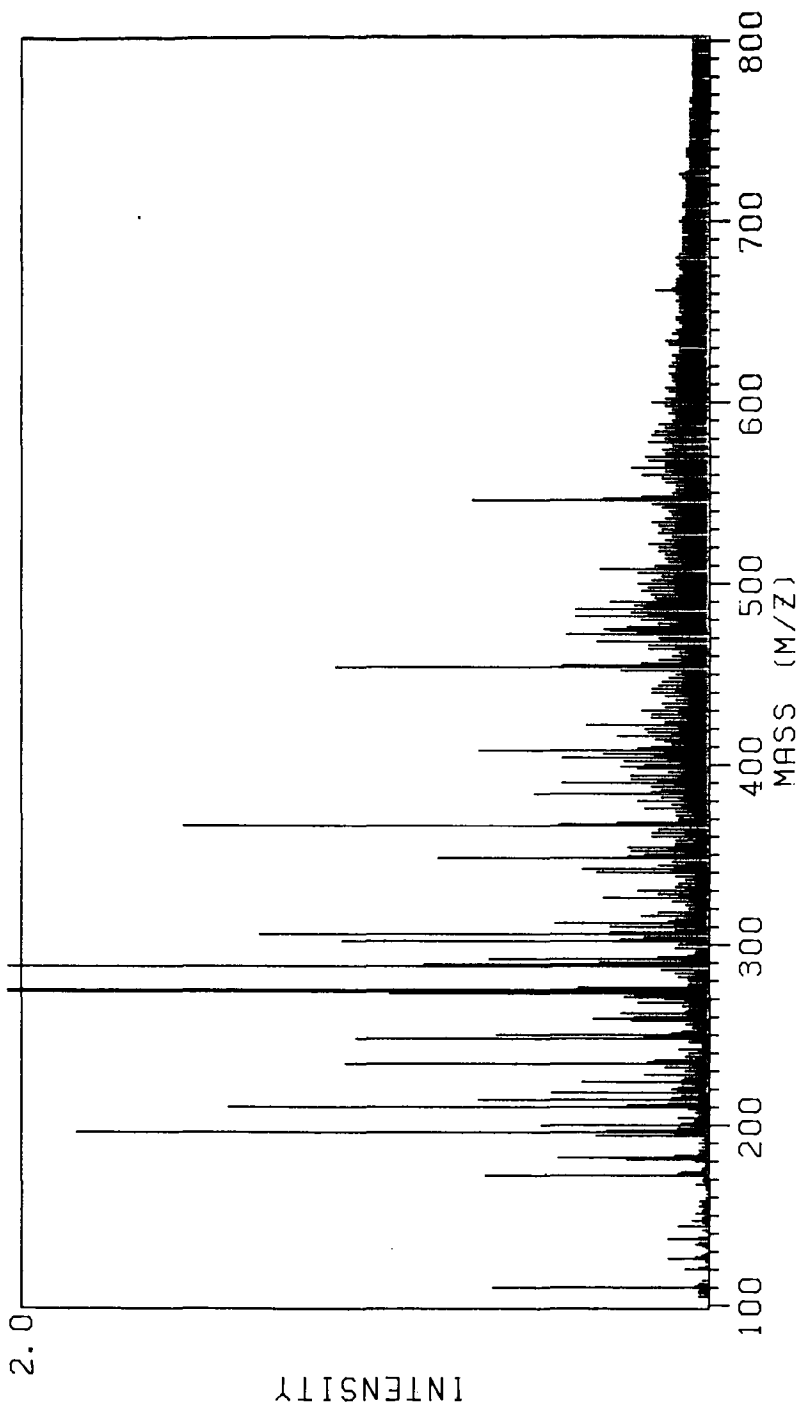


Figure 3. FIMS spectrum of depolymerized Rio Blanco kerogen-toluene solubles.

expected for the least polar fraction from a Western U.S. kerogen. We are currently engaged in studying the effect of phenol-tosyl acid on model compounds.

The Rio Blanco kerogen (MDP-1 core composite) is more reactive toward reductive alkylation and phenol depolymerization than the Hazen kerogen. It is tempting to suggest that the reactivity differences are structure related. However, if this were true, then these differences should be reflected in the soluble reaction products. We cannot adequately detect such differences solely with instrumental methods. We are currently engaged in performing several additional experiments. First, we are performing a depolymerization using ^{13}C -labelled phenol. This will permit an accurate mass balance to be made. Second, we have methylated the toluene-soluble products from unlabelled phenol depolymerization. The methylated fractions should be more easily fractionated by chromatography. Analysis of the chromatographic fractions should be simpler.

ACKNOWLEDGMENT

The authors wish to thank Drs. McNeil, McGinnis, Jeong, Lester, and Larson for helpful discussions.

LITERATURE CITED

- (1) Burlingame, A. L., and Simoneit, B. R., *Nature*, 222, 741 (1969).
- (2) Robinson, W. E., Heady, H. H., and Hubbard, A. B., *Ind. Eng. Chem.*, 45, 788 (1953).
- (3) Robinson, W. E., and Lawlor, D. L., *Fuel*, 40, 375 (1961).
- (4) Ishiwatari, R., and Machihara, T., *Geochim. Cosmochim. Acta*, 46, 825 (1982).
- (5) Yen, T. F., *ACS, Div. Fuel Chem., Preprints*, 19, 109 (1974); Young, D. K., and Yen, T. F., *Geochim. Cosmochim. Acta*, 41, 1411 (1977).
- (6) Resing, H. A., Garroway, A. N., and Hazlett, R. N., *Fuel*, 57, 450 (1978).
- (7) Miknis, F. P., Maciel, G. E., and Bartuska, V. J., *Org. Geochem.*, 1, 169 (1979); Miknis, F. P., Szenerengi, N. M., and Maciel, G. E., *Fuel*, 61, 341 (1982).
- (8) Jackson, L. P., and Decora, A. W., *ACS Div. Fuel Chem., Preprints*, 20 (2), 147 (1975).
- (9) Jacobsen, I. A., Jr., Heady, H. H., and Dinneen, G. U., *J. Phys. Chem.*, 62, 1563 (1958); Jacobsen, I. A., Jr., and Jensen, H. B., *J. Phys. Chem.*, 66, 1245 (1962); Jacobsen, I. A., Jr., and Jensen, H. B., *J. Phys. Chem.*, 68, 3068 (1964).
- (10) Jones, D. G., and Dickert, J. J., Jr., *Amer. Inst. Chem. Eng., Symp. Ser.*, 61 (54), 33 (1965).
- (11) Randsepp, Kh. T., *Izvest. Akad. Nauk SSSR, Otdel. Tekh. Nauk*, (3), 130 (1954); in *Chem. Abstr.*, 49, 4969c (1955).
- (12) Fraenkel, G., Ellis, S. H., and Dix, D. T., *J. Amer. Chem. Soc.*, 87, 1406 (1965).
- (13) Whitesides, G. M., and Ehman, E. J., *J. Org. Chem.*, 35, 3565 (1970).
- (14) a. Franz, J. A., and Skiens, W. E., *Fuel*, 57, 502 (1978);
b. Garst, J. F., *Accts. Chem. Res.*, 4, 400 (1971).
- (15) Ouchi, K., Hirano, Y., Makabee, M., and Itoh, H., *Fuel*, 59, 751 (1980).
- (16) Sternberg, H. W., and Delle Donne, C. L., *Fuel*, 53, 172 (1974); and previous papers in this series.
- (17) Collins, C. J., Homback, H. P., Maxwell, B., Woody, M. C., and Benjamin, B. M., *J. Amer. Chem. Soc.*, 102, 851 (1980).
- (18) Birch, A. J., Hinde, A. L., and Radom, L., *J. Amer. Chem. Soc.*, 103, 284 (1981); also see same authors, *ibid.* 102, 6430, 4074, 3370 (1980) and 100, 4681 (1978).
- (19) Ganem, B., and Small, V. R., Jr., *J. Org. Chem.*, 39, 3728 (1974).
- (20) Olah, G. A., Narang, S. C., Gupta, B. G. B., and Malhotra, R., *J. Org. Chem.*, 44, 1247 (1979).
- (21) Solash, J., Cronauer, D. C., Kobylinski, T. P., Young, D. C., Painter, P. C., and Synder, R. W., *submitted for publication*.
- (22) For a review: Larsen, J. W., and Kuemmerle, E. W., *Fuel*, 55, 162 (1976).
- (23) Heredy, L. A., and Neuworth, M. B., *Fuel*, 41, 221 (1962); Heredy, L. A., Kostgo, A. E., and Neuworth, M. B., *Fuel*, 42, 182 (1963); 43, 414 (1964); 44, 125 (1965).
- (24) Ouchi, K., Imuta, K., and Yamashita, Y., *Fuel*, 52, 160 (1973); 44, 29 (1965); 44, 205 (1965).
- (25) Yurum, Y., and Yiginsu, I., *Fuel*, 60, 1027 (1981); Yurum, Y., *Fuel*, 60, 1031 (1981).
- (26) Transalkylating of fossil fuels substrates, including petroleum resid has been studied by M. Farcaisu (Presentation at Fuel Science Meeting, Gordon Conferences, 1982). The transalkylating reagent used was xylene in the presence of a strong acid catalyst.
- (27) Bandurski, E., *Energy Sources*, 6, 47 (1982).

SYMPOSIUM ON GEOCHEMISTRY AND CHEMISTRY OF OIL SHALE
PRESENTED BEFORE THE DIVISIONS OF FUEL CHEMISTRY, GEOCHEMISTRY,
AND PETROLEUM CHEMISTRY, INC.
AMERICAN CHEMICAL SOCIETY
SEATTLE MEETING, MARCH 20 - MARCH 25, 1983

AN EXAMINATION OF THE PETROPORPHYRINS FOUND IN OIL SHALE FROM
THE JULIA CREEK DEPOSIT OF THE TOOLEBUC FORMATION

By

A. Ekstrom, H. Loeh, and L. Dale
CSIRO Division of Energy Chemistry, Lucas Heights Research Laboratories,
Private Mail Bag 7, Sutherland, NSW, 2232, Australia

INTRODUCTION

The nature of the petroporphyrins found in a variety of crude oils, oil shales, ancient and recent sediments have been a subject of continual interest since these compounds were first isolated from such materials by Treibs et al. (1) some fifty years ago. It is now generally agreed (2) that the petroporphyrins represent the degradation products of chlorophyll and that they consist predominantly of homologous series of deoxophylloerythroetioporphyrin (DPEP) and etio porphyrins. However, as yet unidentified porphyrin compounds which do not belong to either of these two classes have been observed (3) in some samples and the proposition that all petroporphyrins are derived from chlorophyll has also been questioned (4).

The oil shale of the Toolebuc formation in Queensland, Australia has been shown (5) to contain relatively high concentrations of vanadium and nickel porphyrin compounds. Saxby et al. (5) have suggested that these porphyrins are largely of the DPEP and etio-type and also observed significant variations in their concentrations in samples taken from various sites in the deposit. In this paper we describe two further aspects of the porphyrin compounds in this deposit. First, the variations in the concentrations of the chloroform extractable metal porphyrin compounds through well-characterized drill cores was determined, and second, the nature of the vanadium porphyrins was examined using absorption spectrophotometry and insertion probe, fast atom bombardment (FAB) and field desorption (FD) mass spectrometry techniques.

EXPERIMENTAL

Samples of the drill cores from the Julia Creek deposit used were ground and sieved, the -90 μm fraction being used. Samples of 15-20 g were exhaustively extracted with chloroform in Soxhlet extractors. As illustrated in Figure 1, the extract was filtered through a Millipore filter, and analyzed for V, Ni, Fe, Cu and Cr. Atomic absorption, inductively-coupled plasma emission and X-ray fluorescence spectrometry were used to analyze both the extracts and the raw shale.

The separation of the extract into polycyclic hydrocarbons, nickel and vanadium porphyrin fractions was accomplished using $\text{CCl}_4/\text{CHCl}_3$ chromatography with Kieselgel (Merck). The vanadium porphyrin fraction was then further separated into seven fractions using a variety of column chromatography procedures to be described in detail elsewhere (6). Fraction 3 was the predominant one, and comprised approximately 50-60% of the total vanadium porphyrins present. Demetallation of the porphyrin fractions was carried out with methanesulfonic acid (Merck) using published procedures (7).

UV-visible spectra were obtained using a Cary 118C spectrophotometer. Insertion-probe mass spectra were obtained with a Dupont 21-491B mass spectrometer, the FAB spectra with a VG MM-ZAB instrument, and the FD spectra with a JEOL DX-300 mass spectrometer. High pressure liquid chromatography measurements were made with a Waters instrument fitted with dual channel (405 and 546 nm) optical detection and C18 columns.

RESULTS AND DISCUSSION

Table I summarizes the concentrations of trace elements extracted with chloroform from two oil shale samples of the drill cores. Although vanadium is clearly the major element present in the form of metal-organic complexes, significant concentrations of compounds containing nickel, iron, copper and chromium are similarly extracted. As will be shown below, the nickel and vanadium appear to be present largely as porphyrin complexes, but it has not been possible to demonstrate that elements such as iron and copper are also present as porphyrins or as some other form of metal-organic complex.

TABLE I
METAL-ORGANIC COMPLEXES EXTRACTABLE WITH CHLOROFORM FROM
JULIA CREEK SHALE

Element	Concentration Extracted $\mu\text{g g}^{-1}$	
	Sample 1	Sample 2
	Oil Shale, Deep Core 90-92 m	Oil Shale, Shallow Core 31-33 m
Vanadium	104.0	27.0
Nickel	6.0	4.0
Iron	3.0	7.0
Copper	0.26	0.74
Chromium	1.0	0.13
Molybdenum	0.26	0.43
Manganese	0.09	0.09
Magnesium	0.30	0.06
Zinc	0.39	0.20

Variations in the total (i.e. organic and inorganic) concentrations of vanadium, nickel, iron and copper and of the chloroform extractable forms of these elements through the two drill cores are summarized in Figure 2. These results demonstrate the preferential concentration of the chloroform extractable forms of these elements in coquinite and particularly the oil shale segments of the two cores, and the virtually complete absence of these compounds in the mudstone underlying and overlying the deposit. It is also apparent that there are significant differences in the concentrations of the organic forms of these elements within the coquinite and oil shale layers. Indeed, the variations in the soluble organic vanadium concentrations within the individual drill cores are comparable to the variations found in samples from widely different locations of the Toolebuc formation (5). It is also interesting to note that the variation with depth in the cores of the concentrations of the chloroform-soluble forms of vanadium, nickel, iron and copper are significantly different from each other. This observation may indicate that the various metal ions are complexed by different types of organic ligands, and, as indicated below, some evidence was obtained that the porphyrins complexed to the nickel ion are different from those complexed to the vanadyl ion.

Although there are obvious differences in the concentrations of the organic vanadium complexes found in the shallow and deep drill cores, the nature of the vanadium complexes present appears to be virtually identical, as shown (Figure 3) by the HPLC of the vanadium porphyrin fractions from core samples taken at depths of 90-92 m and 29-31 m. It would clearly be desirable to extend such studies to samples taken from much greater depths in the Toolebuc formation.

As indicated in Figure 1, it was possible to separate the vanadium porphyrins extracted from the oil shale (90-92 m) into several distinct fractions using column chromatography. XRF analysis of these fractions showed that all were vanadium complexes and none were found to contain any measureable concentrations of iron, nickel or copper. Comparison of the uv-visible absorption spectra of these fractions (Figure 4) with the spectra of known vanadium chlorin, phylloerythrin and DPEP complexes (8), suggest that fractions 422 and 4422 with absorption maxima at 600 nm were probably vanadium phylloerythrin complexes. These two fractions do not appear to be identical to the rhodo-type petroporphyrins with an absorption maximum at 590 nm isolated by Millson et al. (9) and discussed in detail by Bakér et al. (10) because of the significant difference in the absorption spectra. Also, as will be shown below, the mass spectra of fractions 422 and 4422 are more complex than would be expected for the rhodo-type porphyrin. Sample 630 may be vanadium chlorin derivative, while the spectra of fractions 3, 61, 41 and 441 were typical of vanadium porphyrins with maxima at 412, 538 and 575 nm. However, the ratios of the intensities of the 575 and 538 nm absorption bands, which are in the range 1.15-1.20 for these samples, appear to be more consistent with deoxyphylloerythrin derivatives rather than the DPEP derivatives. No fraction having a spectrum similar to that shown by Hodgson and Baker (8) for the vanadyl-DPEP complex could be isolated from the present samples.

Insertion-probe mass spectra were obtained for these fractions using both EI and CI ionization, typical results being shown in Figure 5. The spectra obtained using these two ionization modes were similar except that the peaks in the CI spectra were located, as expected, one mass unit higher than the corresponding EI peaks. The sequence of peaks at $m/e = 513, 527, 541$ and 555 observed for sample 3 are typical of vanadyl-DPEP homologues. The insertion-probe spectra of samples 422 and 4422 were, surprisingly, virtually identical to those of fraction 3, even though the former two compounds were clearly not vanadyl DPEP derivatives. The mass spectra of samples 61, 441 and 421, which all have typical vanadyl porphyrin visible spectra, showed prominent even mass number peaks at $m/e = 526, 540$ and 554 . Similar observations have been made by Blumer

and Rudrum (11) and are attributed to the effects of the pyrolysis of the sample in probe.

It was also possible to obtain FAB mass spectra of several of the porphyrin fractions. The most notable difference in the insertion probe and FAB spectra were obtained for sample 441 (Figure 6) for which the FAB spectra showed not only a completely different distribution of peaks in the mass range 500-600 amu, but also yielded a second set of prominent peaks in the range 1022-1078 amu. Particularly prominent in this spectrum was the series 495, 509, 523, 537, 551 and 565 i. e. $(541-4) + 14n$; which presumably indicates the presence of unsaturated substituent groups on the porphyrin ring. The high molecular weight peaks appear in a mass range corresponding to 35-40 carbon atoms additional to those of the basic DPEP structure. These compounds are thus superficially similar to the high molecular weight vanadium porphyrins isolated by Blumer et al. (11).

The FAB spectra of the two phylloerythrin fractions (sample 422 and 4422) also showed significant differences from the insertion probe spectra (Figure 6). FAB spectra of samples 4422, 422 and 61 also showed peaks in the range 1000-1200 amu, but these were not as clear as those observed for sample 422, and further work would be required to confirm their presence. The low molecular weight spectra were again dominated by peaks corresponding to $(541-2) + 14n$ and $(541-4) + 14$ indicative of some degree of unsaturation in the substituent groups. These two sequences appear to be similar to those of an as yet unidentified series reported by Thomas and Blumer (3).

The HPLC (C18 Bondapak semipreparative column, methanol 0.5 cc/min) of sample 3 showed seven major and well-separated peaks, of which peaks 4, 5 and 7 were predominant. Fractions containing these peaks were collected as they eluted from the column and examined by FD mass spectrometry. All fractions had UV-visible spectra typical of vanadium porphyrin complexes. As shown in Figure 7, relatively simple mass spectra were obtained. Peak 1 appears to consist of two etio homologues at $m/e = 515$ and 501 , while peaks 2, 3 and 4 are consistent with compounds of the DPEP series. Peaks 5 and 7 show identical mass spectra consistent with a DPEP-2 series but are surprisingly separated by peak 6 which appears to be a mixture of the DPEP (527, 541, 555, 569, 583 and 599) series and DPEP-2 (553, 567) series. To a first approximation, these compounds would be expected to be eluted in order of decreasing polarity of this reverse phase column, and it is difficult to interpret these results without postulating that several compounds having molecular weights corresponding to the DPEP series but of significantly different chemical constitution are present in the samples.

Attempts to demetallate the various porphyrin fractions appeared to be completely successful only in the case of the nickel porphyrins and for sample 3, while demetallation of samples 630, 442 and 4422 yielded no porphyrin type compounds at all. HPLC runs on the demetallated nickel porphyrins and the vanadium porphyrins from fraction 3 showed these to be significantly different. Similar observations have been made previously (12) and may explain why the nickel and vanadium porphyrins appear to have different distributions in the drill cores. However, because of the possibility of decomposition of the porphyrins during demetallation, these observations are far from conclusive.

In conclusion, it should be noted that this investigation described only preliminary attempts to identify some of the porphyrinic compounds present in what appears to be an exceedingly complex mixture in the oil shale of the Toolebuc formation. The possible presence of significant concentrations of chlorin and phylloerythrin type compounds in this shale suggests that the deposit has undergone very little maturation, and a more complete identification of the compounds present should assist in developing a clearer understanding of the origin and of the reactions of petroporphyrins in a geological environment.

ACKNOWLEDGMENTS

The authors would like to thank Dr. A. Ramsden, Division of Mineralogy, CSIRO for samples of the drill cores provided by CSR Ltd and Dr. J. Ellis of Wollongong University for the insertion-probe mass spectra. We would also like to thank VG Analytical Ltd (Mr. C. Hameister) for obtaining the FAB spectra and JEOL (Australasia) Pty Ltd (Mr. J. Wakayama) for the determination of the FD spectra.

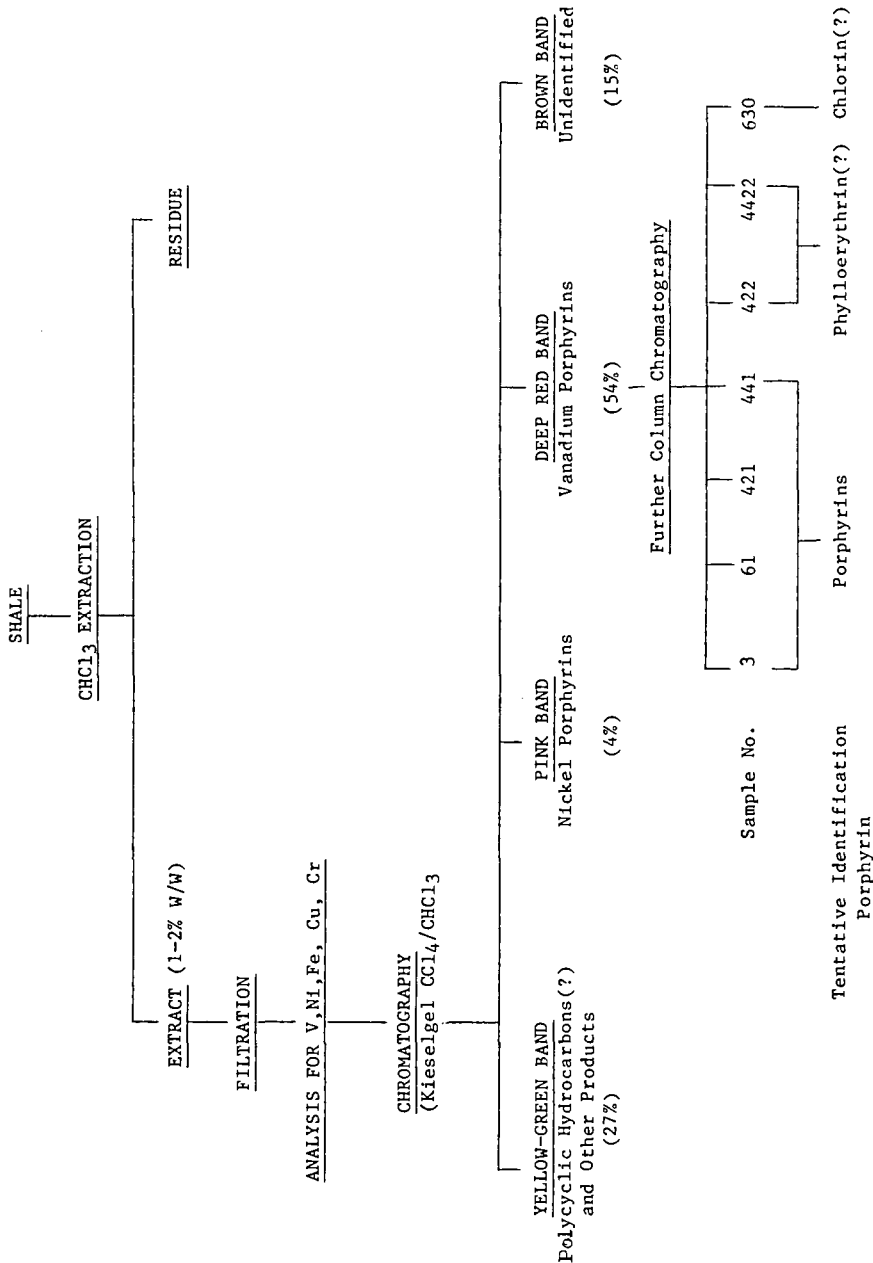


Figure 1. Schematic outline of the separation procedures used in this work.

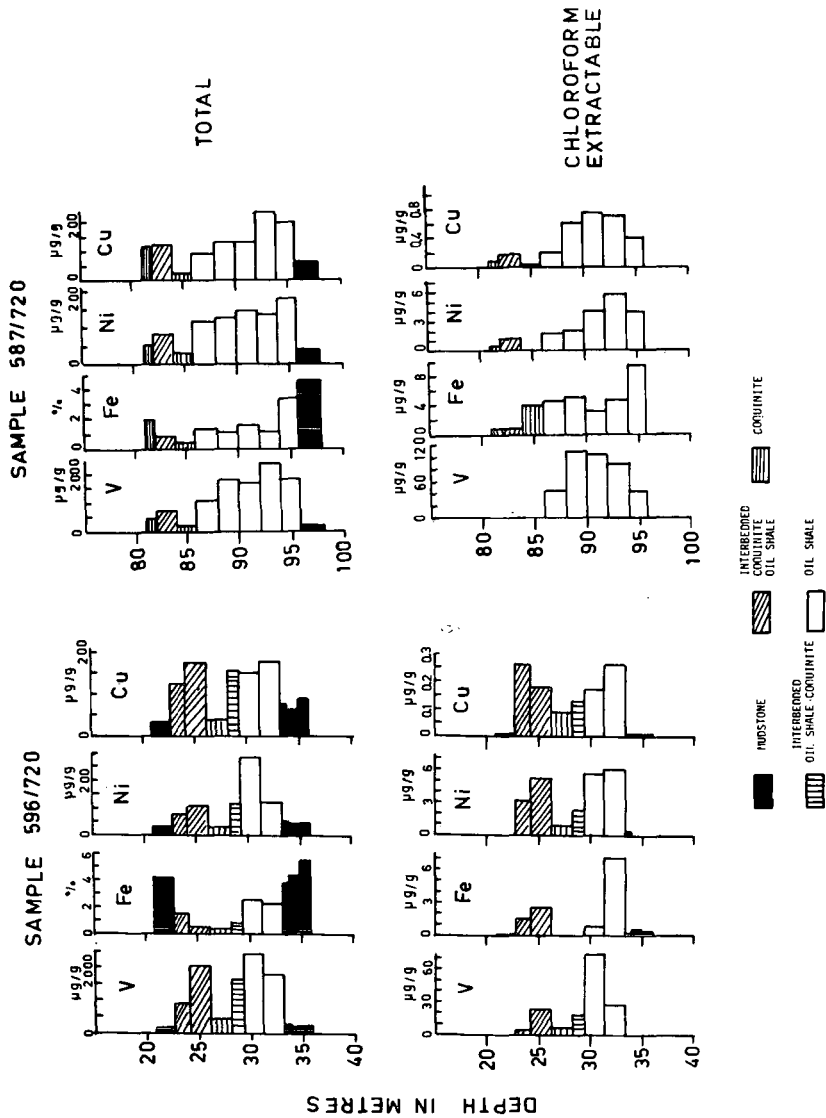


Figure 2. Distribution of the total (upper diagram) and chloroform extractable (lower diagram) concentrations of vanadium, iron, nickel and copper in two drill cores from the Julia Creek deposit.

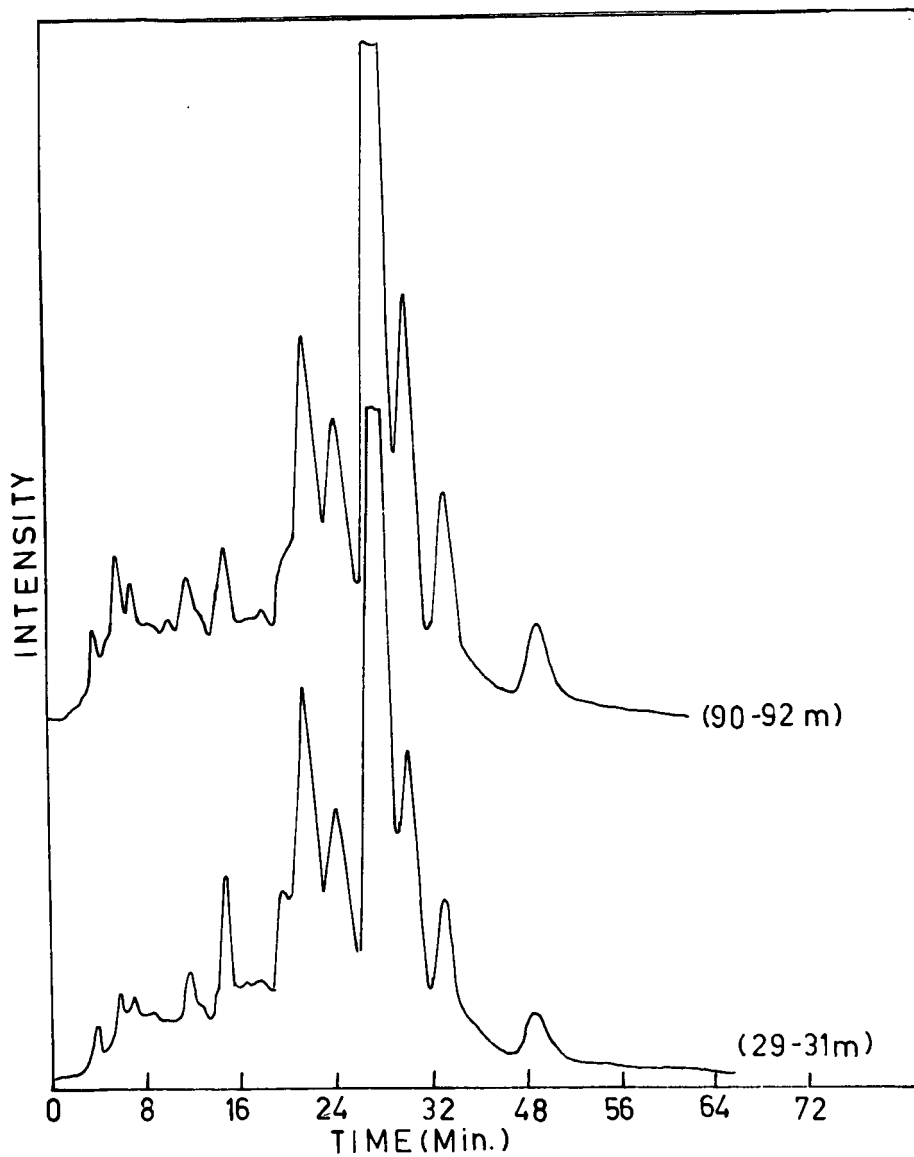


Figure 3. HPLC of the chloroform extracts from samples of oil shale at depths of 90-92 m and 29-31 m. C₁₈ column, methanol 2 cc/min.

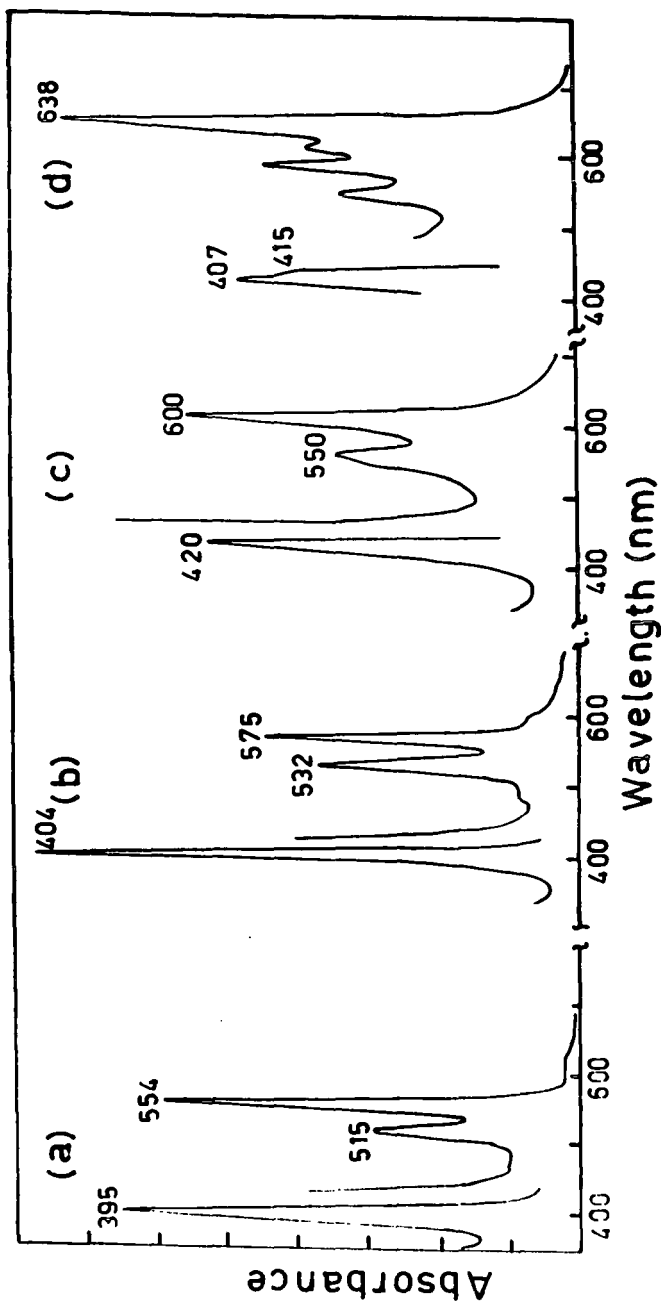


Figure 4. Typical absorption spectra of the various porphyrin fractions determined in chloroform solution. (a):- spectrum of nickel porphyrin fraction, (b) spectrum typical of fractions 3, 61, 421 and 441 and identified as vanadyl porphyrins, (c) spectrum typical of fractions 422 and 4422, tentatively identified as vanadyl phylloerythrin derivatives and (d) spectrum of fraction 630; possibly a vanadyl-chlorin complex. This sample contained some vanadyl porphyrin impurities as shown by the absorption peaks at 407, 575 and 533 nm.

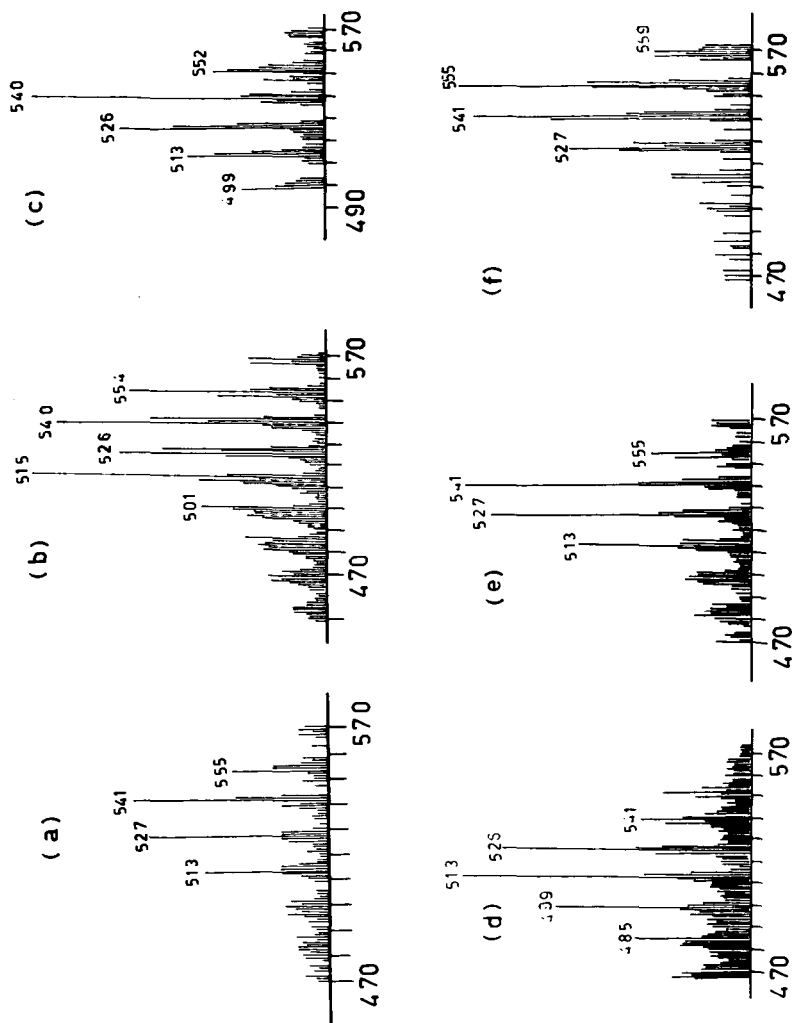


Figure 5. Insertion-probe mass spectra (EI) of various porphyrin fractions. (a) Sample 3, (b) Sample 61, (c) Sample 441, (d) Sample 421, (e) Sample 422, (f) Sample 442.

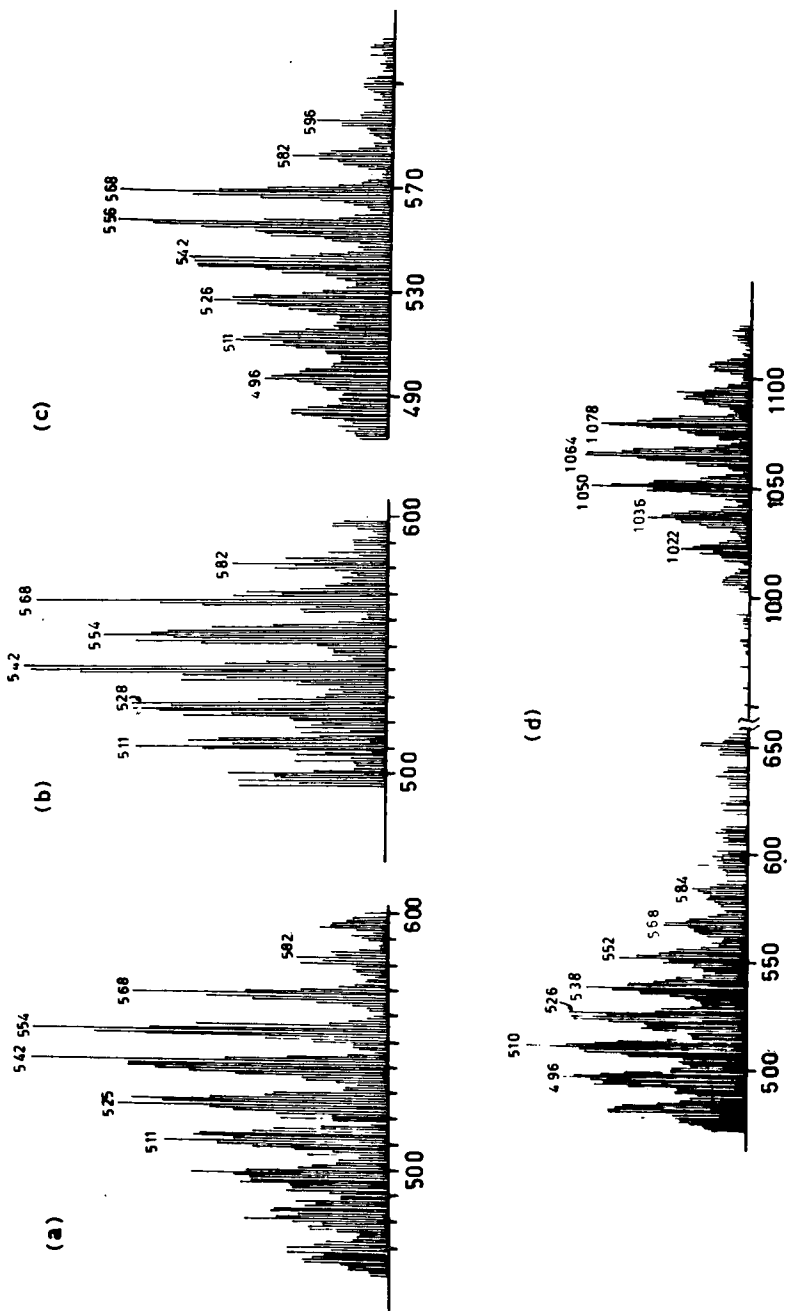


Figure 6. FAB spectra (EI) of various porphyrin fractions. (a) Sample 61, (b) Sample 4422, (c) Sample 422, and (d) Sample 441. The parent peaks would appear as $[M + H]^+$ ions.

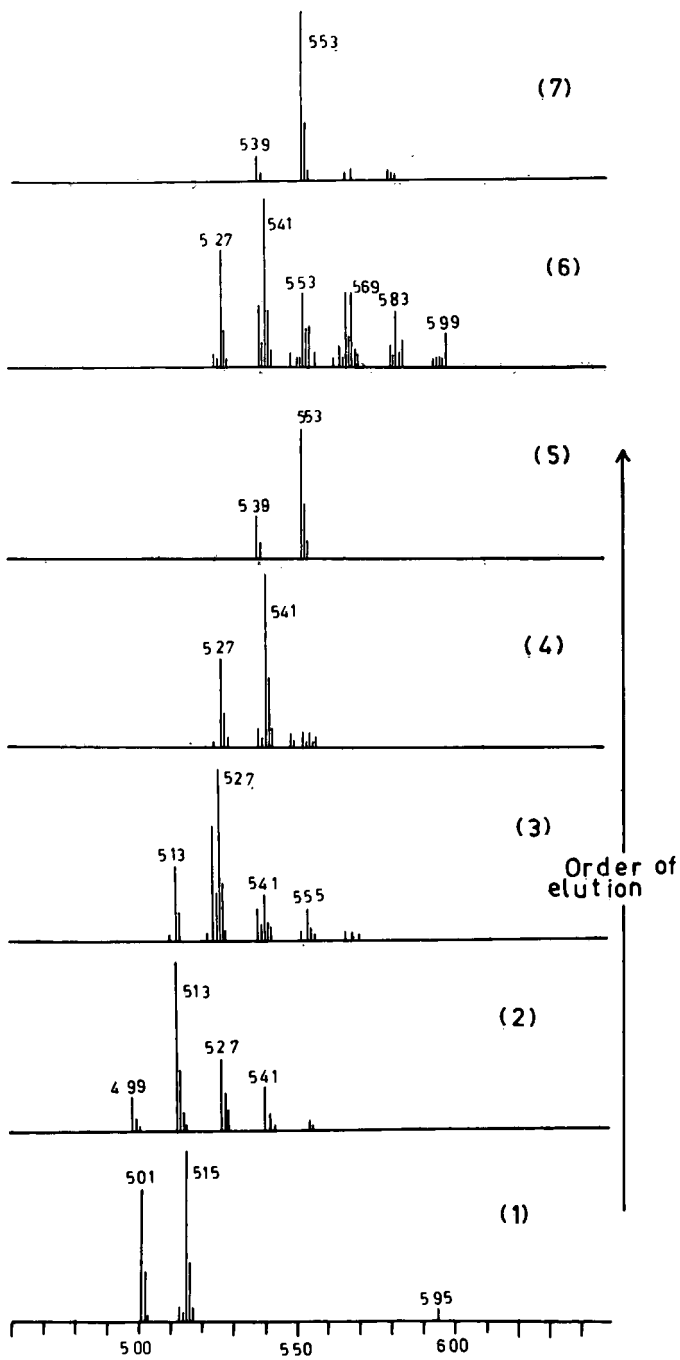


Figure 7. FD mass spectra of the seven major fractions found by HPLC in Sample 3.

LITERATURE CITED

- (1) Treibs, A., *Angew. Chem.*, 49, 682 (1936).
- (2) Baker, E. W., and Palmer, S. E., "Geochemistry of Porphyrins" in "The Porphyrins", D. Delphin (Ed.), Academic Press, New York, N. Y., Vol. 1, pp.485.
- (3) Thomas, D. W., and Blumer, M., *Geochim. Cosmochim. Acta*, 28, 1147 (1963).
- (4) Hodgson, G. W., and Whiteley, C. G., "The Universe of Porphyrins" in Proceedings of the Fourth International Symposium in Environmental Biochemistry. Springer Verlag, p. 35 (1980).
- (5) Saxby, J. D., and Riley, K. W., *Chemical Geol.* (In press).
- (6) Ekstrom, A., and Loeh, H. (to be published).
- (7) Martin, J., Quirke, E., Shaw, G. J., Soper, P. D., and Maxwell, J. R., *Tetrahedron*, 36, 3261 (1980).
- (8) Hodgson, G. W., and Baker, B. I., *Chemical Geol.*, 2, 187 (1967).
- (9) Millson, M. F., Montgomery, D. S., and Brown, S. R., *Geochim. Cosmochim. Acta*, 30, 207 (1966).
- (10) Baker, E. W., Yen, T. F., Dickie, J. P., Rhodes, R. E., and Clark, L. F., *J. Am. Chem. Soc.*, 89, 3631 (1967).
- (11) Blumer, M., and Rudrum, U., *Inst. of Petroleum J.*, 56, 99 (1970).
- (12) Haj Ibrahim, S. K., Presented at 183rd ACS National Meeting, Las Vegas, Nevada March 18-April 2, 1982. Division of Geochemistry Abstracts, paper 51.

SYMPOSIUM ON GEOCHEMISTRY AND CHEMISTRY OF OIL SHALE
 PRESENTED BEFORE THE DIVISIONS OF FUEL CHEMISTRY, GEOCHEMISTRY,
 AND PETROLEUM CHEMISTRY, INC.
 AMERICAN CHEMICAL SOCIETY
 SEATTLE MEETING, MARCH 20 - MARCH 25, 1983

ORGANOMETALLIC GEOCHEMISTRY. ISOLATION AND IDENTIFICATION OF
 ORGANOARSENIC AND INORGANIC ARSENIC COMPOUNDS FROM
 GREEN RIVER FORMATION OIL SHALE

By

R. H. Fish

Lawrence Berkeley Laboratory, University of California, Berkeley, California 94720
 and

F. E. Brinckman

Chemical and Biodegradation Processes Group
 Center for Materials Science, National Bureau of Standards, Washington, D. C. 20234

INTRODUCTION

Transformations and bioaccumulation of trace metals and metalloids, especially arsenic, are well known to occur in modern microorganisms, including the bacteria (1,2) molds (3), and marine plankton or algae (4,5). Such microflora demonstrate capacities for uptake of both inorganic forms of elements, and in some instances, are shown to involve biomethylation of inorganic substrates which result in cellular incorporation of organometal(loid)s, e.g., methylarsonic acid or dimethylarsonic acid (5). Arsenic is known to bioaccumulate in higher marine organisms to a substantial degree (6,7) where it resides in some shellfish tissues as arsenobetaine (8).

Similar considerations for ancient metal(loid) uptake or transformations appear quite reasonable for primordial microflora, especially the algae which account for the present ubiquitous distribution of kerogen in shale rocks (9,10). In general, the fossil deposition record suggests that substantial metal(loid) accumulation also occurred in higher plants which underwent diagenesis to form modern petroleum and coal deposits (11,12). In many instances, various present-day species of plants are known to both selectively and extensively hyperaccumulate various metal(loid)s to such a degree that geochemical prospecting is feasible by correlating metal concentration profiles with local flora (13). It is not unexpected, therefore, to discern characteristic concentration patterns for trace elements in various fossil deposits - whether we regard these as essential or toxic to life - and to expect gross differences in the profiles between the three main types: coal, kerogen, and petroleum, as summarized in Table I (14-18). Similarly expected, though far more subtle, we might anticipate that element distributions for these three main fossil sources also depend upon specific sites, and reflect their terrestrial or marine origins, subsequent geochemical history, and maturation (19-21).

TABLE I
 COMPARISON OF SELECTED ELEMENTAL CONCENTRATIONS* IN
 PETROLEUM, COAL, AND OIL SHALE

<u>Element</u>	<u>Petroleum</u>	<u>Petroleum</u>	<u>Coal</u>	<u>Oil Shale</u>
As	0.111	0.263	15	44.3
Be	--	--	2.0	--
Cd	--	--	1.3	0.64
Cr	0.093	0.008	15	34.2
Fe	10.8	40.7	1.6%	2.07%
Ge	--	--	0.71	--
Hg	0.051	3.236	0.18	0.089
Ni	9.38	165.8	15	27.5
S	0.83%	1.31%	2.0%	0.573%
Se	0.052	0.530	4.1	2.03
Si	--	--	2.6%	15%
U	--	0.060	1.6	4.5
V	13.6	87.7	20	94.2

*Concentrations in ppm except as noted.

The molecular forms of trace metal(loid)s in fossil deposits is doubtless complex, probably consisting of varying proportions of inorganic, metallo-organic (no covalent element-carbon bonds), and true organometallic chemical species residing in unspecified sites within the carbonaceous matrix. Over the years a very substantial solvent differentiation methodology has emerged (22-24), which greatly aids the analyst in assessing the broad matrix categories of fossil materials, and produces reproducible information concerning possible ligation, elements present, and approximate molecular size (weight) of the soluble components.

The determination of the molecular forms of trace metal(loid)s in fossil materials ideally requires a technique with extreme selectivity, lack of interferences, sensitivity to the sub-ppm level, and the ability to deal with heterogeneous samples. The state-of-the-art analytical methods which are capable of meeting these criteria to varying degrees, without extensive sample preparation, are quite limited and have only recently been applied to limited types of fossil samples.

The coupling of chemical separations, which provide selectivity and reduce interferences, with instrumental techniques, which are capable of providing further selectivity and the necessary sensitivity, has been an active area of analytical research, being performed in both off-line and on-line modes. The recent emergence of a number of on-line "hyphenated" techniques (24), GC-MS, MS-MS, LC-ESD (including variable- and scanning UV, IR, NMR, GFAA, FAA and electrochemical detectors) appears to be the most effective and versatile method to quantitate organic, inorganic, organometallic and metallo-organic compounds in complex matrices. Among these, automated coupling of high performance liquid chromatography (HPLC) in normal, reverse phase, ion exchange, or size exclusion modes with element-selective detectors appears most promising for the characterization of metal(loid) containing molecules in complex matrices (25).

RESULTS AND DISCUSSION

Reports of on-line, element-selective detection of chromatographic effluents of fossil materials have appeared more recently and offer the advantages of increased resolution and easier chromatographic optimization because of the real time acquisition of elemental distributions during the chromatographic run. Recently, Brinckman et al. (26), have coupled a graphite furnace atomic absorption (GFAA) spectrometer to a high performance liquid chromatograph, which has been applied by Fish et al. (27), and Weiss et al. (28) to the analysis of arsenic compounds in process waters and oils generated during oil shale retorting.

In order to answer questions on the biogeochemical origin of the methyl and phenylarsonic acids, and arsenate, found in oil shale retorting products (27,28), we extracted a Green River Formation oil shale sample (NBS standard reference material) with refluxing methanol. By using HPLC-GFAA analysis of the extract, and catecholorganoarsonic acid (29) and trimethylsilylation-arsenate derivatization reactions, we have identified, in an unequivocal fashion, methyl- and phenylarsonic acids and arsenate, by the former technique and by capillary column gas chromatography - mass spectrometry analysis with the latter derivatization technique.

Figure 1 gives the arsenic-specific chromatogram of the compounds we identified as methylarsonic acid, phenylarsonic acid, and arsenate, based on retention times of the authentic arsenic compounds. An unknown neutral organoarsenic compound eluted with the solvent front.

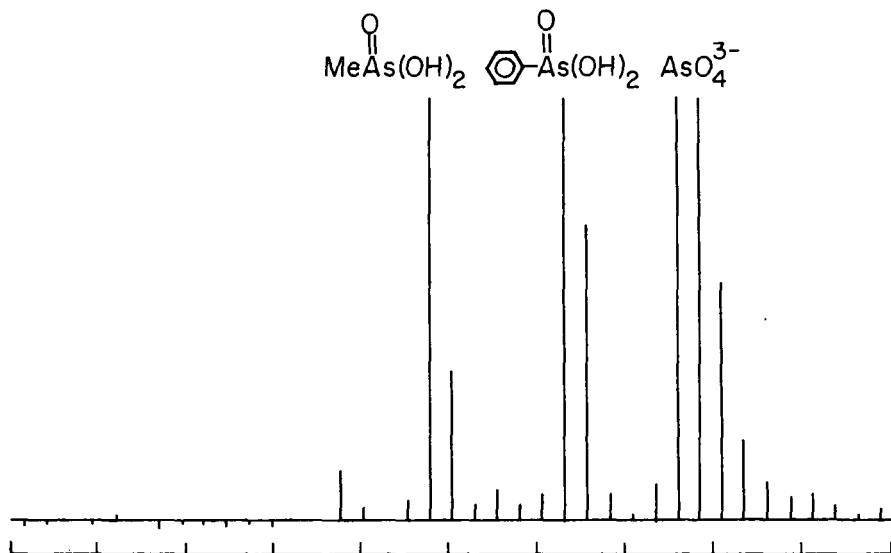
The methanol extract was purified by preparative HPLC (the area from 22 to 35 min. was collected, see Figure 1), lyophilized and dissolved in benzene. To this solution was added excess 3-methylcatechol and the reaction mixture was refluxed for 5 h and worked up to remove the excess 3-methylcatechol. A concentrated sample was subjected to GC-EIMS analysis to provide spectra and scan numbers (retention times) that were identical to the known samples of the 3-methylcatecholates of both methyl- and phenylarsonic acids (29). Additionally, the inorganic anion, arsenate (AsO_4^{3-}), was verified in a similar fashion (preparative HPLC of the region from 35.5-41 min) by preparation of the tris(trimethylsilyl-) derivative of the ammonium salt of arsenate and analyzing the purified extract by GC-EIMS. The organoarsenic compound (Figure 1) that elutes with the solvent front has not been as yet identified and further work is in progress to verify its structure.

We believe these identifications of the organoarsenic acids to be the first such molecular characterizations of trace organometallic compounds to be reported for any fossil fuel precursors and initiates the area of organometallic geochemistry, a field that has hithertofore been totally unexplored (30).

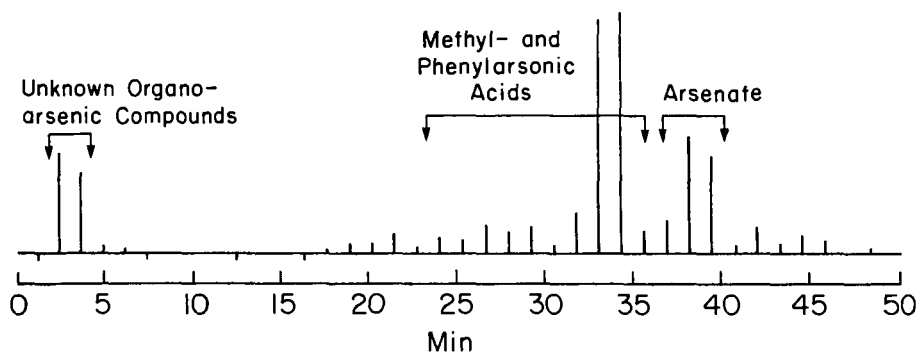
EXPERIMENTAL

The HPLC-GFAA instrumentation and analyses conditions have been described previously (see Literature Cited 25-27). The AA detection of arsenic was at 193.7 nm. The HPLC column was a Dionex anion exchange column with 0.2M $(\text{NH}_4)_2\text{CO}_3$ in aqueous methanol as the eluting solvent. The GC-MS analyses were accomplished using a Finnigan 4023 mass spectrometer system with a 30 m x 0.3 mm DB-5 (J and W) capillary column, conditions: 55° (3 min.) - 300°/min.

Standard



Methanol Extract of Green River Formation Oil Shale



XBL 8210-3116

Figure 1. The HPLC-GFAA analysis of Green River Formation oil shale extracted with refluxing methanol.

Reconstructed ion chromatograms and single ion chromatogram data was done with the INCOS Data System.

ACKNOWLEDGMENTS

The work at LBL was supported by the Offices of Fossil Energy and Oil, Gas and Shale Technology, and the Bartlesville Energy Technology Center (Project Manager, Dexter Sutterfield) of the U.S. Department of Energy under Contract No. DE-AC03-76SF00098. A portion of the NBS study was supported by the NBS Office of Standard Reference Materials. We wish to thank R. S. Tannous and W. Walker of LBL and C. S. Weiss of NBS for assistance in performing these experiments.

LITERATURE CITED

- (1) McBride, R. C., and Wolfe, R. S., *Biochem.*, 10, 4312 (1971).
- (2) Cheng, C. N., and Focht, D. D., *Appl. Environ. Microbiol.*, 38, 494 (1979).
- (3) Cullen, W. R., McBride, B. C., and Pickett, A. N., *Can. J. Microbiol.*, 25, 1201 (1979).
- (4) Bottino, N. R., Cos, E. R., Irgolic, K. J., Maeda, S., McShane, W. J., Stockton, R. A., Zingaro, R. A., "Organometals and Organometaloids Occurrence and Fate in the Environment", Brinckman, F. E., and Bellama, J. M., Eds., pp. 116-129 (ACS Symp. Ser. 82, Washington, D. C., 1978).
- (5) Andrae, M. O., and Klumpp, D., *Environ. Sci. Technol.*, 13, 738 (1979).
- (6) Maher, W. A., *Anal. Chem. Acta.*, 126, 157 (1981).
- (7) Benson, A. A., and Summons, R. E., *Science*, 211, 482 (1981).
- (8) Edmonds, T. S., and Francesconi, K. A., *Chemosphere*, 10, 1041 (1981).
- (9) Cane, R. F., in "Oil Shale", Yen, T. F., Ed., Elsevier, Amsterdam (1976), pp. 27-60.
- (10) Abelson, P. H., "Researches in Geochemistry", Vol. II, Abelson, P. H., Ed., Wiley, New York (1967), pp. 63-86.
- (11) Manskaya, S. M., and Diodzova, T. V., "Geochemistry of Organic Substrates", Pergamon Press, Oxford (1968).
- (12) Yen, T. F., "The Role of Trace Metals in Petroleum", Yen, T. F., Ed., Ann Arbor Sci., Michigan (1975), pp. 1-30.
- (13) Erdman, J. A., and Harrach, G. H., *J. Geo. Chem. Explor.*, 14, 83 (1981).
- (14) Hitchon, B., Filby, R. H., Shah, K. R., "The Role of Trace Metals in Petroleum", Yen, T. F., Ed., (Ann Arbor Sci. Publ., Inc., Ann Arbor, 1975).
- (15) Shah, K. R., Filby, R. H., Haller, W. A., *J. Radioanal. Chem.*, 6, 185 (1970).
- (16) Shah, K. R., Filby, R. H., Haller, W. A., *ibid.*, 6, 413 (1970).
- (17) U. S. National Committee for Geochemistry, "Trace-Element Geochemistry of Coal Resource Development Related to Environmental Quality and Health", Nat'l Acad. Press, Washington, D. C., 1980.
- (18) Fruchter, J. S., Wilkerson, C. L., Evans, J. C., Sanders, R. W., *Environ. Sci. and Tech.*, 14, 1374 (1980).
- (19) Van Krevelen, D. W., and Schuyer, J., Elsevier, Amsterdam, 1957, pp. 96-103 and pp. 211-220.
- (20) Yen, T. F., and Chilingarian, G. V., Eds., "Oil Shale", Elsevier Scientific Publ. Co., New York, 1976.
- (21) Yen, T. F., Nat'l Bureau of Standards Special Publ. NBS-DOE SP 618, p. 9, 1981.
- (22) Saxby, J. D., in "Oil Shale", Yen, T. F., and Chilingarian, G. V., Eds., Elsevier Scientific Publ. Co., New York, 1976.
- (23) Mima, M. J., Schultz, H., and McKinstry, W. E., "Analytical Methods for Coal and Coal Products, Vol. 1, Karr, Jr., Clarence, Ed., Acad. Press, New York, 1978, Chapter 19.
- (24) Filby, R. H., "The Role of Trace Metals in Petroleum", Yen, T. F., Ed., Ann Arbor Science, Michigan (1975), pp. 31-58.
- (25) Jewett, K. L., and Brinckman, F. E., "Detectors in Liquid Chromatography", Vickery, T. M., Ed., Marcell Dekker, New York, in press.
- (26) Brinckman, F. E., Blair, W. R., Jewett, K. L., Iverson, W. P., *J. Chrom. Sci.*, 15, 493 (1977).
- (27) Fish, R. H., Brinckman, F. E., and Jewett, K. L., *Environ. Sci. Technol.*, 16, 174 (1982).
- (28) Weiss, C. S., Brinckman, F. E., and Fish, R. H., Nat'l Bur. of Std. Special Publ., 618, 197 (1981).
- (29) Fish, R. H., and Tannous, R. S., *Organometallics*, 1, 1238 (1982).
- (30) A preliminary account of this study has been submitted for publication. Fish, R. H., Tannous, R. S., Walker, W. S., Weiss, C. S., and Brinckman, F. E. (1982), submitted to *Organometallics*. For a review of this area of speciation of arsenic compounds in fossil precursors and products see: Brinckman, F. E., Weiss, C. S., and Fish, R. H., Chapter in *Chemical and Geochemical Aspects of Fossil Energy Extraction*, Yen, T. F., Ed., Ann Arbor Sci. (1982). In press.

SYMPOSIUM ON GEOCHEMISTRY AND CHEMISTRY OF OIL SHALE
PRESENTED BEFORE THE DIVISIONS OF FUEL CHEMISTRY, GEOCHEMISTRY
AND PETROLEUM CHEMISTRY, INC.
AMERICAN CHEMICAL SOCIETY
SEATTLE MEETING, MARCH 20-25, 1983

BIOMARKERS IN OIL SHALE: OCCURRENCE AND APPLICATIONS

By

Mary F. Singleton, Alan K. Burnham, Jeffery H. Richardson and Jack E. Clarkson
Lawrence Livermore National Laboratory, P. O. Box 808, L-207, Livermore, California 94550

INTRODUCTION

Biological markers, compounds derived essentially unchanged from living organisms, have been used by petroleum geologists to relate oils to their original source rock material (1, 2). This technique is based on the ubiquitous nature of biomarkers in ancient sediments and on the characteristic way in which ratios of biomarkers vary from location to location.

We are extending this technique to the oil shale industry by determining biomarker ratios in oils produced from Green River formation shales and by studying the manner in which these ratios vary with depth and other characteristics of the shale within a given core.

Past work on the biomarkers in oil shale has involved characterization of the biomarkers in bitumen, the soluble organic portion of oil shale and determination of the manner in which their quantity varied with depth in relation to other hydrocarbon types (3, 4). Biomarker derivatives from kerogen, the insoluble organic portion of oil shale, have been determined by a variety of methods (5) and compared to their bitumen analogs (6, 7, 8). Since not all the biomarker compounds from a given shale sample occur in the same proportions in both the bitumen and the oil and since heat treatment is involved in commercial oil production, we have evaluated biomarker occurrence in the whole oil product prepared at a heating schedule comparable to the standard assay procedure (12°C/min, maximum 500°C). We previously established that the biomarkers from kerogen occur in the oil as both unsaturated and saturated compounds (ene and ane) and although the ratios of ene/ane vary with heating rate, the sums of ene plus ane ratios are fairly constant (9). This is important in validating the use of biomarker ratios in oils produced at widely varying heating rates (geological, in-situ retorting, assay, very rapid pyrolysis).

In this work, we have prepared oils from cores in varying locations in the Green River formation in order to compare biomarker ratio characteristics that correlate across the resource, as well as the factors that distinguish one location from another. Beside being of diagnostic value for oil shale retorts, this information provides possible insights into the geochemistry of oil shale and the structure of kerogen and bitumen.

EXPERIMENTAL

Samples

Oil shale core samples were available from two widely separated (East, West) locations in the Green River formation. The first core we studied was from the Geokinetics site near Vernal, Utah. In this area, the Mahogany zone is close to the surface and less than 50 feet thick. Oils were prepared from 1-foot composite samples spanning 45 to 85 feet in depth. These samples had been previously prepared at our laboratory (-20 mesh) and elemental analyses for total carbon, mineral carbon, hydrogen, nitrogen and sulfur were complete. Grade was calculated using a correlation established at our laboratory (10) between organic carbon content and grade that has a standard error of 0.56 gal/ton. These samples varied in grade from 4.05 to 52.30 gal/ton. Geokinetics' designation for this core is "Exp. 22" and they locate the Mahogany Marker at 47.6 feet and the Mahogany Bed at 53.2 feet (11).

The second core we have completed analyzing is Naval Oil Shale Reserve (NOSR) Core 25 from the Anvil Points area near Parachute Creek, Colorado. These shale samples were prepared for a comprehensive study by Giaque et al. (12) and were the consistency of fine talc. Their grade had been determined (at LETC) by the ASTM standard method and varied from 1.95 to 56.50 gal/ton. We prepared oils from 1- and 2-foot composites ranging in depth of burial from 623 to 702 feet. The Mahogany Marker is estimated from the grade variation to occur close to 664 feet. The A-groove, which occurs from approximately 630 to 640 feet, was included in this core, but not in the Geokinetics core. NOSR Core 15/16 from the same source is currently being analyzed and its data will be available shortly.

Procedure

Ten Oil Shale Samples (TOSS) were simultaneously pyrolyzed in a segmented reactor constructed of stainless steel (Figure 1). Approximately 12 g of shale was weighed into each 6-inch high individual sample vessel with stainless steel frit bottom. The vessels were placed into the 10 compartments of the reactor resting on a wire mesh so as to be positioned near the center of the furnace. The lid with 3 thermocouples and a gas inlet was bolted into place with a Viton O-ring seal (the top flange was positioned just outside the furnace). The charged reactor was placed in a 3-zone furnace and the samples were heated at about 10°C/min up to 500°C where the temperature was held for 30 minutes. An argon flow was maintained throughout the experiment to aid in removing vapors from the reactor and to minimize their residence time in the hot zone. Oils were collected in individual U-shaped glass tubes packed with glasswool and immersed in an ice bath. Noncondensable gases were vented through a common manifold and exit line containing a flowmeter.

Chromatography

In order to avoid problems with sample inhomogeneity, the entire oil sample from each sample of shale was dissolved in 1.5 to 2.5 mL of CS₂ (about 1 g oil to 1.5 mL solvent). One μ L of this solution was injected into a Hewlett-Packard Model 5880 Gas Chromatograph equipped with capillary inlet and a 50 m x 0.25 mm Quadrex "007" methyl silicone column. Injection on the column is made with a split ratio of approximately 1 to 100. The column temperature started at 60°C and increased at 4°C/min to 280°C where it remained for a total run time of 90 min. The carrier gas was helium at a pressure of 0.27 MPa flowing at a rate of 1 cm³/min. The injector temperature was 325°C and the flame ionization detector (FID) temperature was 350°C. Data reduction was done using a Hewlett-Packard Model 3354 Laboratory Automation System with a standard loop interface. Identification of various components was based on GC/MS interpretation described previously (9).

Data Analysis

A list of the ratios calculated from the chromatograms are given in Table I. By cores, these ratios for the individual oils were entered into a data file which also included depth of burial, grade and elemental nitrogen/organic carbon of the raw shale. Using computer codes available on an LLNL CDC-7600 (CRSCOR and CROSSPLOT2), we were able to calculate cross-correlation coefficients for all pairs of variables and to plot various data pairs.

RESULTS AND DISCUSSION

We have investigated the variations in two groups of biomarker compounds, chain isoprenoids and steranes, in gas chromatograms of oils produced from two Green River formation cores. The chain isoprenoids ranged from 14 to 20 carbons in size and included several alkene forms. The three steranes we tentatively identified are the tetracycloalkanes, α - and β -ergostane and a stigmastane isomer. We also measured the ratios of normal alkenes to alkanes and the odd/even carbon preference for comparison purposes.

For the Geokinetics core, we prepared 38 oils at 1-foot composites and for NOSR Core 25 we prepared 43 oils at 1- and 2-foot composites. Since the NOSR core included the A-groove immediately above the Mahogany zone, we have used only the 28 samples from the Mahogany zone (600 to 702 feet) in some comparisons, to look for any differences resulting from its inclusion. The C₁₇ odd/even ratio, elemental nitrogen/organic carbon ratio and several biomarker ratios were considerably higher in the A-groove than anywhere in the Mahogany zone.

There has been considerable speculation about the source material responsible for biomarker compounds in oil shale and about the effect of deposition and aging conditions on their distribution (13-17). We are here concerned with the variation in relative amounts of biomarkers with stratigraphy in oils from the Mahogany zone and with the possible application of this information to the commercial development of the resource. At the same time, we have looked at the relationship of biomarkers to other variations in the shale and to the geochemistry of the resource.

Biomarker compounds are present in varying proportions in both the bitumen and kerogen of oil shale, the non-bitumen forms being chemically bound or physically trapped by the kerogen and mineral matrix (9, 18). Burnham et al. (9) observed that the ene/ane ratios of several chain isoprenoid compounds in shale oil behaved like the n-alkanes, e.g., ratios of ene/ane varied over a wide range of heating rates, but sums of ene plus ane were approximately constant. Since pyrolysis of kerogen results in production of both the saturated (ane) and unsaturated (ene) forms of n-alkanes and chain isoprenoids, with ene/ane ratios increasing at varying rates for each compound with increasing heating rate, we have reported some of our ratios as the sums of the ene and ane forms. Phytane, which occurs mainly in bitumen, was an exception for which no unsaturated form was found. Therefore, the ene/ane ratios in shale oil are affected by the severity of the heat treatment and by the distribution of biomarkers between bitumen and kerogen in the raw shale. Based

on these observations we can extrapolate with confidence from high heating rates to very slow ones by using ratios of the ene plus ane forms of the alkanes and biomarkers. In our laboratory, we have found that this relationship applies over a wide range of conditions including very rapid pyrolysis in a fluidized bed and very slow pyrolysis at high pressures (19, 20).

TABLE I
RATIOS CALCULATED FROM THE GC PEAKS FOR EACH OIL SAMPLE

C_8 through C_{28} straight chain hydrocarbons: 1-alkene/alkane	
C_{11} through C_{29} straight chain hydrocarbons: odd/even ratios*	
Pristane/ C_{17} 's + C_{18} 's	(2,6,10,14-tetramethylpentadecane, C_{19})
Prist-1-ene/ C_{17} 's + C_{18} 's	
Prist-2-ene/ C_{17} 's + C_{18} 's	
Pristane + 1-ene + 2-ene/ C_{17} 's + C_{18} 's	
Phytane/ C_{18} 's + C_{19} 's	(2,6,10,14-tetramethylhexadecane, C_{20})
Phytane/Pristane	
Phytane/Pristane + 1-ene + 2-ene	
Phytane/Prist-2-ene	
Phytane/Prist-1-ene	
2,6,10-trimethyldodec-1-ene/ C_{13} 's + C_{14} 's	(1-ene of farnesane)
Farnesane/ C_{13} 's + C_{14} 's	(2,6,10-trimethyldodecane, C_{15})
2,6,10-trimethyldodec-1-ene/Farnesane	
2,6,10-trimethyldodec-1-ene + Farnesane/ C_{13} 's + C_{14} 's	
2-6,10-trimethylundec-2-ene/ C_{13} 's	
2,6,10-trimethyltridec-1-ene/ C_{13} 's + C_{14} 's	
2,6,10-trimethyltridecane/ C_{14} 's + C_{15} 's	
2,6,10-trimethyltridecane + 1-ene/ C_{14} 's + C_{15} 's	
β -ergostane/ C_{29} 's + C_{30} 's,	($C_{28}H_{50}$)
α -ergostane/ C_{29} 's + C_{30} 's	($C_{28}H_{50}$)
stigmastane/ C_{30} 's,	($C_{29}H_{52}$)

Note: C_{17} 's implies the sum of the 1-alkene + alkane of the normal C_{17} hydrocarbon, etc.

* Odd/even ratios were calculated with the formula:

$$\frac{2 \times (C_{\text{odd}} \text{ alkene} + \text{alkane})}{(C_{\text{odd}-1} \text{ alkene} + \text{alkane}) + (C_{\text{odd}+1} \text{ alkene} + \text{alkane})}$$

Although the two cores in this study were located across the formation from each other, we found there was very good agreement between the average values for odd/even preferences (Figure 2) and alkene/alkane ratios (Figure 3) vs carbon number. This demonstrates a consistency in the average values for these ratios in Mahogany zone oils. Another comparison between the two cores is presented in Table II based on biomarker ratios. We find that the average values agree very well for the two cores with the exception of the steranes which are appreciably higher in the NOSR core. This is true even when the A-groove data is excluded.

The ratios of pristane compounds (ane, 1-ene, 2-ene) to phytane are of interest since pristane/phytane ratios in bitumen and/or kerogen are often cited as indicators of terrestrial/laquestrine source material (1-3). Prist-1-ene from kerogens and sediments have been linked to a common precursor of pristane and phytane (21, 22). Anders and Robinson (3) report pristane/phytane ratios averaging 0.44 in Green River formation bitumens. However, these ratios are not indicative of the whole shale oil ratios because most of the phytane comes from the bitumen and most of the pristane compounds are produced from the kerogen. Connan and Cassou (16) discuss pristane/phytane ratios in a variety of crude oils and conclude that ratios lower than 1.5 are indicative of oils derived from "marine shale--carbonate sequences" while ratios greater than 3.0 indicate a significant amount of terrestrial source material. These crude oil ratios are probably more valid

for comparison to whole shale oil samples than are the bitumen ratios. Including the three pristane forms in the ratio of pristane+1-ene+2-ene/phytane gives us values indicative of small, but significant and highly variable terrestrial input at differing levels within each core. The pristane/phytane ratios varied from 0.52 to 1.33 (average 0.78) in the Geokinetics core and from 0.40 to 1.14 (average 0.58) in the NOSR core, while pristane+1-ene+2-ene/phytane ratios varied from 1.54 to 4.35 (average 2.78) and from 1.61 to 5.26 (average 2.63), respectively. It is interesting to note that although these two cores are located near the opposite boundaries of the resource, the ranges and averages for these ratios are nearly the same. However, the maxima and minima do not appear to correspond to the same strata.

TABLE II

COMPARISON OF BIOMARKER RATIOS IN TWO GREEN RIVER FORMATION CORES

Biomarker Ratio*	NOSR Core 25						
	Geokinetics Core			with			
	Min.	Max.	Avg.	Min.	Max.	A-groove Avg.	without A-groove Avg.
pristane	0.09	0.55	0.21	0.03	0.38	0.15	0.16
prist-1-ene	0.15	0.76	0.40	0.13	1.03	0.39	0.39
prist-2-ene	0.05	0.31	0.14	0.04	0.30	0.11	0.10
pristane + 1-ene + 2-ene	0.30	1.22	0.75	0.21	1.62	0.66	0.65
phytane	0.08	0.90	0.29	0.06	0.59	0.28	0.28
prist-1-ene/phytane	0.52	2.63	1.41	0.83	3.13	1.49	1.41
prist-2-ene/phytane	0.26	1.00	0.48	0.20	1.64	0.40	0.35
pristane + 1-ene + 2-ene/phytane	1.54	4.35	2.78	1.61	5.26	2.63	2.33
pristane/phytane	0.52	1.33	0.78	0.40	1.14	0.58	0.56
trimethyldodec-1-ene	0.01	0.19	0.10	0.04	0.25	0.11	0.11
farnesane	0.06	0.20	0.13	0.05	0.29	0.13	0.13
trimethyldodec-1-ene/farnesane	0.55	1.07	0.78	0.47	1.26	0.82	0.80
trimethyldodec-1-ene + farnesane	0.11	0.38	0.22	0.10	0.54	0.25	0.23
trimethylundec-2-ene	0.15	0.47	0.31	0.19	1.07	0.44	0.41
trimethyltridec-1-ene	0.06	0.22	0.14	0.06	0.45	0.20	0.18
trimethyltridecane	0.03	0.37	0.20	0.08	0.56	0.24	0.22
trimethyltridecane + 1-ene	0.16	0.59	0.35	0.14	1.00	0.44	0.41
β -ergostane	0.02	0.26	0.10	0.05	0.69	0.23	0.20
α -ergostane	0.02	0.39	0.12	0.01	1.54	0.27	0.20
?=stigmastane	0.19	1.68	0.65	0.25	5.91	1.56	1.35

* Values reported are for ratios of biomarkers to the respective alkene plus alkanes as expressed in Table I.

The overall prist-1-ene content of the oil is markedly higher than the pristane or prist-2-ene for both cores. It has been suggested that prist-1-ene is related to a kerogen precursor of the pristane and phytane in bitumen (14). Although the correlations are not particularly strong for prist-1-ene vs N/C_{org} (-.10, -.24) and prist-2-ene vs N/C_{org} (+.37, +.69) in the two cores, they are opposite in sign and, thus, may indicate a difference in source material or production mechanism. The unravelling of this relationship will require further work. It is noteworthy that both van de Meent and Larter found prist-1-ene to be present in pyrolysis products from a large variety of kerogens (15, 21).

Both grade and nitrogen/organic carbon atomic ratio in the raw shale vary characteristically with depth in the two cores (Figures 4 and 5) through the Mahogany zone. The A-groove in NOSR Core 25 has the maximum $N/Org.C$ ratio (.24) as well as the leanest shale material (1.65 gal/ton). This inverse relationship between grade and $N/Org.C$ has been noted previously (10). The occurrence of maximum $C_{17}odd/even$ ratio is very pronounced in this region of high $N/Org.C$, as are some of the biomarker compounds (Figure 6).

The depth profiles of three types of compounds studied are given in Figures 6 and 7 and indicate the variation observed in these ratios throughout the two cores. Their behavior is similar at some levels and not at others which would be expected given the complicating factors of natural phenomena at work over geologic time periods.

The cross-correlation coefficients for all pairs of biomarker ratios odd/even ratios, ene/ane ratios, shale grade, $N/Org.C$ and depth were calculated for each core separately. A selection from these data is presented in Table III for comparison of the behavior of biomarkers relative to

each other and to shale properties. This is a very abbreviated list of the cross-correlation data and represents the best correlations in some cases or those with special significance. There was no consistent correlation of biomarkers in both cores with grade or depth over the ranges investigated.

TABLE III
CORRELATION COEFFICIENTS FOR SELECTED VARIABLE PAIRS

Variable 1*	Variable 2*	Coefficient, r		
		Geokinetics core	NOSR with A-groove	Core 25 without A-groove
phytane	pristane	0.90	0.83	0.90
phytane	trimethylundec-2-ene	0.66	0.80	0.64
phytane	farnesane	0.65	0.80	0.61
phytane	trimethyltridecane	0.71	0.79	0.59
phytane	pristane + 1-ene + 2-ene	0.67	0.79	0.85
pristane + 1-ene + 2-ene	trimethylundec-2-ene	0.84	0.84	0.89
pristane + 1-ene + 2-ene	farnesane	0.88	0.81	0.86
pristane + 1-ene + 2-ene	trimethyltridecane	0.64	0.81	0.82
farnesane + 1-ene	trimethyltridecane + 1-ene	0.84	0.95	0.91
farnesane + 1-ene	trimethylundec-2-ene	0.85	0.91	0.84
farnesane + 1-ene	α -ergostane	0.37	0.82	0.62
trimethyltridecane + 1-ene	trimethylundec-2-ene	0.78	0.92	0.87
trimethyltridecane + 1-ene	α -ergostane	0.46	0.79	0.56
trimethyltridecane + 1-ene	β -ergostane	0.22	0.77	0.74
α -ergostane	stigmastane	0.78	0.80	0.89
α -ergostane	β -ergostane	0.23	0.72	0.86
β -ergostane	stigmastane	0.39	0.78	0.82
N/org. carbon	C ₁₇ odd/even	0.54	0.88	0.47
N/org. carbon	prist-2-ene	0.37	0.69	0.23
N/org. carbon	prist-1-ene	-0.10	-0.24	-0.20
N/org. carbon	α -ergostane	0.52	0.58	0.57
C ₁₉ odd/even	trimethyltridecane	0.57	0.77	0.76
C ₁₉ odd/even	phytane	0.50	0.69	0.69
C ₂₇ odd/even	α -ergostane	0.55	0.29	0.61
C ₁₇ odd/even	α -ergostane	0.53	0.62	0.58

* Values reported are for ratios of biomarkers to the respective alkene plus alkanes as expressed in Table I.

In general, the correlations were higher in the NOSR core than in the Geokinetics core data. This was especially evident for the sterane compound correlations and, in particular, the β -ergostane which in the Geokinetics core did not correlate significantly with either of the other two steranes. The reason for this is not evident, but may be due to the fact that the peak is quite small and obscured by nearby peaks. However, there was good correlation in both cores between the following pairs: phytane and pristane, pristane and trimethylundecene, pristane and farnesane, farnesane and trimethyltridecane, farnesane and trimethylundecene, trimethyltridecane and trimethylundecene, stigmastane and α -ergostane. This consistency of correlation among like groups of biomarkers was also observed by Anders and Robinson. It may indicate separate source materials for the chain isoprenoids and the steranes and/or it may indicate a series of degradation products from a different precursor for each group.

The data and discussion presented here are still of a tentative nature, since work on a third core is currently in progress. We anticipate further clarification of the behavior of biomarkers in oil shale with this expanded data base.

CONCLUSIONS

We investigated some biomarkers present in oils produced from two Green River formation cores using capillary column gas chromatography and found strong correlations between chain

isoprenoid compounds and between two of the sterane compounds in both cores. The biomarker compounds showed measurable changes in their ratios to associated alkanes with stratigraphy, thus, supporting the validity of relating shale oils to their source rocks using biomarker ratios. The problem of relating time dependent process variables to an oil product, subject to indefinite migration times through an in-situ-retort, may be resolved with biomarker tracers.

Comparison of these two Green River formation cores shows good agreement in ranges and average values for the alkene/alkane ratios and odd/even ratios of normal hydrocarbons across the resource. Of the two groups of biomarker compounds studied, the chain isoprenoids showed better agreement in ranges and averages than the steranes in the two-core comparison. The maximum variations in ratios of all three groups of compounds occur near the Mahogany marker in both cores and in the NOSR core again near the top of the A-groove. The relationship of variations in these biomarker ratios in oil to other properties of the oil shale source material could provide a better understanding of the structure and geochemistry of kerogen.

ACKNOWLEDGMENTS

We wish to thank Stanley Grotch for help and assistance with the data analysis and Cal Hall and Jim Taylor for mechanical technician support. We also thank Carla Wong and Richard Crawford who identified the steranes by GC/MS and Jane Cupps who helped with the gas chromatography. This work was performed under the auspices of the U. S. Department of Energy by the Lawrence Livermore National Laboratory under contract number W-7405-ENG-48.

EXPERIMENTAL APPARATUS

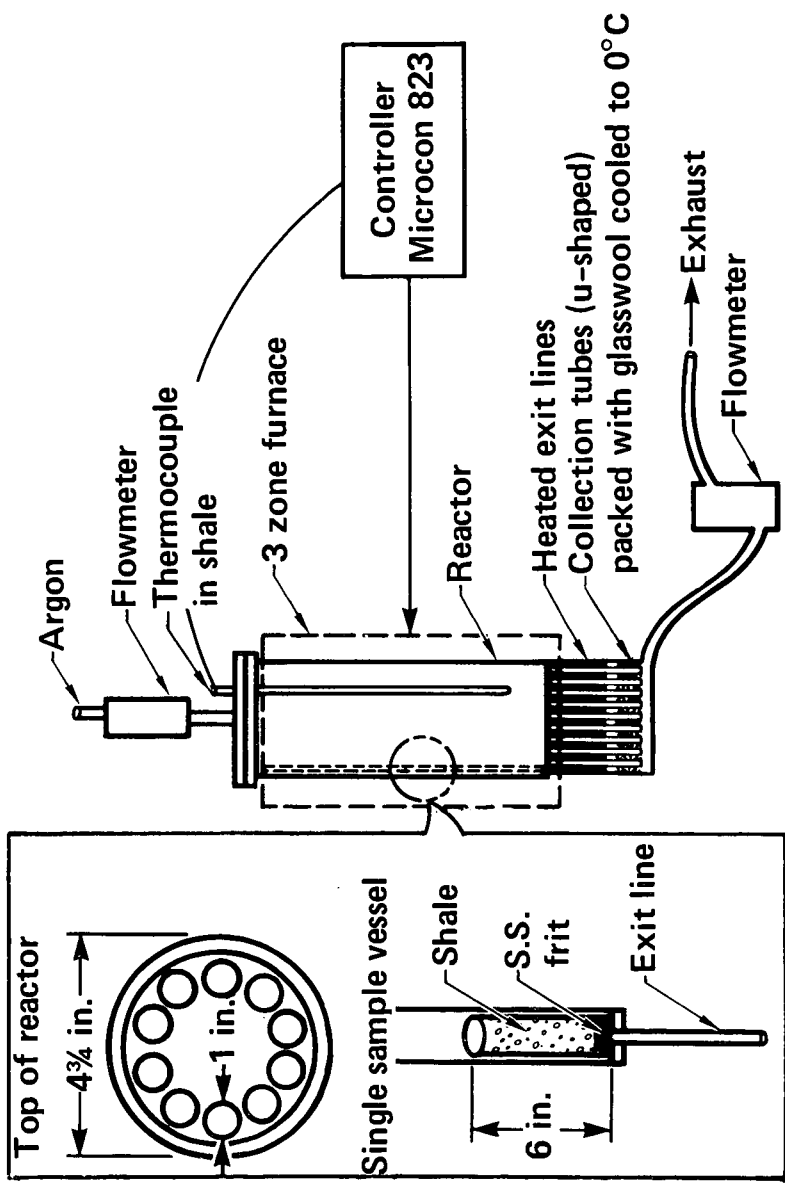


Figure 1. TOSS apparatus for producing oil from ten oil shales simultaneously.

**AVERAGE N-ALKANE + ALKENE ODD/EVEN RATIO
vs CARBON NUMBER**

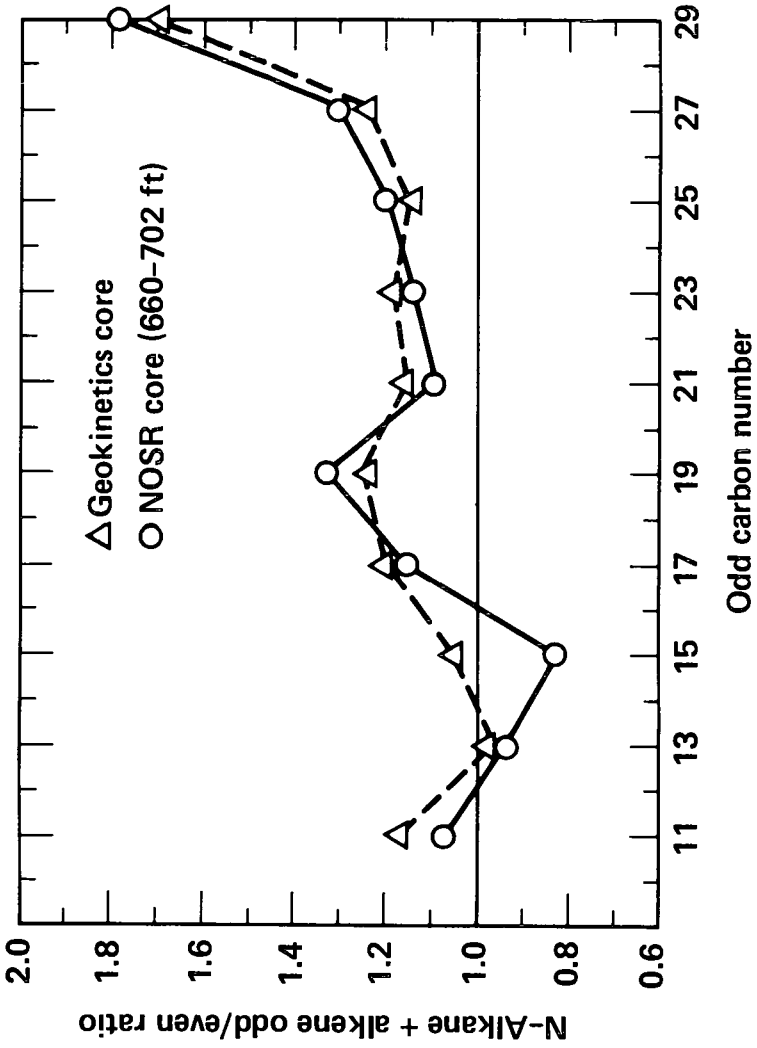


Figure 2. Plot of the average normal alkane + alkene odd/even ratios versus carbon number in the Geokinetics core and NOSR Core 25.

**AVERAGE 1-ALKENE/N-ALKANE RATIO
vs CARBON NUMBER**

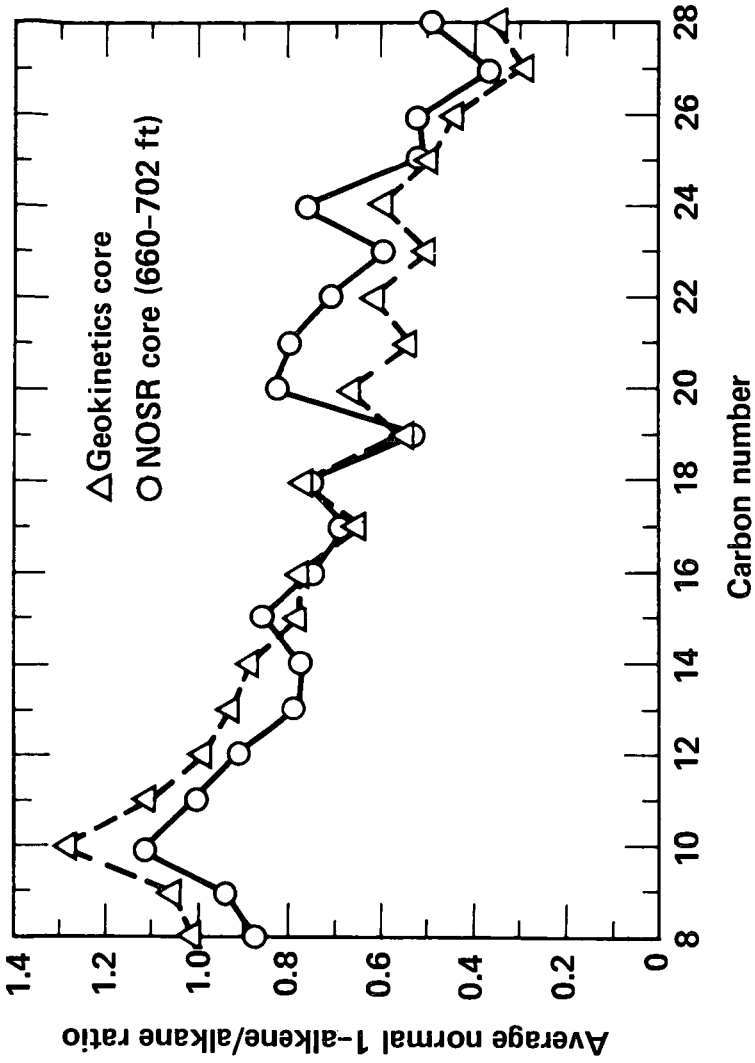


Figure 3. Plot of the average 1-alkene/normal alkane ratios versus carbon number in the Geokinetics core and NOSR Core 25.

**SHALE GRADE AND NITROGEN/ORGANIC CARBON RATIO vs
DEPTH (NOSR CORE 25)**

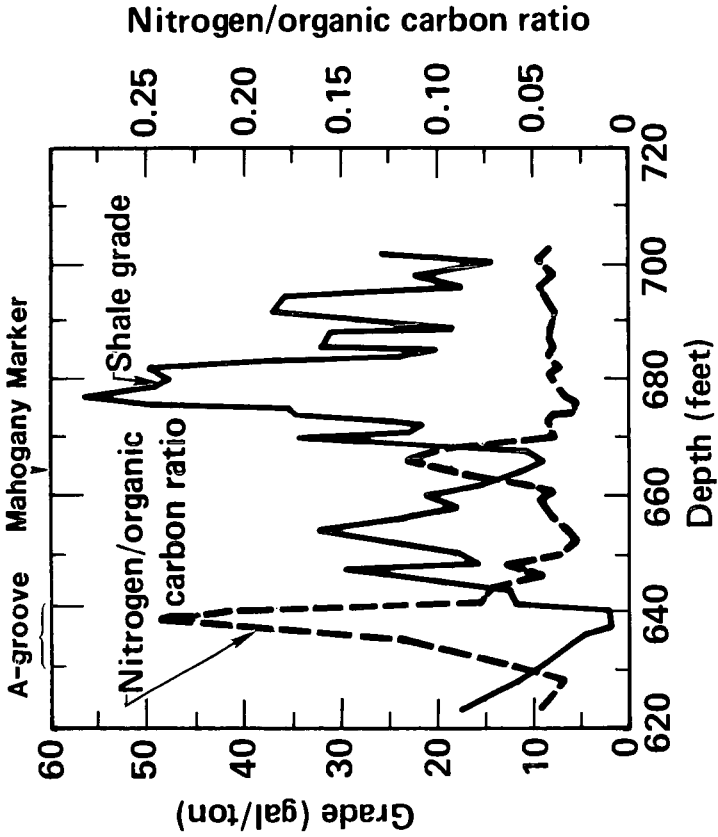


Figure 4. Plot of shale grade and nitrogen/organic carbon ratio versus depth in NOSR Core 25.

SHALE GRADE AND NITROGEN/ORGANIC CARBON RATIO vs
DEPTH (GEOKINETICS)

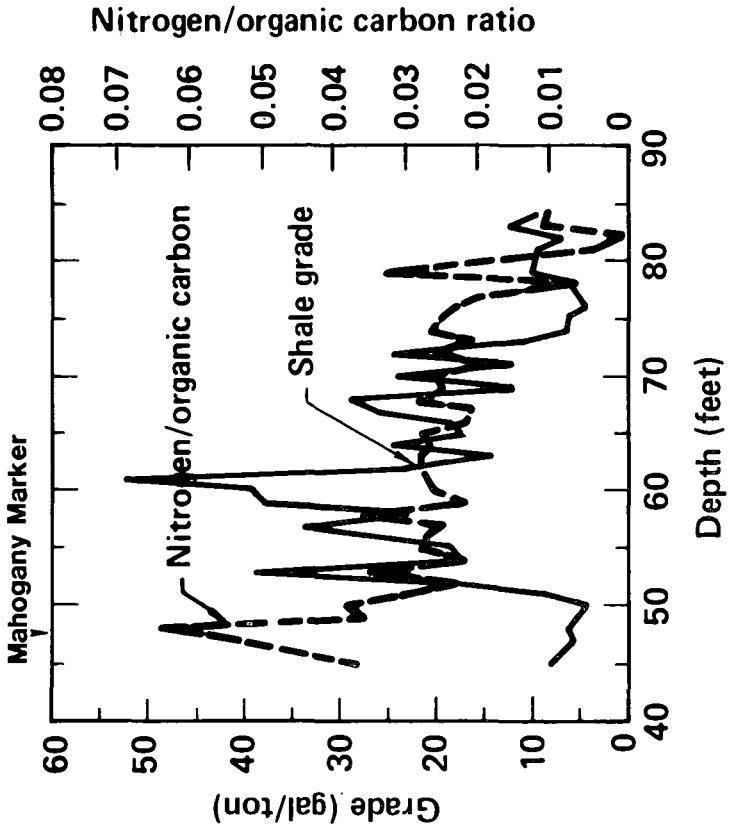


Figure 5. Plot of shale grade and nitrogen/organic carbon ratio versus depth in Geokinetics core.

BIOMARKERS vs DEPTH (NOSR CORE 25)

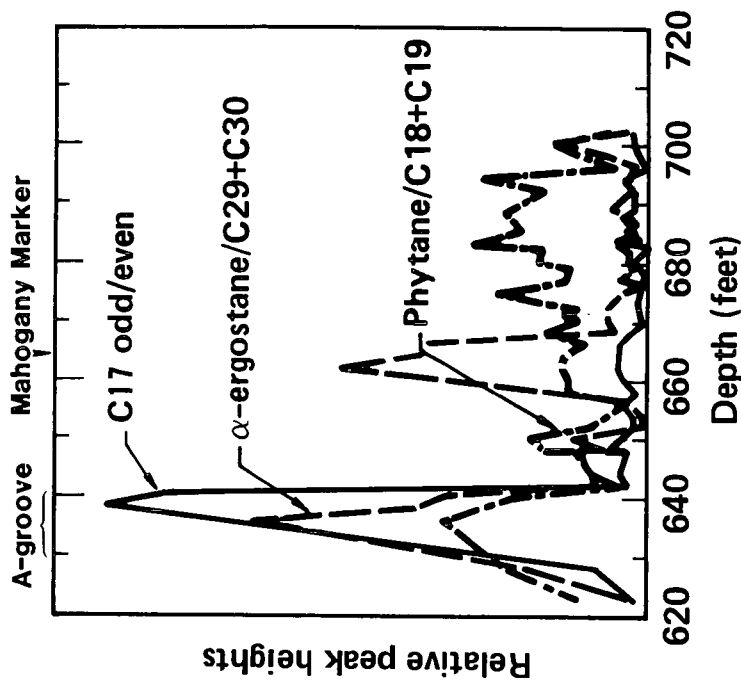


Figure 6. Plot of biomarker compounds versus depth in NOSR Core 25.

BIOMARKERS vs DEPTH (GEOKINETICS)

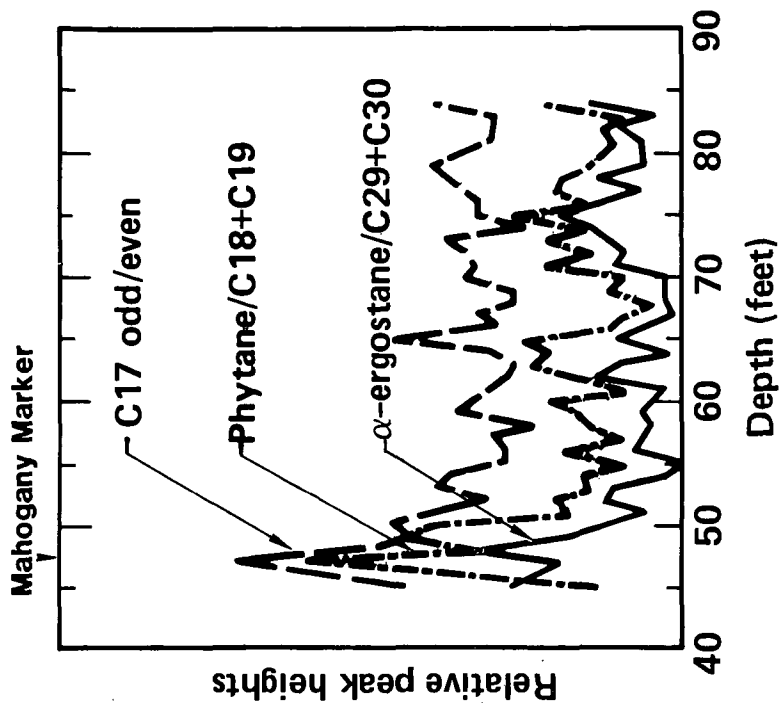


Figure 7. Plot of biomarker compounds versus depth in Geokinetics core.

LITERATURE CITED

- (1) Tissot, B. P. and Welte, D. H., *Petroleum Formation and Occurrence*, Springer-Verlag, New York, NY (1978).
- (2) Seifert, W. K. and Moldowan, J. M., "Paleoreconstruction by Biological Markers", *Geochimica et Cosmochimica Acta* **45**, 783-794 (1981).
- (3) Anders, D. E. and Robinson, W. E., "Geochemical Aspects of the Saturated Hydrocarbon Constituents of Green River Oil Shale - Colorado No. 1 Core", U. S. Bureau of Mines Rep. of Inv. RI 7737 (1973).
- (4) Tissot, B. P., Deroo, G. and Hood, A., "Geochemical Study of the Uinta Basin: Formation and Petroleum from the Green River Formation", *Beochimica et Cosmochimica Acta* **42**, 1469-1485 (1978).
- (5) Gallegos, E. J., *Developments in Petroleum Science* 5, Chapter 8, Teh Fu Yen and G. V. Chilingarian, Eds., Elsevier, NY, 149-180 (1976).
- (6) Cummins, J. J., Doolittle, F. G. and Robinson, W. E., "Thermal Degradation of Green River Kerogen at 150°C to 350°C", U. S. Bureau of Mines Rept. of Inv. RI 7924 (1979).
- (7) Seifert, W. K., "Steranes and Terpanes in Kerogen Pyrolysis for Correlation of Oils and Source Rocks", *Geochimica et Cosmochimica Acta* **42**, 473-484 (1978).
- (8) Burlingame, A. L. and Simoneit, B. R., "High Resolution Mass Spectrometry of Green River Formation Kerogen Oxidations", *Nature*, **222**, 741-747 (1969).
- (9) Burnham, A. K., Clarkson, J. E., Singleton, M. F., Wong, C. M. and Crawford, R. W., "Biological Markers from Green River Kerogen Decomposition", *Geochimica et Cosmochimica Acta* **46**, 1243-1251 (1982).
- (10) Singleton, M. F., Koskinas, G. J., Burnham, A. K. and Raley, J. H., "Assay Products from Green River Oil Shale", Lawrence Livermore National Laboratory Rpt., UCRL 53273 (1982).
- (11) Geokinetics, private communication (1982).
- (12) Giauque, R. D., Fox, J. P. and Smith, J. W., "Characterization of Two Core Holes from the Naval Oil Shale Reserve Number 1", Lawrence Berkeley Laboratory Rept., LBL-10909 (1980).
- (13) Philp, R. P. and Calvin, M., "Kerogenous Material in Recent Algal Mats at Laguna Mormona, Baja California", in *Advances in Organic Geochemistry*, Ensiedema Publishing Co., Madrid, Spain (1977).
- (14) van Graas, Ger, de Leeuw, J. W., Schenck, P. A. and Haverkamp, J., "Kerogen of Toarcian Shales of the Paris Basin. A Study of its Maturation by Flash Pyrolysis Techniques", *Geochimica et Cosmochimica Acta* **45**, 2465-2474 (1981).
- (15) van de Meent, Dik, Brown, S. C., Philp, R. P. and Simoneit, B. R. T., "Pyrolysis-High Resolution Gas Chromatography and Pyrolysis Gas Chromatography-Mass Spectrometry of Kerogens and Kerogen Precursors", *Geochimica et Cosmochimica Acta* **44**, 999-1013 (1980).
- (16) Connan, J. and Cassou, A. M., "Properties of Gases and Petroleum Liquids Derived from Terrestrial Kerogen at Various Maturation Levels", *Geochimica et Cosmochimica Acta* **44**, 1-23 (1980).
- (17) Cane, R. F., *Developments in Petroleum Science* 5, Chapter 3, Teh Fu Yen and G. V. Chilingarian, Eds., Elsevier, New York, NY, 27-60 (1976).
- (18) Vandegrift, G. F., Winans, R. E., Scott, R. G. and Horwitz, E. P., "Quantitative Study of the Carboxylic Acids in Green River Oil Shale Bitumen", *Fuel* **59**, 627 (1980).
- (19) Richardson, J. H., et al., "Fluidized-Bed Pyrolysis of Oil Shale: Oil Yield, Composition and Kinetics", Lawrence Livermore National Laboratory Rept. UCID 19548 (1982).
- (20) Burnham, A. K. and Singleton, M. F., "High-Pressure Pyrolysis of Colorado Oil Shale", Lawrence Livermore National Laboratory Rept. UCRL 88127 (1982).
- (21) Larter, S. R., Solli, H., Douglas, A. G., DeLange, F. and de Leeuw, J. W., "Occurrence and Significance of Prist-1-ene in Kerogen Pyrolysates", *Nature* **279**, 405-408 (1979).
- (22) van de Meent, D., de Leeuw, J. W. and Schenck, P. A., "Origin of Unsaturated Isoprenoid Hydrocarbons in Pyrolysates of Suspended Matter and Surface Sediments", *Advances in Organic Geochemistry*, Pergamon, London, 469-474 (1981).

SYMPOSIUM ON GEOCHEMISTRY AND CHEMISTRY OF OIL SHALE
PRESENTED BEFORE THE DIVISIONS OF FUEL CHEMISTRY, GEOCHEMISTRY,
AND PETROLEUM CHEMISTRY, INC.
AMERICAN CHEMICAL SOCIETY
SEATTLE MEETING, MARCH 20 - MARCH 25, 1983

THE NITROGENEOUS COMPONENTS IN SHALE OIL

By

T. F. Yen, F. F. Shue, and W. H. Wu
University of Southern California, School of Engineering,
Los Angeles, California 90007

ABSTRACT

Nitrogen-containing compounds in shale oil were concentrated by FeCl_3 -clay complexation chromatography. Similarly the nitrogen compounds were also investigated from petroleum as well as coal liquids. Comparison was made for different nitrogen homologues which were identified by GC-MS. Chemical structures of pyridine homologues, and their benzologues, aromatic amines, indoles, etc. will be discussed.

SYMPOSIUM ON GEOCHEMISTRY AND CHEMISTRY OF OIL SHALE
PRESENTED BEFORE THE DIVISIONS OF FUEL CHEMISTRY, GEOCHEMISTRY,
AND PETROLEUM CHEMISTRY, INC.
AMERICAN CHEMICAL SOCIETY
SEATTLE MEETING, MARCH 20 - MARCH 25, 1983

PETROLOGY OF SPENT SHALE: PREAMBLE ON OXYGEN FUGACITY

By

D. C. Melchior and T. R. Wildeman
Department of Chemistry and Geochemistry,
Colorado School of Mines, Golden, Colorado 80401

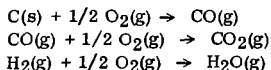
INTRODUCTION

The green River Formation in Colorado, Wyoming, and Utah is well-known for its hydrocarbon content and unique assemblage of minerals. With the increasing need for a petroleum substitute, this area has been investigated for future exploitation. Extraction of the organic compounds from oil shale is accomplished by retorting. Several possible schemes for retorting shale have been proposed (1, 2, 3). The internal conditions of these retorts will be greatly affected by the mineral matrix of the shale. By monitoring the mineral matrix of the shale, questions on retort efficiency and environmental problems may be addressed.

The question this paper will start to investigate is how closely the mineralogy of spent shale may be thermodynamically linked to the conditions that prevailed within the retort. Shales from the Green River Formation contain high amounts of reactive minerals. For example, carbonates are especially prone to decomposition at elevated temperatures and varying atmospheric compositions.

Are these minerals reacting to the products that would be dictated by the thermodynamics? During metamorphism, there are two important factors that will dramatically affect mineralogy: these are temperature and O_2 fugacity. The temperature of a system may be monitored using thermocouples or other devices; however, no such device easily measures O_2 fugacity. "Fugacity" for gas solutions is the same as activity for liquid solution (4). There are primarily two approaches for determining the fugacity of O_2 in a system. The gaseous composition of the system may be determined from which the fugacity is calculated. Alternatively, known redox couples in solid systems such as Fe^{2+} and Fe^{3+} are used to determine the O_2 fugacity in the vapor over the solid.

Campbell and others (5) have studied the gaseous compositions within several retorts and have published results on $CO(g)$, $CO_2(g)$, $H_2(g)$, and $H_2O(g)$ contents as a function of temperature. The reactions of primary concern are:



The iron-containing minerals within unretorted and retorted shales have been studied by Melchior (6, 7). Changes of the iron-containing minerals were observed at various temperatures and internal retorting conditions. Of particular interest, the changes in the mineral pyrite were examined. Are the O_2 fugacities derived from the gases and those determined by the iron-containing minerals consistent?

DISCUSSION

The chemistry of iron is complex; it can be stable as Fe^0 , Fe^{2+} , and Fe^{3+} . The oxidation state of Fe is sensitive to the oxidation-reduction potential of the system and should dictate what oxidation state of Fe is present. Geochemically, the Fe^{2+} and Fe^{3+} species exist in minerals. Melchior (6) has investigated the speciation of iron in minerals within oil shale. The results of this study show that iron in the 2^+ state predominates. The minerals pyrite (FeS_2 (cubic)), siderite ($FeCO_2$ (orthorhombic)), and ankerite ($(Fe, Mg, Ca)(CO_3)_2$) were all detected in unretorted shale using Mössbauer effect spectroscopy. The presence of these minerals indicate that the environment of deposition and development of the shale was relatively reducing and of low energy.

Once removed from these conditions, the minerals are susceptible to change. During retorting, changes occur rapidly and should mimic those observed under metamorphism. The chemical changes of the minerals siderite and pyrite under varying conditions have been investigated (8-10). The chemistry of iron in metamorphic environments has also been exhaustively investigated by Eugster and others (11-13). They have presented the Fe-O-Si buffer system based on mineralogy and varying temperature and redox conditions. The O_2 fugacity within a geologic system may be

obtained from the mineralogy. Within the Fe-O-Si system, fayalite (FeSiO₄) may be present under the least oxidizing conditions, while hematite (Fe₂O₃) is present under the most oxidizing conditions. Figure 1 has been reproduced from Eugster (11,12) and displays the Fe-O-Si buffer system.

In addition to the information on Fe speciation of minerals in unretorted shales, Melchior (6) has determined the speciation of Fe in retorted shales. Table I displays the results of this study for combustion-type retorts. The results show that much of the iron that existed in the 2⁺ state within the unretorted shale has been converted to the 3⁺ state during retorting. The minerals siderite and ankerite underwent conversion prior to conversion of the pyrite. The question of pyrite conversion is essential to answering the ecological questions which abound concerning trace element mobility.

TABLE I
FeMINERALOGY PRESENT IN SPENT OIL SHALES AND OXYGEN
FUGACITIES BASED ON THE MINERALOGY

T°C	Spent Shale Mineralogy	log f _{O₂}	f _{O₂}
600	Hematite, magnetite, carbonate, sulfides, clay	-14.40	3.98 x 10 ⁻¹⁵
750	Hematite, magnetite, carbonate, sulfides, clay	-10.25	5.62 x 10 ⁻¹¹
935	Hematite, magnetite	- 6.20	6.31 x 10 ⁻⁷
1030	Hematite, magnetite	~ 5.0	1.0 x 10 ⁻⁵

Using results in Eugster (11,12), the O₂ fugacity within a retort vessel may be determined based on mineralogy. The presence of hematite (Fe₂O₃) and magnetite (Fe₃O₄) at those retort temperatures places the system in a distinct buffering zone. The O₂ fugacities for these retorts are given in Table I.

The gases CO₂, CO, H₂O, and H₂ will control the fugacity of O₂ in an oil shale retort. Campbell and others (5) studied the evolution of gases during oil shale pyrolysis. This study was performed to simulate conditions that may exist in surface or *in-situ* retorts. Measurements on the gaseous composition within the retort were made. From these measurements, it is possible to compute the O₂ fugacity based on the CO₂-CO and H₂-H₂O couples.

The equilibrium constant for the reaction CO₂(g) → CO(g) + 1/2 O₂(g) is written:

$$K_f = f_{CO} f_{CO_2}^{-1/2} / f_{CO_2} \quad 1)$$

The equilibrium constant for the reaction H₂O(g) → H₂(g) + 1/2 O₂(g) is written:

$$K_f = f_{H_2} f_{O_2}^{-1/2} / f_{H_2O} \quad 2)$$

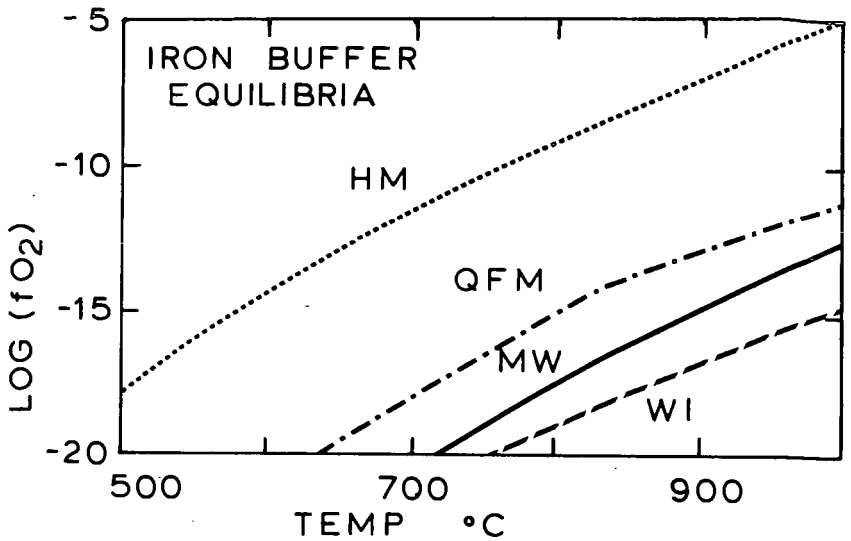
To determine the f_{O₂}, we will assume that the ratios of CO₂(g)/CO(g) and H₂(g)/H₂O(g) are equal to one. This is close to the values usually seen for most retorts (5,14). Using this assumption, it is now possible to use previously determined ΔG_R⁰ values to obtain f_{O₂}. Robie, Hemingway, and Fisher (15) have published ΔG_R⁰ values for the species present from which ΔG_R⁰ for the reactions have been calculated.

Table II presents the ΔG_R⁰, K, and f_{O₂} for the CO₂-CO reaction, plus the f_{O₂} determined based on the H₂-H₂O reaction. Figure 2 shows that the oxygen fugacities derived from the CO₂-CO and H₂O-H₂ couples are similar to each other but quite different from that determined by iron mineralogy.

CONCLUSIONS

The results of this comparison have shown that there is a dichotomy between the oxygen fugacities derived by the two methods presented. This disequilibrium suggests that the mineralogic reactions are kinetically controlled. The results suggest that given sufficient time, it may be possible to promote the reaction of the iron oxides to silicates. A critical question that must be answered is if there is sufficient silica present in the matrix for Fe-silicates to form. This will be addressed in a forthcoming paper. If silicates could form, many of the trace elements thought to reside in the Fe-sulfide minerals would be incorporated into inert structures. This would eliminate some environmental problems involved with spent shale.

Future work in this area should most certainly include a study on possible catalyzing agents that would promote the formation of silicates. One agent that should strongly be considered as a catalyzing agent is steam. The presence of steam may be extremely useful in controlling silicate formation at the lower temperatures that some retorts run at.



H = HEMATITE M = MAGNETITE Q = QUARTZ
 F = FAYALITE W = WUSTITE I = IRON

FIGURE 1 O_2 FUGACITY IN A Fe-O-Si BUFFER SYSTEM.

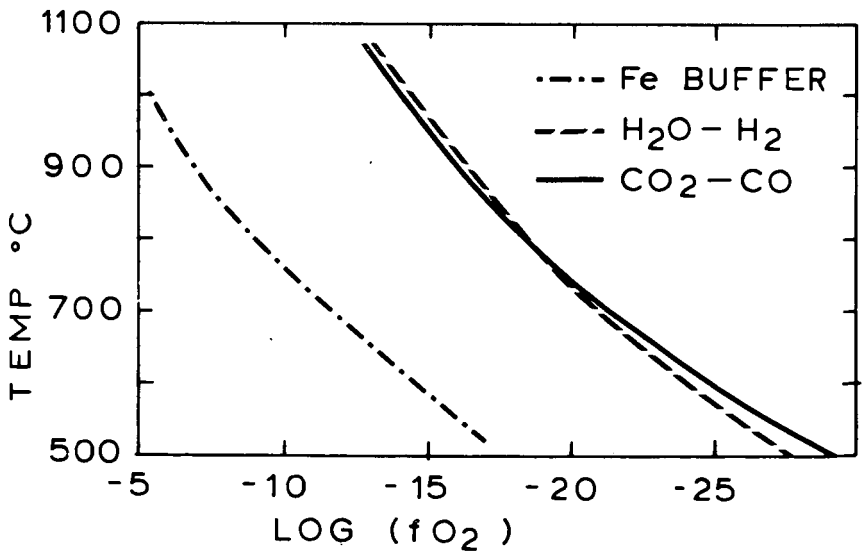


FIGURE 2. O_2 FUGACITY FROM MINERAL & GAS EQUILIBRIA.

TABLE II
THERMODYNAMIC RESULTS FOR THE CO₂-CO AND H₂-H₂O SYSTEM

$\text{CO}_2(\text{g}) \rightarrow \text{CO}(\text{g}) + 1/2 \text{O}_2(\text{g})$				
T°C	ΔG_R° (Kcal/mole)	K	f_{O_2}	log f_{O_2}
527	50.93	1.2×10^{-14}	1.4×10^{-28}	-27.85
627	48.83	1.4×10^{-12}	1.9×10^{-24}	-23.72
727	46.75	6.0×10^{-11}	3.7×10^{-21}	-20.43
827	44.67	1.3×10^{-9}	1.8×10^{-18}	-17.74
927	42.61	1.7×10^{-8}	3.0×10^{-16}	-15.52
1027	40.55	1.5×10^{-7}	2.3×10^{-14}	-13.64

$\text{H}_2\text{O}(\text{g}) \rightarrow \text{H}_2(\text{g}) + 1/2 \text{O}_2(\text{g})$		
T°C	f_{O_2}	log f_{O_2}
500	2.2×10^{-28}	-27.66
600	1.6×10^{-2}	-23.80
700	1.6×10^{-21}	-20.80
800	4.4×10^{-19}	-18.36
900	5.2×10^{-17}	-16.28

LITERATURE CITED

- (1) Jones, J. B., Jr., Paraho Oil Shale Retort: Quarterly of the Colorado School of Mines, 71 (4), 39 (1976).
- (2) Kilburn, P. D., Atwood, M. T., and Broman, W. M., "Guidebook to the Energy Resources of the Piceance Creek Basin, Colorado", D. K. Murray, ed., Rocky Mountain Ass'n of Geologists, Denver, p. 151-164 (1974).
- (3) Mahajan, V. V., Lumpkin, R. E., Gragg, F. M., and Fraser, R. J., Proc. of the 10th Oil Shale Symp., Colorado School of Mines Press, p. 191-199 (1977).
- (4) Moore, W. J., Physical Chemistry 4th Ed.: Prentice Hall, Englewood Cliffs, N. J., p. 977 (1972).
- (5) Campbell, J. H., Ko Jinas, G. J., Gallegos, G., and Gregg, M., Fuel, 59, 718 (1980).
- (6) Melchior, D. C., M. S. Thesis, Colorado School of Mines, 31 pp (1980).
- (7) Melchior, D. C., Wildeman, T. R., and Williamson, D. L., Fuel, 61, 516 (1982).
- (8) Yui, S., Economic Geology, 61, 768 (1966).
- (9) French, B., Am. J. Sci., 271, 37 (1971).
- (10) Marusak, L. A., and Mulay, L. N., J. Appl. Physics, 50, 7807 (1979).
- (11) Eugster, H. P., "Reduction and Oxidation in Metamorphism: Researches in Geochemistry", P. H. Abelson, ed., John Wiley and Sons, Inc., New York, New York, p. 397 (1959).
- (12) Eugster, H. P., and Wones, D. R., J. Petrology, 3, 82 (1962).
- (13) Eugster, H. P., and Skippen, G. B., "Igneous and Metamorphic Reactions Involving Gas Equilibria: Researches in Geochemistry", P. H. Abelson, ed., Vol. 2, John Wiley and Sons, Inc., New York, New York, p. 492 (1968).
- (14) Goodfellow, L., and Atwood, M. T., Fischer Assay of Oil Shale: Proc. of the Oil Shale Corp., Quarterly, Colorado School of Mines, 69 (2), 205 (1974).
- (15) Robie, R. A., Hemingway, B. S., and Fisher, J. R., U. S. Geol. Survey Bull. 1452, 456pp., (1978).

SYMPOSIUM ON GEOCHEMISTRY AND CHEMISTRY OF OIL SHALE
PRESENTED BEFORE THE DIVISIONS OF FUEL CHEMISTRY, GEOCHEMISTRY
AND PETROLEUM CHEMISTRY, INC.
AMERICAN CHEMICAL SOCIETY
SEATTLE MEETING, MARCH 20-25, 1983

ANALYTICAL TECHNIQUES FOR CHARACTERIZATION OF OIL SHALES

By

R. A. Nadkarni
Analytical Research Laboratory, Exxon Research and Engineering Company, P. O. Box 4255
Baytown, Texas 77520

INTRODUCTION

Oil shale, a fine grained sedimentary rock containing insoluble organic material that yields oil by destructive distillation, or retorting, occurs in large quantities in many parts of the world and in the United States. The identified resources of shales outside the United States total over 1.1 trillion barrels of oil (1). The richest deposits in the United States are located in the Eocene Green River formation of Colorado, Utah and Wyoming. In part of this formation, the Piceance Basin, the oil shales are thought to contain energy equivalent of about 1.2 trillion bbl of oil, or about 40 times the nation's present proven reserves of petroleum. Environmental issues associated with shale retorting require substantial monitoring and control of waste products, which can be quite large.

At Exxon Research and Engineering Company's Baytown Research and Development Division, analytical methods for coal and coal products have been developed and are being used (2-4). These methods are now being extended to the characterization of oil shales. This extension is not straightforward in all cases because in several respects shale is almost the exact opposite of coal. For example, shale is high in inorganics and low in organics, the opposite of most coals and shale organics have a high H/C ratio, also the opposite of coal.

The major analytical techniques used for shale analysis are neutron activation analysis (5), X-ray fluorescence (5), and atomic spectroscopy (6-8). In the present paper, we are describing our approach to the multi-element analysis of oil shales and their products utilizing mainly inductively coupled plasma emission spectrometry (ICPES) for metals, and ion chromatography (IC) for some nonmetals. Other major elements such as carbon, hydrogen, nitrogen, sulfur and oxygen, are determined by a variety of combustion techniques.

EXPERIMENTAL

Shale Preparation

The oil shale samples were pulverized to -100 mesh before sampling. Aliquots of the samples were ashed at 750°C for 5 hrs in a muffle furnace. Kerogen was isolated from the shale samples by demineralization with HCl and HF, a procedure developed at the U. S. Bureau of Mines (19).

Parr Bombs

Two types of Parr bombs were used. The acid digestion bombs were used for the ash dissolutions. About 0.2 g of shale or ash was dissolved in 3 mL aqua regia and 2 mL HF in the Parr bomb and heated at 110°C in an air-oven for 2 hours. After the dissolution, 1 g of boric acid was added to each sample solution which was heated on a water-bath for 15 minutes. If any unburned carbon was visible, the solutions were filtered; otherwise, they were diluted to 100 mL. A blank containing the same amounts of the acids was also prepared. The Parr oxygen bombs were used for a rapid ash determination and for sample preparation for IC. About 0.5 g of shale or shale oil was mixed with 0.5 g of white oil in a stainless steel cup. Five mL of water was placed in the bottom of the bomb which was then assembled and pressurized to 30 atmospheres of oxygen. After combustion, the bomb was allowed to cool for 10 minutes and then slowly opened. The inside walls of the bomb were washed with water and all the washings were combined together, filtered if necessary, and diluted to 50 mL. The residue in the cup was dried at 110°C for 15 minutes and re-weighed for ash determination.

Claisse Fluxer Fusion Device

The detailed procedure is described by Botto (9). This is an automated device which simultaneously fuses six samples. In this procedure, the finely powdered sample was mixed with ten

times its weight of lithium metaborate in a platinum crucible and heated at $\sim 950^{\circ}\text{C}$ for 15 minutes. The melt was dissolved in either dilute HCl or HNO_3 and the elements of interest were then determined by AAS or ICPES. Phosphorus was determined from the same solution by a separate molybdenum blue colorimetric procedure.

Inductively Coupled Plasma Emission Spectrometer

Details of our instrumentation are given by Botto (10). It is a Jarrell-Ash AtomComp Model 750 with 34 elemental channels. A list of these elemental channels, the wavelengths used for the determinations, the detection limits and the upper dynamic range for each element is given in the above paper. Six of the elemental channels are also focussed on weaker lines of lesser sensitivity for determining the higher elemental concentrations. This eliminates the necessity of diluting the samples further to prevent major elements in shale from exceeding the upper dynamic limit. The data from ICPES are processed by an on-line PDP-8M computer interfaced to a HP-1000 off-line computer.

Ion Chromatograph

A Dionex Model 14 was used for the determination of anions. The working parameters are given elsewhere (20). Quantitation was done by comparing the peak heights on the strip-chart recorder of the standards with the sample solutions.

Other Instrumentation

An Orion model 901 microprocessor ion analyzer was used for pH and for ion selective electrode measurements. A Norelco PW-1212 was used for X-ray fluorescence measurements. Certain of the ICPES results were checked with an Instrumentation Lab 951 atomic absorption spectrophotometer. Carbon, hydrogen and nitrogen were determined using a Hallikainen CH analyzer or Leco CHN-600 analyzer. Sulfur was determined using a Leco SC-32 analyzer. Oxygen was determined using 14 MeV neutron activation analysis.

Reagents

All of the acids used in this work were of "Ultrex" quality from J. T. Baker Chemical Company. Deionized water was obtained from a Millipore Corporation MilliQ system. An ICPES scan of this water showed a total of 33 elements to be ~ 1 ppm or less. Oil shale standards were provided by Dr. F. J. Flanagan of the U. S. Geological Survey. These were dried for 2 hours at 110°C before analysis.

RESULTS AND DISCUSSION

Ashing of Oil Shales

Because of potential difficulties due to carbonate content of the shales, the normal ASTM ashing procedure for coals was evaluated to find the optimum ashing temperature with minimum elemental losses for shales. A Green River oil shale was ashed at 750°C for 15 hours and then successively ashed for 3 hours each at 850, 950 and 1050°C . From each stage, the percentage ash was determined. All of these ashes and the original shale sample were analyzed for their carbonate content by evolution-gravimetry and for elemental composition by ICPES. The results are summarized in Table I. Essentially all of the carbonate is decomposed at 750°C ; heating further up to 1050°C showed no loss of any element determined. Thus, it seems feasible that a shale sample can be heated overnight to $\sim 800^{\circ}\text{C}$ and the ash subsequently analyzed for the elements of interest with good precision. Thermogravimetric analysis of a Colorado oil shale also indicated $\sim 850^{\circ}\text{C}$ as the optimum temperature for carbonate decomposition in shale.

The Parr oxygen bomb can be used if only a rapid ash determination is desired. The residue left in the ignition cup is equivalent to the ash content of a given shale. Having water as an absorbant in the bomb is not necessary; however, if water absorbant is used, it is probably better to dry the residual ash before final weighing to remove the moisture. Pressing the shale sample into a pellet helps in achieving uniform combustion and in reducing the risk of some sample being blown out of the cup during combustion. Typical results on two raw shales and two shale oil samples are given in Table II. The agreement between the values by the ASTM method for coals and the proposed method is very good (accuracy between 0.2 and 5% with an average of 4%). The precision of the method varies from 0.6 to 13% with an average relative standard deviation of 5%. Thus, the Parr oxygen bomb method can be used for a quick ash determination of coal or shale in a pilot plant laboratory situation as an alternative to the time-consuming ASTM D-3174 procedure.

Claissé Fluxer Analysis

Lithium tetraborate or metaborate fusion for the dissolution of rocks has been in use for many years. The Claissé Fluxer fusion device simply makes this fusion automated. We have used

the method in the past for the fusion of coal and fly ashes (9, 11). Oil shales can be dissolved by this method without pre-ashing. Once the solution is prepared, it may be analyzed for the most part by ICPEs or by AAS. Analysis of U. S. G. S. Devonian Ohio shale SDO-1 by Claisse fluxing followed by AAS or ICPEs measurements is illustrated in Table III.

TABLE I
ANALYSIS OF COLORADO OIL SHALE

Ashing Temperature, °C	Unashed	750	850	950	1050
Ash, wt %	-	63.1	62.8	62.6	61.9
CO ₃ , %	26.4	0.81*	0.42*	0.27*	0.19*
Al, %	3.30	3.15	3.15	3.18	3.14
Ba, wppm	502	515	516	512	513
Ca, %	12.0	12.5	12.8	12.3	12.7
Cr, ppm	31	33	29	24	35
Cu, ppm	134	133	130	136	126
Fe, %	1.69	1.64	1.63	1.62	1.61
K, %	0.98	1.00	0.97	0.95	0.95
Li, ppm	48	50	49	51	49
Mg, %	2.85	2.71	2.85	2.78	2.79
Mn, ppm	302	282	283	282	277
Na, %	1.37	1.35	1.35	1.34	1.36
P, %	0.12	0.11	0.11	0.10	0.10
Si, %	10.7	10.5	10.5	10.6	10.8
Sr, ppm	762	726	738	726	722
Ti, %	0.12	0.10	0.11	0.12	0.12
V, ppm	55	68	56	50	78
Zn, ppm	79	85	79	85	78

* Remaining in ash.

TABLE II
ASH DETERMINATION BY PARR OXYGEN BOMB

Sample	Wt % Ash by: High Temperature Ashing	Parr Oxygen Bomb*
Colorado Shale	62.8	62.7±0.4 (5)
Colorado Shale	72.7	72.2±0.4 (2)
Australian Shale Oil	1.80	1.72±0.11 (3)
Australian Shale Oil	1.87	1.64±0.21 (3)

* Number of replicate analysis.

In the predominantly AAS scheme, phosphorus and titanium are colorimetrically determined. The results obtained on five replicates of the solution by each method are given in Table III and are compared with the values obtained for this standard at the Indiana Geological Survey (7). The ICPEs and AAS results are in very good agreement with each other and with the literature values. The precision and the accuracy of the measurements are ±5% for most elements analyzed.

Combining the Claisse Fluxer fusion with ICPEs measurements gives a rapid and accurate method for the ash element analysis. The total analysis time is reduced to 20-25 minutes per sample. However, although the Claisse Fluxer procedure is excellent for the determination of all major elements, it is not suitable for the determination of trace elements, because the final solution (1 L) is too dilute for detection of trace elements. If the solution volume is kept small, extremely high concentrations of lithium and boron in the solution give an undesirable high background spectrum for trace element measurements. Hence, it is necessary to resort to a separate procedure where both trace and major elements can be simultaneously determined.

TABLE III

ANALYSIS OF SHALE SDO-1 BY CLAISSE FLUXER ICPES-AAS

Oxide Wt % by:	ICPES	AAS	Literature (7)
Al ₂ O ₃	15.6±0.15	15.2±0.12	15.6
CaO	1.37±0.02	1.33±0.01	1.42
Fe ₂ O ₃	11.8±0.1	11.7±0.1	12.2
K ₂ O	4.13±0.12	4.00±0.06	4.23
MgO	1.91±0.02	1.86±0.00	1.87
Na ₂ O	0.46±0.01	0.44±0.00	0.52
SiO ₂	62.4±0.6	63.7±1.1	64.4
TiO ₂	0.87±0.01	0.97	0.90
P ₂ O ₅	0.37±0.07	0.18	0.14
BaO	0.05±0.01	-	0.055
MnO	0.06±0.00	-	0.056
TOTAL	99.0	99.4	101.3

Parr Bomb Dissolution of Shales

Originally the so-called Parr bomb was developed by Bernas (12) for the dissolution of silicate matrices. The bomb is now marketed by Parr Instrument Company of Moline, Illinois. The dissolution procedure has been adapted to shales and consists of mixing 100 to 200 mg of the sample in 2 mL aqua regia and 2 mL HF. After the dissolution, 1 g of boric acid is added to each sample and the samples are heated in a waterbath for 15 minutes. If any unburned carbon is visible at this stage, the solutions are filtered; otherwise, the solutions are diluted to 100 mL for analysis by ICPES. A blank is used throughout the analysis scheme containing the same amounts of aqua regia, HF and boric acid and is used for intensity background corrections in the ICPES measurements.

Other workers have used different acid combinations for the dissolution of ashes in the Parr bomb. Thus, HCl + HF, HNO₃, HClO₄ + HF, aqua regia + HF, and HNO₃ + HClO₄ have all been used in the Parr bombs. We have found the aqua regia + HF mixture to be quite effective in accomplishing the dissolution. It is important to have a boric acid blank subtracted from the sample spectrum in the ICPES analysis to correct for the boron interferences with other elemental lines. It is also necessary to add boric acid to the sample solution immediately after opening the bomb and then to heat the solution on a waterbath for 15 minutes so that all of the boric acid goes in solution and reacts with insoluble fluorides. When boric acid was added only during the final dilution step, low recoveries were obtained, since Al, Ba, Ca and Mg, which form insoluble fluorides, were filtered off along with the unburned carbon.

The results of using the Parr bomb for shales are included in Table IV. These three shales are distributed by the U. S. Geological Survey as "standard" shales: Green River shale SGR-1, Cody shale SCO-1 and Devonian Ohio shale SDO-1. Not enough information is available in the literature on the composition of these shales. The U.S.G.S. values given in Table IV for shales SGR-1 and SCO-1 are averages of values from five papers given in an U.S.G.S. report (13), while the literature values for the shale SDO-1 are from the Indiana Geological Survey (7). We analyzed each sample in four replicates by the Parr bomb procedure. Overall, the agreement between the Parr bomb and the literature results is good. For SGR and SCO shales, chromium and nickel results could not be obtained by Parr bomb, due to contamination from the metal body of the bomb. Somewhat lower silicon results indicate partial volatilization of SiF₄ during dissolution. Phosphorus results for all three shales are lower than the literature values. If phosphorus is partly present as an organic complex in the shale, it will not be totally decomposed by the dissolution procedure.

The Parr bomb dissolution method seems to give satisfactory results on unashed oil shale samples. However, when the method was used for shales which had organic content greater than 20 wt %, lower recoveries for many elements were observed. Agreement between the data on the ashed samples by Claisse Fluxer and the unashed samples by the Parr bomb dissolution was poor, with the latter data always being low. The higher the kerogen content of the shales, the greater the discrepancy. We hypothesize that the mineral matter surrounded by kerogen results in poor

contact between the dissolving acids and the inorganic material, thus, resulting in the low recoveries. Ashing of these kerogen-enriched fractions eliminated this problem. The results in Table V for a typical Green River oil shale concentrate compare the data between the Claisse Fluxer and the Parr bomb methods, the latter with and without preashing. While agreement for the unashed sample is poor, the data from the ashed sample are in good agreement with the Claisse Fluxer procedure. The kerogen concentrates prepared by acid demineralization are analyzed for metals by ICPES after ashing the sample and dissolving it in aqua regia + HF. Typical analyses of an Australian oil shale and the kerogen isolated from it are given in Table VI. Drastic reduction in the metals content of the shale during the kerogen preparation is indicated. Almost complete demetallization of the major metals such as aluminum, calcium and silicon is evident. Pyrite, FeS₂, is the only mineral left in the kerogen concentrate, since only HNO₃ will dissolve it. The elevated levels of fluorine and chlorine in the kerogen compared to the shale, originate from the HCl and HF used for the demineralization. Shale oils are "wet"-ashed with concentrated H₂SO₄ on a hot plate and in a muffle furnace before ICPES analysis for metals.

TABLE IV
ANALYSIS OF OIL SHALES BY PARR BOMB DISSOLUTION

Element, wppm	SGR-1		SCO-1		SDO-1	
	Parr Bomb	USGS ¹³⁻	Parr Bomb	USGS ¹³⁻	Parr Bomb	IGS ⁷
Al, %	3.31+0.27	3.71	7.39+0.17	7.23	6.43+0.25	6.4
As	25-40	75	<13	10.8	-	-
Ba	259+6	337	558+10	594	373+16	-
Be	0.5-1.0	0.91	0.4-2.3	1.58	<0.4	-
Ca, %	6.52+0.12	5.64	2.03+0.07	1.92	0.84+0.04	0.78
Cd	10.3+2.7	-	21.7+2.3	-	-	3
Co	13.5+4.5	11.6	<3	10.3	26+41	-
Cr	-	-	-	64.7	59+9	66
Cu	76+8	65.2	34+3	29.7	58+1	66
Fe, %	1.59+0.05	2.25	3.17+0.07	3.87	6.33+0.68	6.83
K, %	1.26+0.02	1.38	2.00+0.12	2.25	1.92+0.12	2.77
Mg, %	2.28+0.05	2.67	1.56+0.04	1.53	0.93+0.07	0.88
Mn	230+6	295	396+8	444	327+25	325
Mo	36-70	36	<10	2.79	146+5	156
Na, %	2.36+0.08	2.11	0.71+0.04	0.66	0.23+0.03	0.30
Ni	-	34.3	-	29.1	119+18	105
P	562+22	1540	429+33	860-1900	138+36	436
Si, %	11.8+0.3	13.8	25.4+0.8	29.2	19.6+1.1	23.3
Ti, %	0.14+0.002	0.25;0.069	0.36+0.01	0.37	0.44+0.03	0.42
V	114+3	124	119+4	116	156+7	157
Zn	85+3	79	99+5	108	76+9	71

TABLE V
EFFECT OF ASHING ON ELEMENT DETERMINATION IN GREEN RIVER SHALE CONCENTRATE

Element, wt %	Claisse Fluxer	Parr Bomb	
		No Ashing	Preashing
Si	11.6	7.04	11.2
Al	3.09	2.28	2.97
Fe	1.76	1.30	1.71
Mg	1.36	1.02	1.18
Ca	4.78	3.75	4.37
Na	1.39	1.05	1.32
K	0.92	0.56	0.88
Ti	0.13	0.03	0.092
P	0.24	0.10	0.15

Determination of Nonmetals

Ion chromatography (IC) has been used for the determination of fluorine, chlorine, nitrogen and sulfur in oil shales and shale oils. This determination also requires dissolution using the

Parr bomb technique to bring the sample into aqueous solution. Determination of these elements in coal analyses has been described previously (3) where the halogens were determined with ion selective electrodes, nitrogen with a chemiluminescent detector and sulfur by X-ray fluorescence. However, all these elements can be simultaneously determined by IC. With the fast separator columns and 0.0024 M Na₂CO₃ + 0.0030 M NaHCO₃ eluent at 2.30 mL/min flow rate, the retention times for F⁻, Cl⁻, NO₃⁻ and SO₄⁻ were found to be 2.5, 3.5, 9 and 10.5 minutes, respectively. Thus, in less than 15 minutes, four anions can be quantitatively determined; significantly less time than required by the other specific techniques. Typical IC results for the shales are given in Table VII. The difficulty of accurately determining the halogens in the rock matrix is evident from the disagreement between the various literature results for the U.S.G.S. standard shales. Previously using this method on coal samples, good agreement was obtained between certified and IC results (20). Unfortunately, the shale standards have not been extensively analyzed and reported in the literature to enable one to form a true picture of their halogen concentrations. The sulfur results by Parr bomb-IC are in good agreement with the published data.

TABLE VI
ANALYSIS OF AUSTRALIAN SHALE AND KEROGEN

Element, ppm	Shale	Kerogen
Al	6.28%	225
As	-	16
Ba	315	14
Ca	1.13%	391
Cl	412	7070
Co	8.6	9
Cr	34	8.9
Cu	34	81
F	604	1800
Fe, %	4.26	2.66
K	9580	25
Li	28	22
Mg	7040	50
Mn	875	19
Na	4860	132
Ni	41	31
Si	17.0%	107
Ti	1880	12
V	98	-
Zn	97	61

TABLE VII
ION CHROMATOGRAPHIC ANALYSIS HALOGENS AND SULFUR IN OIL SHALES

Sample	Fluorine, ppm		Chlorine, ppm		Sulfur, %	
	Literature	Found ^a	Literature	Found ^a	Literature	Found ^a
U.S.G.S. SGR-1	2285 (14)	307±36	92 (14); 45 (15)	1400±87	1.90 (15); 1.64 (14)	1.71±0.05
U.S.G.S. SCO-1	1500 (16); 779 (14, 17)	425±37	1600 (16); 68 (15); 49 (14)	742±26	0.12 (16) 0.06 (14, 15)	0.052±0.001
Green River Kerogen, %	0.22 ^b	0.25	1.64 ^b	1.48	2.68 ^b	2.42

a. Shale results mean of triplicate analysis.

b. Fluorine and chlorine were determined by ion selective electrodes after Parr bomb combustion, and sulfur was determined by Leco SC-32.

Determination of Carbon, Hydrogen and Nitrogen

Methods for the determination of these elements are based on the combustion of oil shale

samples, usually at 1000°C and measuring the CO₂, H₂O and N₂ produced, by different techniques after scrubbing from the gases the halogens, SO₂ and excess oxygen. Various instruments use gravimetry, infrared, or thermal conductivity for final measurements. Comparative performance of several C/H instruments is illustrated in Table VIII. All appear to give reasonably satisfactory results for carbon and hydrogen. The precision of the results appears to be of the order of $\pm 1\%$ of the C, H, N values.

TABLE VIII
DETERMINATION OF CARBON/HYDROGEN IN OIL SHALES

<u>Instrument</u>	<u>Colorado Shale</u>	<u>Australian Shale</u>
<u>Carbon, Wt %</u>		
Hallikainen	20.4 \pm 0.06 (3)	14.4 \pm 0.10 (3)
Leco CHN-600	20.1 \pm 0.11 (28)	14.04 \pm 0.06 (28)
Leco CR-12	19.8 \pm 0.5 (3)	13.6 \pm 0.17 (3)
Perkin Elmer	20.0 \pm 0.10 (3)	13.7 \pm 0.17 (3)
ASTM Combustion	20.4 \pm 0.12 (3)	14.2 \pm 0.17 (3)
<u>Hydrogen, Wt %</u>		
Hallikainen	2.24 \pm 0.01 (3)	2.24 \pm 0.01 (3)
Leco CHN-600	2.15 \pm 0.04 (28)	2.18 \pm 0.04 (28)
Perkin Elmer	2.10 \pm 0.03 (3)	2.16 \pm 0.02 (3)
ASTM Combustion	2.25 \pm 0.02 (3)	2.31 \pm 0.02 (3)

Numbers in parentheses are the replicate number of analyses.

The classical method for nitrogen determination is the Kjeldahl procedure. The method is very precise and well characterized. However, recently, we have found this method to give erroneously low nitrogen results for some oil shale samples. The data in Table IX illustrate this problem. Two samples of Colorado and Australian shales were analyzed by the Kjeldahl procedure in five different laboratories. The same samples were also analyzed by four different instruments in three different laboratories. Good agreement is apparent among all methods for the Australian shale, but for the Colorado shale there are significant differences. The results can be subgrouped as (a) Kjeldahl data and (b) instrumental data. All of the Kjeldahl results are close, but they are low roughly by a factor of 2 compared to the instrumental techniques. The different instruments have also produced remarkably close results. We believe the non-aminoid nitrogen compounds present in the oil shales are not being determined by the Kjeldahl procedure. Attempts to obtain higher Kjeldahl results by more vigorous digestion did not succeed. We believe it is advisable to use the instrumental methods rather than the Kjeldahl procedure for the determination of true nitrogen content of oil shales. The fact that the Australian shale gave equivalent results by chemical and instrumental methods, but the Colorado shale did not, probably indicates the presence of different specific nitrogen compounds in oil shales as a result of their different genesis.

Determination of Sulfur Forms

A knowledge of the forms and the concentrations of sulfur present in the oil shales is desirable for determining the composition, heating value, thermal degradation properties and eventually relating the sulfur forms found in the shale to those found in the oil. The separation and analysis methods were primarily developed for coal products (ASTM D-2492 procedure). However, when applied to oil shales, this procedure has resulted in reproducible but erroneous results. Smith, et al (18) have pointed out the drawbacks of this procedure and have devised a new procedure based on the HClO₄ dissolution of sulfate and LiAlH₄ reductive dissolution of pyrite. However, many of the laboratories in the U. S. are still using the ASTM procedure. We found the ASTM method to overestimate the sulfate and pyrite forms, thus, resulting in underestimating organic sulfur, even giving negative values in some cases. Our attempts to obtain better results by using a variety of other decomposition aids have not met with success so far. We have been reluctant to apply the U. S. B. M. procedure (18) in our laboratory on a routine basis because of the hazardous nature of HClO₄ and particularly LiAlH₄. The best alternative to the ASTM and U. S. B. M. procedures appears to be the demineralization-kerogen isolation procedure for the determination of pyrite. This U. S. B. M. procedure (19) uses HCl-HF to remove the carbonate and the silicate minerals in the shales, leaving the kerogen residue with only pyrite as the mineral contaminant. In the proposed pyrite determination procedure, this isolated kerogen is analyzed for its iron content by

dissolution in HNO_3 and subsequent AAS or ICPES measurement. A single analysis carried out by this procedure on two shale samples gave results that were definitely lower than the ASTM procedure, but much closer to the LiAlH_4 procedure (Table X). Further work needs to be carried out to determine the quantitative validity of the isolated kerogen procedure.

TABLE IX
DETERMINATION OF NITROGEN IN OIL SHALES

Method	Wt % N	
	Colorado Shale	Australian Shale
Kjeldahl-Lab A	0.42±0.02 (3)	0.38±0.01 (3)
Kjeldahl-Lab B	0.40±0.01 (3)	0.38±0.01 (3)
Kjeldahl-Lab C	0.42±0.00 (3)	0.39±0.02 (3)
Kjeldahl-Lab D	0.49±0.01 (3)	0.41±0.01 (3)
Kjeldahl-Lab E	0.50±0.05 (2)	0.57±0.01 (2)
Leco NP-28	0.70±0.01 (3)	0.42±0.01 (3)
Leco CHN-600	0.79±0.004 (28)	0.57±0.04 (28)
Perkin Elmer	0.79±0.05 (3)	0.46±0.03 (3)
Mettler	0.65±0.02 (3)	0.43±0.01 (3)
Mean-All	-	0.46±0.08
Mean-Kjeldahl (a)	0.45±0.05	0.43±0.08
Mean-Instrumental (b)	0.74±0.06	0.47±0.07
ASTM Kjeldahl Repeatability	0.05	0.05

Numbers in the parentheses are the replicate number of analyses.

TABLE X
DETERMINATION OF PYRITE IN OIL SHALES

Method (Replicates)	Colorado Shale	Australian Shale
ASTM (11)	0.68±0.09	0.79±0.07
LiAlH_4 (3)	0.43±0.02	0.64±0.01
Demineralization (1)	0.41	0.48

In summary, the methods developed using ICPES and IC and other thermal decomposition procedures for metals and nonmetals, are now routinely used at Exxon's Baytown Research and Development Division for the characterization of a large number of oil shales and shale products.

ACKNOWLEDGMENTS

I would like to express my thanks for helpful discussions and encouragement to R. B. Williams and R. I. Botto. Able technical assistance was provided by D. M. Pond, H. L. Chandler, N. J. Bryan and R. B. Cornett.

LITERATURE CITED

- (1) Culbertson, W. C. and Pitman, J. K., U.S.G.S. Prof. Paper, 820, 497-503 (1973).
- (2) Nadkarni, R. A., Anal. Chem., 52, 929-935 (1980).
- (3) idem, Amer. Lab., 13 (8), 22-29 (1981).
- (4) idem, Anal. Chim. Acta., 135, 363-368 (1982).
- (5) Fruchter, J. S., Wilkerson, C. L., Evans, J. C. and Sanders, R. W., Environ. Sci. Technol., 14, 1374-1381 (1980).
- (6) Shendrikar, A. D. and Faudel, G. B., *ibid.*, 12, 332-334 (1978).
- (7) Lechler, P. J. and Leininger, R. K., Jarrell-Ash Plasma Newslett., 2 (1), 8-10 (1979).
- (8) Amini, M.K., DeFreese, I. D. and Hathaway, L. R., Appl. Spectrosc., 35, 497-501 (1981).
- (9) Botto, R. I., Jarrell-Ash Plasma Newslett., 2 (2), 4-8 (1979).
- (10) idem, Proc. Int. Conf. Dev. At. Plasma Spectrochem. Anal., Puerto Rico, in press (1980).
- (11) Nadkarni, R. A., Botto, R. I. and Smith, S. E., At. Spectroscopy (in press).
- (12) Bernas, B., Anal. Chem., 40, 1682-1686 (1968).
- (13) Flanagan, F. J., U.S.G.S. Prof. Paper, 840 (1976).
- (14) Evans, K. L., Tarter, J. G. and Moore, C. B., Anal. Chem., 53, 925-928 (1981).
- (15) Fabbi, B. P. and Espos, L. F., U.S.G.S. Prof. Paper, 840, 89-93 (1976).
- (16) Schultz, L. G., Pourtelot, H. A. and Flanagan, F. J., U.S.G.S. Prof. Paper, 840, 21-23 (1976).
- (17) Malchacek, V., Rubeska, I., Sixta, V. and Sulcek, Z., U.S.G.S. Prof. Paper, 840, 73-77 (1976).
- (18) Smith, J. W., Young, N. B. and Lawlor, D. L., Anal. Chem., 36, 618 (1964).
- (19) Smith, J. W., U. S. Bureau of Mines Rept. Investig. (1961).
- (20) Nadkarni, R. A., Anal. Chim. Acta (accepted for publication).

SYMPOSIUM ON GEOCHEMISTRY AND CHEMISTRY OF OIL SHALE
PRESENTED BEFORE THE DIVISIONS OF FUEL CHEMISTRY, GEOCHEMISTRY,
AND PETROLEUM CHEMISTRY, INC.
AMERICAN CHEMICAL SOCIETY
SEATTLE MEETING, MARCH 20 - MARCH 25, 1983

ORGANIC-MINERAL MATTER INTERACTIONS IN GREEN RIVER OIL SHALE

By

K. M. Jeong and T. P. Kobylinski
Gulf Research & Development Company, Pittsburgh, Pennsylvania 15230

INTRODUCTION

The nature of the association between kerogen or bitumen and the mineral matter phase in oil shales has not been well characterized, yet these interactions are fundamental to any proposed separation and oil recovery procedure. Analogous information has been reported concerning marine sediments (1), but relatively little data are currently available relevant to the organic-mineral matter interaction in oil shales (2-5). Therefore, this study proposed to investigate this problem using a chemical extraction procedure with spectroscopic (FTIR and NMR) identification of the various separated fractions.

Samples of Colorado Green River oil shale (C-a tract, Mahogany zone) were treated in a series of acid/ether extractions in order to preferentially disassociate the mineral matter phase. It is known that carbonate minerals are dissolved by HCl solutions and that pure HF or HF/HCl mixtures effectively remove silicate minerals, quartz, and clay minerals (6, 7). Bitumen, the organic fraction soluble in the common organic solvents, was removed by the Soxhlet extraction method. The fraction of the total mineral content encapsulated by kerogen and thus not accessible to an acid treatment is estimated to be insignificant based on the results obtained by this study.

The relative amounts of acid/ether extracted organics isolated with both the carbonate and silicate minerals were determined. In addition, it was noted that certain fractions of the bitumen were trapped by these two mineral constituents. On the basis of these data, inferences are made concerning possible types of bonding between kerogen and the inorganic mineral matter matrix.

EXPERIMENTAL

The chemical extraction procedure is summarized in flowchart form in Figure 1. A series of acid and ether extractions were used to treat samples of Colorado Green River oil shale (C-a tract Mahogany zone) of three different richnesses: 25, 31, and 44 GPT. These samples were prepared, first, by standard pulverizing and sieving procedures of mine-run oil shale and then, by separation according to organic content using the heavy media liquids gravitational separation technique (8). The final mesh size was 100 x 200.

Bitumen was extracted from dried oil shale using the Soxhlet procedure: 7:3 mixture of benzene:methanol. The resulting fraction was treated with 6N HCl and any iron contamination introduced during the initial grinding step was removed by mechanical magnetic separation. The HCl aqueous phase was further extracted with NaOH yielding three fractions of different acidities: pH = 1, 6.5, >11.

The bitumen, carbonate-free oil shale was neutralized to pH ~5 and the Soxhlet extraction procedure repeated to completely remove physically trapped bitumen. The remaining shale was extracted with a 3:1 mixture of 50% HF:6N HCl followed by an ether extraction and separation of three pH fractions. The Soxhlet extraction procedure was again repeated.

The effectiveness of the chemical extraction procedure was monitored by elemental analysis results obtained by DC arc emission spectroscopy (ARL Model 2100 Film 2m Emission Spectrograph). The structural composition of the various filtrate fractions was characterized using both FTIR (Digilab FTS-20E) and NMR (FT80A, Varian Associates) spectroscopy. In addition, the mineral and elemental compositions of the original oil shale samples were determined from X-ray diffraction (Phillips APD-3500) and energy dispersive X-ray fluorescence (Kevex Model 0700) data. Low-temperature ash samples were prepared using a 13.56 MHz radio frequency ashers (LFE Corporation, Model LTA 504).

RESULTS AND DISCUSSION

Bulk Mineralogical Composition

Elemental analysis of organic C, H, N, O, and S concentrations indicated that 13-23% of the

original Green River oil shale samples was organic matter. The remaining 77-87% consisted of various minerals, primarily ankerite, dolomite, aragonite, quartz, albite, analcime, and illite (see Table I). A concentration dependence as a function of shale richness was found for certain types of minerals. For example, the relative concentrations of clay minerals (illite/smectite) and to a certain extent albite increase with increasing organic carbon content, whereas minerals such as calcite and aragonite are characterized by an inverse relationship.

The low-temperature ash results for the clay mineral constituents were opposite to the expected trend exhibited by the remaining minerals. The clay mineral concentration was found to decrease with low-temperature ashing in contrast to the concentrations of the other minerals which increased in proportion to the organic content removed by the ashing procedure. This irregular feature may be attributed to layer collapse as a result of either organic oxidation (9) or the removal of an associated water phase.

TABLE I
BULK MINERALOGY OF GREEN RIVER FORMATION Ca-TRACT,
MAHOGANY ZONE, OIL SHALE IN WEIGHT PERCENT

Sample Richness (GPT)	Analcime	Clay ^a	Quartz	Feldspar		Ankerite/ Dolomite		Pyrite	TDB ^b	Trace	
				Kspar	Albite	Calcite	Dolomite				
25	Orig	14	8	14	6	5	30	14	<1	.34	Siderite
	LTA	18	7	13	8	9	29	14	<1	.44	Gypsum
31	Orig	12	10	16	<1	10	29	7	<1	.42	Gypsum
	LTA	19	7	14	<1	18	31	10	<1	.34	Aragonite
44	Orig	10	19	15	<1	13	20	2	2	.53	Marcasite
	LTA	14	8	17	<1	24	28	4	2	.75	

a. Clay minerals consist primarily of a mixed layer illite/smectite.

b. Total diffracting intensity, the sum of all fractions before normalization.

Chemical Extraction Results

The HCl extraction step effectively separated carbonate minerals from the oil shale samples as indicated by elemental analysis data summarized in Table II. Approximately 99% of the elemental Ca and approximately 94% of the Mg in the 44 GPT oil shale were removed. On the basis of experimental results of the HCl/ether extracts, it was determined that at least 0.45 and 0.38 wt% of the total organics in the 25 and 44 GPT dried oil shale, respectively, are recoverable (see Table III). Therefore, there appears to be a rather intimate association between this organic fraction and the carbonate mineral matrix. It is also reported that 3.40 and 3.65 wt% of the total organics in these same two samples are trapped by the carbonate mineral matrix and only released after the HCl acid treatment.

The second acid extraction step, leaching by HF/HCl, was equally effective, resulting in the separation of approximately 96% of the elemental Si and approximately 86% of the Al (see Table II). The total amount of organics extracted by the HF/ether combination was at least 1.72 and 1.34 wt% of the initial total organic content of the 25 and 44 GPT samples, respectively. Physisorption by the silicate mineral matrix occurred to the extent that 1.64 and 2.00 wt% of the total organics were trapped yet recoverable by the third Soxhlet extraction. The results of the preferential disassociation procedure are summarized in Table III.

It is determined that approximately four times more bitumen-free organic matter is associated with the silicate mineral matrix than with carbonate minerals. This organic matter is judged to be an interfacial layer between kerogen and the inorganic mineral matrix. The inter-layer structures isolated with either the carbonate or silicate minerals have slightly modified properties compared to the bulk kerogen material due to the presence of mineral binding forces and therefore, are more properly classified as a form of kerogen. The greater majority of the bitumen portion of these Green River oil shale samples was removed by Soxhlet extraction.

It was determined that 27-32 wt% of the bitumen is physically trapped by the mineral matter matrix and to a larger extent by carbonate than silicate minerals. These results are in support of a previous study (3) which suggested a strong interaction between carbonate minerals and carboxylic acid functional groups in Green River oil shale bitumen. In addition, both high-pressure CO₂ dis-aggregation (4) and cation exchange (5) experiments have indicated a close coupling between the mineral matrix and bitumen. The bitumen fractions separated in this work during the chemical

treatment were not specifically analyzed for various chemical components, but the Fischer Assay results summarized in Table III indicate a relatively strong association, particularly in the form of physical trapping, between bitumen and the carbonate mineral matrix.

TABLE II
MULTI-ELEMENTAL ANALYSIS (WT%) OF ORIGINAL AND TREATED
GREEN RIVER OIL SHALE SAMPLES^{a, b} (44 GPT SAMPLE)

Element	Original Oil Shale	Benzene/Methanol Treated Oil Shale	HCl-Treated Oil Shale	HF/HCl-Treated Oil Shale
Weight Fraction	100.0	97.1	68.6	29.6
A1	6.4	5.9	4.6	0.64
As*	87.1 ppm	88.1 ppm		
B	0.021	0.015	0.013	
Ba	0.11		0.08	0.05
Ca	5.1	5.2	0.04	0.04
Cr	0.03	0.03	0.01	0.01
Cu	0.003	0.004	0.003	0.003
Fe	3.6	3.7	1.2	0.96
K	1.9	2.0	1.2	0.23
Mg	4.4	4.5	0.18	0.17
Mn	0.083	0.074	0.013	0.006
Mo				0.005
Na	0.57	0.59	0.04	0.04
Ni	0.018	0.015	0.009	0.003
Si	15	15	14	
Sr	0.08	0.07		0.01
Ti	0.28	0.30		0.07

a. DC Arc Emission Spectroscopy, values given in wt%

b. Mahogany zone C-a tract, 100 x 200 mesh oil shale

* Instrumental Neutron Activation Analysis

TABLE III
ORGANIC MATTER DISTRIBUTION OF TREATED OIL SHALE
EXTRACTS^a BASED ON WT% OF TOTAL ORGANICS

	25 GPT Oil Shale	31 GPT Oil Shale	44 GPT Oil Shale
Bitumen I	13.48	16.14	11.80
II	3.40	3.44	3.65
III	<u>1.64</u>	<u>0.05</u>	<u>2.00</u>
Total Bitumen	18.52	19.63	17.45
Carbonated Associated Organics			
Ether Extract I A/N	0.15	0.18	0.18
Ether Extract I N	0.21	0.19	0.13
Ether Extract I B	<u>0.09</u>	<u>0.11</u>	<u>0.07</u>
Total Extracts I	0.45	0.48	0.38
Silicate Associated Organics			
Ether Extract II A/N	1.33	0.26	0.50
Ether Extract II N	0.09	0.17	0.62
Ether Extract II B	<u>0.30</u>	<u>0.02</u>	<u>0.22</u>
Total Extracts II	1.72	0.45	1.34

a. Total organic concentrations based on elemental analysis are determined to be 13.46, 16.24, 22.93 wt% for 25, 31, and 44 GPT oil shales, respectively.

Spectroscopic Analysis

During the chemical extraction procedure, several major IR bands were monitored in order to determine the extent, if any, of chemical rearrangement. Various references in the literature

have cited the reaction of both hydrochloric and hydrofluoric acids with organic compounds resulting in the modification of specific chemical properties. These reactions include, for example, the hydrolysis and addition reactions of quinones, esters, and olefins with HCl (10,11) in addition to condensation reactions involving HF and olefinic and aromatic compounds (11). The spectroscopic data of the filtrate fractions indicated that HCl or HF generated reactions did not occur to an appreciable extent and that insignificant chemical rearrangement occurred. This is an important point, since it implies that the recoverable organic matter associated with either the carbonate or silicate mineral matrix is of the form which constitutes the *in situ* interfacial layer between kerogen and the inorganic mineral matrix.

FTIR characterization of oil shale was based on the assignment of several IR bands (12) and their respective absorbances (13) (see Table IV). These results, in addition to NMR data discussed below, indicate several similarities as well as differences in the structural composition of the organic matter associated with either mineral constituent studied here. A comparison of FTIR spectra of two ether extract fractions is shown in Figure 2. Both sets of ether extracted organic matter contained trace amounts of molecular water, alcohols, and aromatic compounds. The tentative assignment of the 1125 and 1030 cm^{-1} bands to aryl-alkyl ether groups (14) suggests a preferential silicate--aryl-alkyl ether association, since these bands were identified in the HF/HCl fractions but not in the HCl fractions.

The major constituent of the acid/ether extracted organics was determined to be paraffinic compounds. The $[\text{CH}_3]/[\text{CH}_2]$ ratios determined from FTIR spectra were found to increase with increasing pH for the ether extracted organics associated with the silicate mineral matrix: 0.40, 0.44, and 0.54. This result suggests that the more highly branched compounds and/or the small molecules isolated with the silicate minerals are weaker Lewis acids. The relatively high $[\text{CH}_3]/[\text{CH}_2]$ ratios reported are consistent with the high hydrogen content of Green River oil shales (atomic H/C ~ 1.5 -1.6). This property is also attributed to the observation of a strong band at 720 cm^{-1} due to skeletal vibrations of long chain aliphatic molecules. A relatively higher concentration of aliphatic chains was found in the organic group associated with the silicate mineral matrix.

TABLE IV
IR BAND ASSIGNMENTS

ν (cm^{-1})	Vibrational Mode
3430	OH stretch
3100-3000	CH stretch (aromatics)
2962	Asymmetric CH_3 stretch
2930	Asymmetric CH_2 stretch
2872	Symmetric CH_3 stretch
2860	Symmetric CH_2 stretch
1735	C=O stretch (esters)
1712	C=O stretch (ketones, aldehydes)
1630	C=O stretch (bridged quinones)
1620	C=C stretch
1455	Asymmetric CH_2 and CH_3 bend
1185	C-O stretch
1125, 1030	C-O vibration (aryl-alkyl ethers)
890	$\text{CH}_2=\text{C}$ bend
870, 820, 750	Out of plane deformation aromatic CH
720	Skeletal vibration, straight chains >9 CH_2

A correlation between the C=C stretching vibration and the carbonate mineral matrix was established. Although approximately a tenth as intense as the CH_3 symmetric bending vibration, the 1620 cm^{-1} band due to C=C stretching was identified in all three HCl extracts but in none of the HF/HCl spectra. Further evidence of a preferential association between olefinic hydrocarbons and carbonate minerals was provided by the significantly larger $\text{CH}_2=\text{C}/\text{CH}_2 + \text{CH}_3$ ratio in the case of the HCl spectra. These data are in contrast to the results obtained by Spiro (2) for some Israeli oil shales which reported relatively higher C=C/ CH_3 absorbance ratios for organic matter associated with silicates, suggesting a preferential silicate-olefin interaction. This discrepancy may be attributed to the choice of different oil shales used in both studies.

On the basis of the C=O and C-O stretching vibrations of ester functional groups, a major distinction was determined concerning ester-mineral matter interactions. Significantly larger concentrations of esters were identified in the HF/ether extracts indicating a closer association between esters and silicate minerals. In addition to esters, a relatively larger ketone and aldehyde

content was found with those organics associated with the silicate mineral matrix. The results of Spiro (2) are inconclusive concerning a preferential ester-mineral matter association.

The aromatic content of the original oil shale was determined by NMR spectral analysis to be considerably larger than that of the acid extracted organics. This result is consistent with FTIR data. The NMR results summarized in Table V for the 44 GPT sample also indicate that the aromatic content of the bitumen fraction separated in the first Soxhlet extraction is lower than that of the original oil shale but comparable to that of both sets of acid/ether extracts. However, distinct spectral differences were observed between the initially separated bitumen and the neutral organic fraction isolated with the silicate minerals (see Figure 3). From these differences it can be concluded that the organic matter recovered from the ether extracts of the HCl and the HF/HCl mixture subsequent to the initial Soxhlet extraction is not residual bitumen. The majority of the bitumen was removed initially in the extraction procedure and the organic matter isolated in association with carbonate and silicate minerals is a portion of the kerogen-mineral matter interfacial layer.

TABLE V
¹H-NMR SPECTROSCOPIC ANALYSIS

	<u>Aromatic</u>	<u>Paraffinic</u>
Total Organics in Oil Shale	~20%	~80%
H ₂ O Soluble Organics	<0.1%, mainly monoaromatics	>99%, some olefins, some polar (possibly ester)
Bitumen I	~5.2%, mono and diaromatics	94.8%, methyl, alkyl substituted paraffinic chains (>C ₁₆), 2/3 paraffinic and 1/3 naphthenic
Carbonate Associated Organics ^a		
Ether Extract I, A/N	~3%, mainly monoaromatics	~97%, branched paraffins
Ether Extract I, N	~2%, mainly monoaromatics	~98%, branched paraffins some olefins
Ether Extract I, B	0.2%, mostly diaromatics	~99.8%, highest [CH ₃]/[CH ₂], some olefins
Silicate Associated Organics ^a		
Ether Extract II, A/N	~3%, mono and diaromatics	~97%, paraffinic chains (~C ₁₀), some conjugated olefins
Ether Extract II, N	~1.8%, mainly monoaromatics	~98.2%, small molecules, regularly repeating structural type ~1% olefins
Ether Extract II, B	~1.8%, mainly monoaromatics	~98.2%, long-chain paraffins (~C ₁₀), polar-functional groups

a. Abbreviations: A/N - acidic/neutral, N - neutral, B - basic

Both NMR and FTIR results indicated that the organics associated with carbonate minerals and those associated with silicate minerals are predominantly of paraffinic composition. The NMR data identified approximately equal relative aromatic concentrations in both sets of organic matter in disagreement with Spiro's (2) results for Israeli oil shales. In contrast, Spiro's (2) data indicated that organic matter associated with silicate minerals is composed of relatively more aromatic as well as more polar compounds in comparison to the organic-carbonate group. As mentioned above concerning the FTIR data, this apparent difference in aromatic content between Colorado and Israeli oil shales may be the result of dissimilar mineralogical compositions and/or geochemical properties of the two oil shales (15, 16).

The paraffinic carbon composition was determined to be similar for both groups of acid/ether extracted organics. The relative concentrations of mono- and diaromatic compounds were also comparable. In addition, the NMR analysis identified chain lengths of about C₁₀ with those organics associated with silicate minerals and branched paraffins with the carbonate mineral group. Long chain lengths and branched compounds having a high CH-activity are two important factors which have been reported to affect adsorption processes (17, 18). Therefore, it is not inconceivable that adsorption or a slightly stronger trapping interaction is responsible for certain types of organic-mineral matter bonding.

Organic-Mineral Matter Interactions

The results obtained by this study seem to suggest an equal preference for chemical bonding

as for physisorption. Although one or the other type of interaction cannot be definitively excluded, several inferences are possible. The presence of substantial concentrations of esters in the silicate-organic matter group suggests strongly bonded ester-silicate complexes. However, there remains the possibility that the ester functional group may be providing the linkage necessary for adsorption. Physisorption of esters by the silicate mineral matrix cannot be ruled out, but appears to be rather unlikely considering the bonding forces usually associated with this functional group.

The organic matter-carbonate mineral interaction may preferentially involve chemical bonding between energy rich olefinic functional groups and minerals such as CaCO_3 and $\text{CaCO}_3\text{MgCO}_3$. The relatively large concentration of branched paraffins identified with the carbonate mineral group would seem to suggest an adsorption type of interaction on the basis of these compounds' high CH-activity. Similarly, adsorption of long chain aliphatic compounds on silicate minerals is inferred from the NMR results. In the last two cases, physisorption is also possible, but adsorption and physisorption would seem to be more likely than the formation of chemical bonds. However, hydrogen bonding and other similar covalent or ionic interactions cannot be disregarded. The specific organic structures identified are a portion of the interfacial layer formed between kerogen and the mineral matter, and thus, the possible associations discussed in this section refer to interactions between the carbonate and silicate minerals and a form of kerogen.

SUMMARY

The problem of organic-mineral matter bonding, particularly that involving kerogen, although at first glance rather intractable, has been partially reduced in scale by the data presented here. The chemical extraction technique outlined earlier proved to disassociate successfully in a step-wise manner both carbonate and silicate minerals from several oil shale samples of different richness. The organic matter recovered subsequent to the initial Soxhlet extraction was shown to be bitumen-free.

It was determined that approximately four times more bitumen-free organic matter is associated with silicate minerals than with carbonate minerals. The major structural constituent of the various filtrate fractions was paraffinic compounds. However, spectroscopic analysis indicated relatively larger concentrations of olefins and branched paraffins with the acid/ether extracted organics associated with the carbonate minerals. The silicate mineral matrix was determined to interact with a bitumen-free organic interfacial layer containing relatively more esters, ketones, and long chain aliphatic compounds. In addition, trapping of bitumen-free organic matter was observed, particularly in the case of the carbonate mineral matrix. These interactions involving carbonate and silicate minerals are descriptive of the binding forces in Green River oil shale as they pertain to the interfacial layer between kerogen and the inorganic mineral matrix.

ACKNOWLEDGMENTS

This work was supported by Gulf Research and Development Company. The authors gratefully acknowledge the technical assistance of Mr. D. L. Bash and Dr. J. F. Patzer who obtained the samples for this study. We also appreciate many helpful discussions with Dr. J. F. Patzer and Dr. A. Bruce King.

Figure 1.
 Preferential organic-mineral matter
 disassociation by chemical methods

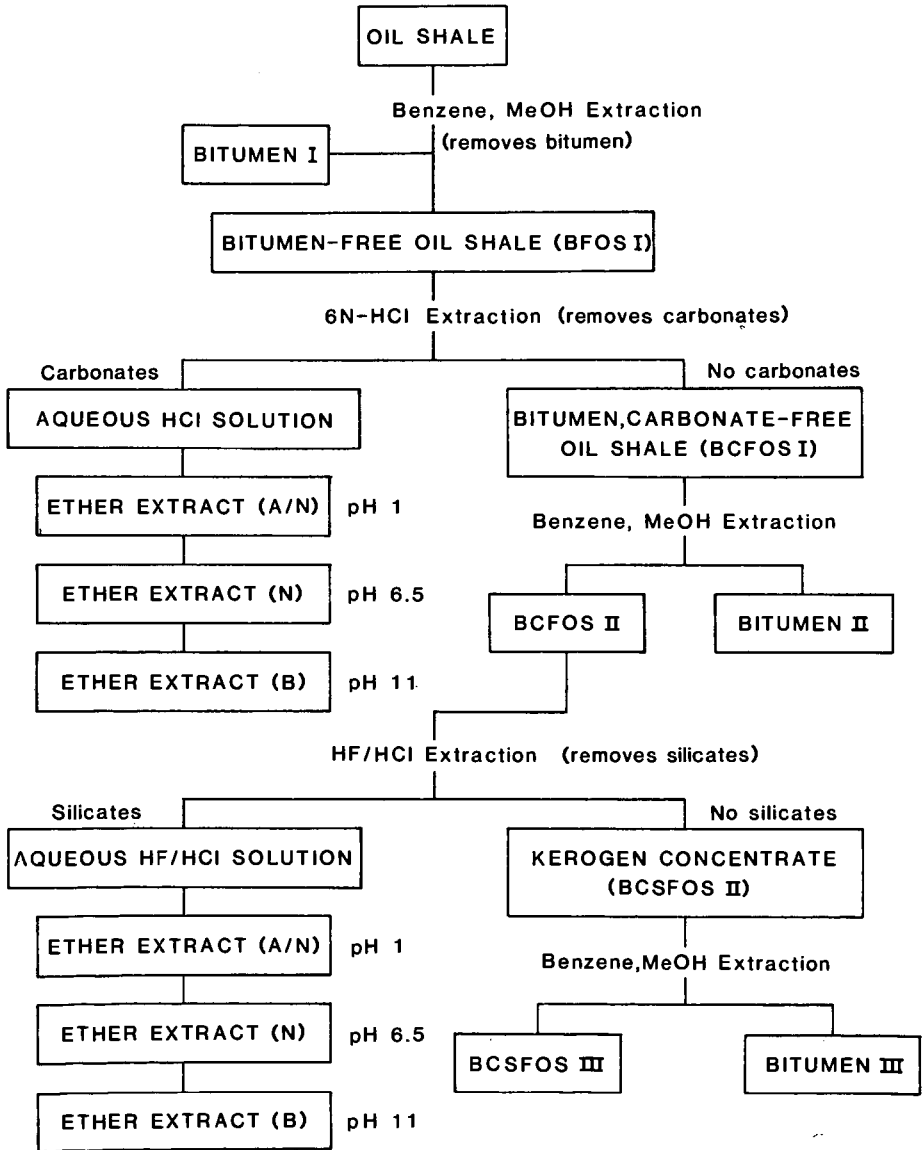


Figure 2. FTIR Spectra of ether extracted (at pH 6.5)
HCl (a) and HF (b) fractions (44 GPT Sample)

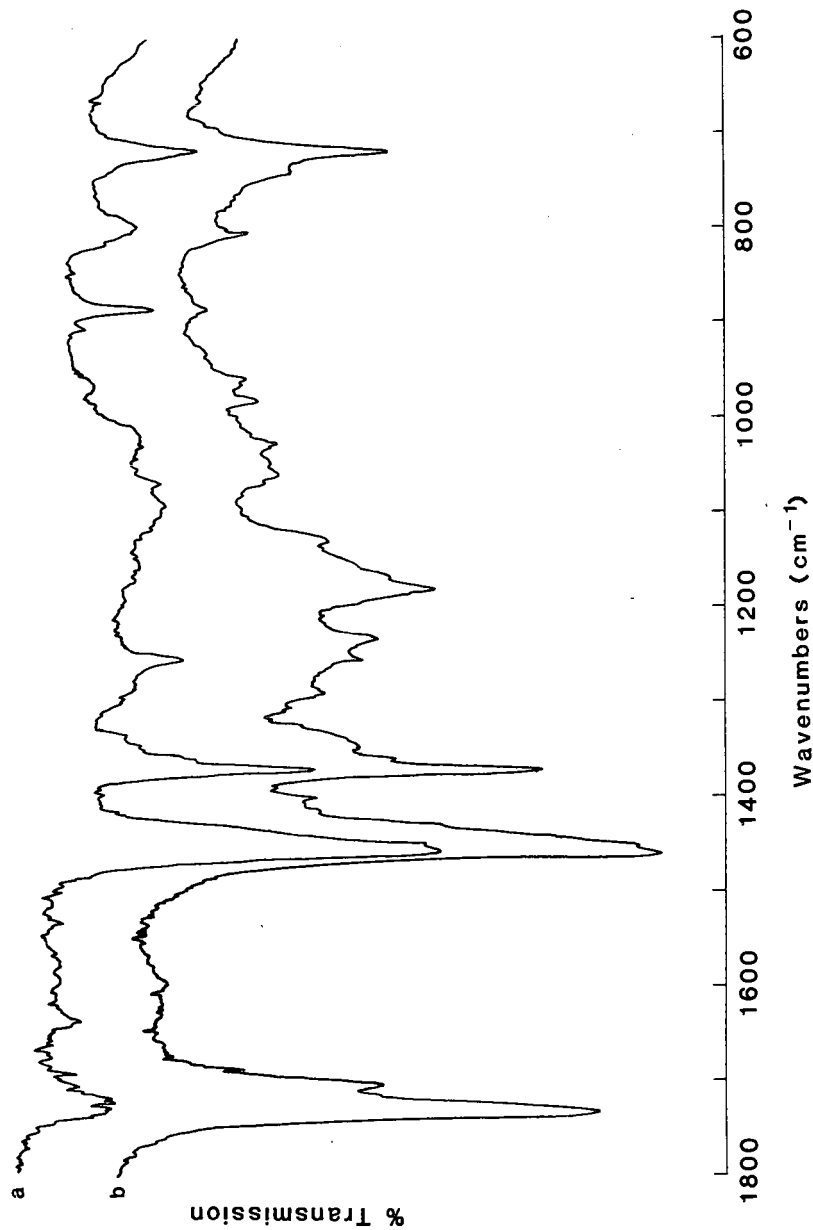


Figure 3a. ¹H-NMR Spectrum of neutral ether extracts of HF/HCl treated oil shale filtrate (44 GPT Sample)

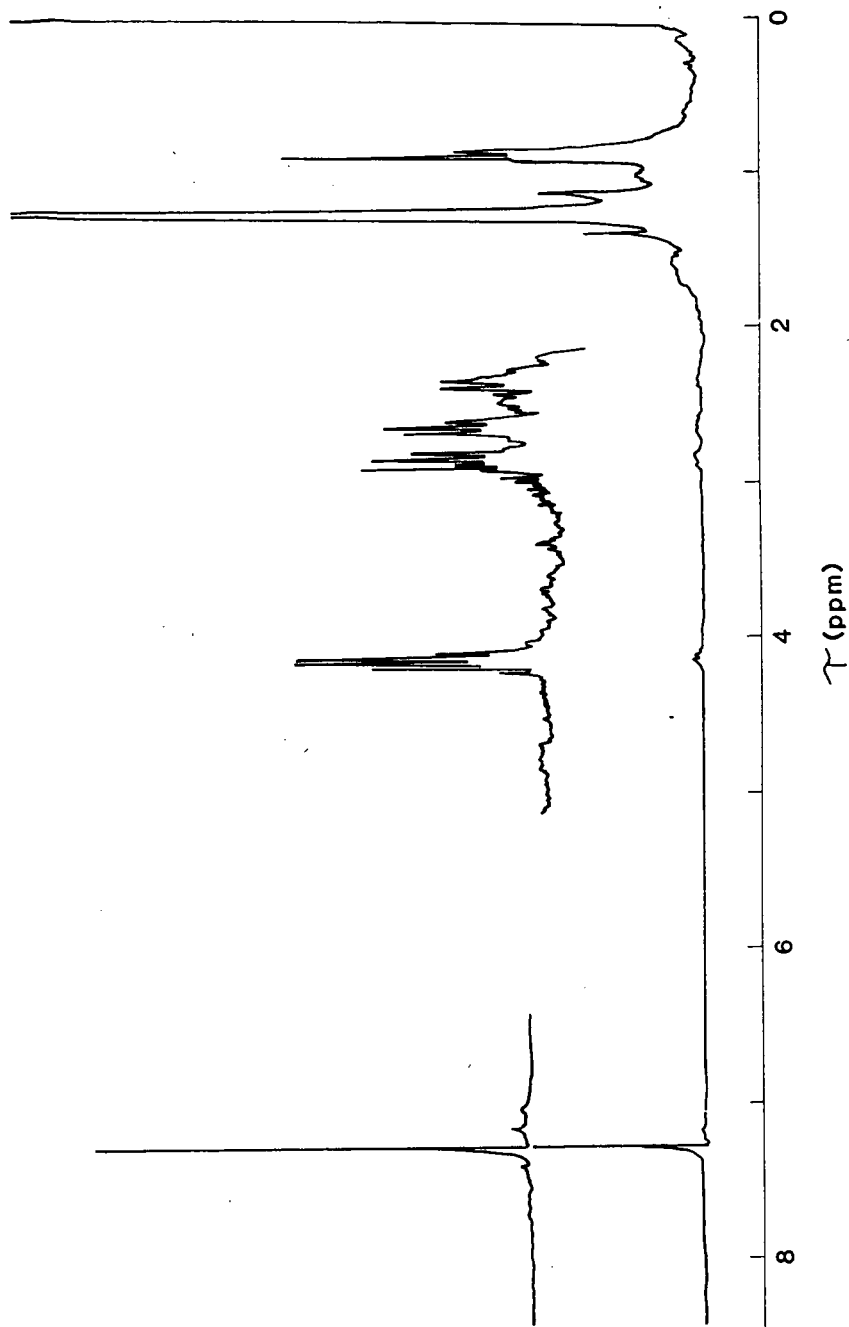
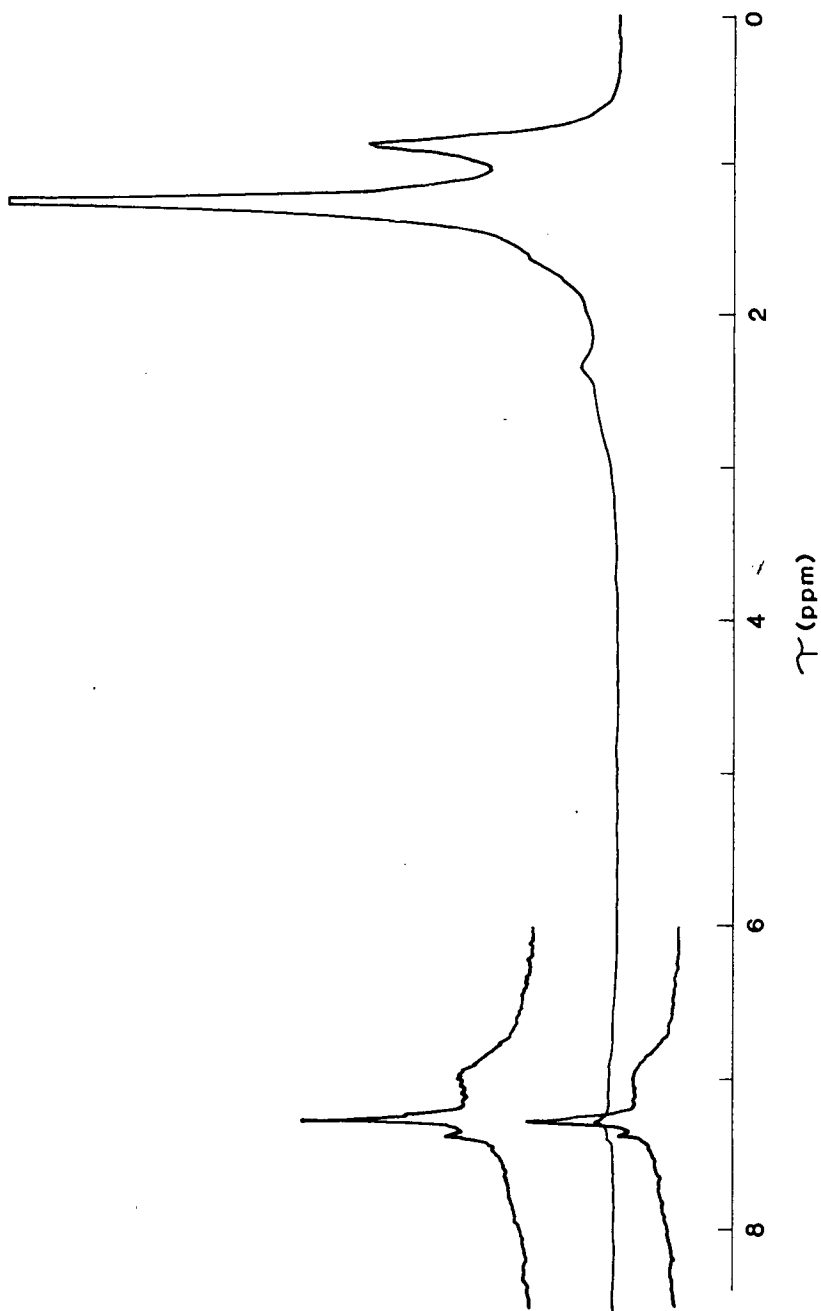


Figure 3b. ¹H-NMR Spectrum of bitumen from 44 GPT Green River
(Mahogany Zone) oil shale



LITERATURE CITED

- (1) a. Aizenshtat, Z., Baedecker, M. J., and Kaplan, I. R., *Geochim. et Cosmochim. Acta*, 37, 1881 (1973).
 b. Brown, F. S., Baedecker, M. J., Nissenbaum, A., and Kaplan, I. R., *Geochim. et Cosmochim. Acta*, 36, 1185 (1972).
 c. Nissenbaum, A., Baedecker, M. J., and Kaplan, I. R., *Geochim. et Cosmochim. Acta*, 36, 709 (1972).
- (2) Spiro, B., *Chem. Geol.*, 31, 27 (1980).
- (3) Vandegrift, G. F., Wimans, R. E., Scott, R. G., and Horwitz, E. P., *Fuel*, 59, 627 (1980).
- (4) Vandegrift, G. F., Wimans, R. E., and Horwitz, E. P., *Fuel*, 59, 634 (1980).
- (5) Rouxhet, P. G., and Robin, P. L., *Fuel*, 57, 533 (1978).
- (6) Saxby, J. D., *Chem. Geol.*, 6, 173 (1970).
- (7) Durand, B., and Nicaise, G., in "Kerogen-Insoluble Organic Matter from Sedimentary Rocks", Editions Technip, Paris, pp. 35-53 (1980).
- (8) Larson, O. A., Schultz, C. W., and Michaels, E. L., in "Oil Shale, Tar Sands, and Related Materials", Am. Chem. Soc. Symp. Ser., 163, 139 (1981).
- (9) Van Olphen, H., "An Introduction to Clay Colloid Chemistry", Second edition, John Wiley and Sons, New York (1977).
- (10) Fieser, L. F., and Fieser, M., "Organic Chemistry", Third Edition, Reinhold, New York (1956).
- (11) Hickinbottom, W. J., "Reactions of Organic Compounds", Third Edition, Longman, London (1957).
- (12) Bellamy, L. J., "The Infrared Spectra of Complex Molecules", Third Edition, Chapman and Hall, New York (1975).
- (13) Matkovsky, P. E., Belova, V. N., Brikenshtein, H. A., Dyachkovsky, F. S., Denisova, Z. A., and Kissin, Y., *Yvsokomol. Soedim.*, A17, 2, 252 (1975).
- (14) Briggs, L. H., Cook, L. D., Fales, H. M., and Wielman, W. C., *Anal. Chem.*, 29, 904 (1957).
- (15) Spiro, B., *Geol.*, 25, 67 (1979).
- (16) Desborough, G. A., Pitman, J. K., and Huffman, C., *Chem. Geol.*, 17, 13 (1976).
- (17) Hoffman, R. W., and Brindley, G. W., *Geochim. et Cosmochim. Acta*, 20, 15 (1960).
- (18) Allen, T., and Patel, R. M., *J. Appl. Chem.*, 20, 165 (1970).

SYMPOSIUM ON GEOCHEMISTRY AND CHEMISTRY OF OIL SHALE
PRESENTED BEFORE THE DIVISIONS OF FUEL CHEMISTRY, GEOCHEMISTRY,
AND PETROLEUM CHEMISTRY, INC.
AMERICAN CHEMICAL SOCIETY
SEATTLE MEETING, MARCH 20 - MARCH 25, 1983

A COMPARISON OF MINERAL REACTIONS FOR
TWO COLORADO OIL SHALE SAMPLES

By

L. G. Thompson and W. J. Thomson
Department of Chemical Engineering, Washington State University
Pullman, Washington 99164-2710

INTRODUCTION

Second generation surface oil shale retorting processes will undoubtedly utilize the residual char on the spent shale leaving the retort. Whether this is done by combustion (1) or steam gasification (2) the temperatures will be sufficiently high that mineral reactions can occur to a significant extent. The more common mineral reactions include dolomite and calcite decomposition as well as solid-solid reactions between mineral carbonates and quartz to form various silicates. The latter reactions proceed at surprisingly fast rates in western shale even at mild temperatures (> 950°K). This is probably due to the small grain sizes (1-10 μ) inherent in western shale (3) which provide for unusual mobility and reactivity.

A knowledge of the mineral reaction rates is important to efficient oil shale processing because the decomposition reactions are highly endothermic and the reaction products can affect the disposal strategy for the shale ash. To date the most extensive study of mineral reaction rates in western oil shale has been conducted by the oil shale group at Lawrence Livermore Laboratory (4,5). Using a 22 GPT oil shale sample from the Anvil Points area, they developed reaction rate expressions for dolomite and calcite decomposition as well as for the formation of silicates which they took to be a reaction between quartz and calcite. Other investigators (6) however, report only the formation of calcium-magnesium silicates.

Because the behavior of calcite appears to be instrumental to the formation of silicates, we decided to investigate the mineral reactions which take place in an oil shale sample which was low in free calcite. This sample, a core sample from the C-a tract, (designated "C-a") has a higher calcium concentration than a sample from the Parachute Creek Member in western Colorado (designated "PCM"), but as Table I shows, it is primarily tied up in ankeritic dolomite. Also shown in Table I are data reported by Campbell (3) for a sample taken from the Anvil Points area.

TABLE I
OIL SHALE SAMPLE DATA

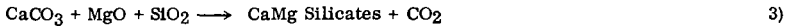
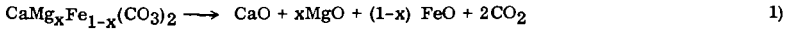
	<u>PCM</u>	<u>Anvil^c</u>	<u>C-a</u>
Assay ^a	50	22	25
<u>Mineral %^b</u>			
Dolomite/Ankerite	21	35.3	44
Calcite	9	19.4	2.4
Quartz	-	41.0	32
Silicates	-		18
<u>Elemental %^b</u>			
Ca	10.2	-	12.3
Mg	3.4	-	3.5
Fe	2.8	-	2.5
Al	5.0	-	4.3
Na	2.6	-	2.0
K	1.7	-	1.7
Si	18.8	-	16.2

a. gallons per ton; b. based on spent shale; c. data reported in Lit. Cited (3).

EXPERIMENTAL

Figure 1 shows a schematic sketch of the experimental equipment. Approximately 1.5 g of spent shale (particle size $\sim 100 \mu$) was placed in a 400 mesh stainless steel basket which was suspended from a recording electrobalance to provide continuous gravimetric readings as the reactions proceeded. The reactor vessel was constructed of 310 stainless steel and placed in a 3" furnace capable of reaching temperatures as high as 1200°K. Any one or a mixture of gases can be metered to the reactor via a 1/4" sparge tube and provisions are made to sample the exit gases with on-line gas chromatography. Tracer tests indicate that the design of the sparge system effectively creates an ideal back-mix state. Temperatures are monitored and controlled by means of two 1.6 mm shielded chromel-alumel thermocouples; one placed approximately 2 cm above the basket and the other so that it barely touches the shale sample.

Attempts were made to isolate the individual reactions to the degree to which it was possible. While this was not too difficult in experiments conducted on the PCM sample, it posed a serious problem with the C-a sample. The problem is best understood by referring to the three sets of reactions shown below.



In all samples the presence of CO_2 can prevent calcite decomposition because of the reversible nature of (2). However, we also found that the ankeritic dolomite in the C-a sample will not decompose (Equation 1) in the presence of CO_2 . As a result it was first necessary to study the silicification reactions (Equation 3) by raising the sample to the desired temperature (1000-1150°K) in the presence of CO_2 . Ankeritic dolomite decomposition was investigated by measuring the decomposition rates of virgin samples in a CO_2 -free environment at temperatures between 800°K and 925°K. Reversible calcite decomposition was then studied by recarbonating the CaO formed in Equation 1 and varying the CO_2 pressure as well as temperature.

RESULTS

Figure 2 shows the results obtained when a virgin C-a sample was allowed to silicate in a CO_2 atmosphere at temperatures between 1000°K and 1140°K. At 1000°K, silicification ceased after about 30% of the available CO_2 had been released. That is, 30% of the mineral carbonates had been converted to silicates. Interestingly, this "staging" effect proceeded as the temperature was subsequently raised. It is possible that this phenomena is due to either the formation of different silicates or, more likely, to the buildup of a silicate layer around a reactant grain. The effect of temperatures in the latter case would be to cause a dramatic increase in the diffusivity of reactants through the layer since solid-solid diffusion is known to be activated (7). However, attempts at fitting the data to various grain diffusion models were not successful and it may be that crystalline phase changes are occurring as suggested by Huang et al. (8). It is also interesting that the silicification reaction rates measured with the C-a sample are approximately 20 times lower than predicted for the Anvil Points sample (9).

Figure 3 is a comparison of first order decomposition plots for both ankeritic dolomite "labelled ankerite" and calcite in the C-a sample with that predicted for dolomite in the PCM sample. As Campbell and Burnham concluded for the Anvil Points shale (9), dolomite and calcite decomposition are indistinguishable at this temperature although the rates are about 30% higher than the C-a shale sample. Figure 4 gives the results for ankeritic dolomite decomposition in the C-a sample at two different temperatures, with and without CO_2 . Note that the presence of CO_2 completely prevents decomposition at the lower temperature and severely inhibits it at the higher temperature. Experiments with both the Anvil Points and PCM samples indicated no effect of CO_2 on dolomite decomposition.

A series of kinetic experiments were also conducted on reversible calcite decomposition using both the C-a and PCM samples. Figure 5 shows an Arrhenius plot for calcite and ankerite decomposition in the C-a sample. The higher activation energy for calcite (171 vs. 146 KJ/mole) produces rate constants which are 2.5 times higher for calcite than for ankerite at 925°K. Table II also shows a comparison of the forward and reverse reaction rate constants for calcite decomposition on the three samples. All three have similar decomposition rate constants although Campbell and Burnham (9) report a higher activation energy for the Anvil Points shale. The rate of recarbonation of the decomposed calcite in both the C-a and PCM shales was found to be relatively insensitive to temperature but approximately first order with respect to CO_2 . The fact that the recarbonation rates are high, leads one to suspect mass transport influences during recarbonation.

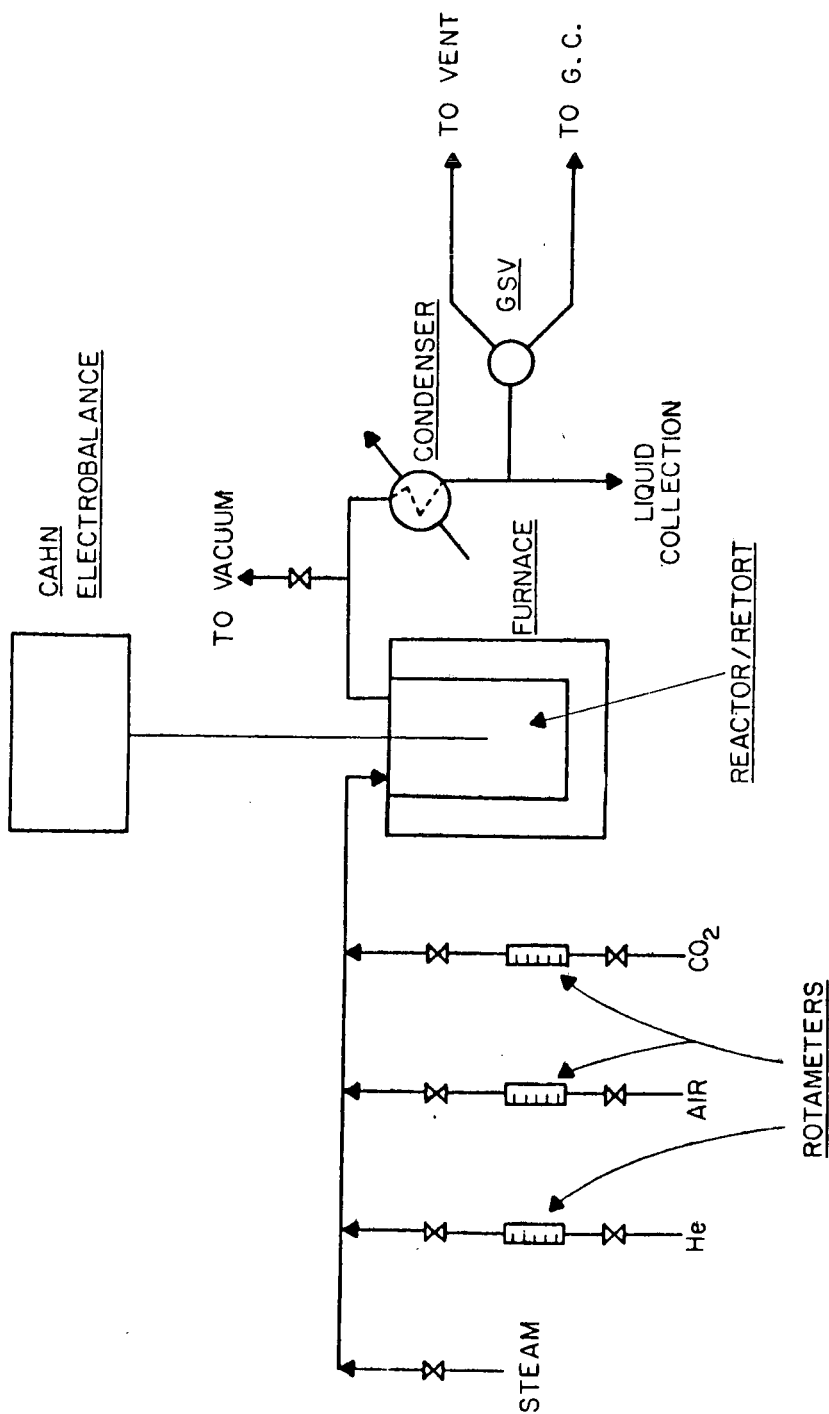


FIGURE 1: EXPERIMENTAL SCHEMATIC

Figure 2

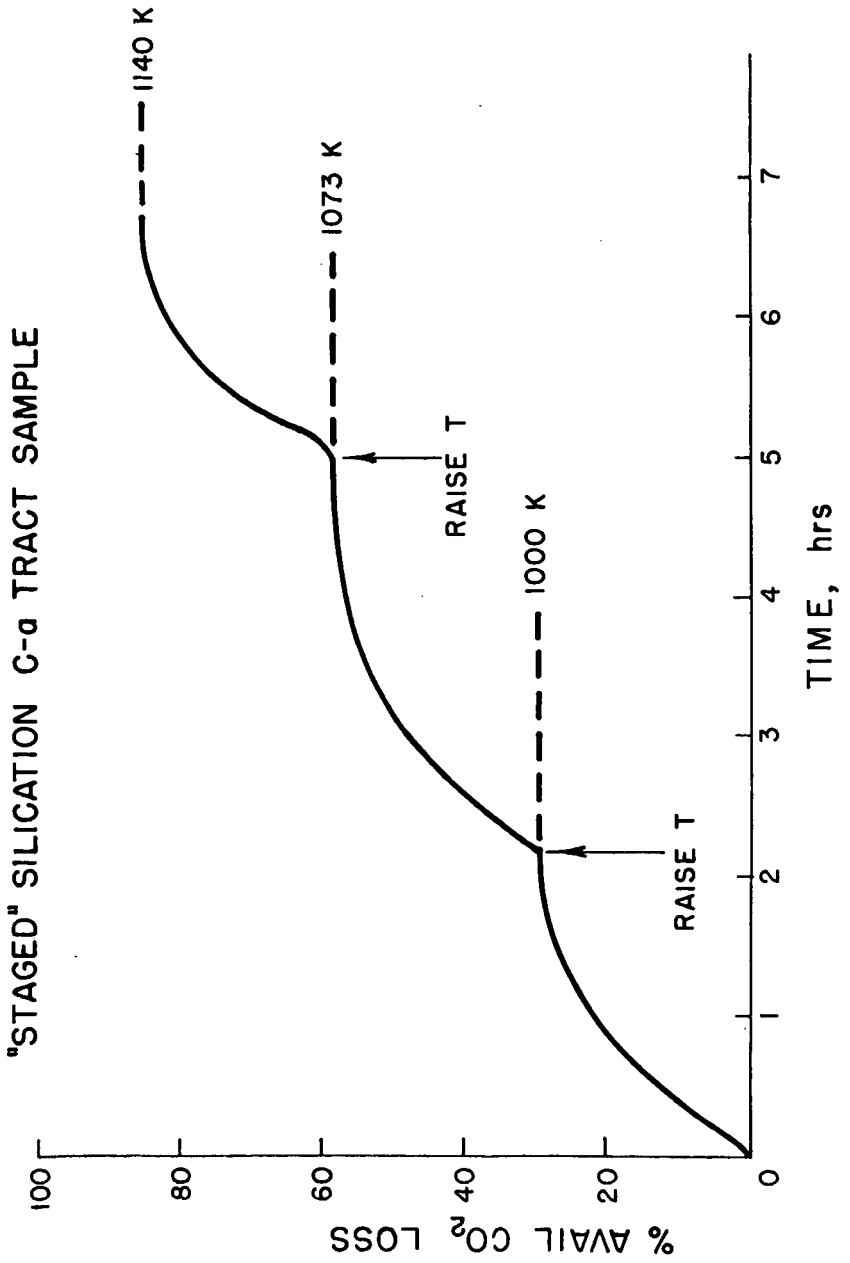


Figure 3

MINERAL DECOMPOSITION 853 K

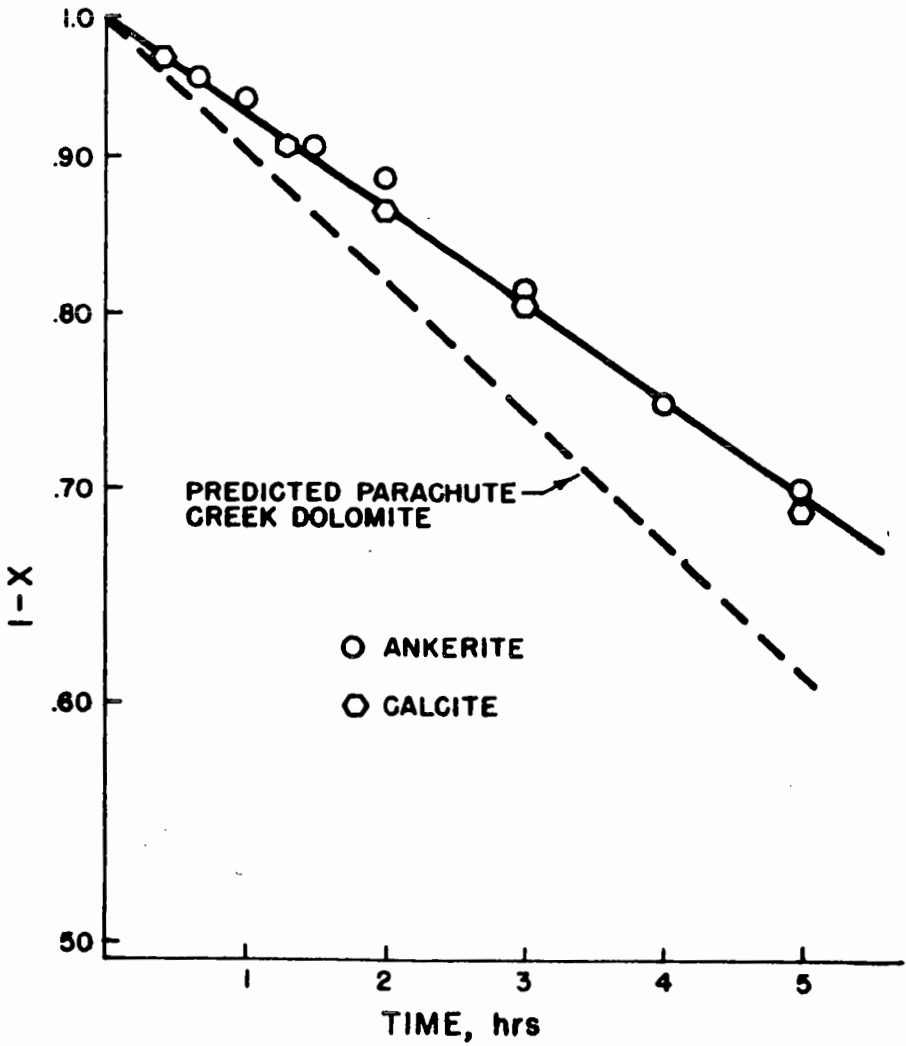


Figure 4

ANKERITE DECOMPOSITION C-a TRACT SAMPLE

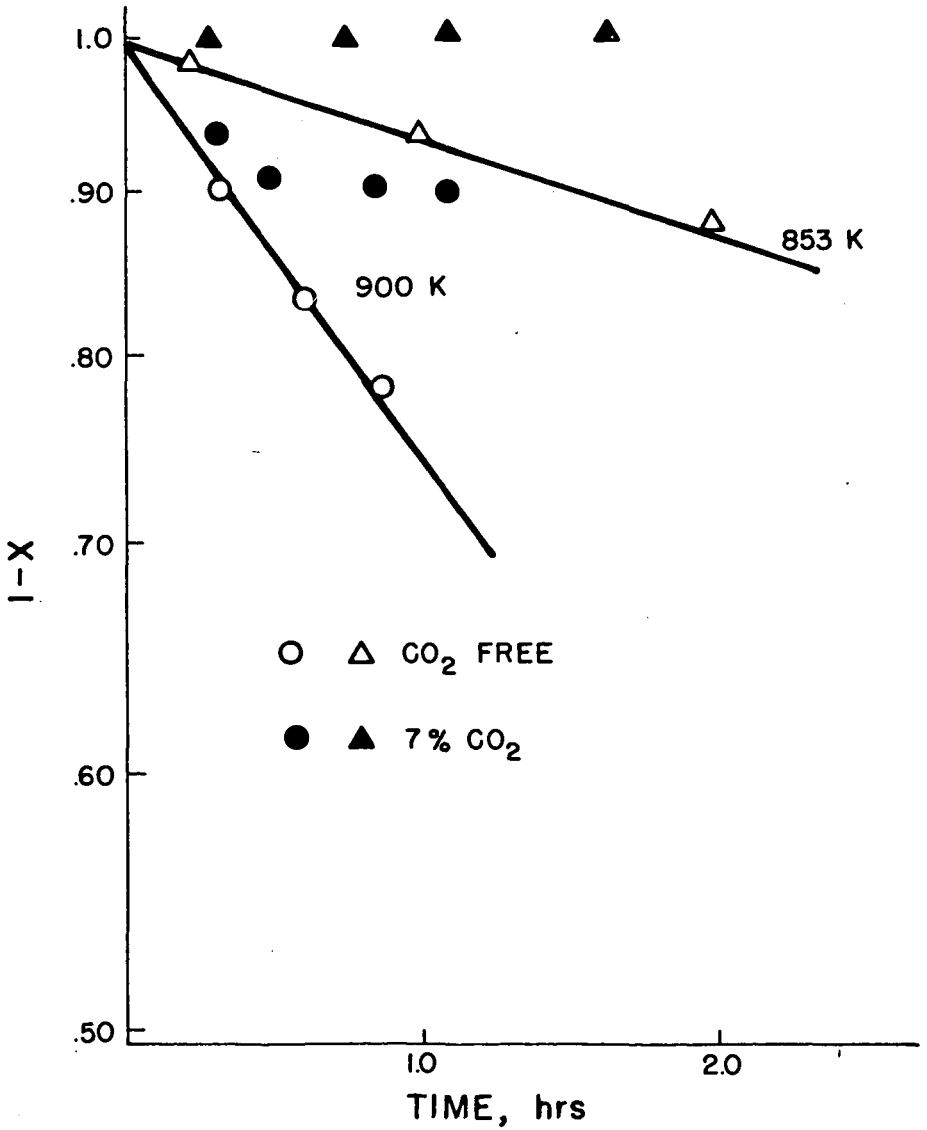
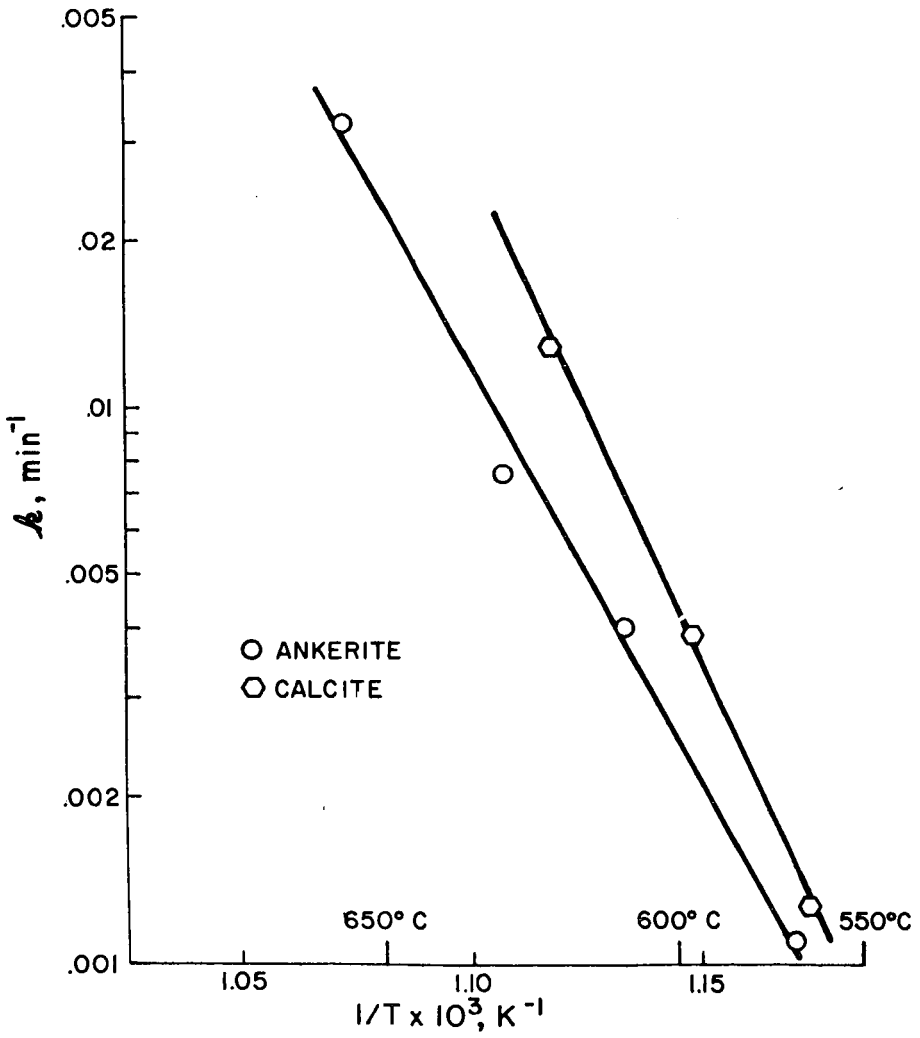


Figure 5

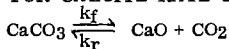
ARRHENIUS PLOT - DECOMPOSITION



Another possibility is that the recarbonation rate is controlled by the rate of adsorption of CO₂. This would be consistent with Soni and Thomson's observations (11) that recarbonation rates are ten times higher when CO₂ is produced on the surface due to char oxidation. If this is the case, then we would have to conclude that CO₂ chemisorption on shale ash is non-activated. Additional studies are now being conducted in order to distinguish between mass transport and chemisorption phenomena.

TABLE II

COMPARISON FOR CALCITE RATE PARAMETERS



$$k_{f,r} = k_{f,r}^0 \exp \left[-\frac{E_{f,r}}{RT} \right]$$

	k_f^a	E_f^b	k_r^c	E_r^b
C-a	.0014	171	6.4	~0
PCM	.0037	171	15	~0
ANV ^d	.0017	242	-	-

a. at T = 855°K, min⁻¹

b. KJ/mol

c. at T = 855°K, (atm-min)⁻¹

d. values from Lit. Cited (9)

CONCLUSIONS

It is apparent that mineral reactions in retorted oil shale are extremely complex. The reaction rates are influenced by a combination of chemical kinetics, grain mobility, solid state crystalline behavior and mass transport. Given the dramatic differences in the dependence of ankeritic dolomite decomposition on CO₂, it is obvious that future kinetic studies must also account for mineralogical structure.

ACKNOWLEDGMENT

The authors wish to express their appreciation to Gulf Research and Development, Pittsburg, Pennsylvania, for the support of this research.

LITERATURE CITED

- (1) Hall, R. N., paper presented at National AIChE Meeting, Anaheim, CA, June 8, 1982.
- (2) "Union Oil's SGR Process", Oil and Gas J., June 17, p. 26 (1974).
- (3) Campbell, J. H., Lawrence Livermore Laboratory Rept. UCRL-52089, Pt. 2 (1978).
- (4) Burnham, A. K., Stubblefield, C. T., and Campbell, J. H., Fuel, 59, 871 (1980).
- (5) Burnham, A. K., and Koskinos, G. K., Lawrence Livermore Laboratory Rept., UCID-18708 (1980).
- (6) Park, Won C., Lindemanis, A. E., and Raab, G. A., IN SITU, 3, 353 (1979).
- (7) Schmalzried, H., "Solid State Reactions", Verlag Chemie, Acad. Press, N. Y. (1974).
- (8) Huang, C. S., Rogan, F. H., and Kun, Li, AIChE Symp. Ser., 77 (202) p (1982).
- (9) Campbell, J. H., and Burnham, A. K., paper presented at AIChE National Mtg., Houston, TX, April 1-5 (1979).
- (10) Thomson, W. J., "The Oxidation/Gasification of Retorted Oil Shale", rept. prepared for DOE, October (1979).
- (11) Soni, Y., and Thomson, W. J., I and EC Proc. Des. and Dev., 18, 661 (1979).

SYMPOSIUM ON GEOCHEMISTRY AND CHEMISTRY OF OIL SHALE
PRESENTED BEFORE THE DIVISIONS OF FUEL CHEMISTRY, GEOCHEMISTRY,
AND PETROLEUM CHEMISTRY, INC.
AMERICAN CHEMICAL SOCIETY
SEATTLE MEETING, MARCH 20 - MARCH 25, 1983

INDIGENOUS MINERAL MATTER EFFECTS IN PYROLYSIS
OF GREEN RIVER OIL SHALE

By

K. M. Jeong and J. F. Patzer, II
Gulf Research & Development Company
P. O. Drawer 2038, Pittsburgh, Pennsylvania 15230

INTRODUCTION

Conventional oil shale processing technology is based upon thermal decomposition of kerogen into various grades of oil products. Historically, a variety of pyrolysis conditions, involving both above ground and *in situ* retorting operations, have been used to obtain shale oil. Numerous kinetic studies (1-6) have investigated temperature and pressure effects. Both isothermal and nonisothermal kinetic methods have been used. These studies (1-6) have established that the decomposition involves a series of consecutive reactions in which the kerogen is first converted to bitumen which, in turn, generates a form of volatile matter which eventually is reduced to coke, oil, and gas. The physicochemical properties of oil shale undoubtedly influence the decomposition process.

A number of studies (7-10) have been published concerning the effects of the mineral constituents of oil shale on the pyrolysis process. The inorganic mineral matrix is known to be intimately associated with the organic fraction, both kerogen and bitumen, and therefore, is believed to affect the release of oil products. Previous thermogravimetric studies of oil shale have attempted to demonstrate the influence of minerals by monitoring the characteristic organic carbon decomposition step of specially prepared mixtures and the composition of the pyrolysate (8-10). The results of both Espitalie, et al. (8), and Horsfield and Douglas (9) indicate that the lower oil yield for oil shale rock as compared to isolated kerogen is due to the release of smaller quantities of higher molecular weight hydrocarbons. These results are interpreted either as the result of a trapping mechanism or condensation/gasification processes, respectively. However, extrapolation of these results to *in situ* oil shale processing is questionable since a physical mixture is not likely to reproduce the exact forms of chemical bonding as they exist in the indigenous material.

The effects of indigenous carbonate and silicate minerals on the pyrolysis of Green River and Eastern oil shales have been studied by TG-DTG and TG-MS methods and are presented in the following sections. The samples were obtained by a chemical extraction method which was shown to stepwise preferentially disassociate both of these mineral components from the oil shale. In addition, the effect of oil shale richness on pyrolysis yield was determined. Since the major mineral constituent not separated by the chemical extraction procedure was pyrite, a pyrite concentrate was prepared by standard sink-float techniques from the carbonate/silicate-free kerogen concentrate. A silicate-induced pyrolysis effect in conjunction with pyrite is also discussed based on TG-DTG data of the original and chemically extracted samples.

EXPERIMENTAL

Green River oil shale obtained from the Mahogany Zone (C-a tract) was reduced to 100 x 200 mesh samples by a mechanical pulverizing and sieving procedure. Standard density separation techniques were used to generate shales having the following Fischer assays: 25, 31, and 44 GPT. Several experiments were performed using samples of Eastern oil shale obtained from Lewis County, Kentucky.

The chemical extraction procedure used to preferentially disassociate carbonate and silicate minerals has been previously described in detail (11) and, therefore, will be briefly summarized in this section. The separation scheme is outlined in Figure 1. Initially, bitumen-free oil shale was isolated using the Soxhlet extraction method based on a methanol/benzene mixture. HCl extraction of the bitumen-free oil shale resulted in a bitumen, carbonate-free fraction, a portion of which was subsequently treated with an HF/HCl mixture to remove the majority of the silicate minerals. The effectiveness of this procedure was verified by elemental analysis data discussed in Lit. Cited (11). The bitumen, carbonate, and silicate-free oil shale was further separated into sink-and-float fractions using both 15 wt% ZnCl₂ in distilled water and pure distilled H₂O as the immersion bath media.

TG-DTG measurements were made with a DuPont Model 951 thermogravimetric analyzer equipped with a 1091 disk memory. Weight loss data were obtained both as a function of time and temperature. Samples were heated from room temperature to 900°C at a rate of 10°C/min. The ambient atmosphere was ultra-pure, 99.9%, N₂ which was generally purged at 100 ml/min. Additional thermogravimetric analysis of the oil shale samples was based on TG-MS results obtained using a Cahn RH microbalance coupled with a Finnigan quadrupole mass spectrometer.

RESULTS AND DISCUSSION

Oil Shale Sample Composition

Green River oil shale is a sedimentary rock consisting of finely laminated layers of marlstone interspersed with varying amounts of organic matter. These oil shales consist of approximately 30-60% carbonate minerals and 30-40% silicate minerals. The bulk mineralogical compositions of the three shale samples obtained by heavy media separation were found to be fairly similar. The major minerals identified included analcime, clay, quartz, aibite, ankerite/dolomite, and calcite. Elemental analysis of the 25, 31, and 44 GPT samples indicated that the organic matter distribution was essentially identical for all three oil shales. The density separation procedure isolated increasingly richer shales, but the fundamental organic composition did not vary.

Eastern oil shales are basically a silicate-rich rock with only about 1% carbonate minerals. The bulk mineralogy of the Kentucky samples primarily consists of quartz, illite, and kaolinite with some chlorite and pyrite. This is consistent with elemental analysis data which indicated that the major constituents are elemental Si, Al, Fe, and K. The elemental Ca concentration was found to be less than 100 ppm for these Eastern oil shale samples.

Thermogravimetric Analysis

Figure 2 shows typical thermogravimetric data for the 25, 31, and 44 GPT samples. All of the weight loss data discussed in this paper were obtained at a heating rate of 10°C/min. Differential analysis of the TG curves indicates two major regions of volatile product release, peaking near 465 and 740°C, respectively. The majority of the observed weight loss below 200°C is believed due to water vaporization.

Based upon TG-MS results, the DTG peak near 465°C is assigned to organic carbon pyrolysis. The TG-MS results, Figure 3, indicate that the hydrocarbon release profile in the range 350 to 500°C, peaking near 430°C, is a broad mixture of C₁₀-C₁₅ alcohols, alkenes, and other compounds which cannot be easily resolved into specific product identifications. Potential contribution of silicate minerals to the weight loss in this region was checked by thermogravimetric analysis of the major individual silicate minerals identified in the shale samples. The silicate minerals showed insignificant thermal decomposition, ≈1 wt%, over the temperature range 360 to 500°C, further supporting the assignment of this DTG peak to organic carbon pyrolysis.

The thermal decomposition of carbonate groups is reflected by the DTG maximum in Figure 2 at 730-760°C. As will be discussed in the next section, this feature of the DTG curves disappears in samples of carbonate-free oil shale. Thermogravimetric analysis of pure calcite and dolomite show carbonate decomposition at 800°C and 730-780°C, respectively, further supporting this assignment. Interference from silicate minerals in this temperature range is precluded on the basis of DTG measurements of standard silicate minerals. The principal volatile product identified by TG-MS (Figure 3) at temperatures higher than those required for organic carbon pyrolysis was CO₂. This result is expected since the decomposition reactions of calcite and dolomite in oil shale release substantial quantities of CO₂ in the temperature range 600-750°C.

The TG-DTG data correspond quite well with other available analytical data for the shale samples. For example, the ratio of the weight loss in the organic evolution peak at 465°C to that of the CO₂ peak at 740°C increased from about 0.4 for the 25 GPT shale to about 1.5 for the 44 GPT sample. This trend is consistent with the relative organic carbon content of the two samples as well as the bulk mineralogy results which indicate that the 25 GPT sample has approximately 14 wt% calcite and 30 wt% dolomite versus less than 2 wt% calcite and about 20 wt% dolomite for the 44 GPT sample. Carbonate carbon concentrations, as determined by acid leaching and evolved CO₂ titration, were found to be 4.8, 3.9, and 3.2 wt% for the 25, 31, and 44 GPT samples, respectively. These values correspond to an expected weight loss in the TG carbonate decomposition region, 740°C, of approximately 18, 14, and 12 wt%, respectively, for the three shales. The expected weight losses compare favorably to measured weight losses of 21, 14, and 12 wt% for the 25, 31, and 44 GPT shales, respectively.

A second feature to be noted concerning the thermal analysis data shown in Figure 2 is a secondary peak at about 520°C following the organic carbon transition. The peak is most pronounced for the 44 GPT sample. TG-MS data, Figure 3, indicate a bimodal H₂S profile with one peak located slightly prior to the organic carbon pyrolysis peak and the second transition occurring at a temperature in between that of carbon decomposition and carbonate decomposition. These combined

results suggest the influence of pyrite on the pyrolysis of the shale samples.

Although DTG analysis of a pyrite standard sample indicated thermal decomposition over the temperature range 480 to 700°C, the major weight loss was observed at 660°C. It is likely that the relatively low concentration of pyrite in the shale samples, about 2 wt%, resulted in the masking of the 660°C peak. On the basis of the TG-MS results, it would appear that the observed 520°C peak is due to pyrite-organic matter reactions involving, for example, FeS₂ and elemental S with aromatic and olefinic compounds. Similar mechanisms have been proposed for the effect of pyrites and iron oxides on the pyrolysis and gasification of coal (12). Rostam-Abadi and Mickelson (10) have shown that for mixtures of Colorado oil shale and pyrite, the pyrolysis rate is reduced.

Weight loss data determined from the TG curves are expressed in terms of the concentration ratio of pyrolyzed organics from TG experiments, to the original organics in the shale $[O_t]^{TG}/[O_t]$. This ratio is an expression of the pyrolysis yield of the sample. Table I summarizes the pyrolysis yields determined for the three oil shales of differing richness and the DTG temperature maxima. The pyrolysis yield is observed to increase with shale organic content from 58.6 to 72.2 wt% of the shale organics. The organic carbon decomposition temperature is reasonably constant as a function of oil shale richness. The temperature at which pyrolysis of carbonates occurs appears to decrease with increasing GPT. The temperature change for the carbonate probably reflects the changing calcite concentrations in the shales. Calcite decomposes at higher temperatures than does dolomite.

For comparison purposes, a sample of Eastern oil shale was thermally analyzed for pyrolysis effects. The mineralogical composition of this oil shale is confirmed by the TG and DTG measurements shown in Figure 2d by the marked absence of the carbonate decomposition characteristic of the 700-800°C temperature range. The pyrolysis yield, 47.4 wt%, determined for this oil shale is substantially lower than that found for the samples of Green River oil shale and is consistent with a lower H/C ratio in the organic fraction. The lower pyrolysis temperature, 453°C, is possibly due to the absence of carbonate mineral bonding and therefore, a lower total enthalpy of reaction. The secondary peak at 520°C was also observed in the TGA data of the Eastern oil shale. This result eliminates a carbonate origin for this transition and is in support of a possible pyrite or pyrite-induced weight loss since this sample contains ~5 wt% pyrite.

TABLE I
SHALE RICHNESS VS. PYROLYSATE CONCENTRATION^{a, b, c}

Oil Shale Richness (GPT)	Elemental Analysis			Thermogravimetric Analysis				Pyrolysis Yield	
	[C _c]	[C _o]	[O _t]	[O _t]	T _i	[C _c]	T _i	Org.	Carb.
	(Ct)	(Wt%)	(Wt%)	(Wt%)	(°C)	(Wt%)	(°C)	(%)	(%)
25	4.79	11.4	14.2	8.32	463	5.76	758	58.6	120
31	3.91	11.9	14.8	9.75	465	3.88	733	65.9	99
44	3.22	19.4	24.1	17.4	467	3.17	729	72.2	98
Eastern ^d	0.03	12.4	----	5.88	453	----	---	47.4	---

- [C_c], [C_o], and [O_t] represent carbonate carbon, organic carbon, and total organic concentration $[O_t] = [C_o]/0.805$; T_i: inflection point temperature.
- T range for organic matter pyrolysis (ΔT_o) is determined to be 350 to 500°C. T range for carbonate carbon decomposition (ΔT_c) is determined to be 600 to 800°C.
- Pyrolysis yield % : $100[O_t]^{TG}/[O_t]$ for organics and $100[C_c]^{TG}/[C_c]$ for carbonates.
- Pyrolysis yield % is based on concentration of organic carbon, [C_o].

TG Results of Extracted Fractions

The influence of the mineral matrix on the pyrolysis of Green River oil shale was investigated for the 44 GPT sample. In contrast to earlier studies (8-10) based on the physical combination of mineral additives with oil shale and/or a kerogen concentrate, the approach used in this work involved a chemical extraction technique (11), Figure 1, which preferentially disassociated the carbonate and silicate minerals. In addition to the original H₂O-washed sample, the following five fractions were analyzed by TG: bitumen-free, bitumen/carbonate-free, bitumen/carbonate/silicate-free or kerogen concentrate, float fraction of kerogen concentrate, and sink fraction of kerogen concentrate. The thermogravimetric data, including pyrolysis yields are summarized in Table II.

The net pyrolysis yield is observed to increase by 2.4% after the removal of the bitumen component contrary to initial expectations. Although the bitumen component is pyrolyzed quantitatively, the kerogen component appears to be converted to products more readily in the absence of bitumen. It is also noted that the secondary peak at 520°C is still present. Thus, the peak is

not associated with bitumen pyrolysis and therefore, by inference, is due to the mainly bitumen-free kerogen component.

TABLE II
THE INFLUENCE OF THE MINERAL MATRIX ON
THE PYROLYSIS OF OIL SHALE^a

Sample	Elemental Analysis			Thermogravimetric Analysis				Pyrolysis Yield	
	[C _c]	[C _o] (Wt%)	[O _i]	W _o (Wt%)	T ₁ ^b (°C)	W _c (Wt%)	T ₁ ^b (°C)	Org. (%)	Carb.
H ₂ O Washed O. S.	2.93	20.49	25.45	15.33	464	11.68	724	60.2	109
Bitumen- Free O. S.	3.05	19.34	24.02	14.81	459	13.04	704	61.7	107
Carbonate- Free O. S.	0.15	25.69	31.91	20.80	472	---	---	68.8	---
Kerogen Conc. ^c	0.18	66.55	82.67	47.59	456	---	---	57.6	---
Float Fraction	0.18	66.64	82.78	56.66	468	---	---	68.4	---
Sink Fraction	0.18	65.28	81.09	45.70	463	---	---	56.4	---

a. Colorado, C-a tract, Mahoghany zone oil shale, 44 GPT, 100x200 mesh

b. ΔT_0 : 350 to 500°C, ΔT_c : 600 to 800°C

c. Kerogen Conc.: Bitumen, Carbonate and Silicate-free Oil Shale

A significant increase in the net pyrolysis yield to 14% was obtained as the result of removal of the carbonate minerals by HCl treatment. The second DTG maximum near 730°C, due to carbonate decomposition, was noticeably absent. An explanation of the increased pyrolysis yield for the carbonate-free shale, as expected, is certainly a combination of several factors. It appears that carbonate minerals, thermochemically and/or kinetically, act to hamper the pyrolysis process or possibly modify the mechanistic reaction scheme to yield a higher percentage of coke. The observed increase in the pyrolysis yield is not due to the release of bitumen trapped by the carbonate minerals since such trapped soluble organic matter was removed by a Soxhlet extraction prior to TG analysis.

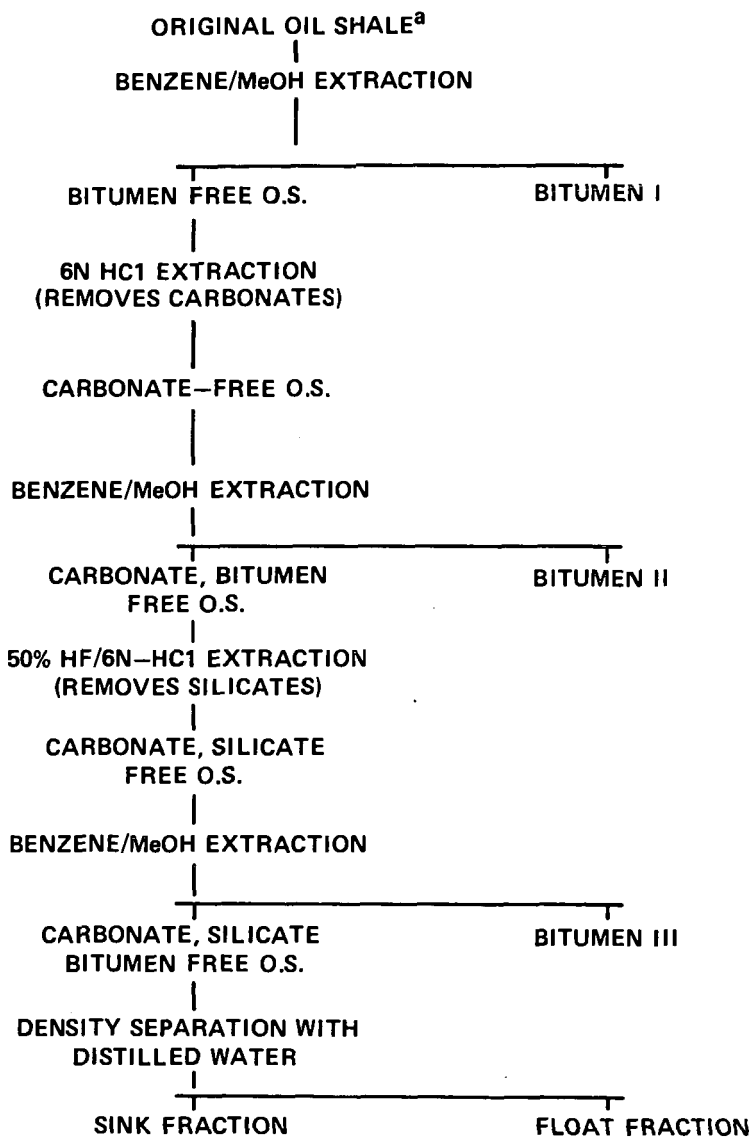
The decomposition of pure phase carbonate minerals has been extensively studied and reviewed (13). The influence of these materials on oil shale pyrolysis kinetics has not been as thoroughly investigated, but the studies of Jukkola, et al. (14), and Campbell (7) are notable. The results of both of these studies indicate that the major calcite decomposition step is not to produce CaO, but rather reaction with silicate minerals in the oil shale to form calcium and calcium-magnesium silicates. The observed enhancement of pyrolysis yield after carbonate removal may be indicative of the catalytic role of silicate minerals in paraffinic and aromatic compound decompositions. In effect, the apparent preference for calcite-silicate interactions precludes silicate-catalyzed organic reactions which would presumably result in enhanced oil recovery.

This proposed silicate mineral catalytic effect is further demonstrated by TG measurements of the kerogen concentrate which indicated a decrease in the pyrolysis yield from 68.8 wt% for the carbonate-free fraction to 57.6 wt% for the carbonate- and silicate-free fraction. These results suggest that the optimum pyrolysis oil yield is achieved for oil shales which are carbonate-free but still retain their original silicate mineral concentration or possibly, an increased silicate concentration.

The positive effect of silicate minerals on oil shale pyrolysis was not a priori predictable and its origin is difficult to precisely quantify. However, one possible explanation seems to involve the combined chemistry of silicate minerals, kerogen, and pyrite. It is known that pyrite usually occurs in the form of microcrystals coated with organic matter which aggregate together to form spherical framboids (15). It is proposed that the dissolution of the pyrite-organic matter interface may be catalyzed by silicate minerals which act as an effective third body for the formation of thiophenic compounds. Liberation of this organic matter coating via pyrite decomposition and subsequent transformation would result in the observed oil yield trend. It has been shown that the reactions of S or H₂S with various organic molecules results in the formation of thiophenic structures as does the reaction of FeS₂ with organics (16).

The catalytic effect of silica and aluminosilicates has been previously suggested in other chemical systems, but to the authors' knowledge, has not been experimentally verified. A possible experimental observation of this catalytic effect may be the 520°C DTG peak. Removal of the

**FIGURE 1 PREFERENTIAL MINERAL MATTER DISSOLUTION
BY CHEMICAL METHODS**



a) COLORADO, C-a TRACT, MAHOGANY ZONE, 100X200 MESH, 44 GPT; IN ORDER TO REMOVE FINES AND CONTAMINATED IRON, THE ORIGINAL OIL SHALE WAS WATER WASHED, FILTERED AND DRIED AT 85°C UNDER VACUUM (400 TORR WITH N₂) FOR 24 HR.

FIGURE 2 NON-ISOTHERMAL TG-DTG CURVES OF WESTERN ((a) 25 GPT (b) 31 GPT (c) 44 GPT) AND EASTERN (d) OIL SHALES (HEATING RATE 10°/MIN)

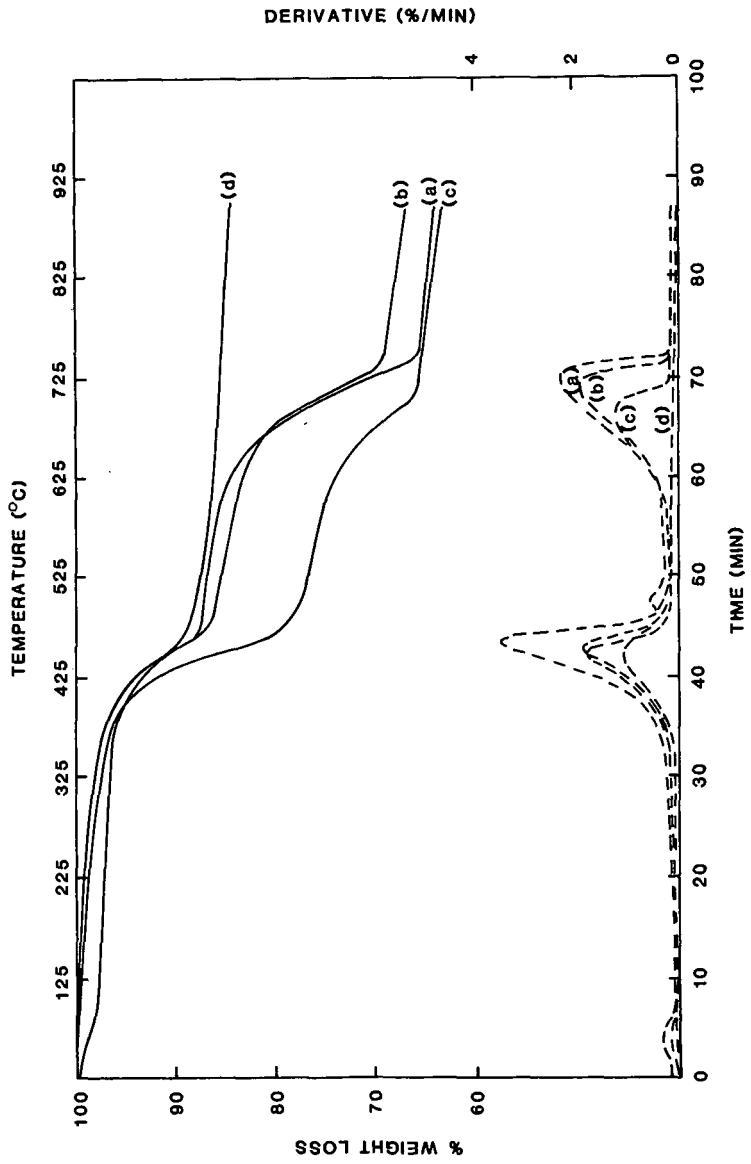
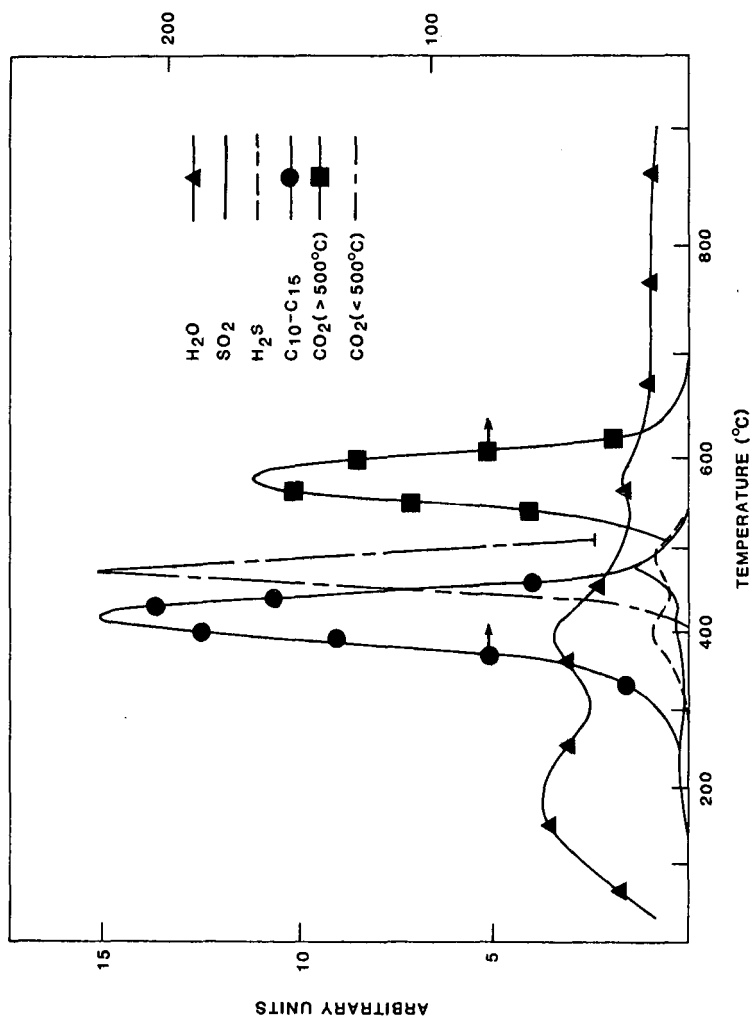


FIGURE 3 TG-MS ANALYSIS OF 44GPT WESTERN OIL SHALE (C₁₀-C₁₅ AND CO₂ (>500°C) REFER TO RIGHT HAND SIDE SCALE)



silicate minerals by HF/HCl extraction resulted in a significant reduction of the thermal decomposition process at this temperature. Reproduction of this peak could only be obtained with substantial additions of the kerogen concentrate to a low temperature ash sample. In addition, an increase in the relative amount of weight loss at 520°C in comparison to the organic carbon decomposition was obtained only by adding to the original 44 GPT sample a fairly large amount of pyrite. On the basis of X-ray diffraction data of the separated fractions, it is probable that both clay minerals and quartz contribute to the catalytic process.

The last step outlined in Figure 1 is the addition of various media to the kerogen concentrate to obtain sink-float fractions. All three GPT oil shales exhibited organic carbon decomposition at 460-470°C in float fractions with density $<1.145 \text{ g ml}^{-1}$. The sink fractions showed a variety of transitions, the most notable being the presence of organic matter as evidenced by the peak near 465°C. This effect is due to very strong organic matter interactions with quartz and pyrite which resulted in the separation of a significant portion of the bitumen-free organic matter with the mineral constituents. This interpretation is consistent with X-ray diffraction results and elemental analysis data. The other major TG inflection point common to all three GPT samples is at $T=530^\circ\text{C}$. This thermal decomposition is especially pronounced for the 25 GPT sink sample. A sample of Eastern oil shale was also sink-floated at $\rho=1.145 \text{ g ml}^{-1}$ with similar results as the Green River oil shale.

Reducing the density to 1.00 g ml^{-1} caused the separation of additional components which previously floated and were not detected due to the relative weight loss of organic carbon. In addition to the transition observed at 470 and 530°C for the higher density separation, two peaks appeared at 670 and 790°C. A shoulder at 370°C prior to the onset of the organic carbon decomposition was observed. It is suggested that the 370°C transition is due to analcime and the 790°C decomposition to calcite based on standard mineral TG-DTG data. The 670°C peak is the first indication of pyrite based on the close match between the observed DTG temperature maximum and that of the pyrite standard at 660°C. This separated fraction is clearly a relatively concentrated pyrite sample as is confirmed by elemental analysis data.

ACKNOWLEDGMENTS

The authors gratefully acknowledge the technical assistance of Mr. D. L. Bash and helpful discussions with Dr. J. E. Lester.

LITERATURE CITED

- (1) Haddadin, R. A., and Mizyet, F. A., *Ind. Eng. Chem. Proc. Des. Dev.*, **13**, 332 (1974).
- (2) Braun, R. L., and Rothman, A. J., *Fuel*, **54**, 129 (1975).
- (3) Herrell, A. J., and Arnold, C., Jr., *Thermochim. Acta.*, **17**, 165 (1976).
- (4) Campbell, J. H., Kuskinas, G., and Stout, N., *Fuel*, **57**, 372 (1978).
- (5) Noble, R. D., Harris, H. G., and Tucker, W. F., *Fuel*, **60**, 573 (1981).
- (6) Thakur, D. S., Nuttall, H. E., and Cha, C. Y., *ACS Div. of Fuel Chemistry, Preprints*, **27**, (2) 131 (1982).
- (7) Campbell, J. H., Lawrence Livermore National Laboratory, UCRL-52089 Part 2, March 13, 1978.
- (8) Espitalle, J., Nadee, M., and Tissot, B., *Am. Assn. Pet. Geol. Bull.*, **64**, 59 (1980).
- (9) Horsefield, B., and Douglas, A. G., *Geochim. et Cosmochim. Acta.*, **44**, 1119 (1980).
- (10) Rostam-Abadi, M., and Mickelson, R. W., *AIChE 1981 Summer Natl. Meeting*, **16b**, F9 (1981).
- (11) Jeong, K-M., and Kobylinski, T. P., 185th ACS National Meeting, Seattle, Wash., March 1983.
- (12) Attar, A., *Fuel*, **57**, 201 (1978).
- (13) Stern, K. H., and Weise, E. L., "High-Temperature Properties and Decomposition of Inorganic Salts, Part 2 Carbonates", *Nat. Stand. Ref. Data Ser.*, Nat. Bur. of Stand., Washington, D. C., 1969.
- (14) Jukkola, E. E., Denilauler, A. J., Jenson, H. B., Barnet, W. I., and Murphy, W. I. R., *Ind. Eng. Chem.*, **45**, 2711 (1953).
- (15) Durand, B., "Kerogen-Insoluble Organic Matter from Sedimentary Rocks", Editions Technip, Paris, 1980.
- (16) a. Hartough, H. D., "Thiophene and its Compounds", Interscience, New York, 1952.
b. Hartough, H. D., and Meisel, S. L., "Compounds with Condensed Thiophenic Rings", Interscience, New York, 1954.

SYMPOSIUM ON GEOCHEMISTRY AND CHEMISTRY OF OIL SHALE
PRESENTED BEFORE THE DIVISIONS OF FUEL CHEMISTRY, GEOCHEMISTRY,
AND PETROLEUM CHEMISTRY, INC.
AMERICAN CHEMICAL SOCIETY
SEATTLE MEETING, MARCH 20 - MARCH 25, 1983

THE EFFECT OF MINERAL SPECIES ON OIL SHALE CHAR COMBUSTION

By

R. P. Cavaliere and W. J. Thomson
Department of Chemical Engineering, Washington State University
Pullman, Washington 99164-2710

INTRODUCTION

In order to increase the energy efficiency of above-ground oil shale processes, the carbonaceous residue ("char") remaining on retorted oil shale ("spent" shale) will either be combusted (1,2) or gasified (3). Although there is no great difficulty in combusting the char, it is important that combustion be carried out in a controlled fashion. Failure to do so can result in high temperatures ($>900^\circ\text{K}$) and the decomposition of mineral carbonates. These decomposition reactions are not only endothermic (4) but some of the products have the potential to cause environmental disposal problems (5).

Control of oil shale char combustion is more easily managed if there is a knowledge of how the rate of combustion depends on O_2 concentration and temperature. This motivation led to an earlier study (6) of the combustion kinetics of spent shale from the Parachute Creek Member in western Colorado. That study provided evidence that one or more of the mineral species present in the shale acted as an oxidation catalyst. Consequently it was decided to follow up on that investigation by examining the combustion activity of other oil shales; specifically those with differing elemental and/or mineral compositions.

Six oil shale samples were selected for evaluation and comparison: one from the Parachute Creek Member (PCM), one from a deep core sample in the C-a tract (C-a), two from the saline zone in western Colorado (S-A and S-B), one from the Geokinetics site in eastern Utah (GEOK) and one sample of Antrim shale from Michigan (ANT).

EXPERIMENTAL

Figure 1 shows a schematic sketch of the experimental equipment. Approximately 1.5 g of spent shale (particle size $\sim 100\mu$) was placed in a 400 mesh stainless steel basket which was suspended from a recording electro-balance to provide continuous gravimetric readings as combustion proceeded. The reactor vessel was constructed of 316 stainless steel and placed in a 4" furnace capable of reaching temperatures as high as 1200°K . Any one or a mixture of gases can be metered to the reactor via a 1/4" sparge tube and provisions are made to sample the exit gases with on-line gas chromatography. Tracer tests indicate that the design of the sparge system effectively creates an ideal back-mix state. Temperatures are monitored and controlled by means of two 1.6 mm shielded chromel-alumel thermocouples; one placed approximately 2 cm above the basket and the other so that it barely touches the shale sample. The latter was used to monitor temperature excursions during initial combustion but never exceeded 10 K and, then, only for 1-2 minutes.

All of the shale samples were retorted in master batches and under identical conditions in a 2.5 cm diameter fixed bed retort. A nitrogen sweep gas at 100 cc/min was employed and the temperature was elevated at a rate of 5 K/min to a maximum temperature of 785°K at which point it was held for 1 hour. Table I shows the quantity of oil collected during retorting, the percentage of organic carbon on the spent shale and the percentage of some of the more important elements (obtained by X-ray fluorescence). Although there is a wide variation in the oil yields, we have previously shown (7) there to be no effect on the combustion activity of spent shale. However, it is interesting to note that the GEOK sample had twice the organic carbon content of the PCM sample even though the two had similar oil yields.

Combustion tests were carried out by heating the sample to the desired temperature in a helium atmosphere and then exposing it to a pre-selected O_2 concentration. In some cases the samples were first subjected to high temperatures ($800\text{--}1050^\circ\text{K}$) in either a helium or CO_2 atmosphere in order to effect changes in the mineral compositions and then cooled to the desired combustion temperature. Combustion activities were evaluated for O_2 pressures between 5 and 20 kPa and at temperatures between 700 and 825°K .

TABLE I
COMPOSITION OF SPENT SHALE SAMPLES

Sample	GPT ^a	C ^b	Wt% Spent Shale						
			Ca	Mg	Fe	Al	Na	K	Si
PCM	50	5.1	10.2	3.4	2.8	5.0	2.6	1.7	18.8
C-a	25	3.5	12.3	3.5	2.5	4.3	2.0	1.7	16.2
GEOK	44	11.9	15.2	4.3	3.1	4.8	2.3	2.0	19.6
S-A	30	3.8	8.4	3.6	3.1	6.3	2.8	2.1	22.3
S-B	40	3.9	1.0	1.0	5.6	10.9	0.4	1.7	30.2
ANT	11	7.0	0.7	1.2	5.4	8.3	0.4	3.4	31.0

a. Gallons per ton

b. Organic carbon

RESULTS

As in our earlier work (6) the combustion reaction rate was found to be first order with respect to both O₂ and char content. Table II lists the apparent rate constants in terms of the pre-exponential factor and the activation energy for all six samples as well as comparative values at 700°K. The S-A sample had the highest activity and has high concentrations of the minerals dawsonite and nahcolite. Although these minerals will have decomposed during retorting, the decomposition products (Na₂CO₃, Al₂O₃) are present and, as we will show, there is strong evidence to indicate that they act as catalysts. In view of this, it is also tempting to conclude that the low apparent activation energy is also due to a catalytic mechanism. However, because of the high reaction rate and the limitations on the maximum gas flow rate in the TGA system, it is possible that gas-solid mass transport has influenced these measurements. It is interesting, but probably coincidental, that the S-B shale had the lowest activity. This sample is similar to S-A except that it is low in dawsonite and nahcolite. Finally, it should be pointed out that the pre-exponential factor listed in Table II for the PCM sample, differs from the value we reported earlier (6). By virtue of our measurements of the actual shale temperature, we have discovered that the measured temperatures in the earlier study were in error. The values listed in Table II are now consistent with the reported measurements of Sohn and Kim (8).

TABLE II
KINETIC PARAMETERS

$$k = k_0 \text{EXP} \left[\frac{-E}{RT} \right] \quad (\text{kPa} \cdot \text{min})^{-1}$$

Sample	$k_0 \times 10^{-5}$	E ^a	k (700 K)
PCM	2.45	97.07	.0140
C-a	8760.	142.3	.0212
GEOK	11.51	91.21	.0236
S-A	.002	49.79	.0385
S-B	.480	93.72	.0049
ANT	5.42	104.8	.0082

a. KJ/mol

One of the experiments which we initially conducted on the PCM sample was to thermally decompose the carbonate minerals (dolomite and calcite) to their oxides at 900°K



When the temperature was lowered to 700°K and the sample exposed to O₂, the observed combustion rate was ten times higher than when the carbonates were left intact. By process of elimination, the increased activity was attributed to the presence of CaO. In order to further investigate this phenomena, the same experiment was carried out with the C-a and ANT sample. The C-a sample was chosen due to the fact that its free calcite was only 2% compared to 10% for the PCM sample. On the other hand, the ANT sample had a very low Ca content.

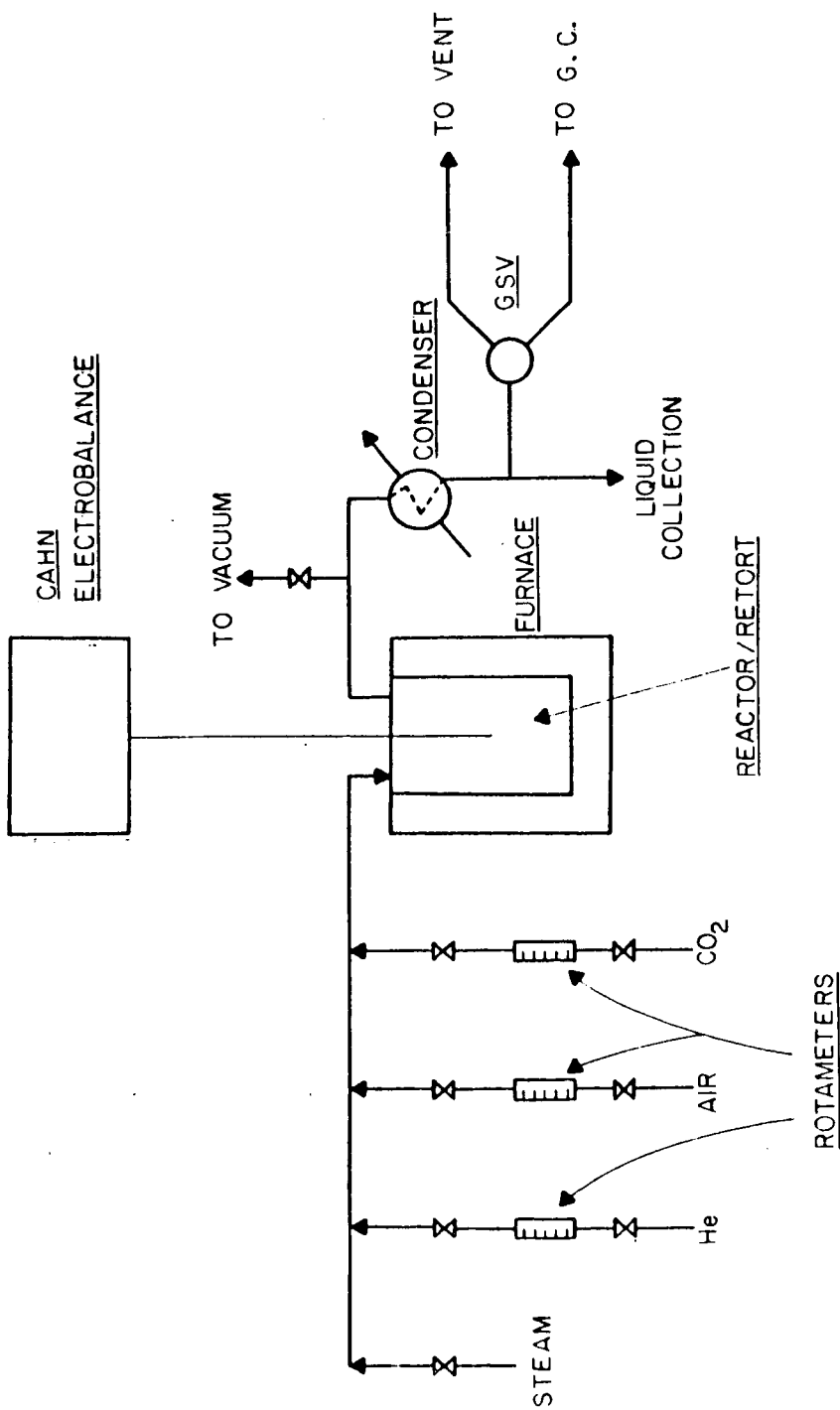


FIGURE 1: EXPERIMENTAL SCHEMATIC.

Figure 2

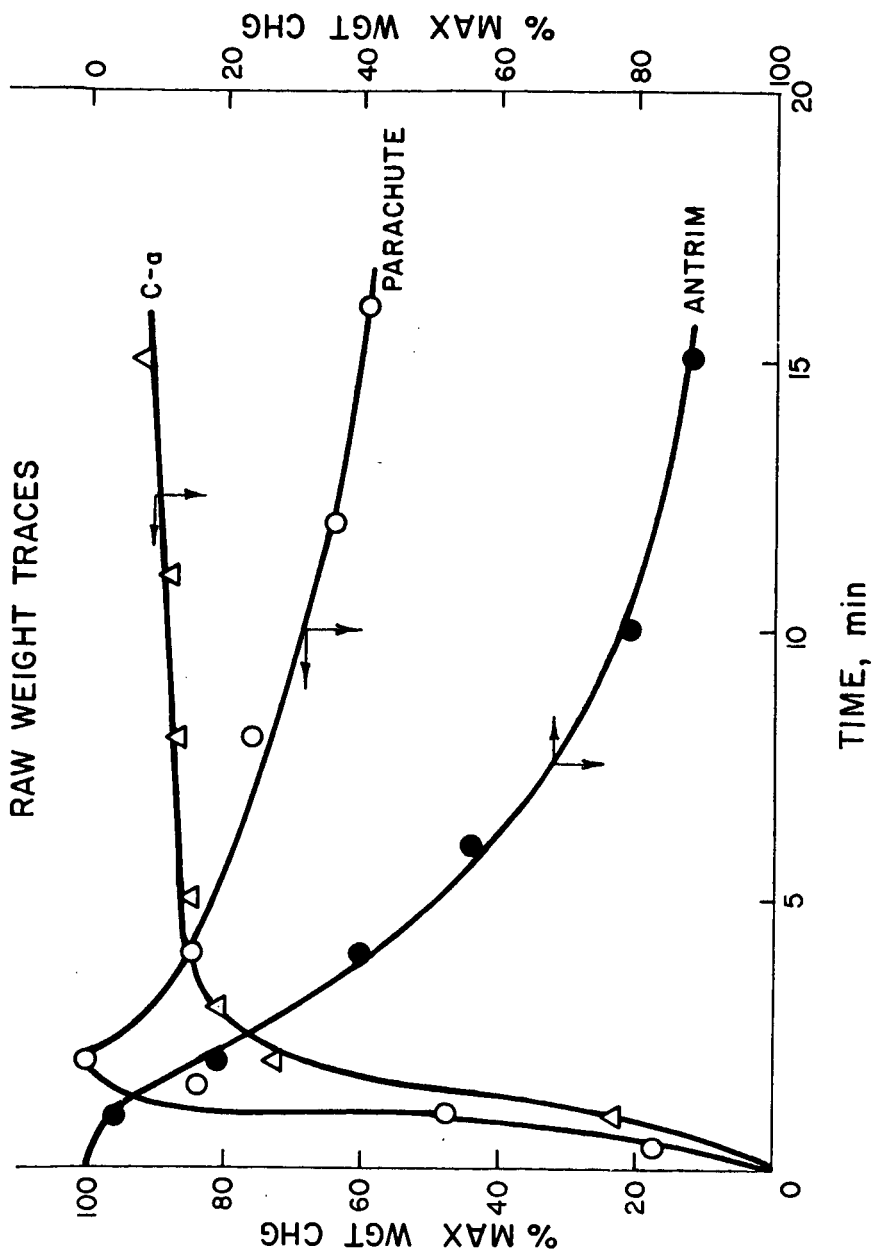


Figure 3

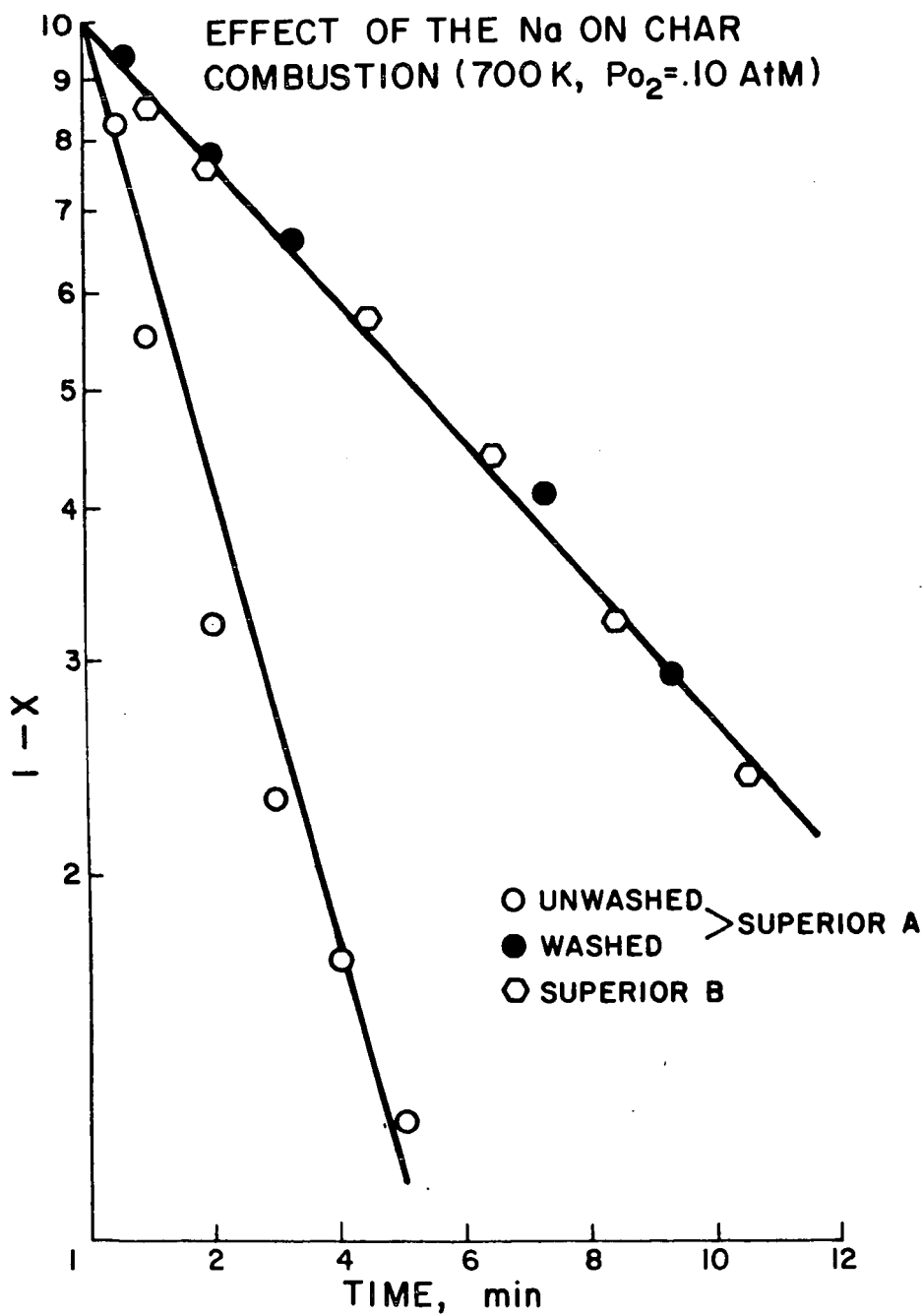


Figure 2 shows the comparative responses of the raw gravimetric readings when the decomposed samples were exposed to 10% O₂ at time = C. Similar behavior is observed for the C-a and PCM samples; that is, the raw weight increases due to the recarbonation of CaO.



Since the combustion rate is at least as fast as the recarbonation rate, the data in Figure 2 correspond to a combustion rate increase of about an order of magnitude in both samples. This also leads to the conclusion that the source of CaO does not appear to be important since most of it is produced from ankeritic dolomite in the C-a sample and over 30% from free calcite in the PCM sample. It is interesting to note that the ANT sample, which has minimal Ca, does not experience a weight gain during combustion. In fact, the combustion rate is identical to that observed for ANT samples which had not been thermally pretreated. Since the latter is also high in iron compounds, these results tend to support the hypothesis of CaO as a combustion catalyst.

Additional experiments were also run in order to examine the effects of mineral species. Figure 3 shows first order plots for two S-A and one S-B sample. As pointed out earlier, the S-A and S-B samples are similar except for high concentrations of nahcolite and dawsonite in the former and this sample had the highest combustion activity (Table II). The effect of the sodium contained in these minerals was examined by water leaching the S-A sample prior to combustion. As can be seen, this reduces the combustion activity so that it becomes identical to the S-B activity. These results are not too surprising since it is well known that the Group I-a and, to a lesser extent, the Group II-a elements are good gasification catalysts (9).

At temperatures between 925-1100°K, western shales will form Ca-Mg silicates if calcite decomposition can be prevented. In order to investigate the consequences of having silicates present during combustion, both the PCM and C-a samples were raised to 1100°K in a 20% CO - 80% CO₂ atmosphere and held at that temperature until silication was completed. The CO₂ atmosphere prevented Reaction 2 from taking place and the CO was used to inhibit the CO₂ - char reaction (10). The samples were then cooled and subjected to combustion conditions. Although both samples had over 50% of their char remaining, it was impossible to combust either at the conditions used in this study. Apparently the silication process acts to encapsulate the char and render it inactive to normal combustion conditions.

CONCLUSIONS

On the basis of the studies conducted here, it is readily apparent that the presence of minerals can drastically alter the reactivity of the residual char on spent oil shale. More detailed quantitative studies are necessary in order to be able to assess their importance under typical oil shale processing conditions and will be the subject of future manuscripts from this laboratory.

ACKNOWLEDGMENT

This work was supported by the U.S. Department of Energy under Contract No. DE-AM06-76RLO2221

LITERATURE CITED

- (1) Hall, R. N., paper presented at National AIChE Meeting, Anaheim, CA, June 8, (1982).
- (2) Griswold, C., and Duir, J. H., paper presented at National AIChE Meeting, Anaheim, CA, June 8 (1982).
- (3) "Union Oil's SGR Process", Oil and Gas J., June 17, p. 26 (1974).
- (4) Campbell, J. H., Lawrence Livermore Lab., Rept. No. UCRL-52089 part 2, March (1978).
- (5) Mavis, J. D., and Rosain, R. M., paper presented at National AIChE Meeting, Detroit, MI, August 16 (1981).
- (6) Soni, Y., and Thomson, W. J., I and EC Proc. Des. and Dev., 18, 661 (1979).
- (7) Soni, Y., and Thomson, W. J., Proceedings of 11th Oil Shale Symp., p. 364, April (1978).
- (8) Sohn, H. Y., and Kim, S. K., I and EC Proc. Des. and Dev., 19, p. 550 (1980).
- (9) Wen, W. Y., Catal. Rev. - Sic. Eng., 22, 1 (1980).
- (10) Thomson, W. J., Gerber, M. A., Hatter, M. A., and Oakes, D. G., "Oil Shale Tar Sands and Related Materials", ACS Symp. Ser. 163, p. 117 (1982).